Development of an Industrial Test Platform for Foot Health Device and Footwear Testing

Zain Shahid

School of Health and Society
University of Salford, Salford, UK

Submitted in Partial Fulfilment of the Requirements of the Degree of Doctor of Philosophy, September 2023

Table of Contents

List of Figures

List of Tables

Acknowledgements

First and foremost, I would like to extend my deepest gratitude to my supervisory team. Dr Dan Parker, your expertise, and insights were invaluable to this project; thank you for your consistent guidance and unwavering support. Thanks also to Chris Nester and Guowu Wei for their input. I would like to extend a special thank you to Scholl for their collaboration and financial support.

This project would not have been possible without the significant guidance, technical expertise, and support offered by the Makerspace and Art department. George Dodgson, Aidan Dunbar and Tim Bailey, your creative insights in the development and manufacture stages were crucial.

To the Robotics Lab, Kieron Duggan, and Andy Baker, thank you for allowing me access to your cutting-edge facilities and for your invaluable technical assistance throughout this research journey. For their technical assistance, I must acknowledge Workshop Technician Bernie Noakes. Your expertise behind the scenes has been invaluable.

I am also thankful for the unwavering support of the CDT Team, especially Joanne Caldwell and Malcolm Granat, whose administrative and logistical assistance made everything run much more smoothly, despite my clear efforts to drive them insane. To my fellow CDT Students, your camaraderie and shared insights have made what has been a difficult journey at times significantly more enriching and far less arduous. Specific thanks must go out to Jennifer Andrews who has been a beacon of positivity on the other side of the desk and a shining example of the values each academic should uphold. I look forward to reading endless her publications and plaudits which will inevitably follow her PhD.

To my family—who have supported me emotionally and in countless other ways throughout this Ph.D.—your love and encouragement have been my most steadfast companions along this journey. You are the foundation upon which all of this has been built. To Abeer, I apologise for leaving you the sole member of the non-doctor club.

Finally, to my wife Alya, words cannot fully capture my gratitude and love for you. Your support, patience and understanding in this final year have made all the difference. I promise I'll be less boring now.

Epigraph

Truth transcends the telling.

- Ino

Statement of Component Contributions

Financial Contribution

ESPRC, Scholl - Provided financial support and collaboration for the research project, allowing the project to advance in the industrial context relevant to foot health devices.

Contributions to Work

BodyParts3D: Supplied the 3D anatomical models utilized in this research, providing a critical foundational element for the development of the test platform.

Makerspace: Contributed to the prototyping and testing phases, with specific thanks to George Dodgson and Aidan Dunbar for their technical assistance.

Art Department: Provided creative insights and support in the manufacturing process, notably Tim Bailey for his contributions.

Laura Smith, Steve Horton: Contributed to the data analysis and interpretation in the Gait lab, providing scientific rigor to the project's findings.

School of Health and Society: Provided the facilities and expertise required for gait analysis, contributing to the validation of the test platform.

Declaration

I declare that this thesis was composed by myself, that the work contained herein is my own except where explicitly stated otherwise in the text carried out while studying at the University of Salford from October 2019 to September 2023. I declare that this work has not been submitted for any other degree or processional qualification except as specified.

Abstract

The current development pathway for medical and non-medical foot health devices faces challenges. Specifically, medical devices often proceed to clinical testing with limited functional testing which can result in spiralling costs and ineffective products. The situation is even more precarious for non-medical foot health devices, which often escape rigorous scrutiny altogether as they are not mandated to undergo clinical trials.

The goal of this PhD was to develop an industrial test platform to address these shortcomings by assessing foot health product performance against performance criteria relevant to those used in clinical testing, and to compliment future clinical trials of products. To achieve this a phantom-foot that closely replicates the form, material properties, and functional movement of a human foot was developed and fitted to a KUKA KR160 robotic arm capable of applying physiologically accurate loading conditions. These were coupled with a measurement system to quantify the effects of orthotics and footwear on plantar pressure and internal foot kinematics. The test platform was validated using experimental data from a healthy population walking in a laboratory setting. The validated test platform was then used to investigate the characteristics of two orthotic products available on the market and compared against in-vivo participants.

This project was the first to use a foot model to test foot health products in an industrial context. The key finding with respect to product performance was the reduction in peak and average plantar pressures due to insole products (compared to a shoe-only condition). However, there was no significant difference between the insole products when compared to a neutral control insole. This challenges whether the specific product designs add any performance value beyond a simple standardised insole design. Secondly, there was little to no impact on the joint kinematics with the application of either insole product. Use of the industrial test platform demonstrated how to use product performance criteria that are used to inform product marketing/performance claims and help evolve future foot health product designs, thus improving orthotic function for consumers. Foot joint segment kinematics were different between test platform and simulated foot and in vivo feet and helps prioritise developments for the next phase of the industrial test platform development (phantom-foot and actuation control system).

Chapter 1: Introduction

1.1. Chapter overview:

This chapter introduces the PhD and describes the academic and industrial motivations which drive decision making within this project. The limitations within the current development pathway for orthotic devices, key components of the test platform and use-contexts as established with the industrial partner are described. Finally, the thesis structure and project plan are outlined. The outcome of this chapter is an outline of the PhD and the literature reviews required to inform the design of the test platform.

1.2. Project context

Medical devices for the foot encompass comfort inserts available over the counter such as insoles and protective pads, as well as devices prescribed by professionals, such as orthotics (Collier, 2011). The development of these devices involves: (1) new products being conceived around a well-defined clinical or market need (2) designed according to clinical and biomechanics criteria (3) sample products produced and iteratively tested and validated against well-defined regulatory requirements (4) before moving into production and consumer/patient use. A flowchart describing in general terms a typical development process can be seen in Figure 1. With a large number of product development processes including marketing, design, procurement, logistics, innovation and product delivery professionals, there exists a risk of inefficiencies, delays, failures, and ultimately unnecessary costs.

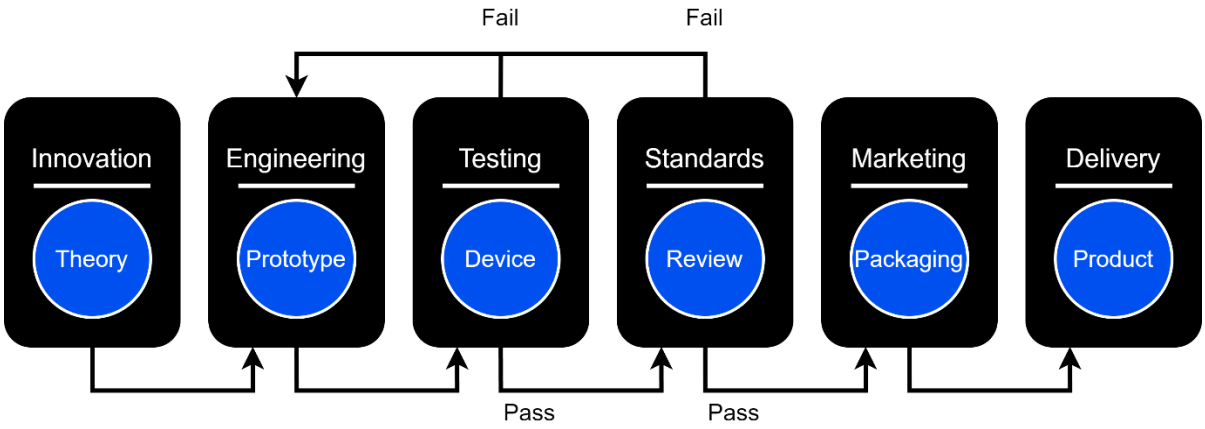

Figure 1: Typical development process for a foot health medical device.

It is important from an industry perspective to de-risk processes where possible, speed up iterative processes and reduce the number of design iterations required before a final product

is achieved. From an academic perspective, there is a significant methodological burden involved with the evaluation of new foot orthotic and related products. Ethical approval is required for clinical and laboratory studies which involve human participants to assess how clinical biomechanical criteria are met by a specific product design e.g., how insole, orthotic and similar protective foot care products change (often reduce) pressure under the foot, typically the heel or forefoot (Understanding health research, 2023). Moreover, these tests can be slow (take many months), costly (>£100k), and difficult to perform (e.g., require specialist skills/laboratories), and consequently impact the innovation process (Emanuel, Lowell, Deborah, Levinson, & Lichter, 2003). Hence, a new approach which could minimise or eliminate the need for laboratory studies involving human participants could open opportunities for research and development both in academia and industry.

The purpose of this PhD is to improve upon the development process and evaluation of new products by providing a means of informing the innovation stage and reducing the burden required to perform product testing. Specifically, how insole, orthotic and similar protective foot care products are designed and how decisions are made based on the outcomes of testing of product prototypes. Also, how product testing results relate to regulatory, performance, and marketing requirements i.e., providing evidence of performance claims.

By way of an example that is linked directly to this PhD project, the industry partner is developing an insole product that aims to reduce pressure and impact forces under the heel as the foot hits the ground during walking or running. The product development process suffered delays due to the product failing during compression mechanical testing. This raised concerns about how design decisions had been made earlier in the design process, what clinical or biomechanical criteria had been used in deciding upon its shape, thickness, volume of liquid in the pad and the nature of the manufacturing processes. Lack of foresight at these earlier stages was now manifesting in unexpected failures in the product performance at a stage in the commercial development that did not allow for thorough redesign and retesting, impacted on manufacturing process/options, and ultimately led to increased risk of taking an inappropriate product to market. A key omission had been the need to understand the magnitude of the 3D forces which are applied to the heel area during walking, which is different than during simple unidirectional compression testing that were industry accepted tests for product development purposes. This posed other issues. Failures in the product performance would make human testing impossible (and so waste money and time), pose a risk to participants (reputational risk and risk of harm being done), and, even if the product

did not fail, it would be uncertain whether changes in foot pressure could be consistently attributed to product design decisions (and thus relate strongly to product marketing claims).

In this example, the preferred process was better quality product testing at an earlier stage, testing that would have informed design decisions rather than just testing already approved designs whose design journey was unclear. Also, adapting product tests according to a specific function/condition (e.g., shock absorption under the heel) at an earlier stage may have made it easier to identify design solutions to the product failure because the link between design and product performance would have been better understood. This new insight could have positively impacted on future iterations of product development too.

One solution to this problem is to develop test protocols/environments that are sufficiently realistic to the context in which the final product will be used such that prototypes/designs are tested under close to market conditions but are simplistic enough to enable testing to be repeatable, trustworthy (e.g., given regulatory requirements), fast and thereby allow for many iterations. Additionally, product performance testing could involve existing lifecycle test processes which simulate wear through cyclic loading, enabling pre- and post-wear performance to be characterised. Currently, in this industry partner but also most others too, all testing of foot care products is done via physical products, whether that be for mechanical characterization, destructive testing, chemical analysis (e.g., for use of products against the skin), or use of human participants. Physical testing is relied upon because often product supplies and samples, including competitor products, are only available in physical form. This prevents, or at least is a barrier to, testing that uses virtual computer models of materials, product samples and the human foot. Virtual models might, in time, be even more efficient than a physical model, but would themselves need to be validated against a physical model before being adopted. This is not trivial because feet come in many sizes, morphologies and are affected over time by aging and disease processes that relate to clinical, biomechanical and market factors (e.g., diabetes, feet in the workplace).

In the context of the above, this industry-linked project aims to develop a physical test platform that can identify the initial and long-term performance of insole, orthotic and related foot protection products (including footwear). Measures of performance would be informed by current industrial practices and literature describing orthotic function experimental protocols. This will enable product claims to be substantiated for products with low-regulatory requirements and inform design decisions for high-regulatory products within industry prior to clinical testing. Additionally, different orthotic design parameters can be

generated and tested iteratively, facilitating research and development within an academic environment. The focus is on the development of a physical test platform that, through iterative testing and variations in foot structures and loading conditions, can speed up, enable more design iterations, and de-risk product development processes. Within the PhD, only off-the-shelf insoles with low regulatory requirements whose performance claims could benefit from testing with the industrial test platform, such as those seen in Figure 2 and Figure 3, will be assessed to present a realistic target within the project timeframe.

Figure 2: Scholl Everyday Knee to Heel Pain Relief Insoles

Figure 3: Scholl Lower Back Pain Relief Insole

The test platform comprises two key parts that form the basis of the PhD and structure of this thesis:

1. A phantom-foot that has form and function (i.e., internal foot kinematics and material properties) close to that of the human feet that will use foot care products.
2. A means of loading the foot similar to in-vivo.

To guide the work of the PhD, two typical use contexts have been agreed with the industry partner:

1. At an early innovation stage, the platform will enable new orthotic product designs to be tested with a standardised methodology, using realistic loading conditions (from heel-strike to mid-stance) to evaluate the initial and long-term performance of the product (with regards to its purpose e.g., to reduce plantar pressure in a given area under the foot). Test cases include the design of prototypes of varied material type (e.g., foams, liquid); density; thickness; components (e.g., multi-material) and variations in the position or size of components.
2. To assess the effects of orthotic materials and/or product geometry on internal foot kinematics by measuring the motion of ‘key’ joints, defined in accordance with each

products' claims (e.g., arch supporting, pronation reducing). As the loading conditions will be constrained from heel-strike to mid-stance within this PhD, the joints of interest are limited to the rear and midfoot.

1.1. PhD plan and thesis structure

The concept of the test platform is that it will have three components:

1. Phantom-foot
2. Actuator system to load the phantom-foot.
3. Measurement system to quantify the effect of products on the foot.

The PhD project plan seeks to develop these three parts in an integrated way and then validate their performance in the context of industrial use.

Four phases of work are proposed:

1. Gather background information by mapping industry and academia requirements and reviews of the literature to inform design specification for (1) the phantom-foot (2) the actuator system and (3) measurement system. This includes a review of the functions of foot orthotics and current evaluation methods employed within clinical studies, anatomical material properties, methods of modelling foot kinematics and actuation systems used to drive cadaveric foot specimens or prosthetic feet. Consequently, this will inform the design specification such that current industrial and academic orthotic practices can be built upon.
2. Establish an integrated design specification which can enable improved and more specific evaluation of orthotic performance for low regulatory products and pre-clinical evaluation of high regulatory products to address the limitations within the current development pathway. Additionally, it will facilitate iterative prototyping to determine the effectiveness of orthotic design features and the representation of samples of different foot size, mass, and pathology.
3. Develop and validate a mechanism to achieve 3 goals: (1) apply physiologically accurate loading conditions from heel-strike to mid-stance. (2) Apply these loading conditions to the phantom-foot which accurately mimics the form, rear and midfoot kinematics, and material properties of a real foot. (3) Capture the effects of orthotic and

footwear products (i.e., changes to plantar pressure and/or internal foot kinematics) as they relate to clinical biomechanical criteria by the measurement system such that product claims can be established.

4. Perform experimental research on orthotic or footwear product prototypes to characterise their effects on the foot, comparing the performance of the industrial test platform to in-vivo gait.

These four phases are outlined in Figure 4 and chapters 2-5 accordingly.

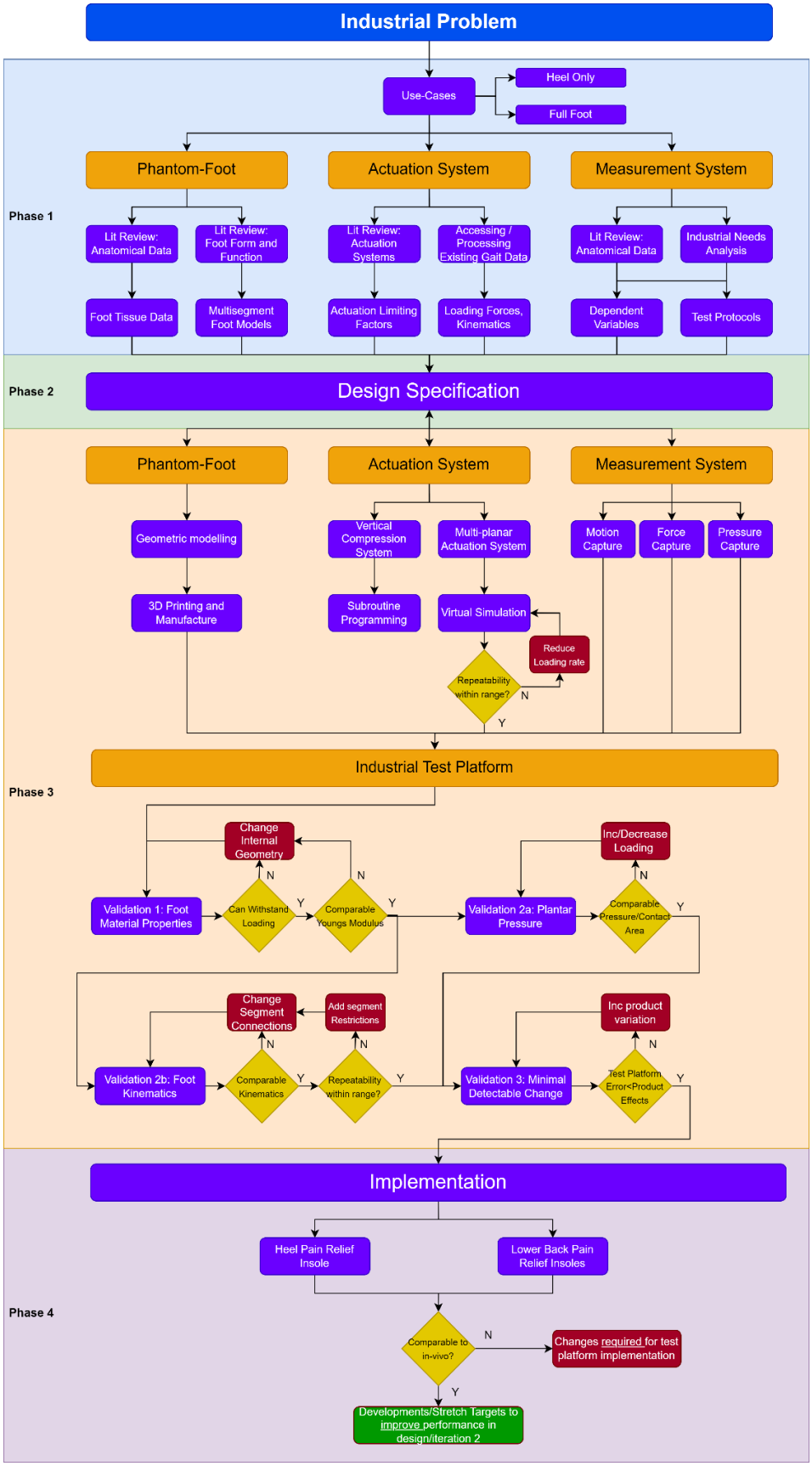

Figure 4: Project Plan

Chapter 2: Literature reviews and industrial needs analysis

2.1. Chapter overview

This chapter aims to gather background information to inform the design specification for the three critical parts of the platform: (1) the phantom-foot, (2) actuator system and (3) measurement systems. Additionally, to ensure that the industrial and academic requirements are clearly defined such that they can be used to inform the design specification. The outcomes of chapter 1 are the requirements that the design specification must meet in chapter 2.

Four literature reviews were completed.

- The first aimed to establish the function of orthotics and how they are evaluated at present within clinical studies. This informed the product performance criteria required to be captured by the test platform to align with clinical studies, such that academic applications (where clinical study methodologies are required to be recreated as closely as possible) and industrial applications (where high resolution is required to evaluate concept designs) could both be executed.
- The second aimed to identify the properties of foot structures and provide material data necessary to design a phantom-foot for the test platform.
- The third aimed to review the form and function of the human foot based on previous attempts to model internal joint kinematics during walking, so that similar models could be considered for the phantom-foot.
- The fourth and final literature review aimed to identify and critique previous actuator systems developed to apply physiological loading to in-vivo, in-vitro and prosthetic feet and thus simulate the conditions of gait.

2.1.1. Literature search strategies

The process for conducting these literature reviews involved searching through IEE Xplore, MEDLINE (Ovid), ProQuest Central and ScienceDirect databases. After completing literature searches and processing the records to remove duplicates and articles falling outside the inclusion criteria, Excalibur, a pdf extraction system was used to obtain the data from each paper (Excalibur: PDF Table Extraction for Humans, 2024).

2.1.1.1. Literature review: orthotic function

The inclusion and exclusion criteria for the orthotic function literature review are detailed below. Table 1 describes the search strategy employed, and Figure 5 details the screening of articles to determine those to be included in the review.

Inclusion criteria:

1. Foot orthotics
2. Healthy and pathological populations
3. Minimum outcomes (changes in biomechanics and foot function)

Exclusion criteria:

1. Orthotics which don't solely interact with the foot e.g. ankle-foot orthotics
2. No data.
3. Qualitative data (commentary on pain and preference)

Table 1: Orthotic function literature review search strategy mapped against the SPIDER tool. TI:title, MP:key term, AB:abstract.

Name	**Description**
Sample	TI Foot OR TI Ankle OR TI Forefoot OR TI Midfoot OR TI Hindfoot OR TI Joint
Phenomenon of Interest	*Undefined*
Design	MP Observational Study OR AB Observational Study OR MP Pilot Study OR AB Pilot Study OR MP Technical Note OR AB Technical Note OR MP Model* OR AB Model*
Evaluation	MP loading OR MP contact area OR MP pressure OR MP kinematics OR MP biomechanics OR MP balance OR MP sway OR TI Performance OR MP Performance OR AB Performance
Research Type	MP Experimental OR AB Experimental OR MP Developmental OR AB Developmental

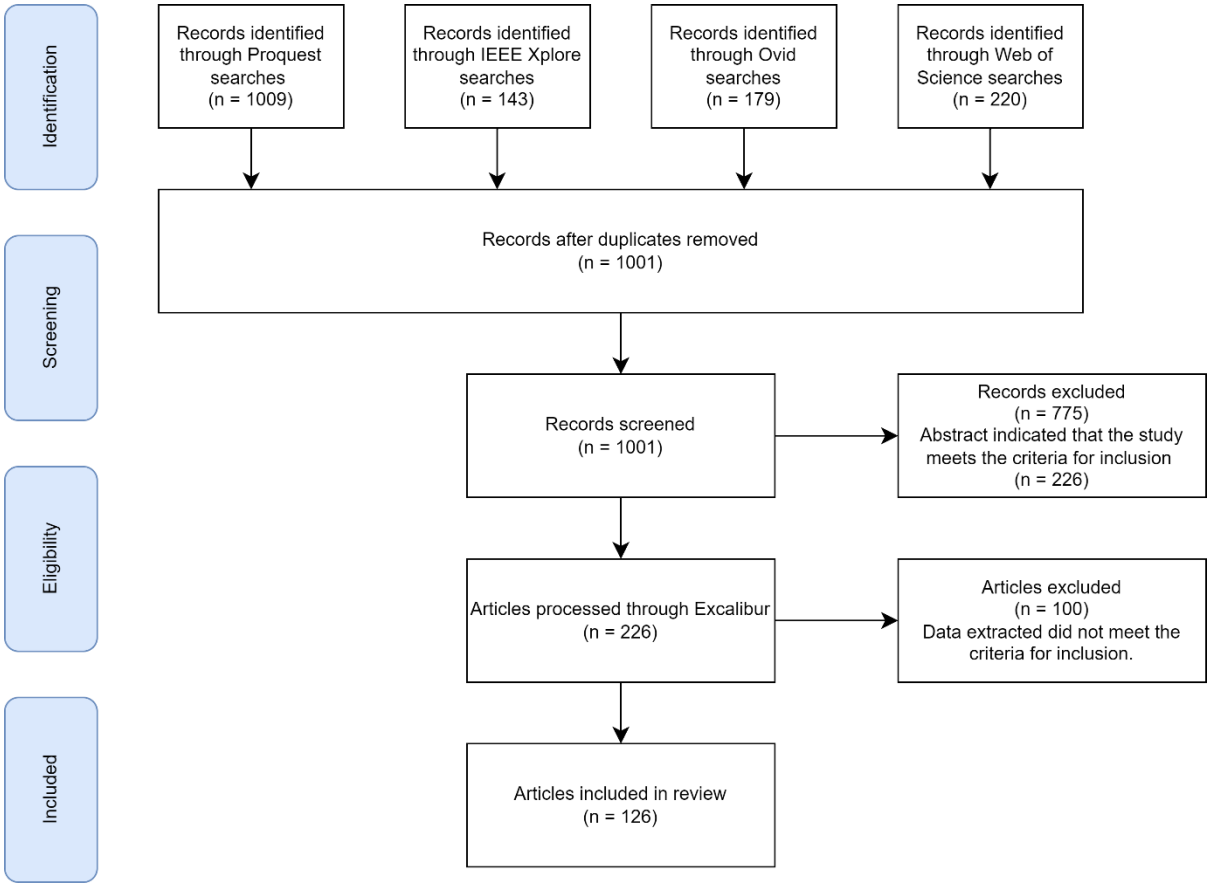

Figure 5: Orthotic function literature search strategy:

2.1.1.2. Literature review: foot anatomy and properties

The inclusion and exclusion criteria for the foot anatomy and material and mechanical properties literature review are detailed below. Table 2 describes the search strategy employed, and Figure 6 details the screening of articles to determine those to be included in the review.

Inclusion criteria:

1. Physical model of the foot and ankle.
2. Represents a healthy population.
3. Minimum outcomes: appropriate variables recorded (repeatability, accuracy, segment number, structures represented).

Exclusion criteria

1. Virtual models.
2. No data.
3. Simulates a population or sub-population with known pathology.

Table 2: Foot anatomy and properties literature review search strategy mapped against the SPIDER tool. TI:title, MP:key term, AB:abstract.

Name	**Description**
Sample	TI Foot OR TI Ankle OR TI Forefoot OR TI Midfoot OR TI Hindfoot OR TI Muscle OR TI Bone OR TI Ligament OR TI Joint OR TI Tissue OR TI Skin OR TI Fat OR TI Cadaver*
Phenomenon of Interest	MP strain OR MP stress OR MP force OR MP density OR MP thickness OR area
Design	MP Observational Study OR AB Observational Study OR MP Pilot Study OR AB Pilot Study OR MP Technical Note OR AB Technical Note OR MP Model* OR AB Model*
Evaluation	TI Mechanics OR MP Mechanics OR AB Mechanics OR TI Performance OR MP Performance OR AB Performance OR TI Characteristic* OR MP Characteristic OR AB Characteristic OR TI Propert* OR MP Propert*OR AB Propert*
Research Type	MP Experimental OR AB Experimental OR MP Developmental OR AB Developmental

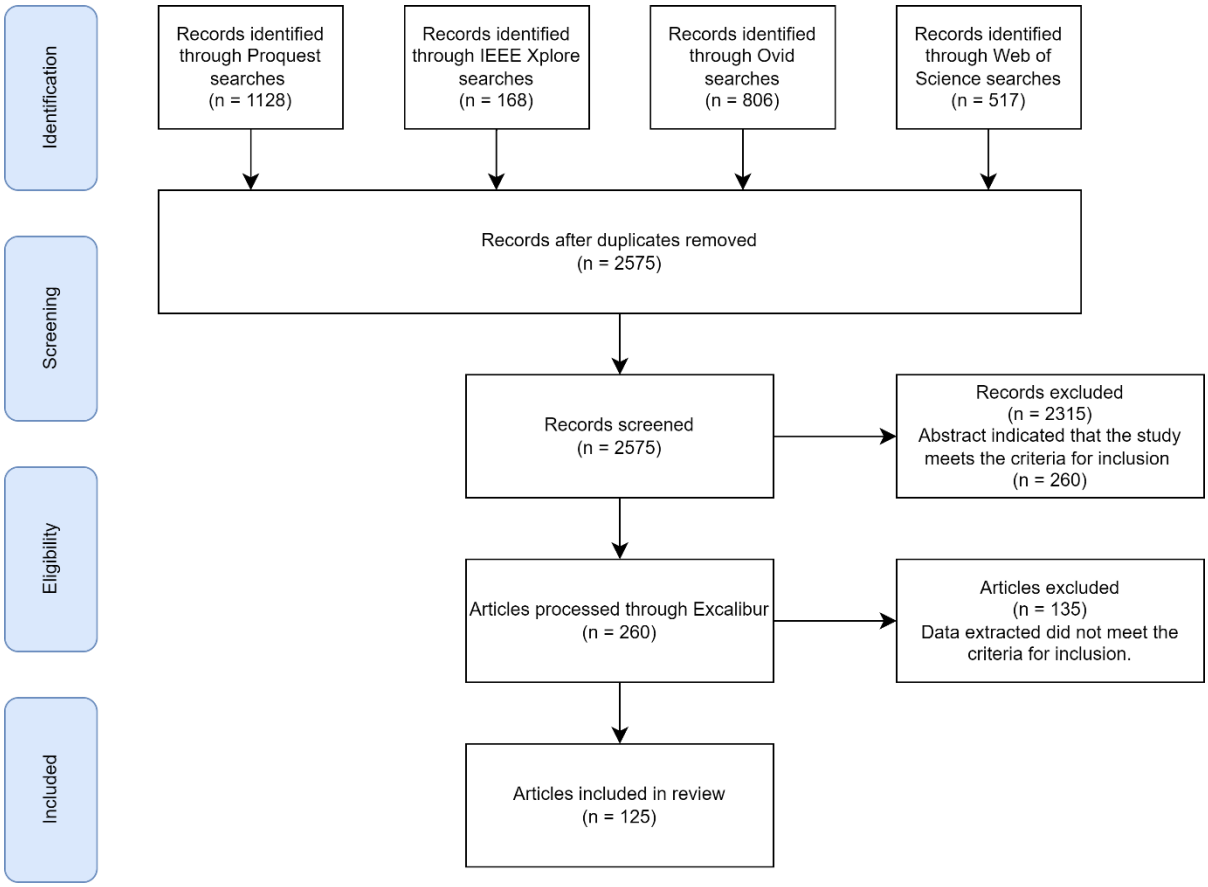

Figure 6: Foot anatomy and properties literature search strategy

2.1.1.3. Literature review: phantom-foot form and function

The inclusion and exclusion criteria for the phantom-foot form and function literature review are detailed below. Table 3 describes the search strategy employed, and Figure 7 details the screening of articles to determine those to be included in the review.

Inclusion criteria:

1. Physical model of the foot and ankle.
2. Represents a healthy population.
3. Minimum outcomes: appropriate variables recorded (repeatability, accuracy, segment number, structures represented).

Exclusion criteria:

1. Virtual models.
2. No data.
3. Simulates a population or sub-population with known pathology.

Table 3: Phantom-foot form and function literature review search strategy mapped against the SPIDER tool. TI:title, MP:key term, AB:abstract.

Name	Description
Sample	TI Foot OR TI Ankle OR TI Simulator OR TI Midfoot OR TI Hindfoot OR TI Muscle OR TI Bone OR TI Ligament OR TI Joint OR TI Tissue OR TI Skin OR TI Fat OR TI Cadaver* OR TI Calcaneus OR TI Talus OR TI Navicular OR TI Cuboid OR TI Cuneiform OR TI Metatarsal OR TI Phalan* OR TI Plantar
Phenomenon of Interest	MP Segment
Design	MP Observational Study OR AB Observational Study OR MP Pilot Study OR AB Pilot Study OR MP Technical Note OR AB Technical Note OR MP Model* OR AB Model*
Evaluation	TI Mechanics OR MP Mechanics OR AB Mechanics OR TI Performance OR MP Performance OR AB Performance OR TI Characteristic* OR MP Characteristic OR AB Characteristic OR TI Propert* OR MP Propert*OR AB Propert*
Research Type	MP Experimental OR AB Experimental OR MP Developmental OR AB Developmental

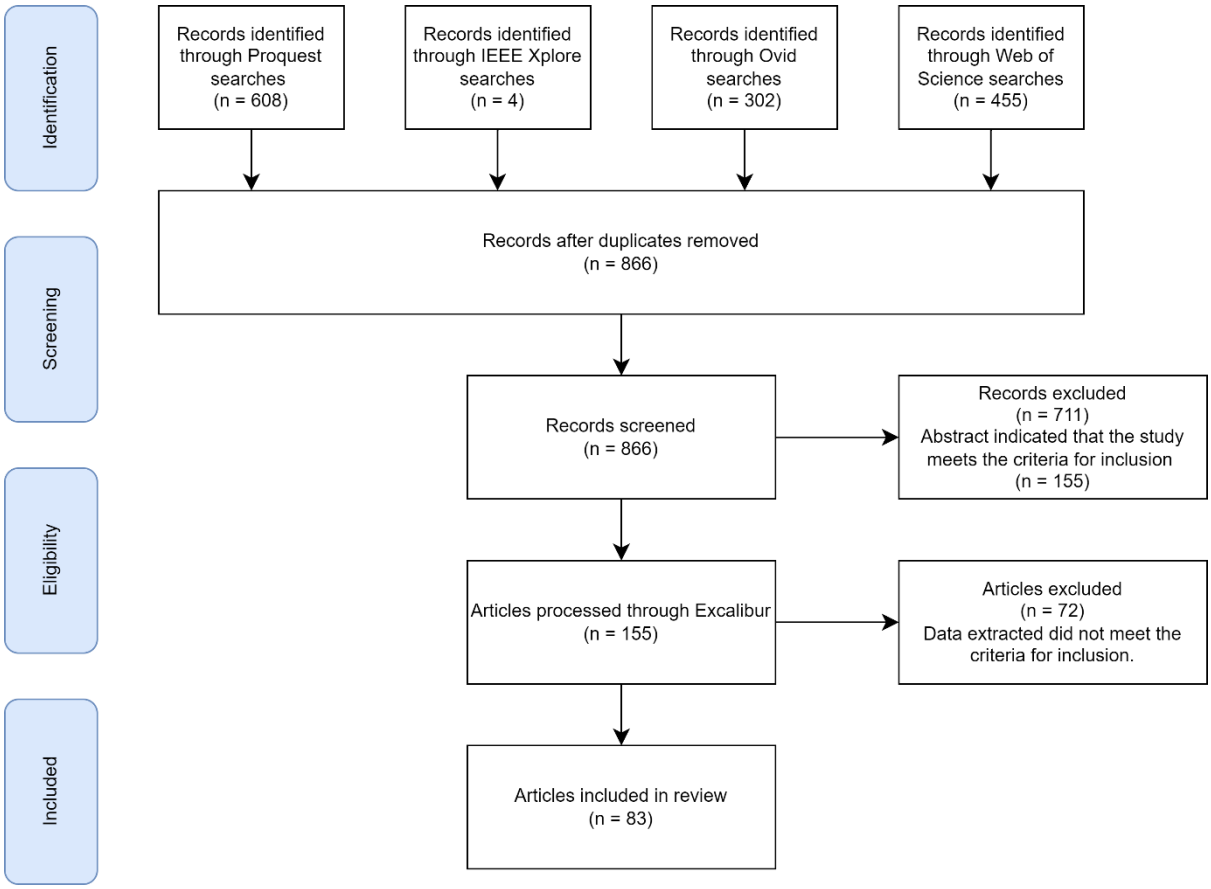

Figure 7: Phantom-foot form and function literature search strategy

2.1.1.4. Literature review: human ankle-foot actuation systems

The inclusion and exclusion criteria for the human ankle-foot actuation systems literature review are detailed below. Table 4 describes the search strategy employed, and Figure 8 details the screening of articles to determine those to be included in the review.

Inclusion criteria:

1. Lower limb actuator.
2. Represents a healthy human population.
3. Minimum outcomes: appropriate variables recorded (repeatability, accuracy, degrees of freedom, joints represented)
4. Observational studies, pilot studies, technical notes (or systematic review or meta-analysis of these study types)
5. Prosthetic test systems

Exclusion criteria:

1. Virtual model or FE analysis
2. Non-human model i.e. animal model
3. No data
4. Simulates a population or sub-population with known pathology

Table 4:Ankle-foot actuation system literature review search strategy mapped against the SPIDER tool. TI:title, MP:key term, AB:abstract.

Name	**Description**
Sample	MP (Foot OR Ankle) AND Simulat*
Phenomenon of Interest	*Undefined*
Design	MP Observational Study OR AB Observational Study OR MP Pilot Study OR AB Pilot Study OR MP Technical Note OR AB Technical Note OR MP Model* OR AB Model*
Evaluation	*Undefined*
Research Type	MP Experimental OR AB Experimental OR MP Developmental OR AB Developmental

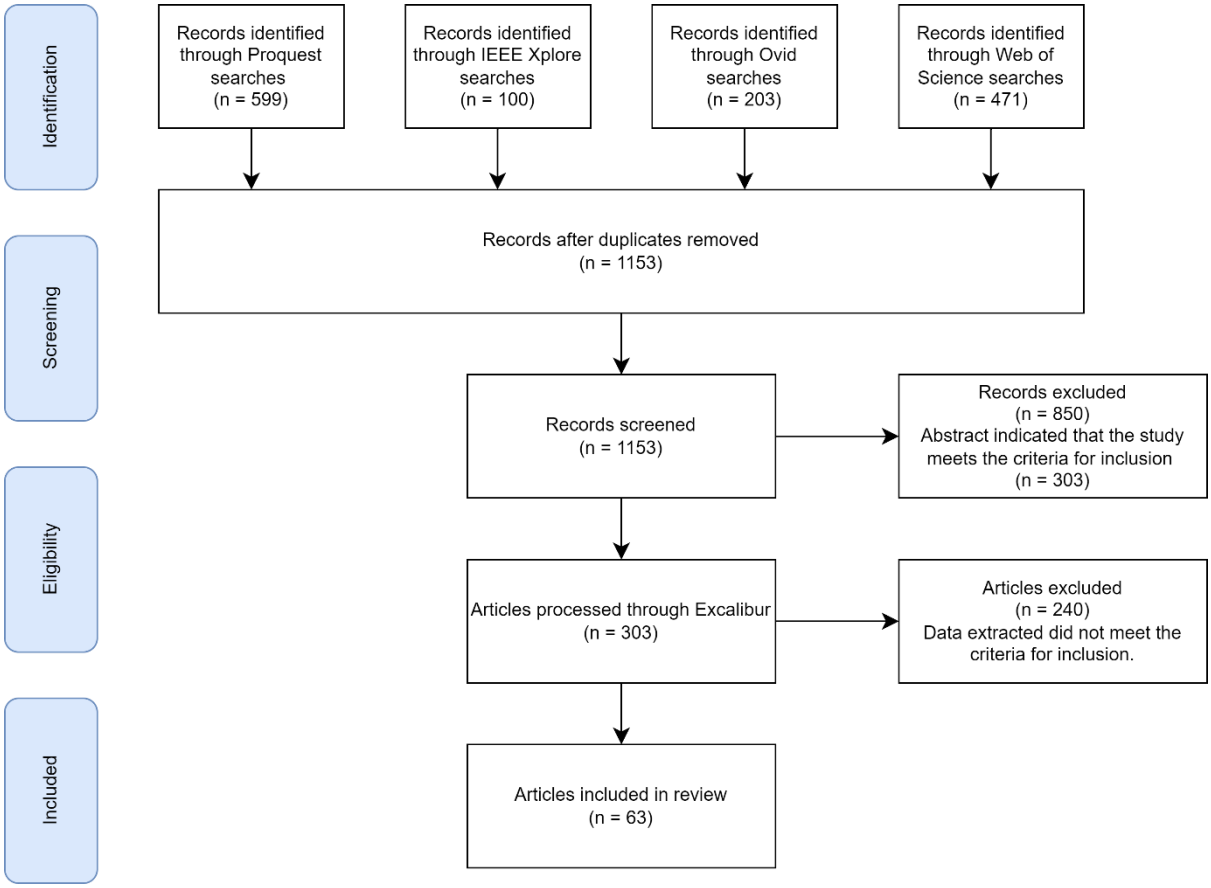

Figure 8: Human ankle-foot actuation systems literature search strategy

2.2. Literature review: orthotic function

Foot orthotics (FOs) can be broadly classified as two groups: 1) prefabricated off-the-shelf orthoses and 2) custom-made orthoses manufactured using a plaster cast or three-dimensional laser scan of the foot (Tran & Spry, 2019; Landorf, 2001). Prefabricated FOs are mass-produced, generic devices available over the counter intended for use by patients with no pathology, to provide pain relief through cushioning, shock attenuation and pressure redistribution among other functions (Redmond, Landorf, & Keenan, 2009). Their advantages include lower costs and immediate availability. Custom-made orthotics can be subdivided into three categories: soft (accommodative), rigid and semi-rigid (Elatter, Smith, Ferguson, Farber, & Wapner, 2018). Soft FOs provide cushioning and protection to provide shock absorption and a reduction of shear forces, at the expense of reduced durability (Janisse & Janisse, 2008). Conversely, rigid FOs offer minimal cushioning, shock absorption and protection, however, are used to control the motion of the foot, provide arch support, and redistribute loading forces (Rome & Brown, 2004). They are significantly more durable than soft FOs. Finally, semirigid FOs, the most commonly used orthoses, combine the advantages of soft and rigid FOs by utilizing a rigid core and soft, upper layer for cushioning (Springett, Otter, & Barry, 2007). The FO prescribed depends on the pathology and treatment required. Examples of off-the-shelf and custom-made orthoses can be found in Figure 9.

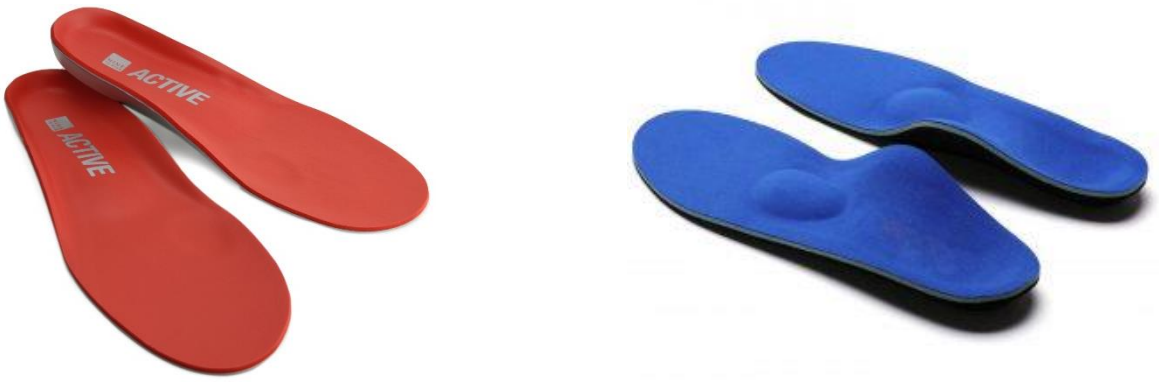

Figure 9: Off-the-shelf orthotic (left) (Healthy Step, 2024) and custom-made orthoses (right) (Podiatry Station, 2024).

Rigid and semi-rigid FOs designed for musculoskeletal interventions in conditions such as rheumatoid arthritis restore normal foot function by achieving a near-neutral subtalar joint alignment, where the foot adapts to the FO by re-orienting its motion (Elatter, Smith, Ferguson, Farber, & Wapner, 2018; Kogler, 1996). This leads to musculoskeletal compensations in the hip and knee; hence these types of FO can impact the entire kinetic chain from hip to foot (Hajizadeh, Desmyttere, Carmona, Bleau, & Begon, 2020). The

success of these FOs in restoring typical function is variable and largely dependent on the degree of pathology. Soft FOs provide cushioning to distribute pressure or reduce impact forces during gait via arch support, medial/lateral wedges, and heel cups (Fong, Lue, Chung, & Chu, 2020). They have been found to reduce the forefoot plantar pressure-time integral more immediately than semi-rigid FOs (Tenten-Diepenmaat, 2019). The management of foot pain may involve various treatment modalities, with a special emphasis on non-surgical treatment of which orthotics are one of the highest priorities (Tahririan, 2012).

Various improvements on pain management and foot function via the application of FOs during weight bearing activities have been claimed. The management of plantar heel pain may involve various treatment modalities, with a special emphasis on non-surgical treatment of which orthotics are one of the highest priorities (Tahririan, 2012). However, conclusions vary between studies, and within different populations experiencing foot pathology e.g., rheumatoid arthritis (RA) groups have shown much better pain relief than osteoarthritis (OA) groups (Paterson, et al., 2022; Zafar, Zamani, & Akrami, 2020; Menz H. , 2015). Moreover, there is debate as to the effectiveness of off-the-shelf vs custom FOs: Evans noted minimal delineation in functional and pain reduction between both cases in paediatric populations with flat feet (Evans AM, 2022) and Rome found no significant health quality gain using custom orthoses with RA groups (Rome K, 2017). The application of a FO may also result in unwanted consequences For example, FOs have been demonstrated to redistribute plantar loads, with the contoured geometry resulting in a reduced peak and average plantar load under the region targeted by the device e.g., under the heel (Balsdon, 2022) or forefoot (Chapman, 2016). This intervention is intended to provide pain relief in these target areas for groups experiencing foot pathology e.g., plantar heel pain or osteoarthritis. However, a consequence of this redistribution often leads to greater midfoot contact area (Gibson, Woodburn, Porter, & Telfer, 2014) or vice versa (i.e, offloading is achieved by increasing contact area in a plantar region).

To design a test platform capable of characterising the performance of these orthotic devices, a review was conducted to determine the measurement systems and assessment protocols utilised to capture primary outcomes of interest and evaluate the performance of FOs. This included plantar pressure redistribution and joint kinematic changes. Alongside an industrial needs analysis and academia needs analysis, this informed the product performance criteria to be evaluated using the test platform. The review focused on devices situated under the foot only to align with the use-contexts established in the previous chapter.

2.2.1. FO effects on loading pattern:

Plantar pressure measurements are the primary method of determining changes made to foot function by FOs, either using an in-shoe system or pressure plate. Contact area, average and peak pressures across different regions of the plantar surface e.g., hindfoot, midfoot, forefoot, and changes to centre of pressure have typically been utilised in the literature (see Table 5). The centre of pressure measurements obtained from in-shoe plantar pressure systems and pressure plates have been shown to be precise, and the measurements produced by these two methods are comparable. (Debbi, 2012). Nevertheless, in-shoe systems are largely preferred within FO studies as the interaction between the plantar surface and product is of primary interest, as opposed to the interaction between the FO and the ground. Studies involving these systems have used sports shoes (Balsdon, 2022; Gibson, Woodburn, Porter, & Telfer, 2014) and shoes with extra depth/width (Chang, Wang, Huang, Lin, & Lee, 2012; Tenten-Diepenmaat, 2019) to accommodate the orthotic intervention underneath the pressure sensor and foot, although details of footwear have not been provided in all cases. Footwear has been shown to decrease maximum tibial rotation, internal tibial rotation, and acceleration (Cornwall & McPoil, 1995; Morio, Lake, Guéguen, Rao, & Baly, 2009) and hence uniformity of footwear between participants across a study requires control to ensure changes in foot function can be solely attributed to FOs.

2.2.1.1. Orthotic function experimental protocol

There were several common features in the assessment protocols of the studies cited in Table 5. Firstly, participants were made to walk either on a treadmill or along a gait lab walkway during assessments with plantar pressure measurement systems; the differences between walking overground vs on a treadmill are typically not clinically relevant (Papegaaij & Steenbrink, 2017). Healthy participant groups were typically elected when evaluating the effects of orthotic designs such as heel plugs or heel lifts (Balsdon, 2022; Zhang, Li, Kaiyun, Qiufeng, & Vanwanseele, 2016), lateral wedges (Tse, Ryan, Dien, Scott, & Hunt, 2021) and medial arch supports (Fong, Lue, Chung, & Chu, 2020). However, some groups experiencing foot pathology have also involved evaluation of metatarsal bars, domes and arch support (Hodge, Bach, & Carter, 1999; Jackson, Binning, & Potter, 2004; Partovifar, Safaeepour, & Cham, 2021; Yu-Ping, Hsien-Te, Wang, Zong-Rong, & Chen-Yi, 2020; Farzadi, Safaeepoor, Mousavi, & Saeedi, 2014).

In assessments involving populations experiencing foot pathology, assessment via plantar pressure measurement system frequently followed an acclimatisation period with a product between 1-12 weeks (Chang, Wang, Huang, Lin, & Lee, 2012; Gibson, Woodburn, Porter, & Telfer, 2014; Chapman, 2016; Halstead, et al., 2016). During this assessment, each participant was asked to walk at a comfortable walking pace for a set duration (if on a treadmill), or until they completed a defined number of passes back and forth along a gait lab walkway. This was repeated for each study condition, including a control condition which usually involved walking without any insole.

Table 5: Studies investigating orthotic effects on plantar pressure in different populations. ISPP = In-shoe plantar pressure, OA = Osteoarthritis, RA = Rheumatoid arthritis

			Types of Orthoses Investigated				
Reference	**Participants**	**Intervention Type**	**Off-the-shelf/Prefabricated**	**Soft**	**Semi-rigid**	**Rigid**	**Foot Function (Plantar Pressure Only)**
(Balsdon, 2022)	**Number:** n=14 **Diagnoses:** none **Age (years):** 35.4 ± 7.7	Accommodative			x		ISPP (Average pressure, peak pressure, and pressure contact area)
(Chang, Wang, Huang, Lin, & Lee, 2012)	**Number:** n=19 **Diagnoses:** RA diagnosis **Age (years):** 58.6 ± 10.1	Accommodative		x	x		ISPP (peak pressure, pressure-time integral, mean force contact area)
(Gibson, Woodburn, Porter, & Telfer, 2014)	**Number:** n=16 **Diagnoses:** RA diagnosis (for minimum 2 years) **Age (years):** 50.7 ± 8.4	Motion Control			x	x	ISPP (forefoot peak pressure, midfoot contact area pressure-time integral, mean force contact area)
(Hodge, Bach, & Carter, 1999)	**Number:** n=11 **Diagnoses:** RA diagnosis **Age (years):** 65 (49-82)	Accommodative		x	x		ISPP (peak pressure, pressure-time integral, average pressure, time in mask)
(Jackson, Binning, & Potter, 2004)	**Number:** n=10 **Diagnoses:** RA diagnosis **Age (years):** 61 (32-79)	Accommodative	x	x			ISPP (peak pressure, pressure-time integral, stance time, contact area)
(Jin, 2019)	**Number:** n=30 **Diagnoses:** none **Age (years):** 20.52 ± 2.5	Accommodative				x	Pressure plate (COP position changes, COP moving speed, peak pressure, and peak contact area).
(Telfer, Woodburn, Collier, & Cavanagh, 2017)	**Number:** n=20 **Diagnoses:** Type 2 Diabetes **Age (years):** 64.4 ± 9.2	Accommodative			x		ISPP (peak pressure)
(Chapman, 2016)	**Number:** n=33 **Diagnoses:** Midfoot OA **Age (years):** >18	Accommodative	x		x		ISPP (Maximum force, peak pressure, contact area and contact time)
(Halstead, et al., 2016)	**Number:** n=33 **Diagnoses:** Diagnosed OA **Age (years):** 58.4 ± 11.6	Accommodative and Motion Control	x		x		ISPP (Maximum force, peak pressure, contact area and contact time)

(Jimenez-Perez, Gil-Calvo, Aparicio, Cibrian Ortiz de Anda, & Perez-Soriano, 2021)	**Number:** n=30 **Diagnoses:** none **Age (years):** 32 ± 7	Accommodative			x		ISPP (Mean Peak Pressure, pressure-time integral, relative pressure, stance time)
(Tse, Ryan, Dien, Scott, & Hunt, 2021)	**Number:** n=40 **Diagnoses:** none **Age (years):** 26.6 ± 2.9	Accommodative				x	ISPP (Peak pressure, pressure-time integral, time of peak pressure, contact area)
(Partovifar, Safaeepour, & Cham, 2021)	**Number:** n=15 **Diagnoses:** RA diagnosis **Age (years):** 50 ± 1.2	Accommodative	x			x	ISPP (Mean Peak pressure, maximum force, contact area)
(Fong, Lue, Chung, & Chu, 2020)	**Number:** n=12 **Diagnoses:** none **Age (years):** 38.5 ± 8.0	Accommodative				x	ISPP (Peak pressure, pressure-time integral, peak force, force-time integral)
(Yu-Ping, Hsien-Te, Wang, Zong-Rong, & Chen-Yi, 2020)	**Number:** n=15 **Diagnoses:** Flatfoot diagnosis **Age (years):** 19.7 ± 4.3	Accommodative				x	ISPP (Peak pressure, stance time, cadence, step frequency)
(Zhang, Li, Kaiyun, Qiufeng, & Vanwanseele, 2016)	**Number:** n=20 **Diagnoses:** none **Age (years):** 22.4 ± 0.9	Accommodative			x		ISPP (Peak pressure, contact area, force-time integral)
(Song, et al., 2015)	**Number:** n=20 **Diagnoses:** none **Age (years):** 21.19 ± 3.66	Accommodative	x			x	ISPP (Peak pressure, pressure-time integral, GRF).
(Farzadi, Safaeepoor, Mousavi, & Saeedi, 2014)	**Number:** n=16 **Diagnoses:** Hallux valgus **Age (years):** 21.19 ± 3.66	Accommodative	x			x	ISPP (Peak pressure, maximum force, contact area).

2.2.1.2. Product performance criteria

The most used plantar pressure variables used to describe foot function included the mean peak pressure, pressure-time integral, force-time integral, plantar contact area, contact time and centre of pressure. The mean peak pressure is defined as follows:

$$\overline{PP} = \frac{\sum PP_{peak}}{n_{steps}}$$

Equation 1: Where $\overline{PP}$ is the mean peak plantar pressure, PP_{peak} is the peak plantar pressure during each stance phase and n_{steps} is the number of steps recorded.

There are two reported calculations of the pressure-time integral in the literature which can be distinguished as 1) the plantar pressure-time integral (PPTI) and 2) the peak plantar pressure-time integral ($PPTI_N$), where the latter is the calculation method employed within a common in-shoe plantar pressure measurement system (Novel GmbH Inc., Munich, Germany). These are defined as follows:

$$PPTI = \int PP \text{ x } \Delta t$$

Equation 2: Where PPTI is the plantar pressure-time integral, PP is the average plantar pressure per time sample across a given region and Δt is the duration of that time sample.

$$PPTI_N = \sum PP_i \text{ x } \Delta t$$

Equation 3: Where $PPTI_N$ is the peak pressure-time integral, PP_i is the peak pressure in the i-th sample and Δt is the duration of that time sample.

As a result, the $PPTI_N$ is not a true integration of pressure over time for a plantar area as it ignores sub maximal pressures, as described by Melai et al (Melai, et al., 2011). For comparing the operation of orthotics on foot function in this project (i.e., a reduction in pressure-time integral in a plantar region) there is no significant impact in utilising either of these measures as only the peak pressure is required. However, this is not appropriate for academic applications of the test platform where the summative loading of a particular plantar area is of interest.

The force-time integral is defined as follows:

$$FTI = \int F \text{ x } \Delta t$$

Equation 4: Where FTI is the force-time integral, F is the force per time sample and Δt is the duration of that time sample.

Force is typically estimated by in-shoe pressure measurement systems using piezo resistive force sensors, whose electrical resistance decreases as mass is applied, and can be calibrated to provide highly accurate force measurements. Within force plates, forces are measured using force transducers such as strain gauges, which produce an electrical current proportional to the load applied to the transducer (Beckham, Suchomel, & Mizuguchi, 2014).

The remaining variables i.e., contact area, peak pressure, and contact time can be derived from the pressure sensor software. Contact area is the sum of active sensors multiplied by the area of each sensor; this is dependent on the pressure system hardware i.e., the number of sensors within a pressure measurement system. Peak pressure is the maximum sensor value for a given timepoint and the maximum peak pressure is the highest value across stance. Finally, contact time is the number of samples recorded where the contact threshold (typically 5kPa) is exceeded and represents time between heel contact and toe off multiplied by the sampling rate.

2.2.2. FO effects on gait

FOs have been found to change lower limb kinematics and kinetics during gait events e.g., in participants with RA, OA or exhibiting patellofemoral pain, ankle dorsiflexion and eversion moments have been demonstrated to decrease via rigid FOs designed the longitudinal arch (Simonsen MB, 2022; Whittaker, 2020; Hart HF, 2020) (see Table 6). Rigid and semi-rigid FOs are typically employed to alter foot kinematics during gait. The effects of several FO designs were evaluated by a recent systematic review and meta-analysis (Hajizadeh, Desmyttere, Carmona, Bleau, & Begon, 2020) including medial/lateral posting and arch and heel support. Firstly, medial posting decreased ankle eversion and increased knee adduction moments and these effects have been referred to a less everted position of foot (bringing the foot towards neutral) and the medial shift of centre of pressure (CoP) imposed by the FO design investigated (Fukuchi, Lewinson, Worobets, & Stefanyshyn, 2016). Next, lateral posting reduced knee adduction moment, medial knee contact force and loading. It is used to help bring the heel of the foot into valgus and prevent inversion, thus enhancing ground reaction force to increase subtalar joint supination resistance and lateral ankle instability (Palomo-Fernández, et al., 2023). However, findings were limited and inconclusive for arch and heel support. This could be attributed to differences in biomechanical test methods: variation in foot model (lower vs higher resolution) and the characteristics of the FO

investigated (contoured vs flat). Therefore, the need for a more standardized biomechanical test method is apparent.

2.2.2.1. Orthotic function experimental protocol

Various methods have been used to measure kinematic changes made to the foot and establish changes in foot function. Manual measurement of joint positions such as the knee and ankle joints when weightbearing has been carried out in the literature (Whittaker, 2020). However, gait analysis more commonly employs the use of 3D motion capture systems which are often paired with force plates embedded into the floor of a gait laboratory to capture ground reaction forces (GRF) as a person ambulates over them. In the studies listed within Table 6, healthy or individuals experiencing foot pathology were fitted with retro-reflective markers to capture the kinematics of the hip, knee, ankle and foot as they walked. Markers are applied in accordance with multi-segment foot model protocols to separate the foot into segments whose relative motion can then be analysed to determine changes made by FOs (these models are discussed in greater detail in literature review three). Participants were asked to walk in two conditions: a control condition, where no FO was applied, and an intervention, where an FO was applied.

Biomechanics analysis tools such as Visual3D (C-Motion Inc, Washington DC, USA) could then be used to perform analysis to determine the effectiveness of an FO using the following steps. 1) Building a biomechanical model which would be informed by the number and type of segments (inertial properties), joint properties (number of degrees of freedom) and kinds of actuators that move the segments. 2) Calculating the kinematics of the model by determining the transformation from recorded tracking markers to the pose of each segment of the biomechanical model. 3) Finally, applying inverse dynamics to the kinematics of the biomechanical model and to the location, magnitude, and direction of externally applied forces e.g., ground reaction forces from the force plate, which results in calculated joint moments. Although the process to build biomechanical models within analysis tools involves many nuances, joint angle and joint moment calculations can be made easily within the software.

There are some noted limitations with motion capture systems, specifically around the implementation of the body worn retro-reflective markers. The placement of these markers can have great implications on the kinematics measured, although some markers have a greater impact than others (Fonseca, et al., 2022; Schallig, van den Noort, Maas, Harlaar, &

van der Krogt, 2021). For example, Fonseca et al found highest marker sensitivity values for markers that solely define the direction of an axis of a segment coordinate system (e.g. as the origin), like the marker at the posterior aspect of the calcaneus in the Oxford foot multisegment model (multisegment models are discussed in greater detail in the next section). Additionally, the stability of these markers during dynamic tasks can be reduced e.g., due to soft tissue artifacts, where the motion of markers is affected by the motion or elasticity of skin and underlying anatomical components. Finally, low sampling frequencies have been shown to affect peak kinematic and kinetic data capture, and influence sample entropy (Lee & Kim, 2012; Raffalt, McCamley, Denton, & Yentes, 2019). Force plates, plantar pressure capture and motion capture systems implemented in the studies identified within this review operated at around 100-120Hz. Heinemann et al found the natural frequency of walking to be less than 2.0Hz (Heinemann & Kasperski, 2017). Following the Nyquist theorum which states that a sinuisoidal function in time or distance can be regenerated with no loss of information as long as it is sampled at a frequency greater than or equal to twice per cycle, a capture rate of at least 100Hz is more than sufficient to capture gait data sufficiently (Colarusso, Kidder, Levin, & Lewis, 1999).

Table 6: Studies examining orthotic effects on joint kinematics in different populations. OA = Osteoarthritis, RA = Rheumatoid arthritis

			Types of Orthoses Investigated				
Reference	**Participants**	**Intervention Type**	**Off-the-shelf**	**Soft**	**Semi-rigid**	**Rigid**	**Foot Function (Kinematics only)**
(Simonsen MB, 2022)	**Number:** n=25 **Diagnoses:** RA and foot pain **Age (years):** 56.2 ± 10	Motion Control				x	Gait characteristics (Ankle plantar flexion and eversion moments)
(Whittaker, 2020)	**Number:** n=52 **Diagnoses:** Plantar heel pain **Age (years):** 42.9 ± 10.9	Motion Control	x		x		Gait characteristics (Ankle range of motion)
(Hart HF, 2020)	**Number:** n=42 **Diagnoses:** Patellofemoral pain **Age (years):** 35.9 ± 6.8	Motion Control	x			x	Gait characteristics (Ankle inversion/eversion, ankle dorsiflexion/plantarflexion)
(Gibson, Woodburn, Porter, & Telfer, 2014)	**Number:** n=16 **Diagnoses:** RA diagnosis (for minimum 2 years) **Age (years):** 50.7 ± 8.4	Motion Control			x	X	Gait characteristics (rearfoot eversion, ankle internal moment, forefoot dorsiflexion, navicular height)
(Halstead, et al., 2016)	**Number:** n=33 **Diagnoses:** Diagnosed OA **Age (years):** 58.4 ± 11.6	Motion Control	x		x		Gait characteristics (kinematics)
(Huerta, Moreno, Kirby, Carmona, & Garcia, 2009)	**Number:** n=12 **Diagnoses:** none **Age (years):** 24.58 ± 5.56	Motion Control				x	Gait characteristics (peak foot abduction during stance, peak internal tibia rotation during stance, net ankle inversion moments)

2.2.2.2. Product performance criteria

The criteria used to describe lower limb kinematics include joint angles. These are defined as the angle of a segment relative to another segment and can be calculated using a X-Y-Z rotation sequence; in biomechanics, a common sequence is mediolateral (ML) - anterior/posterior (AP) - axial (AX).

$$R_{zyx} = R_z R_Y R_x$$

$$R_x = \begin{bmatrix} 1 & 0 & 0 \\ 0 & \cos\alpha & \sin\alpha \\ 0 & -\sin\alpha & \cos\alpha \end{bmatrix} \quad R_y = \begin{bmatrix} \cos\beta & 0 & -\sin\beta \\ 0 & 1 & 0 \\ \sin\beta & 0 & \cos\beta \end{bmatrix} \quad R_Z = \begin{bmatrix} \cos y & \sin\gamma & 0 \\ -\sin\gamma & \cos y & 0 \\ 0 & 0 & 1 \end{bmatrix}$$

Equation 5: Equation 5: Where R_{zyx} is the joint angle described in each plane, R_x is the rotation about the ML axis by α degrees, R_y is the rotation about the AP axis by β degrees and R_Z is the rotation of the AX axis by γ degrees.

Solving for the Euler angles α (x angle), β (y angle) and γ (z angles):

$$\alpha = \tan^{-1}\left(\frac{-\sin\alpha}{\cos\alpha}\right), \qquad \beta = \tan^{-1}\left(\frac{\sin\beta}{\sqrt{\cos\gamma}}\right), \qquad \gamma = \tan^{-1}\left(\frac{-\sin\gamma}{\cos y}\right)$$

These calculations are carried out within the biomechanical analysis software. Similarly, joint reaction moments can be computed automatically and are defined as the product of two measurable quantities: 1) the joint segments' moments of inertia (requires segment mass and length) and 2) the joint's angular acceleration. The internal joint moment can then be calculated using Equation 6 where the instantaneous total moment is calculated by the software and force plate data is used to calculate the ground reaction moment.

$$M_{Total} = M_{IJ} + M_{JR} + M_{GR}$$

Equation 6: Calculation of joint moments where M_{Total} is the instantaneous joint moment, M_{IJ} is the internal joint moment, M_{JR} is the joint reaction moment and M_{GR} is the ground reaction moment.

The joint angles and internal joint moments of interest differ depending on the intended mechanism of the FO e.g., reducing ankle inversion moments (Hsu, Lewis, Monaghan, Saltzman, & Hamill, 2014). Angular rotations provide insights into the dynamic movement patterns of the foot during the stance phase of gait and are essential for assessing the effects of orthotics, footwear, and pathological conditions. Angular rotations are typically measured using motion capture systems or inertial measurement units (IMUs) that track the orientation of foot segments in three-dimensional space. The primary angular rotations of interest in foot biomechanics include:

1) Dorsiflexion/Plantarflexion (Sagittal Plane): This rotation occurs around the medial-lateral axis, describing the upward (dorsiflexion) or downward (plantarflexion) movement of the foot.
2) Inversion/Eversion (Frontal Plane): This rotation occurs around the anterior-posterior axis, describing the inward (inversion) or outward (eversion) tilting of the foot.
3) Abduction/Adduction (Transverse Plane): This rotation occurs around the vertical axis, describing the outward (abduction) or inward (adduction) rotation of the foot.

Angular rotations are calculated based on the angular displacement of foot segments over time. The angular velocity (ω) and angular acceleration (α) can also be derived from these measurements: Equation 7 calculates the angular displacement, Equation 8 the angular velocity and Equation 9 the angular acceleration.

$$\theta = \theta_{final} - \theta_{initial}$$

Equation 7: Calculation of total rotation angle of a foot segment relative to a reference position where θ is the total angular displacement, θ_{final} is the final angular position and $\theta_{initial}$ is the initial angular position.

$$\omega = \frac{d\theta}{dt}$$

Equation 8: Calculation of the rate of change of angular displacement over time where ω is the angular velocity, $d\theta$ is the change of angular displacement and dt is the change in time.

$$\alpha = \frac{d\omega}{dt}$$

Equation 9: Calculation of the rate of change of angular velocity over time where α is the angular acceleration, $d\omega$ is the change in angular velocity and dt is the change in time.

2.2.3. FO effects on shock absorption

FOs designed for shock absorption properties are often composed of a gel or similar shock absorbing material to reduce impact forces, loading rates and thereby prevent overuse injuries (Turpin, et al., 2012; Orvitz, 2015). They may be seated underneath the entire plantar surface or solely under the heel region (Withnall, Eastaugh, & Freemantle, 2006). Unfortunately, the term “shock absorption” is often misused within orthotic studies, or assumptions are made on the shock absorption properties of a FO without any direct measurements being taken (Yi, Lee, Son, & Sohn, 2022; Yu-ping, Peng, Wang, Zong-Rong, & Chen-Yi, 2020; Wright, Neptune, van der Bogert, & Nigg, 1998) as cited in (Turpin, et al., 2012). Changes in peak plantar pressure are used to make these assumptions, however, this does not take the loading rate into account (Windle, Gregory, & Dixon, 1999).

Studies have involved healthy populations to assess the benefits of shock-absorbing FOs in reducing exercise-related injuries, particularly with military personnel and athletes (Franklyn-Miller, Wilson, & Bilzon, 2011; Kaalund & Madeleine, 2014). However, a recent systematic review found no notable injury prevention effects due to the application of a shock-absorbing FO. (Bonnano, Landorf, Munteanu, Murley, & Menz, 2017). All the FOs included within this review were minimally contoured and prefabricated or made from a commercially available material. Table 7 describes the types of orthotics investigated and the measures used to evaluate changes in foot function.

2.2.3.1. Orthotic function experimental protocol

Two calculation methods exist to describe the condition of shock absorption: 1) capturing the pressure-time integral via a pressure measurement system or 2) capturing the loading rate using accelerometers. In the case of the former, a flexible pressure measuring insole was placed between the plantar surface of the foot and FO (Chen, Tang, Hong, & Tang, 2015). In the latter, an accelerometer was fitted to the tibia of a participant (aligned with its longitudinal axis) and synchronised with a force plate to determine tibial accelerations. Tape and self-adherent wrap were applied to the accelerometer to minimise skin movement artifacts (O'Leary, Vorpahl, & Heiderscheit, 2012). In each case, participants were then asked to walk/run (depending on the study) at a comfortable pace across a gait laboratory walkway until a set number of passes had been completed.

Table 7: Studies examining orthotic effects on shock absorption in different populations.

Reference	Participants	Intervention Type	Types of Orthoses Investigated				Foot Function
			Off-the-shelf	Soft	Semi-rigid	Rigid	
(Franklyn-Miller, Wilson, & Bilzon, 2011)	**Number:** n=200 **Diagnoses:** none **Age (years):** 24.75	Shock Absorption	x	x			Peak pressure
(O'Leary, Vorpahl, & Heiderscheit, 2012)	**Number:** n=16 **Diagnoses:** none **Age (years):** 28 ± 8	Shock Absorption	x	x			Ground reaction forces, tibial accelerations, lower-extremity kinematics, and participant-perceived comfort
(Chen, Tang, Hong, & Tang, 2015)	**Number:** n=11 **Diagnoses:** unilateral heel reconstruction **Age (years):** 39.4	Shock Absorption	x	x			Walking velocity, maximal force, peak pressure, pressure-time integral
(Kim, Cho, Jung, Kim, & Chung, 2010)	**Number:** n=12 **Diagnoses:** none **Age (years):** 25.08 ± 2.43	Shock Absorption	x	x			Joint range of motion, GRF, peak pressure, average pressure, contact area, contact time
(Pawelka, Kopf, Zwick, Bhm, & Kranzl, 1997)	**Number:** n=6 **Diagnoses:** none **Age (years):** unknown	Shock Absorption		x			Peak pressure, pressure time integral.

2.2.3.2. Product performance criteria

Calculation of the pressure time integral was previously described in Equation 2 and Equation 3. There are several methods to calculate the magnitude of acceleration:

$$|a| = \left|\frac{F}{m}\right|$$

Equation 10: Where |a| is acceleration magnitude, F is the net force and m is the object's mass.

$$|a| = \sqrt{|a_x|^2 + |a_y|^2 + |a_z|^2}$$

Equation 11: Where |a| is the acceleration magnitude, a_x is the acceleration magnitude in the x-axis, a_y is the acceleration magnitude in the y-axis and a_z is the acceleration magnitude in the z-axis.

The mean peak vertical tibial acceleration has been used to characterise shock absorption. Hence only the magnitude of the z component is relevant for this calculation.

2.2.4. FO effects on balance/sway

An additional measure commonly described within clinical studies is balance (also known as sway/stability). Within the context of human gait, balance has been defined as the ability of a person not to fall, and postural control is the act of achieving/maintaining a state of balance in static and dynamic conditions (Pollock, Durward, & Rowe, 2000). Numerous methods have been adopted to evaluate balance and factors which could affect postural control in both static and dynamic conditions (Du Pasquier, et al., 2003). These include the implementation of inertial measurement units (Brognara, Mazzotti, Rossi, & Lamia, 2023), force plates (Asgari, Yeowell, & Sadeghi-Demneh, 2022; Robb & Perry, 2020; Azizan, et al., 2018; Abdallah, 2016; Tahmasebi, Mohammad, Behnaz, & Francis, 2015; Qiu, et al., 2013), plantar pressure measurement systems (Ting-Ting, Shin-Liang, Hui, Jeng-Sheng, & Hsien-Te, 2022; Tarrade, Doucet, Saint-Lo, Llari, & Behr, 2019; Hsiao-Yun, Yun-Chi, Shih-Chung, & Chun-Hou, 2019; Nobili, Mannacio, Ciccarelli, Tajani, & Ripani, 2017; Ma C. Z., Wong, Lam, & Wan, 2016; Annino, et al., 2016) in addition to qualitative evaluation techniques. These studies typically involve older populations (Gross, Mercer, & Feng-Chang, 2012). Table 8 describes the types of orthotics investigated and the measures used to evaluate changes in foot function.

2.2.4.1. Orthotic function experimental protocol

Clinical assessments involved static and dynamic movements in each experimental condition (with and without orthoses) performed in a gait laboratory. Static assessments involved the

participant standing with feet close together or in tandem, and some studies performed assessments with and without visual perturbation and on different surfaces (soft and rigid). Dynamic assessments included walking and sport-specific exercises (squats) which were performed before and after each experimental condition was assessed. In studies utilizing inertial measurement units, the sensor was placed at the fifth lumbar spine vertebrae (L5) (Brognara, Mazzotti, Rossi, & Lamia, 2023). Otherwise, force/pressure plates were placed underneath the foot and/or pressure measurement systems placed within the shoe of the participant prior to static and dynamic assessments.

Table 8: Studies examining orthotic effects on balance/sway in different populations. OA = Osteoarthritis.

Reference	Participants	Intervention Type	Types of Orthoses Investigated				Foot Function (Kinematics only)
			Off-the-shelf	Soft	Semi-rigid	Rigid	
(Brognara, Mazzotti, Rossi, & Lamia, 2023)	**Number:** n=42 **Diagnoses:** none **Age (years):** 32.5 (25-42)	Balance Control				x	Sway area, antero-posterior displacement, medio-lateral displacement
(Asgari, Yeowell, & Sadeghi-Demneh, 2022)	**Number:** n=30 **Diagnoses:** plantar callosity **Age (years): >**60	Balance Control			x		Antero-posterior and mediolateral sway velocity
(Azizan, et al., 2018)	**Number:** n=18 **Diagnoses:** none **Age (years):** 22.4 ± 1.9	Balance Control				x	GRF, centre of pressure, centre of mass
(Abdallah, 2016)	**Number:** n=33 **Diagnoses:** Knee OA **Age (years):** 55.03 ± 7.52	Balance Control				x	GRF peak, loading rate, relative timing to stance phase, walking speed
(Tahmasebi, Mohammad, Behnaz, & Francis, 2015)	**Number:** n=15 **Diagnoses: Fl**atfoot **Age (years):** 22.3 ± 2.3	Balance Control				x	Centre of pressure excursion, path length, mediolateral and anteroposterior velocities
(Qiu, et al., 2013)	**Number:** n=20 **Diagnoses:** Parkinson's **Age (years):** 65 ± 9	Balance Control		x			Anterior-posterior postural sway, medial-lateral postural sway,
(Ting-Ting, Shin-Liang, Hui, Jeng-Sheng, & Hsien-Te, 2022)	**Number:** n=15 **Diagnoses:** none **Age (years):** unknown	Balance Control				x	Centre of pressure excursion, location of peak pressure
(Tarrade, Doucet, Saint-Lo, Llari, & Behr, 2019)	**Number:** n=34 **Diagnoses:** foot pain **Age (years):** 43.8 ± 10.9	Balance Control				x	Centre of pressure path length, anteroposterior and medial-lateral velocity, and amplitude of displacement

(Hsiao-Yun, Yun-Chi, Shih-Chung, & Chun-Hou, 2019)	**Number:** n=25 **Diagnoses:** chronic ankle instability **Age (years):** 19.8 ± 1.38	Balance Control				x	Centre of pressure path length, sway area
(Nobili, Mannacio, Ciccarelli, Tajani, & Ripani, 2017)	**Number:** n= 50 **Diagnoses:** none **Age (years):** 20.7 ± 2.09	Balance Control				x	Load percentage ratio, peak pressure.
(Annino, et al., 2016)	**Number:** n=24 **Diagnoses:** none **Age (years):** 67.75 ± 6.04	Balance Control	x				Net velocity, anteroposterior velocity, mediolateral velocity, centre of pressure sway path

2.2.4.2. Product performance criteria

The centre of pressure (COP) is defined as the centroid of the ground reaction force vector (Eun-tae & Hwi-young, 2020). On the other hand, the centre of pressure excursion index (CPEI) quantifies the amount of deviation of the centre pressure curve from a reference line, which connects the maximum pressure points at the heel strike and toe off (Shibuya, Kitterman, & Jupiter, 2013). Displacement from the COP medial-laterally or anterior-posteriorly is defined as COP excursion/path length. The sway area is defined as the displacement area of the centre of mass in the unit of time, however, the calculation depends on the method employed to calculate the COP trajectory: convex hull, principal component analysis or mean of circle areas (Wollseifen, 2011).

2.2.5. Clinical outcomes

Several foot pathologies have been highlighted within this review which impact foot function and are linked to foot pain including rheumatoid arthritis, osteoarthritis, and plantar heel pain. The evaluation of foot function in these pathologies has involved patient reported factors during clinical assessments. Table 9 describes the evaluation methods utilised in the studies extracted from this literature review.

Table 9: Studies involving self-reported and clinically assessed foot function and foot pain measures. RA = Rheumatoid arthritis, OA = Osteoarthritis.

Reference	Population	Measure	Evaluation Method
(Chang, Wang, Huang, Lin, & Lee, 2012)	RA	Pain Level	Visual Analog Scale (0-10)
(Gibson, Woodburn, Porter, & Telfer, 2014)	RA	Comfort, fit, self-reported efficacy, symptoms, activity	Numerical rating scale, Likert scales
(Hodge, Bach, & Carter, 1999)	RA	Pain level	Numerical rating scale
(Tse, Ryan, Dien, Scott, & Hunt, 2021)	Healthy	Comfort	Numerical rating scale
(Simonsen MB, 2022)	RA and foot pain	Pain intensity	Visual Analog Scale (0-10)
(Whittaker, 2020)	Plantar heel pain	Foot pain level, foot function level	Foot Health Status Questionnaire foot pain and foot function subscales
(Halstead, et al., 2016)	OA	Comfort, pain, patient impression	Numerical rating scale, Manchester Foot Pain and Disability Index
(O'Leary, Vorpahl, & Heiderscheit, 2012)	Healthy	Comfort	Visual Analog Scale (0-10)
(Chen, Tang, Hong, & Tang, 2015)	Unilateral heel-reconstruction	Pain intensity	Numerical rating scale

(Pawelka, Kopf, Zwick, Bhm, & Kranzl, 1997)	Healthy	Wearing comfort, perceived discomfort location	Visual Analog Scale (0-10)
(Tarrade, Doucet, Saint-Lo, Llari, & Behr, 2019)	Foot pain	Pain, comfort level and preference	Numerical rating scale

The evaluation methods identified within the review included: 1) the visual analogue scale, 2) numerical rating scale, 3) Likert scales, 4) foot health status questionnaire, 5) Manchester Foot Pain and Disability Index.

2.2.5.1. Visual analogue scale

The visual analogue scale is a validated method in which participants rate acute/chronic pain on a 10cm line that represents a continuum between 0 (no pain) and 10 (worst pain) (Delgado, et al., 2018). Measurements are then recorded from the starting point by measuring the position of the participants mark in centimetres and interpreting this as their pain score. The scale has also been employed to measure comfort by O'Leary (O'Leary, Vorpahl, & Heiderscheit, 2012).

2.2.5.2. Likert scale

A Likert scale is a set of statements for which participants are asked for their level of agreement on a scale from "strongly disagree" to "strongly agree" (Joshi, Kale, Chandel, & Pal, 2015). The combined statements and scores then describe the sentiment towards the issue e.g., foot pain. Similarly, the Manchester Foot Pain and Disability Index is a validated, patient-reported outcome tool to measure foot pain and pathology. Several versions of this index exist including Chinese and Dutch versions (González-Sánchez, Ruiz-Muñoz, Li, & Cuesta-Vargas, 2018; Martijn, Sierevelt, Wassink, & Nolte, 2023).

2.2.5.3. Numerical rating scale

The numerical rating scale has several versions including an 11-, 21- or 101-point scale, describing pain between the extreme end points of "no pain" and "worst pain" (Williamson & Hoggart, 2005). It was the most commonly utilised evaluation method to describe pain within the studies extracted within this review, featuring in 6 studies (Gibson, Woodburn, Porter, & Telfer, 2014; Hodge, Bach, & Carter, 1999; Tse, Ryan, Dien, Scott, & Hunt, 2021; Halstead, et al., 2016; Chen, Tang, Hong, & Tang, 2015; Tarrade, Doucet, Saint-Lo, Llari, & Behr, 2019).

2.2.5.4. Foot health status questionnaire

The foot health status questionnaire is a method to measure quality of life is, which includes 4 subscales: foot pain, foot function, footwear, and general foot health (Bennett & Patterson, 1998; Bennett, Patterson, Wearing, & Baglioni, 1998). However, Whittaker only employed the foot pain and foot function subscales (Whittaker, 2020). Each subscale (excluding footwear) employs a 5-point Likert scale to rate pain (from painless to severe pain) or function (no limitation to severe limitation). Each items scores are then transformed to a scale ranging from 0 to 100 to indicate foot health for each of the 4 domains.

2.2.5.5. Manchester Foot Pain and Disability Index

Comprising the Manchester Foot Pain and Disability Index are 19 statements, grouped into three subscales: functional limitation, pain intensity and personal appearance (Garrow, et al., 2000). Each statement has three possible responses: “none of the time” (score=1), “on some days” (score=2) and “on most/every day(s) (score=3) (Menz, Auhl, Ristevski, Frescos, & Munteanu, 2014). Halstead utilised the functional limitation subscale to capture patient reported foot function over the course of 12 weeks (Halstead, et al., 2016).

Unfortunately, given the test platform doesn’t involve human participants when testing, these user-reported measures cannot be implemented. Consequently, measures such as pain level, comfort and foot function cannot be directly recorded, and instead need to be inferred-estimated using changes in the measures described previously e.g., reduction in peak plantar pressure gradients, greater shock absorption etc. This mostly impacts commercial non-medical products (as they don’t undergo clinical testing that could address these limitations), but customer feedback within the current development pathway could fulfil this role.

2.2.6. Product performance criteria

The literature review highlighted several design factors (e.g., material, geometry such as medial/lateral posting) which impact the performance of a FO and defined four product performance criteria: impact on gait, impact on loading pattern, impact on shock absorption, and impact on stability/balance. The academic and industrial requirements provided greater clarity on the most appropriate measurement systems to employ within the test platform. Some measures used to define these performance criteria may not be achievable in the test platform (e.g., tibial rotation), given the differences between a human and industrial test platform.

Gait analysis utilises motion capture systems to capture foot kinematics during gait activities and gold standard marker-based systems such as Qualisys (Qualisys, Sweden) and Vicon (Vicon Industries Inc, USA) have been evaluated comprehensively within the literature and include hardware and software packages which are CE marked in Europe and cleared for clinical use in the USA. The placement of reflective markers and variables that can be captured are dependent on the foot model design; these are discussed in greater detail in a later literature review. Pressure based measurements describe either (1) the interaction between the product and foot or (2) between the foot and the ground, depending on if a pressure plate or in-shoe pressure capture system is utilised. As this project involves the characterisation of products interacting with the phantom-foot, an in-shoe pressure capture system is preferred, and will account for effects of the geometry of the product on plantar pressure to a greater extent than could be captured by a flat plate. Finally, to capture force-based measures, force plates are often utilised alongside Qualisys and Vicon motion capture systems. They can fulfil an additional purpose within the test platform by ensuring the actuation system consistently loads the phantom-foot and product in the same way. Used in conjunction with the pressure- capture system, clear product claims can be established (i.e., under the same loading conditions, product A reduces the peak loads experienced by a plantar region). The product performance criteria, suitability for assessment with the industrial test platform and potential sources of measures have been identified in Table 10 and are defined in Appendix H: Product Performance Criteria Definitions.

Table 10: Product performance criteria and clinical sources of measure.

Product Performance Criteria	Measure		Suitability for assessment using test platform?	Potential Source of Measure
Impact on gait	Rearfoot angle at contact		Yes	Motion capture
Impact on gait	Maximum rearfoot angle		Yes	Motion capture
Impact on gait	Velocity (stride)		No – this is an input parameter for the actuation system	Motion capture
Impact on gait	Tibial rotation		No – the talus will be fixed to the actuation system so won't experience unguided rotation	Motion capture
Impact on gait	Rearfoot eversion velocity		No – this is an input parameter for the actuation system	Motion capture
Impact on gait **Impact on shock absorption** **Impact on loading pattern**	Kinetic data	Vertical force	Yes	Force plate
		Vertical impulse	Yes	Force plate
		Ankle inversion moment	Unknown – this is dependent on what foot joints are represented in the phantom-foot	Force plate
		Ankle eversion moment	Unknown – this is dependent on what foot joints are represented in the phantom-foot	Force plate
Impact on shock absorption **Impact on loading pattern**	Peak pressure	Ball of Foot	Yes	In-shoe pressure capture
		Medial arch	Yes	In-shoe pressure capture
		Heel	Yes	In-shoe pressure capture
Impact on shock absorption **Impact on loading pattern**	Pressure time integral	Ball of Foot	Yes	In-shoe pressure capture
		Medial arch	Yes	In-shoe pressure capture
		Heel	Yes	In-shoe pressure capture

Impact on shock absorption **Impact on loading pattern**	Force time integral		Yes	In-shoe pressure capture
Impact on shock absorption **Impact on loading pattern**	Contact area	Heel	Yes	In-shoe pressure capture
		Medial arch	Yes	In-shoe pressure capture
Impact on loading pattern	Time to peak pressure	Ball of Foot	Yes	In-shoe pressure capture
		Medial arch	Yes	In-shoe pressure capture
		Heel	Yes	In-shoe pressure capture
Impact on loading pattern	Contact time	Ball of Foot	Yes	In-shoe pressure capture
		Medial arch	Yes	In-shoe pressure capture
		Heel	Yes	In-shoe pressure capture
		Total	Yes	In-shoe pressure capture
Impact on stability/balance	Centre of pressure and mass displacement	Displacement of centre of pressure	Yes	In-shoe pressure capture

2.2.7. Conclusion

This literature review revealed several primary outcomes which can be grouped into four FOs product performance criteria:

- impact on loading pattern (change to location of peak pressure),
- impact on gait (change in foot kinematics),
- impact on shock absorption (reduction in loading rate/force), and
- impact on stability/balance (change to COP).

The principal methods to capture these outcomes in clinical studies have been established as: 1) an in-shoe pressure capture system or pressure plate to capture changes in plantar pressure, 2) a motion capture system to monitor changes in foot kinematics, 3) pressure capture systems or accelerometers to determine changes in shock absorption and 4) force plates, pressure plates or inertial measurement units for changes to stability/balance. An in-shoe pressure capture system is more appropriate than a pressure plate given the interaction between the foot and product is of interest when using the test platform. Additionally, force plates provide a pragmatic solution given their availability within the

FOs which use various geometric features to modify foot pressure, kinematics and thereby function have been utilised within healthy groups and populations experiencing foot pathology, with varying degrees of success in improving foot function and reducing pain. FO material, geometry and placement under the foot were highlighted as key design factors in changing foot kinematics, location of peak pressure, shock absorption and balance. Soft insole materials reduced peak plantar pressures more effectively than rigid materials and geometric features such as metatarsal bars/domes reduced average peak pressures in the area under which they are fitted.

However, meta-analysis findings for the effects of some interventions were conflicting, due to the heterogeneity of test protocols and variables describing foot function. For example, Hajizadeh et al. hypothesised that differences in kinematic data collection (i.e., different retroreflective marker placement protocols) may have resulted in low biomechanical data quality (Hajizadeh, Desmyttere, Carmona, Bleau, & Begon, 2020). High inter-individual variability was also noted in previous studies (Telfer, Abbott, Steultjens, & Woodburn, 2013; Wahmkow G. , Cassel, Mayer, & Baur, 2017; Liu, et al., 2012) cited in (Hajizadeh, Desmyttere, Carmona, Bleau, & Begon, 2020). It suggests the need for standardised test

methods to accurately evaluate FO performance in terms of both pressure and kinematics, which the test platform would be capable of fulfilling provided the phantom-foot can function with a high degree of repeatability.

It is not possible to capture all the product performance criteria detailed above within a single test platform. Specifically, self-reported measures such as pain and comfort levels cannot be captured without the involvement of human participants. However, this does not significantly impact the implementation of the test platform within academia or industrial contexts. In the former, clinical studies carried out with human participants post product development/evaluation using the test platform can be used to capture these product performance criteria (if required). This is also true if a medical device is to be developed in industry due to the requirements to complete clinical testing with this class of product. Otherwise, current methods of user feedback via surveys will be sufficient, given that these product performance criteria are primarily of interest with populations experiencing foot pathology who would require a medical device rather than an off-the-shelf product. Consequently, the test platform will compliment and inform clinical studies and provide opportunities to capture product performance criteria to aid product innovation, development and evaluation in industry and academia.

2.3. Literature review: foot anatomy and properties

The design of the test platform was informed by the anatomical structure and biomechanics of the foot, as they play a key role in producing the PPD, location of COP and GRF during gait. Description of the components that comprise foot anatomy are widely available in the literature (Shimaa Shehata, 2022; Kelikian & Sarrafian, 2011; Logan, Sardesai, Daivajna, Robinson, & Hutchings, 2012; Jastifer, 2023). In essence, the foot-ankle complex comprises numerous bones, muscles, ligaments, synovial joints, and tissues (Qian, Ren, Ding, Hutchinson, & Ren, 2013). Bones are connected by means of joint containers and ligaments which determine the range of motion permitted in each plane. The articular surface of bones is covered with articular ligament. Muscles are connected to bones via tendons which act as pulleys and are surrounded by synovial sheaths to enable them to glide. Complex movement occurs in all three planes of motion due to large loading conditions and the action of 13 extrinsic and 21 intrinsic muscles, whose actions maintain balance and stability during gait. The tibia is subjected to the resultant GRF and moment, which varies according to the

location of the COP and PPD (Wang, et al., 2020). The normal mechanics of the foot-ankle complex result from the combined effect of its components. To reproduce a foot model that is sufficiently realistic for the intended purpose, the material and mechanical properties of each foot structure must be determined. Material properties define the inherent characteristics of a material whereas mechanical properties describe how a material behaves under mechanical loads. This will allow physical equivalents to mimic as far as is possible and necessary, real foot structures.

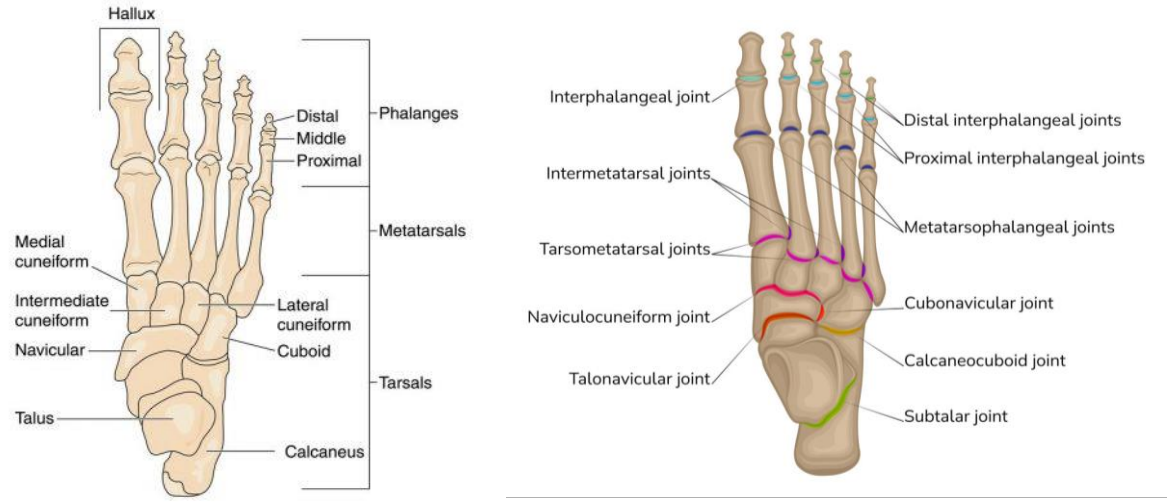

Figure 10: Bones of the foot (left) (Bone and Joint Specialists, 2024) and joints of the foot (right) (Matt Appleton, 2024).

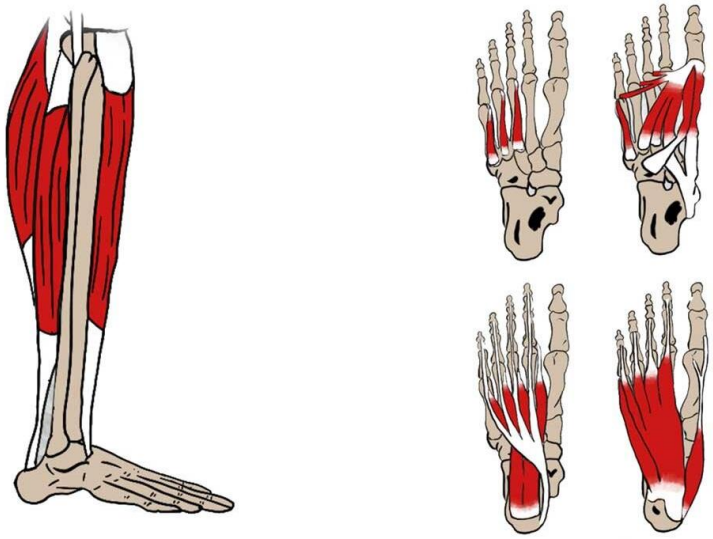

Figure 11: Extrinsic (left) and intrinsic (right) muscles of the foot (Ioannou, 2024).

Experimental methods to characterise the behaviour of plantar soft tissue during loading involve both live participants (in-vivo) and cadaveric samples (in-vitro). In-vivo studies offer the most realistic setting for capturing foot tissue behaviour, however, pose difficulties due to

constraints involved with living participants around recruitment, access to tissue structures and the forces that can be applied to live tissue without causing pain/discomfort. In-vitro studies provide greater access to anatomical components and more realistic loading conditions (i.e., close to bodyweight loading forces, however, there may be differences in the behaviour of cadaveric samples under load compared to live participants. Hence, both in-vivo and in-vitro studies will be compared within this review.

Efforts have been made to create more specific musculoskeletal databases investigating the response of structures under mechanical manipulation (Neumann, et al., 2018) (Schimmoeller, et al., 2020), however, Neumann and Schimmoeller focused on the arm and leg only. A database featuring all the data required to fully define the mechanical and material properties of each anatomical component of the foot has yet to be created, hence the need for this review. The breadth and dynamic nature of the material properties of the plantar tissue indicate that there is no single ideal material property to achieve; rather, the choice in material properties must relate to the context in which the phantom-foot is to be used. In the case of this project, the phantom-foot must recreate the morphology and stress/strain response of the foot to allow for the product performance criteria defined in the industrial needs analysis to be analysed.

2.3.1. Material and mechanical characteristics of interest

Several material properties are of interest in relation to this project including Young's modulus, viscoelasticity, composition, and environmental sensitivity. The first of these, Young's modulus, describes the stiffness of a material and represents the ratio of stress to strain in the elastic region of deformation. This is commonly used in studies investigating the properties of in-vivo and in-vitro tissue, such as in a recent study by Qian (Qian Z, 2021). Viscoelasticity expresses both a materials ability to return to its original shape after deformation, and its ability to dissipate energy over time. Additionally, viscoelastic materials behave differently during loading and unloading, displaying dependency on the rate of loading (Naemi, 2015). The composition of components such as the plantar tissue contribute to their material properties, affecting stiffness, strength, and extensibility. Finally, materials may be sensitive to changes in temperature and humidity (among other environmental conditions).

With regards to mechanical properties, the strength of a material describes its ability to withstand applied forces without failing. This is important for the internal structures of the

foot to support body weight and resist external loads. Next, damping (or shock absorption) refers to the ability to dissipate impact forces during weight-bearing activities, which is particularly important during periods of high rates of loading. Fatigue resistance indicates a tissue's ability to withstand repeated loading over time without failure, while joint stability relates to the stability of foot and ankle joints and is important in maintaining proper alignment and function during movement. Finally, given the foot-ankle complex involves the interaction of various different structures during gait, the muscle-tendon dynamics, joint kinematics, and ground reaction forces can be jointly described as biomechanical interactions. Below, the foot is divided into its sub-components, with the material and mechanical properties of each described using existing literature.

2.3.2. Plantar tissue anatomy and properties

Plantar tissue differs in thickness across the foot and can be divided into several layers including: skin, subcutaneous fat pad (soft tissue), plantar fascia, muscles and tendons, ligaments and fascial layers (Guo, 2018; Morrison T, 2021; Angin S. M., 2018). The properties of each are described below.

2.3.2.1. Plantar skin

Significant literature exists which details the biophysical properties of plantar skin, however, its importance as a structure in enhancing the tolerance of the foot to mechanical loads has also been examined (Hashmi, Nester, Wright, Newton, & Lam, 2015; Boyle, 2019). Deformations are distributed evenly across the surface of skin due to its morphology and composition (M. F. Leyva-Mendivil, 2015). Additionally, it presents a viscoelastic response under loading (Everett & Sommers, 2012; Clancy NT, 2010). The thickness of plantar skin differs across the foot, varying from 0.51 ± 0.17mm under the hallux and 0.66 ± 0.13mm under the heel pad, with a general increase in thickness from forefoot to hindfoot. The Young's modulus varies between skin layers; the stratum corneus has a very value of 2GPa, while the viable epidermis and dermis have lower Young's moduli of 0.1-0.2 MPa and 0.02-0.04 MPa respectively (Boyle, 2019). When the skin was considered as a single layer in recent study, a mean Young's modulus of 0.83 ± 0.49 MPa was observed from 5 cadaveric donor samples (Crossland, Sairally, Edwards, Culmer, & Brockett, 2024). Some environmental factors can impact the material and mechanical properties of plantar skin. Increased hydration levels appear to reduce the stiffness of plantar skin and thus reduce the

resistance to indentation (Wendland & Sprigle, 2018; Wu, van Osdol, & Dauskardt, 2006). Additionally, Wu et al observed increased temperatures reduced the cohesive strength and stiffness of plantar skin via the increased mobility of lipids.

2.3.2.2. Subcutaneous fat pad (soft tissue)

The plantar fat pad is composed of adipocytes, fat cells, surrounded by a regular series of fibrous tissue septa which act as a shock absorber and distributes force during gait (Dalal, Widgerow, & Evans, 2015). The heel pad is specialised and consists of distinct layers: a superficial layer which attaches to the plantar skin and is made up of smaller components of adipocytes, and a deep layer that attaches to the calcaneus and consists of larger adipocyte components. Several factors have been identified within the literature which influence the behaviour of plantar soft tissue. A review was completed on the effects of ageing on foot and ankle biomechanics (Menz H. , 2015). The stiffness of soft plantar tissue was found to increase with age, which was somewhat contributed to by increased skin hardness (Hsu, et al., 2005; Hsu, Wang, Tsai, Kuo, & Tang, 1998; Kwan, Zheng, & Cheing, 2010; Ju-Wen, Wen-Chung, & Tung-Yang, 2014). Aging also contributes to a deterioration of the mechanical properties of bone and can cause bone fragility fractures (Maghsoudi-Ganjeh, Wang, & Zeng, 2020). In addition to age, sex, height, and mass have been shown to change the stiffness of plantar tissue: there is a positive correlation with weight, and a negative correlation with height and BMI (Kim, Koh, Hwang, Han, & Lee, 2016). The effects of these aspects specifically on the heel pad have been detailed in a previous review (Parker D. , 2013). Attempts were made to account for the effects of age within Table 11 by separating young (<50 years old) and elderly (>50 years old) populations, however, participant specific data such as mass and height was not available for each study. Data was averaged for each group (and the collective groups) and the standard deviations (SD) combined using Equation 12 (SD was noted as "–"if not specified):

$$\frac{SD_a^2}{n_a} + \frac{SD_b^2}{n_b} = SD_{combined}^2$$

Equation 12: Where SD_a is the standard deviation of group a, SD_b is the standard deviation of group b, n_a is the sample size of group a, n_b is the sample size of group b and $SD_{combined}$ is the combined standard deviation.

The in-vivo studies included within this review which investigated the stress/strain of the heel pad, sub-metatarsal tissue and sub-hallux tissue implemented similar experimental methods, by palpating the plantar surface of the foot with a probe placed in series with a load cell (Kwan, Zheng, & Cheing, 2010; Sun, et al., 2011). The indentation rate varied between

experiments from 9.2mm/s to manual incremental control in addition to variations in indenter size and the maximum tissue deformation permitted (Teoh, Shim, & Lee, 2014). Additionally, the maximum tissue deformation permitted varied, with some studies using a fixed value e.g., 5.6mm (Haeun, et al., 2019) while others used a percentage change from the initial thickness e.g., 10% initial thickness (Zheng, et al., 2012). However, neither of these correspond to the actual deformation experienced by plantar tissue during gait, which is greater (Teoh, Shim, & Lee, 2014). The rate of indentation and indentation depth at which the Young's modulus is calculated both greatly impact the stress/strain behaviour of the plantar tissue due to its non-linear loading response (see Equation 13); it was noted that the response of the plantar tissue to loading was frequency dependent (Wearing, Hooper, Dubois, Smeathers, & Dietze, 2014).

In-vitro studies have involved stress relaxation experiments using cadaveric samples dissected from underlying muscle and bone (including removal of skin), and cut into cylinders to suit loading system indenter size/constraints to determine the Young's modulus of various sites across the plantar tissue (Pai & Ledoux, 2010; Ledoux & Blevins, The compressive material properties of the plantar soft tissue, 2007). This allows for the properties of individual structures e.g., fat pads, to be characterised, or the entire plantar tissue to be considered together. Unfortunately, this may have impacted upon the stress/strain properties of the plantar tissue and makes direct comparison between in-vivo and in-vitro studies difficult.

Table 11: In-vivo and in-vitro Young's modulus properties compiled from existing literature. 1: (Teoh, Shim, & Lee, 2014), 2: (Klaesner J. W., Commean, Hastings, Zou, & Mueller, 2001), 3: (Chao, Zheng, Huang, & Cheing, 2010), 4: (Kwan, Zheng, & Cheing, 2010), 5: (Zheng, et al., 2012), 6: (Sun, et al., 2011), 7: (Teng, et al., 2022), 8: (Pai & Ledoux, 2010), 9: (Ledoux & Blevins, The compressive material properties of the plantar soft tissue, 2007)

	In-Vivo (kPa)				**In-Vitro (kPa)**			
	Average	**Young**	**Elderly**	**References**	**Average**	**Young**	**Elderly**	**References**
Hallux	43.32 (38.50)	24.80 (7.00)	49.50 (37.85)	1, 4, 6	731 (-)	830 (30)	632 (-)	8, 9
1st Met	88.65 (-)	109.00 (-)	78.48 (55.40)	2, 4, 6	671.5 (-)	730 (30)	613 (-)	8, 9
2nd Met	74.33 (-)	65.95 (-)	93.40 (-)	1, 3, 6	-	-	-	-
3rd Met	107.15 (-)	127.00 (-)	87.30 (48.70)	2, 4	695.5 (-)	715 (30)	676 (-)	8, 9
4th Met	-	-	-	-	-	-	-	-

5th Met	81.60 (-)	84.00 (-)	79.20 (46.10)	2, 4	654 (-)	700 (30)	608 (-)	8, 9
Heel	133.91 (76.73)	140.25 (34.58)	136.76 (68.50)	1, 2, 4, 5, 6, 7	621 (-)	740 (30)	508 (-)	8, 9

This review found significant differences in the Young's modulus values reported from in-vivo and in-vitro studies, with the latter reporting values more than an order of magnitude greater across all plantar tissue sites. Additionally, cadaveric samples have been demonstrated to present less energy loss (46.5%-65.5% energy loss vs 90%) and greater stiffness (~900kN/m vs ~100kN/m) (Ledoux & Blevins, The compressive material properties of the plantar soft tissue, 2007). Several hypotheses may explain this difference. 1) In-vivo data was only collected from intact feet whereas in-vitro samples were cut down to only include plantar tissue: consequently, this will have resulted in differences in the outward spreading of the tissue when loaded, although these isolation effects were accounted for (Miller-Young, Duncan, & Baroud, 2002). 2) In-vivo tissue will have been compressed against uneven bony structures as opposed to in-vitro tissue compressing against a flat, metal plate. 3) In-vitro samples had previously been frozen and thawed and were stored on ice until tested; there are numerous papers which study the impact of different cadaveric preservation techniques on the material properties of bony and tendinous structures, however, none which investigate their effects on plantar tissue.

Although these factors may also be significant, it is likely that the non-linear stress/strain behaviour of plantar tissue presents the greatest source of error in Young's modulus calculations, as the equation developed by Hayes et al assumes linear elastic material properties (Hayes, 1972).

$$E = \frac{(1 - v^2)}{2ak\left(v, \frac{a}{h}\right)} . \frac{f}{w}$$

Equation 13: Where E is the effective Young's modulus, v is the Poisson's ratio, a is the radius of indenter stylus, h is the tissue thickness, k is the scaling factor dependent upon v and a/h, w is the depth of indentation and f is the force of indentation.

Consequently, the relatively low loading forces used to calculate the Young's modulus of the plantar tissue at various sites in in-vivo studies may misrepresent the actual material properties. Using loading forces akin to those experienced during gait will reduce this error, which suggests the results extracted from in-vitro experiments may be more reliable in this case. Ultimately, although Young's modulus is the most noted measure of anatomical

components stress/strain response (hence it's inclusion within the project), a measure which takes the frequency and load dependent response of plantar tissue into account would be more appropriate.

Both in-vitro studies included within this review cut down plantar tissue specimens to align with previous in-vivo studies, hence only in-vivo data was included in Table 12. Several techniques exist for the measurement of plantar tissue thickness, each presenting different sources of potential error. The most prevalent method involves a tissue ultrasound palpation system which uses a linear array ultrasound probe in series with a load cell (Chao, Zheng, Huang, & Cheing, 2010; Kwan, Zheng, & Cheing, 2010; Zheng, et al., 2012; Sun, et al., 2011; Chatzistergos, Behforootan, Allan, Naemi, & Chockalingam, 2018; Behforootan, Chatzistergos, Chockalingam, & Naemi , 2017). Placement of the probe under each plantar tissue region would influence the measurement derived, due to the internal morphology of the foot.

Dynamic fluoroscopy was used to measure changes in plantar thickness during gait, using edge detection algorithms to determine tissue thickness (Tenten-Diepenmaat, 2019; Wearing, Hooper, Dubois, Smeathers, & Dietze, 2014; Wearing, Smeathers, Yates, Urry, & Dubois, 2009). The definition of bone and tissue edge boundaries and the location at which tissue thickness was measured were the greatest sources of error. The primary disadvantage of dynamic fluoroscopy is the high radiation dose absorbed by the participant (West, 1993).

Optical coherence tomography (CT) scans using standard reconstruction algorithms were performed by Klaesner and Campanelli, although the former also included data collected via a tissue ultrasound palpation system to calculate tissue thickness (Klaesner J. W., Commean, Hastings, Zou, & Mueller, 2001; Campanelli, et al., 2011). Following scanning, Campanelli then constructed a 3D model of the foot, with sub-metatarsal and sub-calcaneal tissue sliced coronally to determine tissue thickness across each entire region, although there was difficulty defining sections of the heel pad using this method due to a region of unstructured fat. CT scans were of interest within this project as it provides measures of volume, not just thickness. Consequently, it can be utilised to define and recreate the three-dimensional structures that the foot comprises.

As with the Youngs modulus properties of plantar tissue, age has been determined to affect tissue thickness, which increased in thickness with age (Kwan, Zheng, & Cheing, 2010). Hence results were separated by age group: young (<50 years old) and elderly (>50 years

old). Table 12 describes the plantar tissue thickness values found for sites across the plantar surface for young and elderly populations, as well as an average and standard deviation values calculated using Equation 12. Table 15 describes the measurement technique used to capture the plantar tissue thickness.

Table 12: Compilation of in-vivo unloaded thickness data from existing literature of various plantar tissue sites.

	In-Vivo Unloaded Tissue Thickness (mm)			
	Average (mm)	**Young (mm)**	**Elderly (mm)**	**References**
Hallux	6.11 (2.00)	7.20 (0.70)	5.75 (1.88)	3, 5, 7
1st Met	8.91 (3.55)	9.27 (2.36)	8.64 (2.65)	1, 2, 3, 5, 7
2nd Met	11.20 (7.43)	12.72 (7.19)	9.69 (1.82)	2, 5, 8
3rd Met	10.26 (-)	11.00 (-)	9.52 (1.77)	1, 3
4th Met	7.45 (1.20)	7.50 (0.90)	7.40 (0.80)	7
5th Met	8.70 (-)	9.00 (-)	8.39 (2.51)	1, 3
Heel	16.64 (8.78)	16.19 (10.56)	17.27 (4.42)	1, 3, 4, 5, 6, 7, 8, 9, 10, 11, 12, 13, 14

Table 13: Measurement technique utilised per study to determine in-vivo tissue thickness.

Reference		**Measurement Technique**
1	(Klaesner J. W., Commean, Hastings, Zou, & Mueller, 2001)	Ultrasound
2	(Chao, Zheng, Huang, & Cheing, 2010)	Ultrasound
3	(Kwan, Zheng, & Cheing, 2010)	Ultrasound
4	(Zheng, et al., 2012)	Ultrasound
5	(Sun, et al., 2011)	Ultrasound
6	(Teng, et al., 2022)	Dynamic fluoroscopy
7	(Mo, Li, Yang, Zhou, & Behr, 2019)	Ultrasound
8	(Haeun, et al., 2019)	Ultrasound
9	(Chatzistergos, Behforootan, Allan, Naemi, & Chockalingam, 2018)	Ultrasound
10	(Behforootan, Chatzistergos, Chockalingam, & Naemi , 2017)	Ultrasound
11	(Chatzistergos, Naemi, Sundar, Ramachandran, & Chocklingam, 2014)	Ultrasound
12	(Wearing, Hooper, Dubois, Smeathers, & Dietze, 2014)	Dynamic fluoroscopy
13	(Campanelli, et al., 2011)	Optical coherence tomography
14	(Wearing, Smeathers, Yates, Urry, & Dubois, 2009)	Dynamic fluoroscopy

2.3.2.3. Plantar fascia and muscles

The plantar fascia is comprised of collagen fibres and connects the medial tubercle of the calcaneus to the proximal phalanges of each toe, blending with the fibrous flexor tendon sheaths (Stecco, et al., 2013). The collagen fibres are primarily arranged longitudinally, however there are additional fibres arranged in multiple directions, with some elastic fibres present in the loose connective tissue between the collagen fibre bundles (Snow SW, 1995). Wang et al determined the maximum Young's modulus of the plantar fascia bundles to be approximately 300kPa, although this decreased with distance from the calcaneus (Qian, et al., 2021). However, similarly to plantar soft tissue, cadaveric and in-vivo specimens appear to produce significantly different Young's modulus; Isvilanonda et al found significantly higher values in cadaveric specimens, as well as regional differences with higher values in the proximal middle and distal middle regions (400 and 522 MPa) than the medial and lateral regions (225 and 242 MPa). The plantar fascia demonstrates viscoelastic behaviour and can withstand very high tensile loads, which is expected given its role in maintaining arch stability (Todros, Biz, Ruggieri, & Pavan, 2021).

Plantar intrinsic muscles can be divided into four layers. The first layer (i.e. the most superficial) includes the abductor hallucis which abducts/flexes the hallux, flexor digitorum brevis which flexes the lateral phalanges and abductor digiti minimi which abducts the 5th phalanx. Next, the second layer includes the quadratus plantae which assists the flexor digitorum brevis, and the four lumbricals which flex the metatarsophalangeal joints and extend the interphalangeal joints. The third layer consists of the flexor hallucis brevis which flexes the hallux at the metatarsophalangeal joint, adductor hallucis which adducts the hallux and flexor digiti minimi brevis which flexes the 5th phalanx. Finally, the deepest layer contains the plantar and dorsal interossei which adduct and abduct phalanges 2-4. Studies have found no link between the stiffness of these intrinsic muscles and plantar pressure distribution; however, the morphology of the muscles and body mass have been noted to affect plantar pressure (Taş & Çetin, 2019; Panichawit C, 2015). Passive muscle demonstrates some joint motion restriction and non-linear elastic responses under loading (Herbert & Gandevia, 2019). Unfortunately, material properties for these muscles appear to be absent from the literature.

2.3.3. Bone, joint, ligament, and cartilage anatomy and properties

2.3.3.1. Bones

The bones of the foot can be divided into three main groups: tarsals, metatarsals, and phalanges. The anatomy, articulations, functions, attachment points and clinical relevance to pathologies are widely discussed in the literature (Rizzo, 2015; Ledoux, Rohr, Ching, & Sangeorzan, 2006; Chuto, Richelme, Cermolacce, Nicaud, & Puech, 2018). Several factors have been found to impact the characteristics of bone including age, gender, health status and ethnicity (Vulović & Filipovic, 2020). The material and mechanical properties of whole bones depend upon the compilation of cortical and trabecular bone. Cortical bone is significantly stronger than trabecular bone, with the former producing a Young's modulus between 15-25GPa in comparison to 0.1-5GPa and demonstrates anisotropic behaviour (Jameson, 2014; Morgan, Unnikrisnan, & Hussein, 2018). The individual properties of each foot bone have not been investigated as of yet, however FE models typically model bony structures with a Young's modulus between 7300MPa and 29,200MPa (Niu, Wang, Feng, & Jiang, 2014; Morgan, Unnikrisnan, & Hussein, 2018).

2.3.3.2. Joints, ligaments, and cartilage

The foot comprises a number of different joint types including planar/gliding intertarsal joints, ellipsoid/condyloid metatarsophalangeal joints, hinge-like interphalangeal joints, the hinge-type ankle joint, and the tarsometatarsal articulations. Each individual foot bones motion has been described previously (Dawe & Davis, 2011). The articulating bones, type of joint, movement and stabilising ligaments are described in Table 14.

Table 14: Joints of the foot and the associated movements and stabilising ligaments.

	Movement	**Joint**	**Articulating bones**	**Stabilising ligaments**
Synovial hinge joint	Plantarflexion and dorsiflexion	Talocrural joint	Tibia, fibula, and talus	Medial ligament, lateral ligament complex and interosseous ligament

Plane synovial joint	Limited gliding and sliding	Calcaneocuboid Joint	Calcaneus and cuboid	Long plantar ligament and dorsal ligaments
		Talonavicular Joint	Talus and navicular	Calcaneonavicular, cuboid-intermediate cuneiform and cuboid-lateral cuneiform ligaments
		Cuboid-Cuneiform Joints	Cuboid and cuneiform bones	Cuboid-intermediate cuneiform, cuboid-lateral cuneiform, cuboideonavicular, cuneocuboid, interosseous cuboideonavicular and interosseous cuneocuboid ligaments
Ellipsoid/Condyloid Joints	Flexion, extension, abduction, adduction and circumduction	1st MTP Joint	1st metatarsal and proximal phalanx of the hallux	Medial collateral ligament
		2nd MTP Joint	2nd metatarsal and proximal	Lateral collateral ligament

			phalanx of the 2nd phalanx	
		3rd MTP Joint	3rd metatarsal and proximal phalanx of the 3rd phalanx	Medial and lateral collateral ligament
		4th MTP Joint	4th metatarsal and proximal phalanx of the 4th phalanx	Medial and lateral collateral ligament
		5th MTP Joint	5th metatarsal and proximal phalanx of the 5th phalanx	Medial and lateral collateral ligament
Hinge-like joints	Flexion and extension	Proximal interphalangeal joint	The proximal and middle phalanges of each toe	Medial and lateral collateral ligament

		Distal interphalangeal joint	The middle and distal phalanges of each toe	Medial and lateral collateral ligament

Ligaments present in the foot and ankle have a much higher Young's modulus than soft plantar tissue, with ligaments of higher stiffness limiting a greater range of motion (Siegler, Block, & Schneck, 1988). Articular cartilage presents a slightly higher Young's modulus to plantar soft tissue (Boschetti & Peretti, 2008). Numerous FE models have been created which utilise mechanical and material properties collected by Gefen, Athanasiou and Siegler; a Young's modulus of 10MPa has been used to represent foot cartilage and 700MPa for foot ligaments. (Gefen, Megido-Ravid, Itzchak, & Arcan, 2000; Athanasiou, Liu, & Lavery, 1998; Siegler, Block, & Schneck, 1988).

2.3.4. Conclusion

The foot-ankle complex comprises a series of linear and non-linear components operating across well-defined interfaces including the plantar tissue, cartilage, ligaments, and bony structures. The response of these components under load is sensitive to loading and the magnitude of the force applied. Moreover, participant-specific factors such as age, gender and body morphology play a significant role in the behaviour of the foot-ankle complex. The implications of these factors on the industrial test platform relate to the sample represented during testing. As such, in the context of the industry challenge this project is addressing, it is important to initially model the phantom-foot on an individual of known mass, with no pathology related to the foot-ankle complex (in the first case, non-medical products will be tested using the test platform), with as much detail of their anthropometric measurements (as required by this project) as possible. The resulting model will provide opportunities to test product design iterations against the product performance criteria and allow inferences on how the product will perform with real product users by considering variations in foot structure and form that are known to exist due to participant-specific factors. However, representing the non-linear, anisotropic material properties to a high degree of accuracy presents a difficult challenge given the limited budget and manufacturing capabilities available within the PhD project. Hence a simplified foot with linear material properties

which align with a given rate of loading should be used as a first case to achieve, with a more complex foot suggested in future.

Young's modulus was a common material property stated for components of the foot, despite the non-linear behaviour of biological tissues and anatomical structures. It provides a quantitative measure of the stiffness or elasticity of biological tissues and structures. As described above, its value can vary depending on various factors and experimental determination of Young's modulus can be challenging given the irregular morphology of bones, tissues etc. Ultimately, it may provide a limited view on the characteristics of anatomical components. However, given that non-biological materials are commonly described by this property, it provides a useful starting point in choosing the materials the phantom-foot would be constructed by. The use-context of the industrial test platform may influence the final material properties selected i.e., the ability of the phantom-foot to withstand repeated loading at representative loads may require a material of a higher Young's modulus value to be selected.

The material properties of the individual bones within the foot skeletal system are not well defined. Moreover, no study comparing the properties of the hindfoot, midfoot and forefoot appear to be present in the literature, with only 2 sources in the literature describing the viscoelastic behaviour of the hindfoot bones (Son & Munroe, 2018; Son & Latt, Hindfoot Bone Viscoelasticity and Stress Relaxation, 2019). However, differences between hindfoot, midfoot and forefoot bones are not critical to replicate with regards to the industrial application as they form very rigid structures, and enough data is present to define the required material properties of the components to be replicated within the phantom-foot. Enough data is present to model the skeletal structure, passive muscle, ligaments, cartilage, and plantar tissue of the phantom-foot.

Tissue thickness can vary across participants due to age, gender, and pathology amongst other factors. Hence, the relatively low standard deviation of the unloaded tissue thickness under the Hallux, 1st and 3rd - 5th metatarsals could be attributed to natural variation between participants. However, larger variations in tissue thickness, for example, the greater variation found for unloaded tissue thickness under the 2nd metatarsal, may be attributed to the different measurement techniques utilised to capture sub-heel tissue thickness. Moreover, differences in the definition of plantar tissue may have contributed to variation in measurements, as previous studies have attempted to distinguish the individual layers comprising the heel e.g., macro-chamber and microchamber (Mo, Li, Yang, Zhou, & Behr,

2019). Consistency in the measurement technique utilised, and the creation of a phantom-foot model based on an individual (rather than an average population) will nullify both of these issues, hence a CT scan of an individual to define and model 3D structures is suggested.

2.4. Literature review: phantom-foot form and function

Literature review 2 provided data to inform the material properties that parts of the phantom-foot might possess. However, a fundamental decision is how many parts to use to define the foot and how to validate the behaviour of the phantom-foot against in vivo data. In experimental studies (such as those discussed in literature review 1), the human foot is divided into "functional segments" because there are too many individual bones and structures to measure simultaneously. These multisegment models (MSMs) allow foot kinematics of subsections of the foot to be measured during gait, enabling normal and abnormal function to be studied. These models offer possible examples of how to model the functional behaviour of the foot and in many cases will provide in-vivo kinematic (and perhaps other data) that would allow validation of the phantom-foot in later stages of this project. Khazzam postulates the choice of foot model depends on the focus of the research and population of interest; the phantom-foot is intended to represent a healthy individual of a typical consumer and will be used to test products that are used under the heel only, the forefoot only, and the entire foot, in the first case (Khazzam, Long, Marks, & Harris, 2006). As a result, this review was undertaken with the focus to establish a low-risk starting point in the design of the phantom-foot which was likely to be sufficient in representing the foot in these applications (i.e., the simplest MSM capable of representing foot kinematics such that orthotic performance can be assessed), with the idea that further complexity could be added if required following validation.

2.4.1. Comparison of MSMs

Over 40 MSMs developed for clinical and research applications were identified within the literature, however only the most commonly implemented models and those most relevant to the phantom-foot were compared and contrasted. The aggregation of these themes informs the completion of the design specification of the phantom-foot. The MSMs identified within the review are (in order of increasing complexity):

1. The Conventional Gait Model (CGM)

2. The Oxford Foot Model (OFM)
3. Milwaukee Foot Model (MFM)
4. Rizzoli Foot Model (RFM)
5. Salford Foot Model (SFM)
6. Kinfoot Foot Model (KFM)
7. Glasgow-Maastricht Foot Model (GMM)

These models and the segments within them are shown in Figure 12, with each rigid foot segment represented by a different colour. Models with fewer than 5 segments have been defined as “low complexity”. Table 15 compares the number of segments, segment definitions and samples represented by each MSM reviewed.

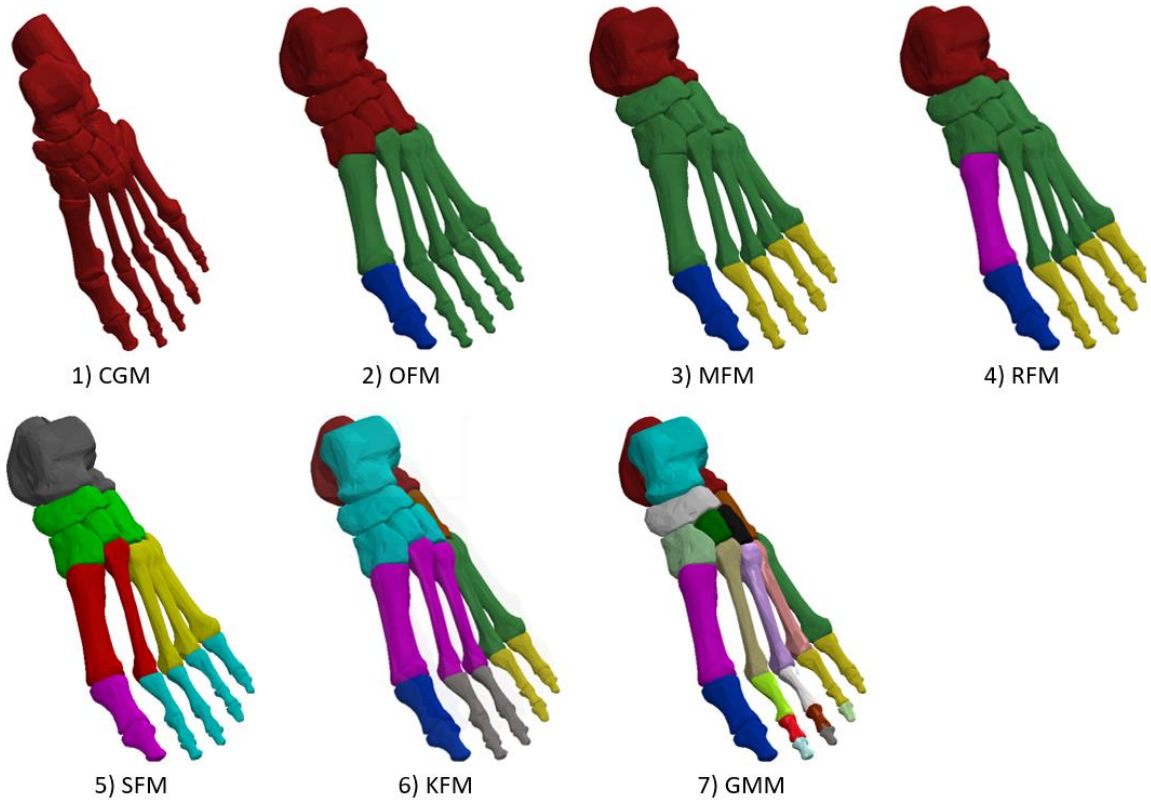

Figure 12: Diagrammatic representations of the foot models examined within the review.

Table 15: Comparison of MSMs identified within the review.

Complexity	Model	Reference	Number of Segments	Segment Definitions	Sample Represented
Low	CGM	(Baker, 2018)	1	Whole Foot	Healthy Adult Adults experiencing foot pathology
	OFM	(Curtis, 2009)	4	Tibia, Hindfoot, Forefoot, Hallux	Healthy Adult Adults experiencing foot pathology Healthy Paediatric
	MFM	(Myers, 2004)	4	Tibia/Fibula Hindfoot (Talus, Navicular, Calcaneus) Forefoot (Cuboid, Cuneiforms, Metatarsals) Hallux	Healthy Adult Adults experiencing foot pathology Healthy Paediatric
	RFM	(Portinaro, 2014)	5	Tibia Hindfoot Midfoot First Metatarsal Hallux	Healthy Adult Adults experiencing foot pathology Healthy Paediatric
High	SFM	(Nester, Jarvis, Jones, Bowden, & Liu, 2014)	6	Leg Calcaneus/Talus Midfoot (Navicular, Cuboid, Cuneiforms) Lateral Toes Medial Toes Hallux	Healthy Adult
	KFM	(Cowley, 2001)	9	Tibia/Fibula Talus, Navicular, Cuneiforms Cuboid Calcaneus Lateral Toes Medial Toes Hallux	Healthy Adolescent Healthy Paediatric
	GMM	(Al-Munajjed, Rasmussen, Carbes, & Tørholm, 2013)	26	Each bone (except the sesamoid bones)	Healthy Adult Adults experiencing foot pathology

2.4.2. Low complexity MSMs

Almost all the models identified within the review have been utilised in healthy populations with extensive commentary on their ease of use, accuracy in representing the kinematic movements of the foot and inter-participant repeatability. However, ease of use and lower data variation between studies and laboratories is not particularly relevant to the use of the phantom-foot within the test platform. Rather, the accuracy by which foot kinematics are accurately reported by the models is the key criteria determining which model, or combination of models, should the phantom-foot seek to emulate. Moreover, models can be adapted to suit specific industrial test requirements e.g., if the movement of a particular section of the foot is of particular interest.

The conventional gait model (CGM) is a grouping of biomechanical models developed in 1980 which modelled the foot as a single segment, assuming the separate components of the foot function as a single rigid segment (Baker, 2018; Kadaba M. P., 1990). Although multiple laboratories developed their own models, their characteristics were very similar (Sutherland, 1972; Shoemaker, 1978; Kadaba M. P., 1989; Kadaba M. P., 1990; Davis, 1991) and allowed the analysis of kinematics, forces and kinetics generated about the ankle in normal and populations experiencing foot pathology becoming the standard for gait analysis in the 1990s (Novak A. a., 2009; Brodsky, 2011). However, despite a large body of literature concerning the repeatability of the model, few studies have investigated its accuracy and those which did, have focussed on the hip joint centres or knee flexion axis orientation rather than the foot and ankle (Sangeux M. a., 2011; Peters, 2012; Sangeux M. a., 2014; Passmore, 2016; Sauret, 2016). Moreover, technological limitations prevented CGMs from using more than two markers on a small foot, leading to the foot being represented as a single axis rather than a three-dimensional structure. Consequently, kinematic alterations at joints within the foot and distal to the ankle could not be measured and variations in kinematics, either due to participant specific differences, changes over time with disease or interventions, might be attributed to the ankle joint however, may have actually taken place within other joints in the foot (Benedetti, 2011; De Ridder, 2015). This is problematic as unless this motion is attributed to the correct areas of the foot, informed decisions in insole geometry to change the kinematics cannot be made.

Numerous low complexity models have been developed since to improve and standardise foot measurement during gait (Carson, 2001; Stebbins, 2006). The OFM models the foot and lower leg as the tibia, rearfoot, forefoot and hallux, and is one of the most widely used models to date due to its implementation within Vicon system software (Vicon, UK), an early leader in motion capture technology (Curtis, 2009). Similarly, the four rigid segments defined within the MFM include the tibia and fibula; hindfoot-talus, navicular, and calcaneus; forefoot-cuboid, cuneiforms, and metatarsals; and hallux (Myers, 2004). Both models have been used within adult and paediatric populations (Alonso-Vázquez, Villaroya, Franco, Asín, & Calvo, 2008; Stebbins, 2006; Kidder, Abuzzahab, Harris, & Johnson, 1996) and calculate segment kinematics 4 segments in the sagittal, coronal and transverse planes (Khazzam, Long, Marks, & Harris, 2006), however, only the OFM has been implemented with orthotics. Orthotic studies involving the OFM have investigated devices applying changes to the rearfoot such as a medial heel bar (Klein, Chapman, Lastovicka, Janura, & Richards, 2022) and the midfoot via medial arch support (Wahmkow G. , Cassel, Mayer, & Baur, 2017; Dombroski, Balsdon, & Froats, 2014). However, there was poor agreement in the forefoot transverse and sagittal planes with a different 4 segment MSM when using the medial heel bar, which suggests the forefoot segment may present less reliable responses to orthotics when using this model.

The RFM is a 5 segment MSM that represents the tibia, hindfoot, midfoot, first metatarsal and hallux, developed with a greater focus on frontal plane alignment of the hindfoot, as well as transverse and sagittal plane alignment of the forefoot (Portinaro, 2014; Novak A. C., 2014). It has been validated within different populations (Caravaggi P. a., 2011; Deschamps K. a., 2012; Arnold J. B., 2013), utilized in clinical studies (Caravaggi P. a., 2010; Bishop, 2012; Deschamps K. a., 2013) and displayed to be more reliable when directly compared to others (Mahaffey, 2013; Powell, 2013). As well as describing intersegmental kinematics, the RFM describes functional and clinically pertinent angles such as the medial longitudinal arch, navicular drop and first ray mobility; these measures were previously collected from static radiographic images (Novak A. C., 2014).

Each of these models are able to capture sufficient rearfoot and forefoot kinematic motions of the foot, however, the lack of representation of medial/lateral motions which have been evidenced to take place during gait are problematic in their application within this project, as the kinematic changes made by orthotic products which feature geometry to act on the outer

borders of the planter surface of the foot, e.g., under the medial arch, would not be able accurately captured.

2.4.3. High complexity MSMs

Higher complexity models can capture and represent foot motion during gait more accurately through the definition of a greater number of rigid segments, particularly due to the separation of lateral and medial components. Several high complexity models were included within this review including the SFM, KFM and GMM. Firstly, the SFM is a 6-segment model introduced by Jarvis to capture foot movement in healthy individuals (Nester, Jarvis, Jones, Bowden, & Liu, 2014). It separates the forefoot into lateral and medial segments which addresses the issue raised by lower complexity models. The KFM, a 9-segment model developed by Cowley, adds additional complexity through decomposition of the midfoot and individualisation of the hallux and was used to create a database of normative kinematic and kinetic data for the adolescent population (Cowley, 2001; MacWilliams, 2003). Finally, the GMM is the most complete kinematic model to date, featuring all 26 bones of the foot (except the sesamoid bones) and the corresponding joints (Al-Munajjed, Rasmussen, Carbes, & Tørholm, 2013), with joint types, location and orientation data extracted from existing literature (Winson, 1995; Arampatzis, 2003; MacWilliams, 2003).

Each of the SFM, KFM and GMM models have produced results comparable to existing literature with respect to the kinematic data (Leardini, 1999; Oosterwaal, et al., 2016). However, in the context of this project and the industrial problem, the SFM presents several advantages. Firstly, a large dataset of a healthy adult population is available from previous studies, where anthropometric data is present for each participant. As noted in literature review 1, the sample selected to be represented is key as demographics such as age, pathology and gender can all impact the material properties and behaviour of the foot-ankle complex under loading. Therefore, the SFM presents a low-risk starting point in the design of the phantom-foot. Additionally, the greater the number of segments, the greater the difficulty in skin marker placement due to the positioning of markers on less obvious bony landmarks, which can lead to larger vibration artefacts that misrepresent joint motion (MacWilliams, 2003). Within the context of the industrial project, vibration artifacts are not present as markers will be placed directly onto bony landmarks, but this makes comparison between the motion of the phantom-foot and in-vivo data difficult when the bone/segment motion of the

phantom-foot will be validated. As a result, the SFM will be significantly easier to validate compared to the KFM and GMM.

2.4.4. Conclusion

Very little comparative literature and orthotic-specific studies were found during this literature review; hence it focused on the development of the most commonly implemented models, the sample populations studied and key benefits/limitations between low and high complexity MSMs. The key advantages of more complex MSMs are that they are better able to accurately represent in vivo foot kinematics, in that more bones are individualised, and fewer segments motion is grouped together. Several models have evidenced movement between the medial/lateral sides of the foot separately to rearfoot and forefoot movement. This suggests that these "areas" need to be separately represented otherwise movement will need to occur in parts of the phantom-foot in abnormal ways to enable the overall foot to behave normally. This being the case, a less complex phantom-foot may enable adequate representation of in-vivo kinematics, without needing to address the inevitably greater practical complexities associated with a phantom based on the most detailed MSM (i.e., comprising 26 segments). Consequently, as a starting point, the SFM was selected as the segment range of motion, the motion pattern and timing of motion are largely comparable to that of existing literature for the most complex model (GMM), which we assume to be most accurate, however, the complexity of implementing the model is reduced. Additionally, variation in foot motion between individuals can occur for numerous reasons including individual variation, disease, age, activity, and interventions, and a large dataset based on this model is available, which reduces the risk of these factors negating the effectiveness of the industrial test platform through allowing the selection of participants data according to whose anthropometrics closely match those of the phantom-foot.

2.5. Literature review: human ankle-foot actuation systems

Ankle-foot simulators are mechanical systems that apply loading to a foot specimen or phantom-foot (e.g., prosthetic foot) to recreate functional tasks such as walking or parts of the walking cycle. The literature primarily comprises in-vitro "gait simulators" using cadaveric feet and detailed reviews have already been completed documenting the development of these systems, as well as their applications in investigating the properties of the foot and

ankle. Other ankle-foot simulators include those developed to test lower-limb prosthetic devices and those intended for destructive or safety/regulatory testing of orthotic and footwear products.

The test platform being designed and implemented through this PhD has a different application than the cadaver-based systems (which aim to study foot anatomical and biomechanics in detail) and prosthetic device systems (which focus on clinical prosthetic component design), and destructive testing (which are often highly repetitive iterations of loading situations that are not recreating any functional task or too few functional tasks).

Rather, the test platform aims to produce a foot that responds to external loads in a manner that is sufficiently realistic (with regards to the industrial requirements) to enable product design decisions to occur with confidence. However, cadaver-based, prosthetic-based, and destructive test actuation systems still represent the general concept being investigated in this project and could help inform the design of the test platform.

2.5.1. Ankle-foot simulator functional characteristics

The functional characteristics of simulators and their importance within the context of the project can be found in Table 16. These factors are important in allowing comparison between cadaveric and prosthetic actuation systems to determine the most appropriate solution for the industrial test platform. Unfortunately, the performance indicators are not clearly disclosed for destructive test systems due to patent and copyright protections and have not been included.

Table 16: Functional characteristics of simulators that are of interest to this project.

Functional Characteristic	**Definition**	**Importance of characteristic within this project**
Control strategy	Any means of inter/intra-step feedback control	Determines the method of tuning the trajectory and load applied to the phantom-foot. This may change over time as the phantom-foot material is pre-conditioned prior to orthotic testing.
Degrees of freedom of the end effector to which the phantom-foot is attached.	Defines the number of planes the phantom-foot can be actuated in.	This would allow for more complex gait patterns including the representation of shear and medial/lateral rotations
Method of loading the foot	If either the tibia, ground or both are moved relative to one another and thereby used to load the foot. *Active simulators* hold and apply load through the tibia by performing a spatial movement, whereas *passive simulators* apply load through a ground plate whilst the tibia is held in place (Wang, et al., 2020). Systems that incorporate a combination of tibial spatial movements and ground plate loading are defined as *hybrid systems*.	Determines the positioning of the measurement system e.g., force plate, with respect to the actuation system, to capture the loading of the phantom-foot. Additionally, it determines how the phantom-foot will be fixed to the actuator and how its bone/segment motion will be validated against in-vivo data.

Maximum applicable loading force	The loading force defined as % of body weight, which the actuation system can apply, with the represented sample assumed to have a mass between 588 – 784 N.	The system must allow testing of orthotic products against all expected sample conditions, i.e., a range of body masses, to determine its suitability for a given population (e.g., adults, children). The system must be also run significantly below its loading capacity to ensure longevity.
Stance duration	The length of time the actuation system must hold the phantom-foot in stance phase (from heel-strike to heel-off)	Determines the maximum rate of motion required to simulate normal walking speeds.
Measurement Devices	Sensors utilised within the mechanism to capture the behaviour of the phantom-foot foot/end effector.	Defines the performance indices which can be captured by the measurement system to quantify product performance.
Product Performance Criteria	The measures used to describe product performance	Determines the capability of the system to capture product performance against the characteristics defined in literature review 1.

2.5.2. Control Strategies

There are two categories of control systems: open loop/feedforward control systems which involve no means of feedback from the output, and closed loop control systems which do employ a method of feedback. Feedforward control is based on models of the systems to compute control signals but can only be effective if two key problems are addressed: disturbances (i.e. friction) and model inaccuracies (i.e., a difference between the planned and performed motion) (Plooij, Wolfslag, & Wisse, 2015). Compensating for friction can be divided into non-model and model-based approaches. The former requires on a method of feedback to compensate for the system while the latter relies on the control algorithm and flexibility within the system (Li, Zhang, Wei, & Yue, 2018). Consequently, as no method of feedback is present in feedforward control systems, model design and adaptability to unexpected changes are critical to the operation of the test platform. Stable walking and running have successfully been recreated in monopedal and bipedal robots using open loop systems (Mombaur, Longman, Bock, & Schlöder, 2005; Mombaur, Bock, Schlöder, & Longman, 2005). Similarly, robotic arms have been shown to perform stable periodic motions using open loop control systems (Wolfslag, Plooij, Babuška, & Wisse, 2015; Kim, et al., 2001).

Keemink describes some closed loop control methods used for controlling actuation systems in contact with a mechanical environment including: (in)direct force control, impedance control and admittance control (Keemink, van der Kooij, & Stienen, 2018). Direct force controllers involve 2 nested loops; the internal loop is torque controlled, and the external loop is force controlled. The purpose of the internal loop is to achieve desired torque in each of the joints, considering the manipulator dynamics in a known condition i.e., a full dynamic model (Siciliano & Villani, 1999). Direct force control has several advantages including its precise control over contact forces and its adaptive responses to changes in the environment. However, it requires accurate force sensors which can be costly, its implementation may involve complex control algorithms and its direct reliance on force measurements may make it susceptible to noise and disturbances (Siciliano & Khatib, Force Control, 2017).

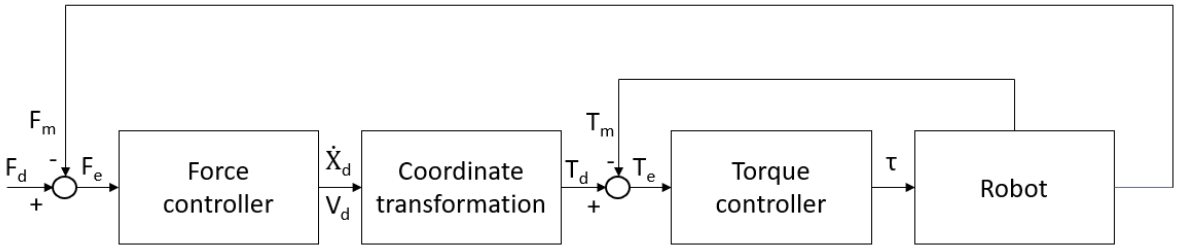

Figure 13: Direct force control. F_d is desired force, F_m is the force measured with the force transducer, F_e is the force error, X_d is the desired velocity (continuous time domain), V_d is the desired velocity in the discrete time domain, T_d is the desired torque, T_m is the measured torque, T_e is the torque error and τ is the control applied to the motors.

Indirect force control is similar, but the internal loop is position controlled. This is usually easier to develop than direct force control as it's often built on top of a typical industrial manipulator controller, and it can be difficult in practice to accurately model friction and thereby obtain an accurate dynamic model required for direct force control (Winiarski & Woźniak, 2012). Although widely utilised in industrial robots, it has limitations in precise force control and may require fine-tuning of position or impedance parameters to achieve desired force behaviour. The decision to implement direct or indirect force control is largely dependent on the application required, specifically the budget, required precision and adaptability.

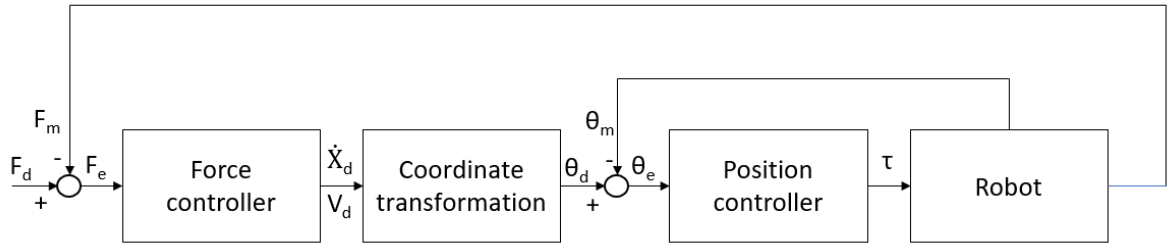

Figure 14: Indirect force control. F_d is desired force, F_m is the force measured with the force transducer, F_e is the force error, X_d is the desired velocity (continuous time domain), V_d is the desired velocity in the discrete time domain, θ_d is the desired position, θ_m is the measured position, θ_e is the position error and τ is the control applied to the motors.

Impedance control is considered as a prominent approach in robotics to avoid large impact forces while operating in unstructured environments. In such environments, the conditions under which the interaction occurs may significantly vary during the task execution. This demands robots to be endowed with online adaptation capabilities to cope with sudden and unexpected changes in the environment (Abu-Dakka & Saveriano, 2020). However, the complexity in commissioning these controllers have resulted in reduced implementation in industry (Cruz, Radke, Haninger, & Krüger, 2021). Impedance controllers require the output force measured by a sensor and the desired position as inputs, however, torque-based impedance control systems also exist.

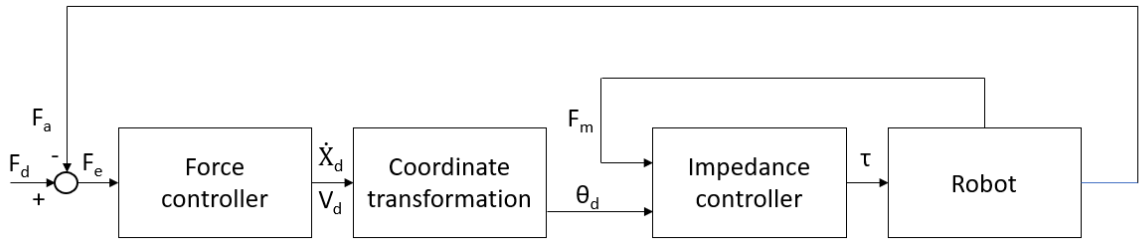

Figure 15: Impedance control. F_d is desired force, F_a is the force exerted on the environment by the robot, F_e is the force error, X_d is the desired velocity (continuous time domain), V_d is the desired velocity in the discrete time domain, θ_d is the desired position, F_m force measured with the force transducer and τ is the control applied to the motors.

Finally, admittance control, although sometimes interchanged with position-based impedance control, differs as it controls motion after a force is measured, whereas impedance control operates after a deviation from a set point is measured (Keemink, van der Kooij, & Stienen, 2018). The equations for both control schemes are the same, but the inputs/outputs differ; impedance control requires displacement/velocity and outputs a force, whereas admittance control requires a force and outputs a displacement/velocity (Maithani, Ramon, & Mezouar, 2019). An example of the implementation of this control method is human-robot interaction tasks e.g., power-assisted assistive robotics.

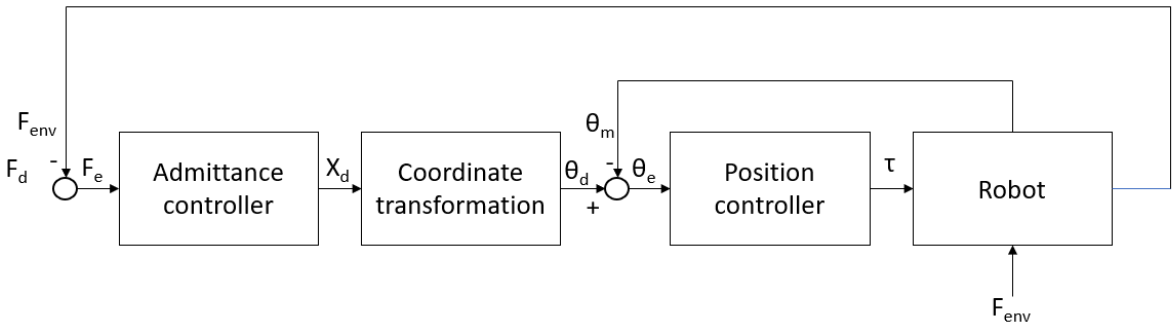

Figure 16: Admittance control: F_d is desired force, F_{env} is the force applied by the environment, F_e is the force error, X_d is the desired velocity, θ_d is the desired position, θ_m is the measured position, θ_e is the position error and τ is the control applied to the motors.

2.5.3. Degrees of freedom (DOF)

The degrees of freedom define the motion capabilities of robots, referring to the number of independent joints that can provide freedom of movement of the manipulator (Nüchter, 2009). Grübler's formula defines the degrees of freedom in relation to the number of joints and constraints:

$$DOF = m(N - 1 - J) + \sum_{i=1}^{J} f_i$$

Equation 14:Degrees of freedom, where m is the degrees of freedom for a single body, N is the number of bodies (including ground) and J is the number of joints

Pamungkas et al. described the degrees of freedom in each joint in the lower limb (see Table 17) (Pamungkas, Caesarendra, Soebakti, Analia, & Susanto, 2019). Actuators may drive one or many of the joints listed in order to recreate gait. The fewer the DOF represented, the less closely the final trajectory of the ankle-foot actuation system will be able to represent gait. However, there are a number of factors to consider with respect to degrees of freedom. While higher degrees of freedom enable more accurate replication of natural gait, they also increase the complexity of the robotic system. This complexity can lead to challenges in control, increased weight, and higher energy consumption due to a greater number of actuators (Karimi, 2022). Additionally, more complex systems with higher DOFs are generally more expensive to design, manufacture, and maintain given the requirement of a greater number of sensors to provide accurate position/force feedback (Tran, Nguyen, Dinh, & Tran, 2023). Therefore, it is important to choose a robotic system which balances the biomechanical fidelity with practical considerations such as cost, depending on the use contexts.

Table 17: Degrees of freedom in each joint in the lower limb

Joint	DOF	Movement
Hip	3	Flexion-extension
		Abduction-adduction
		Internal-external rotation
Knee	2	Flexion-extension
		Rotation
Ankle	3	Plantar flexion-dorsiflexion
		Abduction-adduction
		Eversion-inversion

2.5.4. Cadaveric ankle-foot simulators

In-vitro experimentation on cadaveric foot samples is a common practice because it allows easy access to structures deep to the skin surface and thus measurement of biomechanical phenomena not otherwise possible. Several actuation systems have been designed to apply loading forces to a cadaver foot similar to those experienced by the in vivo foot during gait

(see Figure 17). This review includes systems which utilise tendon actuators (Noble, Colbrunn, Lee, Van Den Bogert, & Davis, 2010) (Kim, et al., 2001) (Nester, et al., 2007) (Peeters, et al., 2013) (Hurschler, Emmerich, & Wülker, 2003) (Aubin, Cowley, & Ledoux, 2008) (Sharkey & Hamel, 1998) as well as a robotic arm-based system (Prisk, Imhauser, O'Loughlin, & Kennedy, 2010). A comparison of these systems can be found in Table *18*.

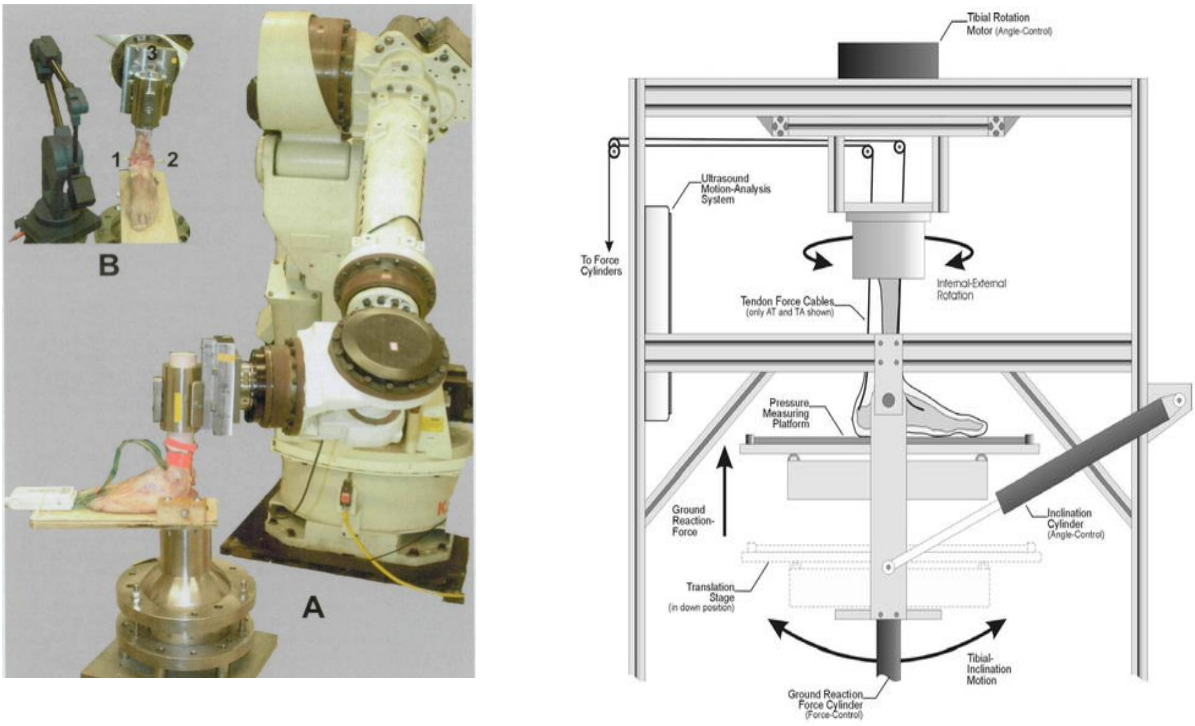

Figure 17: (Prisk, Imhauser, O'Loughlin, & Kennedy, 2010) Robotic system with a pressure-measurement sensor that was inserted into the ankle joint (left) and (Kim, et al., 2001) kinematic and kinetic gait simulator (right)

Cadaveric systems are limited by the fragility of the cadaveric foot sample, which can quickly suffer damage under loading. A common solution to this issue is to scale down the gait loading forces applied by the system, although, as identified in literature review 1, this likely results in a different plantar soft tissue response due to the non-linear nature of tissue behaviour.

Table 18: Main performance indexes of cadaveric ankle-foot gait dynamic simulators. BW:body weight, DOF:degree of freedom

Reference	Control System	Tibia Loading Method	Simulated BW (%)	Stance Duration (s)	Freedom of Motion (DOF)	Measurement Devices	Product Performance Indicators
(Noble, Colbrunn, Lee, Van Den Bogert, & Davis, 2010)	Pseudo-fuzzy iterative logic and real-time hybrid control	Passive	100	2.8	6	Force Plate, Load Cells	Foot kinematics, Tendon actuator forces
(Kim, et al., 2001)	Open loop	Hybrid (passive shear)	40	20	3, in sagittal plane	Force Plate, Electromagnetic Tracking System	Foot kinematics, GRF, COP advancement
(Nester, et al., 2007)	Open loop	Active	50	2	3, in sagittal plane	Force Plate, Motion Capture System	Foot Kinematics, GRF
(Peeters, et al., 2013)	Inertial force feedback controller	Hybrid	50	10	3, in sagittal plane	Force Plate, Motion Capture System, Load Cell, Pressure Plate	Foot kinematics, GRF, COP
(Hurschler, Emmerich, & Wülker, 2003)	Force and angle feedback controller	Passive	50	60	1, rotation about its own axis	Motion Capture System, Pressure Plate	Foot kinematics, COP
(Aubin, Cowley, & Ledoux, 2008)	Fuzzy iterative learning control	Passive	75	2.7	Tibia held fixed	Force Plate	GRF
(Sharkey & Hamel, 1998)	Open loop	Passive	100	12	3, in sagittal plane	Force Plate, Pressure Plate	Foot kinematics, GRF, Tendon actuator forces
(Prisk, Imhauser, O'Loughlin, & Kennedy, 2010)	Closed loop	Active	-	-	6, in sagittal plane	Force-moment Sensor, Pressure Sensor, Load Cell	Ankle Joint Contact Force, GRF

2.5.5. Prosthetic ankle-foot simulators

Prosthetic test systems have also incorporated in-vitro test methods to develop new lower-limb prosthetics, as a lack of test standards can lead to unsafe in-vivo test methodologies (Marinelli, Giberti, & Resta, 2017). Additionally, individual control parameters can be studied in isolation and tuned e.g., the flexion and extension motion control of a prosthetic knee/ankle. These systems operate in much the same fashion as cadaveric-based systems, however, prosthetic devices aren't susceptible to the same limitations as cadaveric feet hence the loading forces applied by these systems are much greater. The primary difference is that prosthetic device simulators do not consider/represent internal foot motion. The systems identified within this review can be found in Table 19 and examples can be seen in Figure 18.

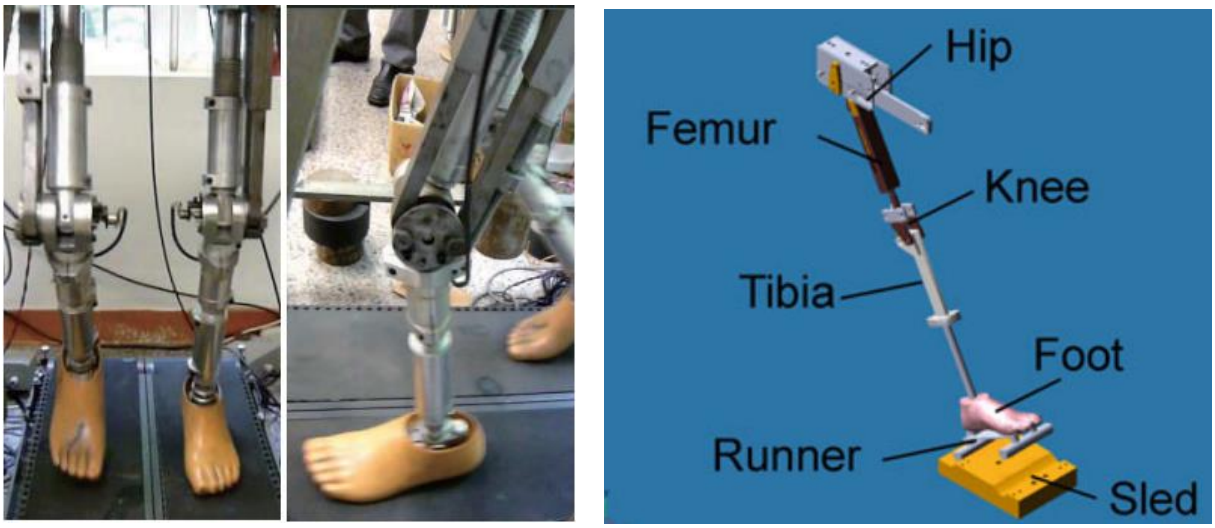

Figure 18: Zhang 2010, lower prosthesis and force test table (left) and Giberti 2013, Virtual model of the leg prosthetic test bench (right)

Table 19: Ankle-foot gait dynamic simulators used to test prosthetic devices and the main performance indexes. DOF:degree of freedom, GRF:Ground reation force, COP:Centre of pressure

Reference	Control System	'Tibia' Loading Method	Loading Force (N)	Stance Duration (s)	Freedom of Motion (DOF)	Sensors	Product Performance Indicators
(Marinelli, Giberti, & Resta, 2017)	Closed loop	Hybrid	900	1.1	8	Force Plate, Motion Capture System	Foot kinematics, GRF
(Giberti, et al., 2013)	Closed loop	Active	1125	1	3	Load cells	GRF
(Zhang, Shen, Shen, & Li, 2010)	Closed loop	Active	700	-	2	Force sensor Photoelectric encoder	GRF, Knee joint angle
(Richter, Simon, Smith, & Samorezov, 2015)	Closed loop	Active	1200	-	2	Force sensor Incremental encoder	GRF, Thigh Angle
(Kim & Oh, 2001)	Closed loop	Active	-	1.2	3	Gyro sensor	Knee joint angle, Gait period

2.5.6. Industrial ankle-foot test systems

The primary function of industrial ankle-foot test systems can differ greatly to cadaveric and prosthetic based systems, as they are explicitly designed to perform specific test routines i.e., repeating a portion of the gait cycle to test the life cycle of prosthetic components. Furthermore, the systems identified within this review are primarily concerned with the external effects on a product e.g., material degradation, rather than internal foot motion, similarly to prosthetic device simulators. They are thus focussed on product durability and failure rather than product effectiveness in terms of reducing foot pressure or modifying foot motion in ways that are consistent with clinical or biomechanical concepts, or product marketing claims.

Industrial systems are not well documented within the literature due to patent and copyright protections, however several International Organization for Standardization (ISO) standards exist for the testing of prosthetic devices which can inform design specification. Two ISO standards define prosthetic device test practices. 1) ISO 10328 specifies procedures for static and cyclic strength tests on lower-limb prostheses which typically produce compound loadings by the application of a single test force, which occur during different instants during the stance phase of walking. 2) ISO 22675 primarily specifies a cyclic test procedure for ankle-foot devices and foot units of external lower limb prostheses, distinguished by the potential to realistically simulate those loading conditions of the complete stance phase of walking from heel strike to toe-off that are relevant to the verification of performance requirements such as strength, durability, and service life. Test systems that fulfil these ISO standards or perform footwear testing have been listed in Table 20 and examples seen in Figure 19.

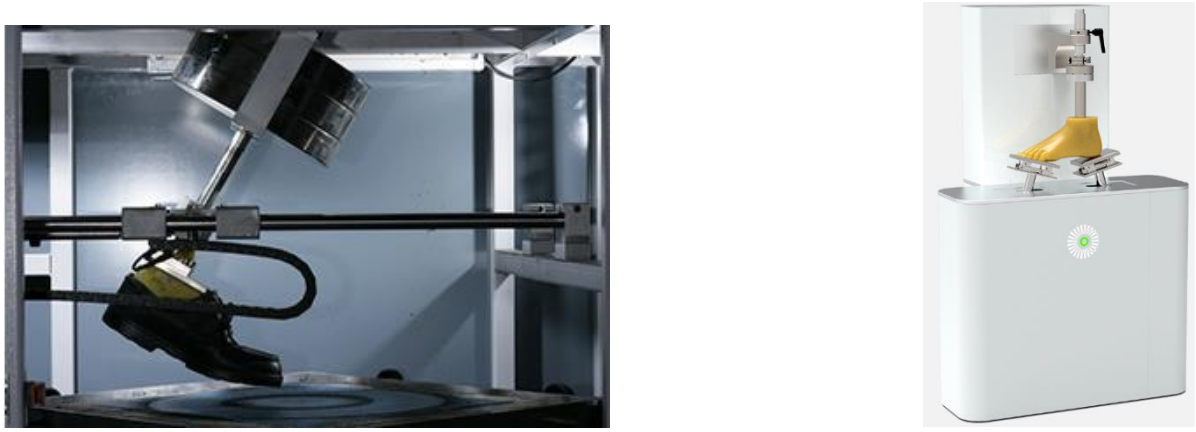

Figure 19: Satra Pedatron (left) and Thelkin lower limb prosthesis simulator (right)

Table 20: Ankle-foot gait dynamic simulators used to test devices in industry.

Actuation System	Control System	'Tibia' Loading Method	ISO Standard	Load Capacity (N)	Stroke (mm)	Frequency (Hz)	Number of Axes
Pedatron Satra	Closed loop	Active	-	-	-	-	2
Lower limb prosthesis simulator Thelkin	Unknown	Hybrid	10328	5000	150	10	2
810E5 TestResources	Closed loop	Active	10328 22675	30,000	-	15	2
Ankle-foot prosthesis simulator Shore Western	Closed loop	Hybrid	22675	6800	150	1.5	2
Foot and ankle prosthesis simulator Thelkin	Unknown	Hybrid	22675	10,000	150	2	2
Prosthetic ankle-foot testing capability Bionix	Unknown	Hybrid	10328 22675	25,000	150	-	-

2.5.7. Discussion

A variety of control methods have been developed for cadaveric ankle-foot gait dynamic simulators. Open-loop systems were previously preferred as recreating stance close to physiological speeds was easier to achieve, however more recent systems tend to incorporate some form of feedback control based on GRF to reach the target force. This also aligns with prosthetic ankle-foot simulators, and whilst industrial ankle-foot test systems don't disclose their control methodologies, closed-loop control is assumed based on their outputs; an example of this is the Pedatron, which features force and pressure measurement systems. Consequently, a closed-loop system is preferable for the test platform as iterative optimisation for an open-loop system would be extremely time-consuming to perform, and a force plate can provide the between-step feedback required through GRF measurements, which can be aligned to available gait data sources.

Industrial ankle-foot test systems vary in loading methodology depending on their purpose: Shore Western and Thelkin systems which simulate wear on prosthetic device implement hybrid loading methods while the Pedatron actively loads the 'tibia' because it is used in a range of footwear/orthotic applications. Although cadaveric systems feature a mixture of active and passive tibia loading systems, prosthetic-based systems employ active and hybrid systems exclusively. This may be attributed to the additional simulation of muscle forces through the control of tendons; the system is easier to control when the cadaveric sample is fixed, such that the tendon cables don't need to stretch/move with the foot during gait. The test platform aligns much more closely with prosthetic-based systems where tendinous control is currently not considered and the Pedatron, as its implementation is to be focused on the testing of foot health devices. Following this and noting the scale of design required to produce a passive system vs implementing an off-the-shelf robotic arm, an active system is preferred for this project.

The stance duration, maximum loading force and DOF vary significantly between cadaveric and prosthetic ankle-foot systems. This may relate to the specific research aims of each system, as some attempt to simulate the action of the knee as well as the ankle, which inherently requires a greater number of DOF. Additionally, as mentioned before, the fragility of cadaveric specimen and additional control of tendons influences the maximum loading force and DOF. Industrial ankle-foot systems use much fewer axes, however, it is unclear how closely they align with cadaveric and prosthetic test systems as this information is not

available. The test platform does not intend to simulate the action of the knee or implement tendinous control, however, given it doesn't feature an ankle joint, the DOF around this joint would need to be fulfilled by the actuation system. A stance duration close to real gait (approximately 0.6s (Whittle, 2014)) is expected to be achieved.

The performance indicators obtained from cadaveric and prosthetic test systems mostly involve force and pressure measurements although systems using ultrasound measurements to measure tissue displacement and gyroscopes to estimate gait periods. Potential sources of measure used to capture product performance were previously identified in literature review 1 and these align with the measurement systems utilised within the reviewed actuation systems.

2.5.8. Conclusion

The implementation of the test platform with a phantom-foot aligns more closely with systems involving prosthetic feet, with a man-made structure representing the foot. No muscular control is required hence loading solely through the tibia satisfies the requirements of the system. Of the ankle-foot gait dynamic simulators investigated, the robotic arm-based systems implemented by Prisk and Marinelli are of greatest interest within an industrial environment as they offer a simple method of achieving the required loading forces and stance duration required. They also provide a feasible example of a robotic system to capture the product performance criteria required within this project. Given a similar robotic arm would also be capable of achieving 6 DOF, this would enable the key motion occurring during gait to be represented. Given the phantom-foot does not feature an ankle-joint unlike some cadaveric specimens utilised in cadaveric simulators, the action of this joint would need to be simulated using the robotic arms end-effector joint.

Additionally, robotic arms can be purchased "off-the-shelf" and so won't require significant adaptation for application within this project, are able to apply the required loading forces at physiologically accurate speeds and allow flexibility in test conditions as subroutines defining static and dynamic simulations can be programmed. Consequently, a robotic arm will be utilised within the test platform to fulfil the requirements of the system and enable orthotic and footwear product testing under sufficiently realistic loading conditions.

Chapter 2 has identified methods of analysing foot orthoses' performance, typical foot tissue properties, models of representing the foot in ways that are functionally relevant, reviewed existing models to actuate in-vitro and prosthetic foot models, and considered the

measurement needs of industry in use of the foot platform. Literature review 1 and the industrial needs analysis provided product performance criteria, informing the measurement systems required and test protocols. Literature review 2 provided mechanical and material properties of the components of the foot, while literature review 3 informed the phantom-foots' design to accurately represent foot kinematics during gait, with the SFM also providing kinematic data to inform the actuation system. Finally, literature review 4 provided a means of loading the foot.

Following the background information gathered in chapter 2, there are 4 key elements which the industrial test platform must satisfy.

1) Replication of the form, material properties and functional movement of an anatomical foot under gait-like loading which would allow foot health devices to be fitted and tested.

2) A manufacturing methodology capable of producing phantom-foot models with a high degree of repeatability, with the flexibility to change the sample population represented. This manufacturing process would ideally be accessible to the industry partner or the University of Salford (depending on where the test platform is situated), to allow for greater control in changing samples and to reduce outsourcing wait times and costs.

3) Reproduction of the loading forces and trajectory representative of a healthy human adult during gait; these variables should be adjustable so that samples of different populations can be represented.

4) The capacity to capture product performance criteria of interest such as location of peak pressure and joint motion to indicate product performance and allow product claims to be substantiated.

The next chapter describes a design specification for the test platform including the design of the phantom-foot, actuation system and measurement system required to characterise orthotic and footwear products to address the industrial problem.

2.6. Outcomes from literature reviews

Following the completion of the literature reviews several outcomes have been drawn out to inform the aims, objectives, and device specification of the test platform. Firstly, the orthotic function literature review revealed several primary outcomes which can be grouped into four FOs product performance criteria: impact on loading pattern (change to location of peak

pressure), impact on gait (change in foot kinematics), impact on shock absorption (reduction in loading rate/force), and impact on stability/balance (change to COP). The chosen methods to capture these outcomes within the test platform (to correspond with instrumentation used in clinical studies) are an in-shoe pressure capture system to capture changes in plantar pressure, a motion capture system to monitor changes in foot kinematics, and force plates for capturing loading. Next, the foot anatomy and material properties literature review examined material and mechanical characteristics of interest across the components of the foot and ankle. The primary conclusions drawn from this review were the importance of modelling the phantom-foot on a healthy individual with clear anthropometric information and the use of a single model rather than a range of models reduces the complexities of modelling various components in the foot-ankle complex. Additionally, within this PhD the use of Young's modulus to determine appropriate materials for modelling the phantom-foot is a pragmatic choice, given the difficulty in reproducing the non-linear anisotropic properties of human tissue and widely reported Young's modulus across biological and non-biological materials.

The phantom-foot form and function literature review compared and contrasted existing multisegment models to determine the most appropriate choice to model the phantom-foot. Less complex models provided an easier starting point with respect to manufacture but provided less accurate kinematic information. Conversely, more complex models offer better representation, but are more difficult to implement in practice. Ultimately the Salford foot model offered the best solution within this project with kinematic representation similar to the most complex model (Glasgow-Maastricht Foot Model), but easier manufacture. Moreover, a large existing dataset of healthy in-vivo participants modelled using this multisegment model was available to help validate the test platform. Finally, the human ankle-foot actuation systems literature review compared existing actuation systems to determine an appropriate solution to implement within the test platform. The implementation of the test platform with a phantom-foot aligns more closely with systems involving prosthetic feet, with a man-made structure representing the foot. A robotic arm was the most appropriate solution given the high load capacity (robot dependent), flexibility in changing actuation profiles and availability within the University of Salford. Given the test platform is designed to be used in a variety of test cases with different products and representing different gait patterns, a flexible system where the trajectory and loading parameters could be changed easily was important. A robotic arm offers this flexibility without comprising on

repeatability or other factors and therefore presented the best solution to meet the industrial requirements of this project.

Chapter 3: Device specification

3.1. Chapter overview

This chapter defines the aims, objectives, user needs and forms an industry test platform specification by integrating the information, data, and insights from chapter 1. Additionally, the specification is informed by the time-constraints of the PhD; a series of achievable targets and stretch goals were identified to ensure an operational test platform was delivered, with the option to add functionality and more appropriately address the industrial partners requirements where time permitted. Decisions have been made to primarily address the industrial requirements, rather than accurately reproduce human foot anatomy, as this was the primary goal of the test platform. Material tests were carried out to inform the design of the plantar tissue component of the phantom-foot. The outcome of this chapter is an initial design/iteration of the industrial test platform designed to fulfil the specification.

3.2. Aims and objectives

Following the literature reviews and assessment of the academic and industrial needs, the aims and objectives of the PhD project are defined as follows.

3.2.1. Aim 1:

To create a phantom-foot model that replicates the material and mechanical properties of the human foot during gait for orthotic testing purposes.

Objectives:

1. Identify the key material and mechanical properties of the human foot during gait.
2. Develop a prototype phantom-foot model that closely mimics these properties, including flexibility, impact absorption, and biomechanical response.
3. Validate the phantom-foot model through comparative studies with real human subjects to ensure accurate replication of foot behaviour during gait.

3.2.2. Aim 2:

To develop a comprehensive test platform that accurately assesses orthotic product designs under realistic loading conditions.

Objectives:

1. Design and engineer a versatile test platform that can simulate a range of biomechanical loading conditions representative of real-world scenarios encountered during gait.
2. Manufacture the test platform using materials and components that ensure durability, reliability, and precision in assessing orthotic product performance.
3. Validate the test platform through rigorous testing against established standards and comparative studies to ensure accuracy and repeatability of results.

3.2.3. Aim 3:

To evaluate the effectiveness of the developed test platform through comparison with in-vivo orthotic experimental protocols.

Objectives:

1. Define an experimental protocol that replicates in-vivo orthotic testing conditions and parameters used in clinical studies.
2. Conduct experiments using both the developed test platform and clinical studies on existing therapeutic products.
3. Analyse and compare the results obtained from the test platform with those from clinical studies to assess correlation and effectiveness.

3.3. User needs

Clinical studies are fundamental to evaluating existing and new orthotic products. However, studies performed by industry and those performed by investigators within academic institutions differ in their goals and protocols. The results of an academic clinical study are not intended to be used for commercial or promotional purposes (Bhatt, 2019). Rather, research is aimed at understanding FO mechanisms and providing an evidence-base for the prescription/usage of FOs by healthy and populations experiencing foot pathology. Conversely, industrial clinical studies are to fulfil regulatory requirements and provide evidence for success of a new FO for marketing and promotional purposes.

From an academic perspective, there are barriers in current practices which the test platform will overcome. There are significant ethical regulations and practices which must be followed in trials involving human participants, particularly populations experiencing foot pathology.

The test platform provides an opportunity to model a healthy or populations experiencing foot pathology and test FOs, without the need for any ethical approval, burden on participants and associated costs. As a result, clear indications of product performance can be established quickly and efficiently. Moreover, it provides a baseline to separate the effects of a product and inter-subject variation more clearly. To achieve this, the test platform is required to align with clinical test protocols as closely as possible. This includes the product performance criteria captured (e.g., impact on gait), assessment protocol (e.g., walking for a specified number of steps), and the measurement systems employed (e.g., force plate). Additionally, the test platform is required to be flexible such that different populations can be represented; this includes but is not limited to flexibility in scaling the phantom-foot, changing the loading force applied, tibial angle at initial contact, stance time (represented by loading time) and changing the stiffness properties of the plantar tissue such that different foot sizes, age ranges and bodyweights can be investigated.

The current pathway for product testing by the industrial partner includes mechanical testing (e.g., with the Satra Pedatron), clinical studies (if the product is classified as a medical device) and finally customer surveys, to establish product claims. The Satra Pedatron is a test platform that applies a trajectory similar to human gait to a foot-shaped indenter and repeatedly loads footwear for the purpose of durability testing.

There are several issues present. Firstly, products that aren't classified as medical devices do not undergo clinical testing or human trials in controlled settings. Most orthotic devices are class 1 medical devices (and hence require a clinical evaluation) however, this is only the case when a product is "intended for a medical purpose" (Medicines & Healthcare products Regulatory Agency, 2002). Outside of these cases, where a product does not fulfil a medical purpose, the industry partner has previously relied on consumer surveys to determine the effectiveness of a product. This is problematic as product claims cannot be well-substantiated without quantitative data on the mechanisms of effect (e.g., pressure, which is known to be related to pain), and qualitative surveys of this type can be skewed by various means including brand awareness, the nature of the questions asked and even the placebo effect (J. Lee et al., 2015). Moreover, the orthotic function literature review highlighted conflicting evidence on the performance of different FOs due to variations in test protocols. As non-medical products comprise most comfort products, this heavily impacts the industrial partners ability to make product claims and appears as a large issue within the broader orthotics

market as a whole – in 2020 approximately 88% of insole sales came from off-the-shelf products (Fact.MR, 2021).

Secondly, the nature of in-vivo clinical trials limits the ability of the industrial partner to test design iterations to a high resolution (i.e., small changes in material density, thickness etc) due to the nature variations in human gait (e.g., change in stride length, walking speed), and potential response bias if a participant changes how they walk within a test environment (Christopher, Drouin, & Houglum, 2006). Insufficient and ineffective product efficacy testing prior to clinical trials poses high risks to the development process, with several iterations of clinical tests leading to delays and escalating costs. This may also cause functional deficits due to the pressure to keep design iterations to a minimum. The test platform addresses this deficiency by providing a highly repeatable test environment but is not required to recreate the nature variation observed between in-vivo participants.

Finally, it is important to recognise the function of the test platform within the existing product development cycle. The test platform is intended to compliment, not replace clinical studies; these are required to fulfil regulatory requirements for FOs defined as medical products. Specifically, the test platform is required to characterise product performance such that product claims can be verified, and design iterations compared, but is not required to determine the physical performance of the product over time e.g., its' durability, longevity etc. This will influence the number of loading cycles performed within the test protocol and allow a more accurate but less robust plantar tissue model to be selected which aligns closely with the anatomical foot. Fidelity in the representation of internal foot structures is important given their impact on the plantar pressure and joint kinematics e.g., different foot shapes have been shown to influence plantar pressure patterns (Hillstrom, Song, & Kraszewski, 2013; Mootanah, Song, & Lenhoff, 2013). Moreover, plantar pressure is determined by bony prominences which would not present the same way if a prosthetic foot was used for example. Hence why the phantom-foot is required as opposed to e.g., a Sach foot.

3.3.1. Industrial considerations and partnership

Given the link between this project and the industrial partner, it was important to establish methods of communication and a decision-making process at the beginning of the project. Primary decision-making responsibilities lay with the student and University of Salford with quarterly meetings established with the industrial partner to provide progress updates. The products to be evaluated by the test platform in its first implementation were decided by the

industrial partner; given the first phase of testing would focus on the hindfoot and midfoot, products which were intended to act upon this area of the foot were elected. Additionally, a product performance criterion was established based upon the existing criteria used by the industrial partner to characterise previous orthotic products.

3.4. Final specification

Chapter 2 informed the specification of requirements for the industrial test platform from each literature review. Literature review 1 called for a test platform capable of evaluating product performance based on criteria commonly reported in clinical studies, which acknowledges the needs of academic and industrial stakeholders. Literature review 2 called for a requirement of a stable/repeatable phantom-foot structure such that the test platform is an improvement on current variability seen in vivo. Literature review 3 called for the phantom-foot to align closely with the anatomy of the human foot, and the representation of the foot using a multi-segment model. Finally, literature review 4 called for a robotic arm-based actuation system capable of delivering loads representative of an adult human at speeds representative of normal walking gait.

The requirements of each literature review are not necessarily complimentary. For example, literature review 2 called for the manufacture of a phantom-foot whose material properties aligned as closely as possible with a human foot. However, this may have reduced the durability of the phantom-foot and hence compromised the requirements of literature review 1, as sufficient data would not be captured to characterise orthotic product performance. Consequently, the design process involved iterations to identify a solution which sufficiently satisfied the requirements of each literature review, with priority given to literature review 1 as it was critical to the implementation of the test platform.

The test platforms' requirements are available within

Table 21 and the specification is defined in Table 22.

Table 21: Test platform requirements

Component		Purpose	Material and Mechanical Requirements
Phantom-Foot	Bone Segments	Transfer load from actuation system to plantar tissue	(R1) Young's Modulus: 7300 MPa
	Plantar Tissue	Mimic plantar tissue under loading and interface with products	(R2) Young's Modulus: 700-1000 kPa (R3) Unloaded Thickness: 15mm (Heel), 10mm (Metatarsals, Phalanges)
	Pseudo-ligaments	Connect bone segments and allow motion	(R4) Young's Modulus: 10MPa
	Pseudo-cartilage	Reduce friction between bone segments	(R5) Lower coefficient of friction than produced skeletal components
Actuation System	Robotic Arm	Actuate phantom-foot and apply repeatable, realistic loading forces	(R6) Peak velocity: >=3ms^{-1} (R7) Peak acceleration: >=55ms^{-2} (R8) Continuous load rating: >=1000N (R9) Degrees of freedom: >=6 (R10) Workspace: >=1m^{2}
Measurement System	In-shoe Pressure Capture System	Capture plantar pressure under loading	(R11) Shoe size: UK men's 8.5 (R12) Permitted load: >=1000N (R13) Capture rate: >=100Hz
	Motion Capture System	Capture joint segment motion during loading	(R14) Marker size: <9.5mm diameter (R15) Capture rate: >=100Hz (R16) Number of markers: >=11 (R17) Marker placement: Salford foot model
	Force Plate	Capture force profile during loading	(R18) Permitted load: >=1000N (R19) Capture rate: >=100Hz

Table 22: Test platform specification

Component	Specification
Phantom-Foot	(S1) Design anatomically accurate bone segments and plantar tissue that mimic human foot biomechanics (S2) Utilize materials with specified Young's modulus and thickness for realistic load transfer and deformation (S3) Incorporate pseudo-ligaments and pseudo-cartilage with defined mechanical properties for joint stability and reduced friction between bone segments
Actuation System	(S4) Implement robotic arm with ≥ 6 degrees of freedom for realistic foot motion simulation (S5) Ensure peak velocity, acceleration, and continuous load rating meet or exceed specified requirements (S6) Design control interface and programming software for precise, repeatable motion control and load application
Measurement System	(S7) Select and integrate in-shoe pressure sensors, motion capture cameras, and force plates (S8) Ensure measurement accuracy, capture rates, and compatibility with experimental conditions (shoe size, load, capture frequency) (S9) Develop data processing and analysis methodology for biomechanical data interpretation and visualization

3.5. Conceptual design

A conceptual design was designed where the components of the test platform were developed virtually prior to any manufacture, to guide the decision-making process following the definition of the design specification. Guidance was taken from similar models within the literature such as the BAREFOOT model (Johnson, 2018) to determine possible manufacturing pathways, particularly with regards to the phantom-foot (as the robotic arm and measurement systems wouldn't require manufacturing processes). Additionally, low-cost choices were preferred to ensure the project budget wasn't exceeded, and low-risk options were favoured given the context in which the PhD was undertaken; Covid-19 significantly altered the project plan and provided a risk to the project throughout. An example of this

included choosing manufacturing methods which required less in-person laboratory time e.g. 3D printing rather than more intensive methods.

3.5.1. Phantom-foot

A key element of the industrial platform was the creation of a realistic foot interface between the loading mechanism and orthotic/footwear product, which mimics the material properties and kinematics of a human foot. A phantom-foot was proposed comprising a rigid skeletal system which follows the morphology of a healthy adult foot. It was designed to fit each element of the design specification, featuring bone segments, plantar tissue, pseudo-ligaments, and pseudo-cartilage as defined previously.

Bone segments would be grouped according to the SFM which was elected in chapter 2. The SFM was preferable to other models given the segment range of motion, the motion pattern and timing of motion for this model were largely comparable to that of existing literature for the most complex model, which individualised each bone and was assumed to be the most accurate. However, it presented an easier target to achieve within this project as the manufacture of components durable enough to withstand loads representative of gait would be significantly easier with larger bone segments. Additionally, extensive data from previous studies which utilised the SFM were available which would help validate the test platform, which made it more appropriate than creating an entirely new multisegment model.

Solidworks (Dassault Systèmes, France) is 3D modelling software used to design components and includes material property definition as well as virtual test capabilities. It was used to develop a virtual conceptual model of the phantom-foot, with bones linked together using a flexible, elastic material which acted as a pseudo-ligamentous structure; the material could be used to vary the range of motion for each segment by varying the spacing between bone segments, and varying the tension placed on the material once the phantom-foot would be produced. A thin coating was suggested to line the ends of each segment to act as a low-friction cartilaginous substitute as employed by Zhu in an anthropometric robotic finger (Zhu, Wei, Ren, Luo, & Shang, 2023). Finally, a plantar tissue model was designed to encapsulate part of the skeletal system whilst allowing access to the dorsum to allow the measurement system to capture segment motion. The material properties of the virtual model corresponded to those of cadaveric plantar tissue discussed in chapter 2. Figure 20: shows the conceptual virtual phantom-foot.

Figure 20: Conceptual Skeletal and Plantar Tissue parts which form the phantom-foot

3.5.2. Actuation system

To translate the phantom-foot along gait-like trajectories and thereby apply accurate loading forces, an actuation system is required. Chapter 2 examined actuation systems currently used within industrial and research applications. Given the test platform is designed to be used in a variety of test cases with different products and representing different gait patterns, a flexible system where the trajectory and loading parameters could be changed easily was important. A robotic arm offers this flexibility without comprising on repeatability or other factors and therefore presented the best solution to meet the industrial requirements of this project.

As a 588-784N sample was intended to be sampled, and during gait-like trajectories for walking the real foot can experience loads of 120% bodyweight, the continuous load capabilities of the arm was required to support approximately 1000N. RoboDK (RoboDK, Canada), a robotic simulation platform which supports a range of robotic arms, was utilised to create a virtual environment in trajectories could be generated and applied to any robotic arms supported by the software. Figure 21 shows the expected layout of the phantom-foot and robotic arm within the RoboDK platform. Several existing data sources were available to inform the specification of the actuation system. This included gait parameters such as the velocity, acceleration and loading required to represent a 588-784N male sample. However, adaptation of the system may be required in future when representing different samples,

hence the actuation system was required to exceed these initial parameters. Jarvis' work is a primary source of this data (Nester, Jarvis, Jones, Bowden, & Liu, 2014).

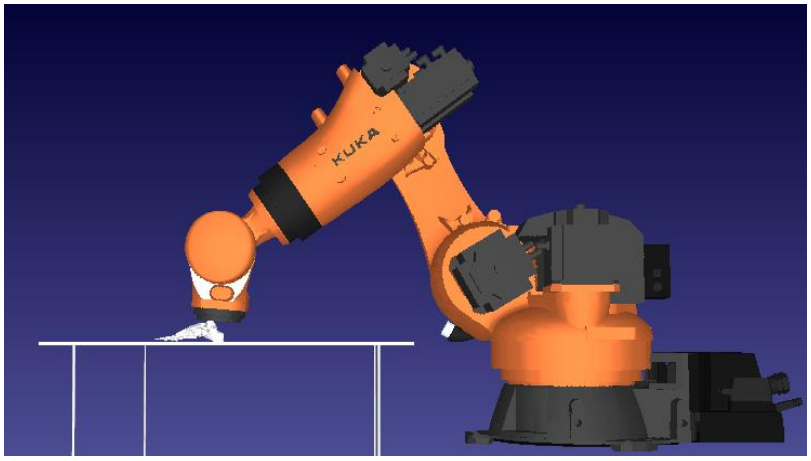

Figure 21: RoboDK software simulation package with skeletal foot model

3.5.3. Measurement system

A measurement system implemented in conjunction with the phantom-foot and actuation system would allow the product performance criteria of interest identified in the industrial needs analysis to be captured, and product claims to be verified. As detailed in the industrial needs analysis, the following were required: a method of capturing foot kinematics, location of peak pressure and ground reaction forces. An in-shoe pressure capture system was selected for plantar pressure mapping, and a force plate for ground reaction force measurements. Additionally, force-feedback is not available with all robotic arms to provide a means of force-feedback, hence the force plate was also utilised to tune the trajectory of the actuation system between steps. The arrangement of the force and pressure sensors were similar to the protocol implemented within clinical studies identified in chapter 2. A conceptual arrangement of the measurement system can be seen in Figure 22.

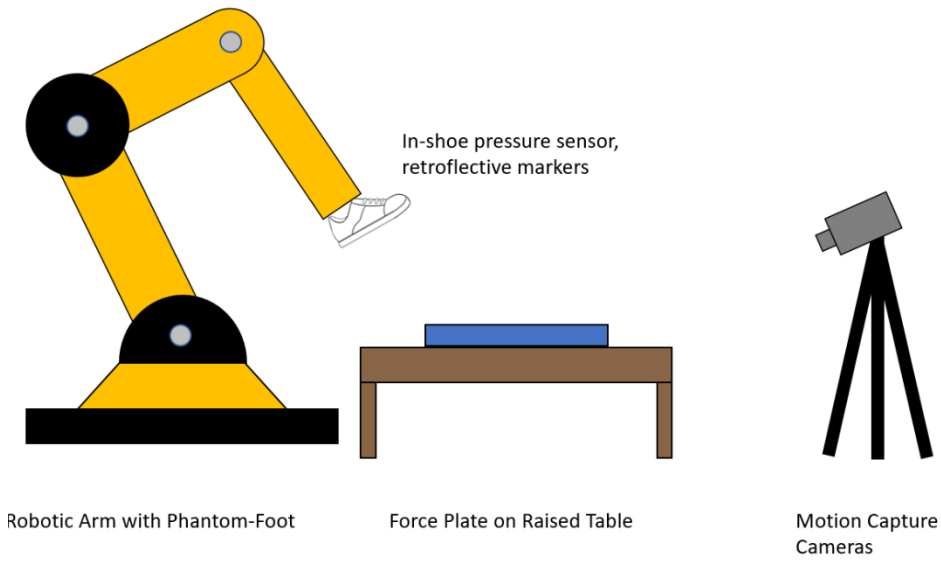

Figure 22: Conceptual Design of the Measurement System

3.5.4. Stretch goals

The PhD timeframe was sufficient to produce an industrial test platform capable of fulfilling the two established use-cases of the industrial partner. However, the flexibility to 1) change test protocols to facilitate the testing of new products and 2) add complexity to the actuation system or phantom-foot to represent different populations and gait conditions, was key for the industrial test platform to effectively satisfy the needs of the industrial partner for potential future test requirements. This flexibility would also allow for the test platform to applied within research contexts e.g., in the study of lower limb prosthetic devices. The additional elements which could be applied to the test platform were defined as “stretch goals” and would be incorporated within the project depending on 1) the performance of the industrial test platform after meeting the core requirements and 2) the timeframe remaining following this initial implementation. Figure 23 describes the proposed stretch goals and their dependencies determining their fulfilment.

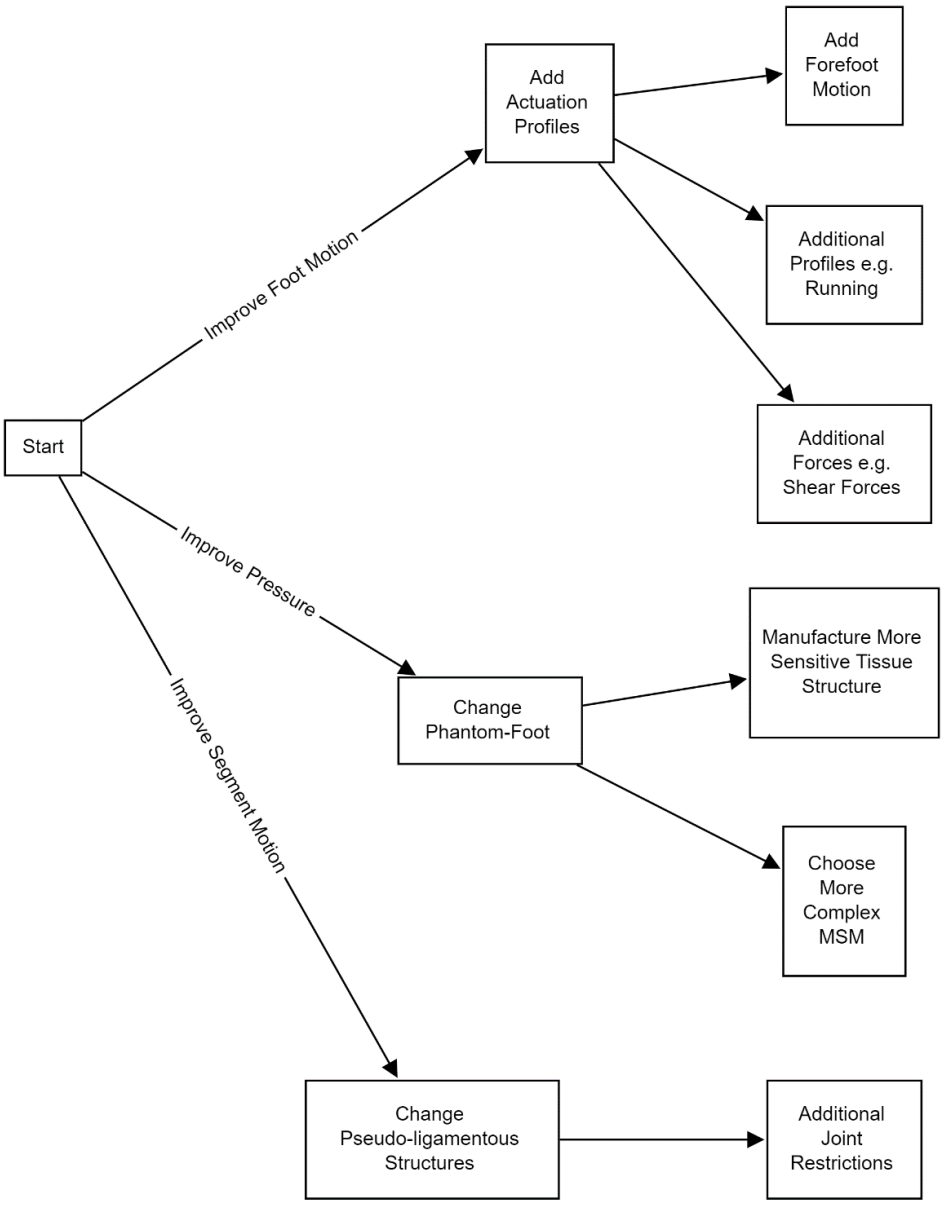

Figure 23: Possible stretch goals depending on the variable elected to improve

3.6. Phantom-foot design and manufacture

3.6.1. Material selection

The material requirements of the phantom-foot were defined in the previous chapter to correspond to in-vitro data. However, the material also had to be stable enough under cyclic loading to function within an industrial test setting. A previous project with the industrial partner involved testing insoles with layers of different materials. This work indicated that material changes plateaued after ~200 cycles, with the ground reaction force decreasing until stable due to the material compressing/relaxing over time. Hence, 100-1000 cycles were

selected to characterise product performance, to ensure both the phantom-foot and foot health product are stable i.e., producing a consistent response under loading, and their behaviour when stable is evident. None of the materials were expected to degrade over a short time span when unused (i.e., weeks/months).

Numerous technologies exist which could be used to produce materials which met the requirements of the phantom-foot (properties and morphology) including casting and 3D printing. Both technologies allow for the materials of varying Young's modulus to be utilised, from 0.01 to 1000MPa, and the stress/strain properties of these materials to be tuned: in casting by using deadener to soften silicon gels (Ahmadzadeh & Hukins, 2014) and through producing lattices rather than solid parts in 3D printing (Reddy, Davuluri, & Boyina, 2020) or by printing using multi-materials (Lopes, Silva, & Carneiro, 2018). 3D printing was preferred within this project for several reasons. Firstly, changes to the sample to be printed and rapid prototyping could more easily be performed, and less manual work would be required to manufacture each part, making it suitable within both research and commercial environments. Next, it aligned with the current development and testing pathway utilised by the industrial partner, with product stress-testing already incorporating the use of 3D printed indenters (Satra, UK), and changes to the sample could be made efficiently via 3D modelling. Finally, given the context in which this project was developed during the covid pandemic, availability to the manufacturing facilities at the University of Salford were limited and prone to change. As such, a manufacturing methodology where less manual work was required provided a lower risk solution in comparison to casting, or a similar manually intensive method.

Stereolithography (SLA) printing involves the use of an ultraviolet laser to fuse photosensitive resin into the desired shape (Huang, Qin, & Wang, 2020). There are several benefits and limitations associated with this printing method. Advantages include the production of high-quality 3D models, strong pattern/lattice structures with small layer heights which decrease or eliminate layer lines entirely and unused resin can be saved and reused (Melchels, Feijan, & Grijpma, 2010). All the disadvantages of this method are linked to the resin printing material: care must be taken to add drainage holes to hollow models to prevent cupping and allow excess resin to be removed, models must be washed, cured, and dried which adds additional time to the manufacturing process, and only a single material can be used at a time. An alternative printing method is Polyjet, which also uses ultraviolet light to fuse material together, however, uses photopolymer droplets rather than photosensitive

resin (Patpatiya, Chaudhary, Shastri, & Sharma, 2022). Consequently, Polyjet parts are produced fully cured and don't require additional post-processing. Multiple materials can be used simultaneously, meaning support structures can be produced in a soluble gel to allow for easy removal, and the material properties of each part can be tuned i.e., the Young's modulus can be altered. The only method to achieve this effect using SLA printers is to vary the internal structure of the model, designing a 3D lattice rather than producing a solid part (Johnson, 2018). Lattice microstructures can be generated and encapsulated by a thin outer shell to increase the compressibility of a given material.

Both SLA and Polyjet printers can produce flexible parts, however, the latter are significantly more expensive to purchase (minimum £6000-£70,000 compared to £3000) and have significantly higher operational costs due to high energy consumption. This large cost reduced the feasibility of Polyjet printing within this project, and SLA printing was elected instead. However, if costs were to reduce in the future, it would serve as a more effective manufacturing method in the production of phantom-foot models.

3D printable materials which accurately represent the properties of human soft tissue are currently not available (Mashiko, Konno, Kaneko, & Watanabe, 2015). Flexible resins compatible with SLA printers are available with shore hardness values between 50-80A. Shore hardness is a description of an elastomers' hardness, and can be roughly correlated to Youngs' modulus values using Gents' equation (Gent, 1958):

$$E = \frac{0.0981(56 + 7.62336S)}{0.137505(254 - 2.54S)}$$

Equation 15: Where E is the Youngs modulus (MPa) and S is the ASTM D2240 Type A durometer

Conversion between shore hardness and Young's modulus presented some error according to the shore hardness of the material being tested (Qi, Joyce, & Boyce, 2003). However, it was sufficient within this project to provide an approximation of the range of materials that would be suitable to produce the phantom-foot, with the exact Young's modulus of the material varied using internal lattice structures. From Equation 15 (assuming E = 0.7 – 1MPa), the estimated shore A hardness ranges between 30-37. As the phantom-foot is expected to require greater than in-vitro tissue durability (given its industrial application), a resin of shore hardness 80A was selected for manufacture. It was difficult to accurately compute the elastic properties of a lattice design prior to manufacture, hence trial and error was the primary method to manufacture parts of a specific elasticity (Molodov, 2013). Consequently, several

lattice profiles were generated and tested to identify the most appropriate structure (see Figure 24).

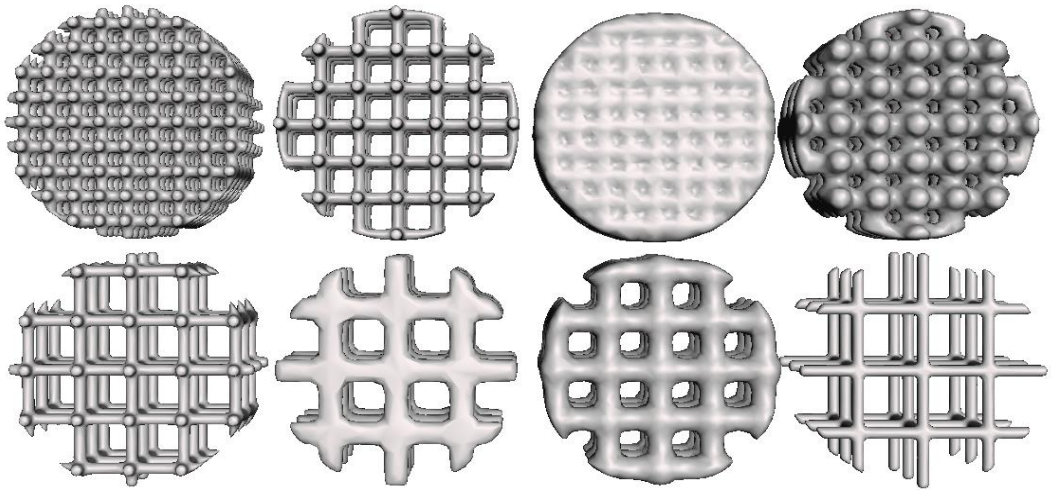

Figure 24: Examples of lattices generated using Meshmixer

Autodesk Meshmixer (Autodesk, California, USA) was used to generate each cubic lattice. Meshmixer only allowed square lattices with cylindrical columns, and samples varied in element diameter and element spacing. Cylinders with a diameter of 19mm and a height of 11mm were generated to match the dimensions of cadaveric samples from a previous study and the samples printed by Johnson (Pai & Ledoux, 2010; Johnson, 2018). Figure 25 shows an example of a lattice structure generated from a solid cylinder.

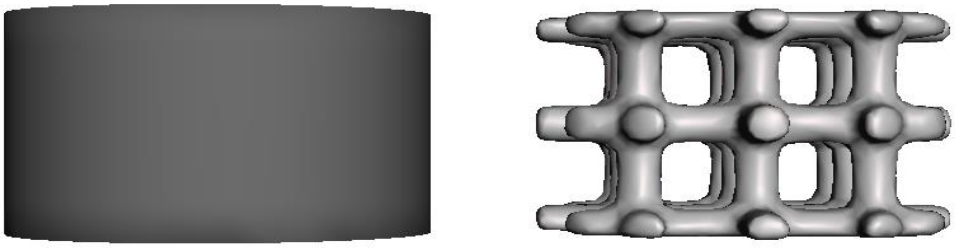

Figure 25: Decomposition of solid cylinder to mesh lattice using Meshmixer

Element diameter and element spacing were limited to integer values as a starting point, with the former varied between 1-2mm and the latter 2-5mm due to the maximum resolution of the printer. Samples were printed using a Formlabs Form 3 SLA printer (Formlabs, Massachusetts, USA): this was due to its high resolution (25 microns), small layer thickness (25-300 microns) which enabled a greater range of lattice structures, user friendly and large library of flexible resins. Samples were post-processed following the manufacturer's instructions using isopropyl alcohol to clean the print before drying and curing.

A Zwick Roell (Zwick Roell Group, Germany) hydraulic press was used to test the material properties of each sample (cite). 15 triangular waves were applied at a frequency of 1Hz, with materials loaded to 300N of force. The first 14 cycles were used to condition the material, with the stress/strain characteristics calculated using the final cycle. Young's Modulus values were calculated using Equation 2 at 50% peak strain using the proprietary software TestXpertII (Zwick Roell Group, Germany) to correspond with the test protocol applied by Pai and Ledoux (Pai & Ledoux, 2010).

$$E = \frac{\sigma}{\varepsilon} = \frac{F/A}{\Delta l/l}$$

Equation 2, where E is the Youngs modulus, σ is the stress, ε is the stress, F is the applied force, A is the cross-sectional area, Δl is the material displacement and l is the initial thickness.

Figure 26 shows the calculated Young's modulus values for each lattice design compared to the cadaveric sample range from chapter 2.

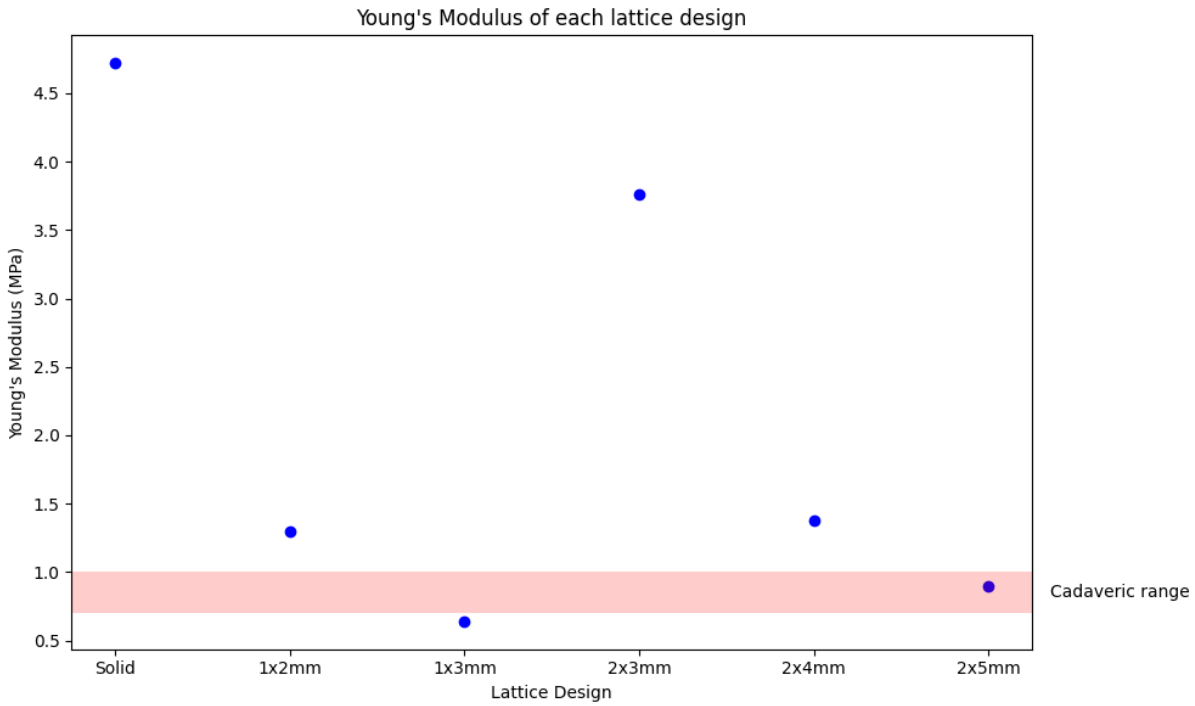

Figure 26: Lattice designs and their corresponding Young's modulus values compared to the cadaveric sample range (yellow area)

Of the designs tested, the 2x5mm lattice fell within the cadaveric Young's Modulus range derived in chapter 2. However, when loaded up to 800N during a feasibility test, the phantom-foot was unable to withstand 200 cycles of loading without deteriorating. Consequently, a lattice design of a greater than in-vitro Young's modulus was required to fulfil industrial test requirements. The 1x2mm and 2x4mm designs were both investigated as alternatives; the latter was significantly easier to produce due to the maximum printing

resolution available, and able to withstand a minimum of 500 loading cycles of 800N. The effects of this higher-than-expected Youngs modulus value on the behaviour of the phantom-foot (namely location of peak pressure) is addressed in chapter 4 during validation of the test platform.

3.6.2. Phantom-foot development and production

Two subsystems of the foot core are relevant for the design of the phantom-foot: the passive subsystem consisting of the bones, ligaments and joint capsules that maintain the various arches of the foot, and the active subsystem consisting of the muscles and tendons that attach on the foot (McKeon et al., 2015). Within the passive subsystem of the human foot, numerous joint interfaces exist to produce the complex movements that occur during gait. The talocrural joint is a hinge joint formed between the distal tibia-fibula and talus that allows dorsi/plantarflexion in the sagittal plane (Claassen, et al., 2019). Within the test platform, this motion would be satisfied by the actuation system i.e., via the connection between phantom-foot and actuation system. The interphalangeal joint formed between the phalanges of the hallux performs the same motions in the sagittal plane (Angin & Demirbuken, 2020). The calcaneocuboid joint is a modified saddle joint which forms part of the midtarsal joint and is found between the anterior facet of the calcaneus and posterior cuboid; very little movement occurs although slight flexion/extension in the sagittal plane has been observed (Bonnel, Teissier, Colombier, Toullec, & Assi, 2013). The subtalar joint, a condyloid joint formed between the talus and calcaneus, is not represented as the calcaneus and talus are represented by a single segment; this will result in a loss of the kinematics and deformation which takes place in the joint such as its stabilising of the surrounding soft tissues (Noginova, 2021). Although the tarsometatarsal joint complex is divided into 3 columns physiologically (Wang, Li, & Zhang, 2014), the SFM simplifies this to a medial and lateral segment, both of which are planar joints formed between the cuneiforms and metatarsals. Finally, the condyloid metatarsophalangeal joints formed between the metatarsal heads and proximal phalanxes are represented by medial and lateral segments which primarily produce flexion/extension in the sagittal plane, and additionally some abduction/adduction in the transverse plane (Wang, et al., 2021). Figure 27 displays some of the joints modelled within the phantom-foot.

Figure 27: Metatarsophalangeal (left), Tarsometatarsal (centre) and Calcaneocuboid (right) joints modelled within Solidworks.

To design the phantom-foot in accordance with specification point S1 (see Table 22), an adult Japanese male model was downloaded from BodyParts3D (Mitsuhashi et al., 2009), a dictionary-type database for anatomical structures. The model was based on a single sample, created from a whole-body set of MRI images and supplemented by 3D editing (Nagaoka et al., 2004). The sample is a representative 22-year-old Japanese male with a mass of 588-784N and 172.8cm tall; these values are close to the average height and mass of Japanese 18-30-year-old males, which are 171.4cm and 620.97N respectively. This is slightly different to the average UK male: 175.3cm and 820.12N. Additionally, the feet of Japanese males and females have been found to be wider than Australoid and Caucasoid participants of similar foot length (Kouchi, 1998; Jurca, Zabkar, & Dzeroski, 2019), and differ in forefoot shape (Hawes, et al., 1994). The larger plantar surface area of the phantom foot model may result in a slightly different plantar pressure distribution compared to an actual human foot. However, this was not expected to invalidate the performance characterization of the product or reduce the capacity of the test platform to enable testing of design iterations. Nevertheless, if the industrial partner plans to launch country-specific products, it would be more appropriate to use phantom foot models that correspond specifically to the foot anthropometry of those populations when implementing the test platform. The manufacturing process to produce the phantom-foot can be seen in Figure 28.

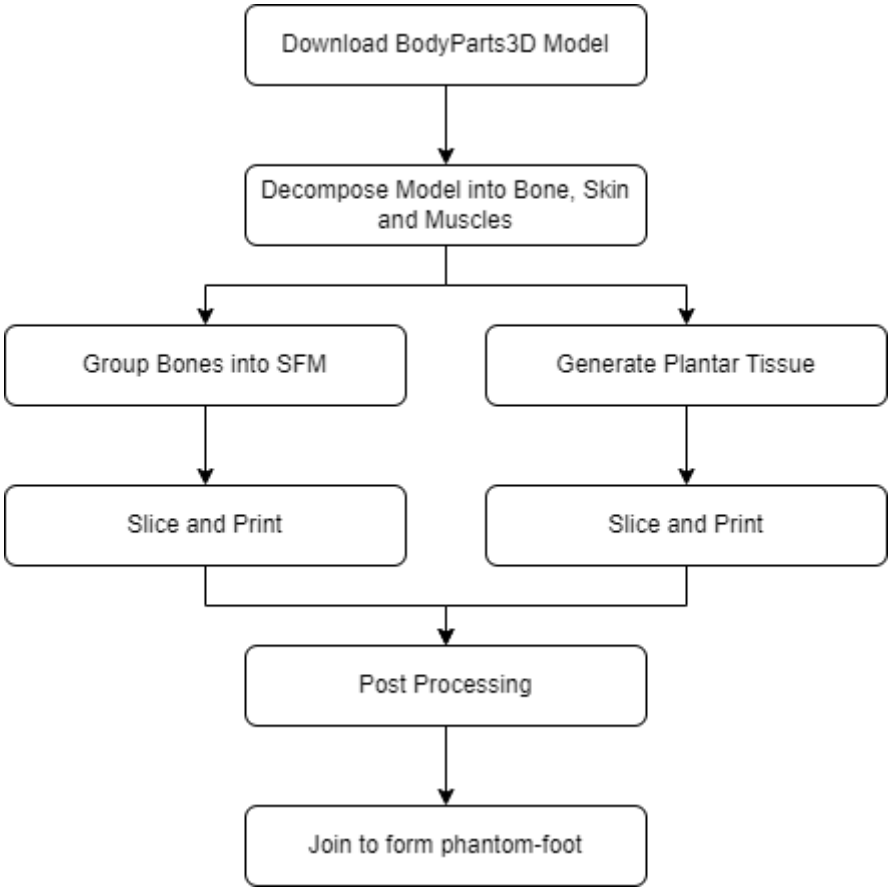

Figure 28: Manufacturing process to produce phantom-foot model.

A full body skeleton model and skin model were downloaded from the online repository BodyParts3D in STL format and imported into Solidworks as solid bodies. Several extruded cut commands reduced the models to only represent the left foot, before each solid body was individualised to separate muscular, skeletal, and skin components. Muscular components were then suppressed before a Boolean combine operation filled the gap between the skin and skeletal frame to form the plantar tissue model. The tissue and skeletal models were then imported and managed separately within Meshmixer. Bones were grouped together according to the SFM; this was achieved by adding struts between bones to be linked together, which when 3D printed would fuse the parts together. Bone segments were also hollowed to allow the pseudo-ligamentous structure to be threaded through them; the hollow command was performed such that the geometry of the downloaded foot model would be preserved. This would reduce the structural integrity of the parts; however, they would still sufficiently meet the specification and support full weightbearing. Finally, a flange plate designed to fit to the end effector of the actuation system was modelled and fused with the calcaneus-talus segment, with slots to accommodate bolts. This process was designed to satisfy specification points S2 and S3 (see Table 22).

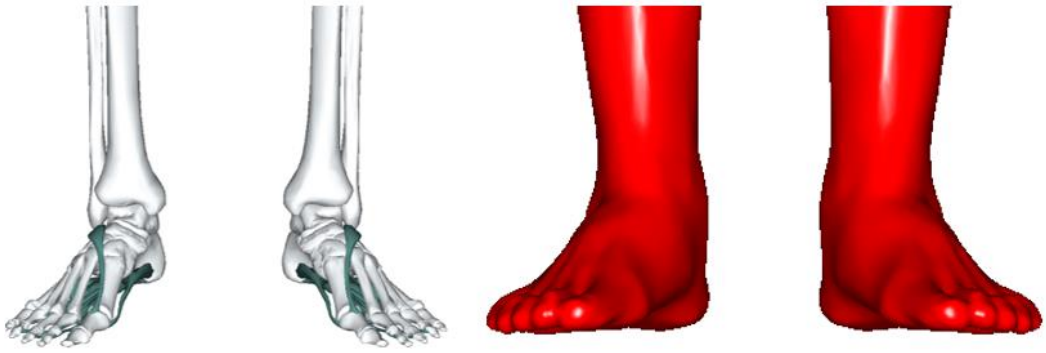

Figure 29: Skeletal and Skin Models Imported from BodyParts3D prior to processing

An Ultimaker S5 (Ultimaker, Netherlands) was chosen to produce the skeletal components as its print bed size allowed multiple models to be printed at once and models of sufficient accuracy could be created rapidly. Ultimaker Cura Express, the 3D printers' proprietary software, was used to slice the skeletal components and reduce the infill percentage to improve the rate of production; this allowed initial prints of 20% infill to be produced to confirm the quality of the created model prior to producing the final parts of 50% infill. The skeletal model was 3D printed using PLA (satisfying requirement R1). Polyethylene terephthalate (PET) tape was added between joint articulation surfaces to reduce surface friction (satisfying requirement R5).. Support material was removed from the PLA parts using pliers and a file before threads of NinjaFlex filament was glued into each phalange using two-part epoxy and threaded through the centre of each bone segment to link the segments together and form the pseudo-ligamentous structure (satisfying requirement R4).. This maintained the geometry of the phantom-foot and restricted joint motion to result in similar joint ranges of motion to the anatomical foot, as the space between bone segments could be modified by reducing the tension placed on the filament. However, it is different to the anatomical foot as individual ligaments have been represented as grouped structures within the phantom-foot. The recreation of accurate skeletal structures was expected to result in arthrokinematics comparable to the in-vivo foot (Loudon and Bell, 1996). Datasheets for the materials used can be found appendices I – L.

Kinematic analysis of the foot joints helps to establish joint axis centres and dominant planar motions. The most important joints within the ankle joint complex (in the context of the use cases identified), which have the primary responsibility of transferring load during the early parts of gait, are the talocrural and subtalar joints, however, the latter is fixed within the phantom-foot. The axis of rotation of the talocrural joint is approximately 13°-18° laterally

from the frontal plane at an angle of 8°-10° from the transverse plane (Houglum, 2012; Lundberg et al., 1989). Typical ranges for dorsiflexion and plantarflexion are 0°-25° and 0°-50° respectively. Consequently, the pseudo-ligamentous structure was designed to recreate

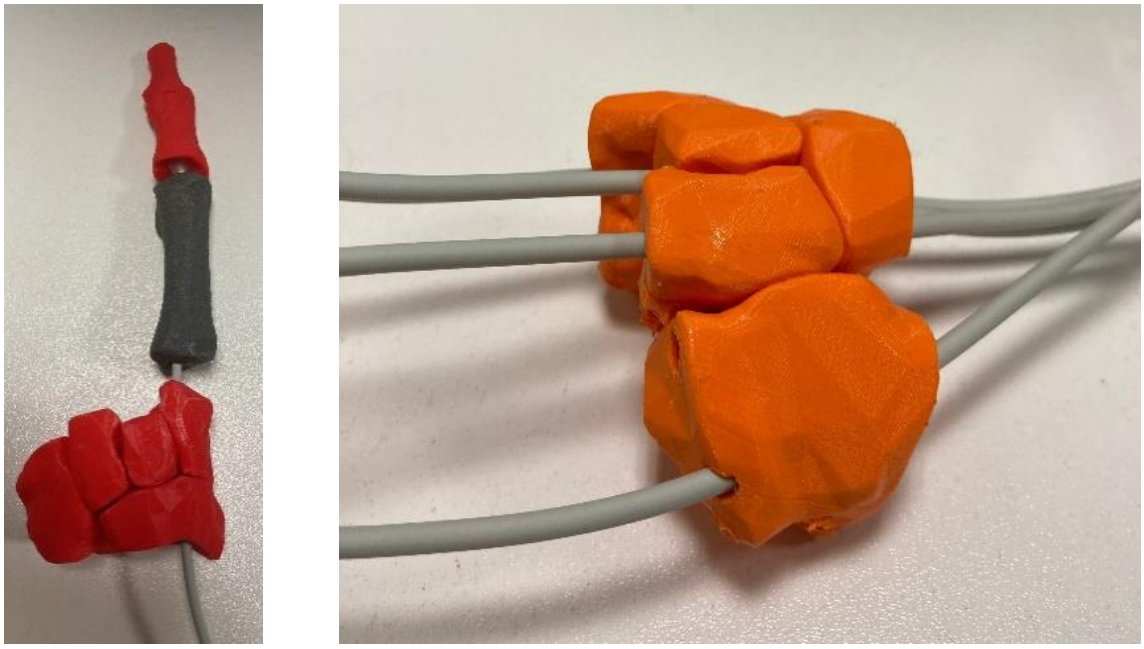

Figure 30: Pseudo-ligaments threaded through bones and linking segments

this range of motion within the phantom-foot.

An important mechanism in the propulsion of the human foot during stance phase is made possible by the midtarsal joint locking and unlocking (Okita et al., 2014). During gait, the foot has been described to transition from providing shock absorption during heel strike, weight support and transfer in mid-stance and acting as a rigid lever arm for propulsion in the terminal stance (Tweed et al., 2008). The phantom-foot may exhibit slight differences in joint motion during loading due to the grouping of bony segments; the smaller movements performed by these individual bones in-vivo may contribute to larger movements at the distal and proximal segments when the bones are grouped. Moreover, the simplification of the foot model i.e., the exclusion of tendinous structures, would result in much less force applied through the forefoot in the terminal stance, likely moving the final COP further posteriorly than in the human foot. And the phantom-foot did not represent the sub-talar joint as the talus and calcaneus are grouped in the SFM. Consequently, the representation of the midtarsal joint locking mechanism did not directly align with the human foot. However, this was not expected to affect the behaviour of the phantom-foot with the orthotic products during the beginning of stance phase to mid-stance, which would be sufficient for the characterisation of each products' performance.

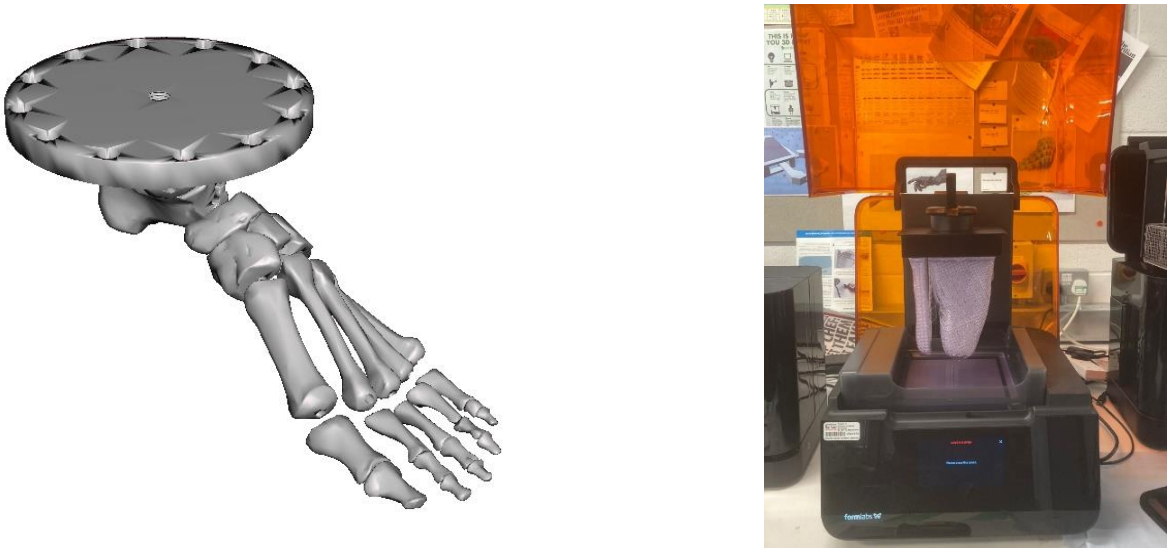

Figure 31: SFM Model as modelled in Meshmixer (left) and Formlabs Form 3 used to print plantar tissue components (right)

A 3D printed plantar tissue component made from Formlabs flexible 80A resin was chosen to recreate the shock absorption characteristics of the plantar tissue, maintaining the arches of the foot alongside the pseudo-ligamentous resin threaded through the bony segments by being fixed to the heel and phalanges (satisfying requirements R4-R5). This helped recover the unloaded position of the skeletal anatomy between cycles via elastic recoil. The plantar tissue model was imported into Meshmixer and hollowed to a 1mm shell before which a lattice pattern was applied to fill the structure. A cubic lattice of 2mm element diameter and 4mm spacing filled the solid, which was the structure selected following the material tests completed earlier in this chapter. A Formlabs Form 3 was used to produce the plantar tissue models, allowing two models to be printed per cycle, however, the limited print bed size meant that the model had to be printed in two separate pieces which would be joined together following production. This was acceptable within the context of the PhD project as the two pieces were aligned and joined using the same resin used to produce each part to create a strong, seamless bond, and as only heel-strike to mid-stance would be simulated, the forefoot section of the plantar tissue where the parts were joined would not experience bending which may have impacted plantar pressure mapping. The print variability was evaluated by comparing the forefoot and hindfoot of various phantom-foot copies by fitting different parts together to visually determine differences between prints. It was important to join the rearfoot and forefoot to ensure appropriate tension was applied to the skeletal components once they were secured to the plantar tissue, to enable the elastic recoil. However, the introduction of a hard boundary in the plantar tissue would be likely to produce unusual force transmission

through the forefoot hence a larger printer which could accommodate production of the entire plantar component at once would be preferred in future iterations. Preform (Formlabs, USA) was used to slice the models and included tools to check printability prior to manufacture, ensuring cupping was avoided.

Following production, support material was removed from the plantar tissue parts by hand before each component was washed in isopropyl alcohol (IPA) for 15 minutes using the Form Wash, left to dry for at least 1 hour and cured according to the manufacturer's instructions using the Form Cure. The front and rear plantar tissue parts were then joined by coating each face to be joined in resin, clamping them together and using a UV light to cure the resin. The join was tested by manually flexing the plantar tissue component between the manufacturers hands to ensure a strong bond had been achieved and the join would not break when the part was loaded. Finally, the skeletal and plantar tissue components were mated together mechanically using two screws in the posterior and lateral heel, and tape to secure each phalange into the indentations in the plantar tissue forefoot. Typically, in the human foot strong fibrous ties at the soft tissue/bone interface allow soft tissue to be adhered to the bone at the calcaneus. However, at the metatarsals the soft tissue is adhered to the plantar fascia, the plantar fascia is internally bound into the joint capsule and plantar plate (but not the bone as this happens at the point of the metatarsophalangeal joint so would interact with movement if strongly bound). The phantom-foot differs in this approach as the bones are directly secured to the plantar tissue using non-elastic materials, screws at the calcaneus, and tape at the phalanges. These don't allow motion between the bone segment and tissue areas which are joined. This simplification was made due to the omission of the plantar fascia from the design of the phantom-foot in this initial iteration, and to reduce complexity during manufacture; it was expected to impact the foot kinematics, but it was unknown to what extent. However, it did allow skeletal components to be reused between phantom-foot models once the plantar tissue degraded following testing. Figure 32 displays the complete manufactured phantom-foot, with the skeletal component adhered to the plantar tissue using screws and tape as aforementioned.

Figure 32: Complete Manufactured Phantom-foot

3.7. Actuation system design and setup

3.7.1. Test platform actuation system

The muscles acting on the foot can be divided into extrinsic and intrinsic, where the former are located within compartments of the leg and are responsible for eversion/inversion and plantarflexion/dorsiflexion, and the latter are located within the foot and responsible for fine motor actions (Zelik, Scaleia, Ivanenko, & Lacquaniti, 2015). Intrinsic muscles located within the dorsal aspect of the foot assist extensor muscles in their actions, while those located in the sole play a role in postural control of the arches during static stance, flexion of the toes and production of small movements within the foot to position the toes and shift weight across the forefoot during gait (Fourchet & Gojanovic, 2016; Headlee, Leonard, Hart, Ingersoll, & Hertel, 2008; Mckeon & Fourchet, 2015).

The purpose of the actuation system is to move the phantom-foot in a gait-like trajectory and thereby apply realistic loading forces to it. To simplify the actuation system, the active subsystem (i.e., control of fine motor actions within the foot) was excluded from the design of the phantom-foot; it was assumed, for the purposes of simplicity, that a passive foot was sufficient to characterise the foot health products investigated within this project, and to only add complexity when and how it was warranted. Moreover, the inclusion of intrinsic and extrinsic muscle control would require significant changes to be made to the robotic arm or the inclusion of an additional actuation system altogether in conjunction with the robotic arm to achieve accurate foot motion. The product performance criteria identified within the industrial needs analysis and main performance indexes of cadaveric and prosthetic-based ankle-foot gait simulators in chapter 2 guided the choice of a robotic arm to act as the

actuation system. Robotic arms provide an off-the-shelf solution capable of future adaptation where required to add complexity in future test platform iterations.

A pragmatic approach was taken to choose the actuation system for the test platform, given the tight budget constraints of the PhD project. The University of Salford had an existing suite of KUKA and ABB robotic arms of varying sizes and payload capabilities. Given the only two capable of producing forces which fulfilled the specification were KUKA KR160's, one of these was selected (see Figure 33): the arm could support a payload of 1570N, was highly accurate in that it could achieve a pose repeatability of ±0.06mm and had 6 axes, which is sufficient for the current expectations of the industrial test platform (specification points S4 and S5, and requirements R6 – R10), with scope for added complexity in future applications. For example, the KUKA KR160 can be implemented in industrial applications with automatic tool switching, which could be used to rapidly change between products/phantom-feet during testing.

Figure 33: KUKA KR160 Robotic Arm

The robotic arm required commissioning before it could be used which included positioning and securing the arm within a workspace, calibration of the global coordinate system to ensure the virtual and real environments coordinates matched and the setting up of safety barriers around the work envelope. The actuation systems identified in chapter 1 connect to cadaveric/prosthetic specimens via the fibula when representing the hip, knee, and ankle (Marinelli, Giberti, & Resta, 2017) or the tibia when representing the knee and/or ankle (Zhang, Shen, Shen, & Li, 2010). Within the test platform, the phantom-foot was connected to the robotic arm via a flange plate, connecting to the proximal end of the calcaneus-talus segment. Actuation would only occur in the sagittal and coronal planes, as shear forces and

transverse plane movements were not included in the recreation of gait using the test platform. While shear forces provide important kinetic information particularly in assessing gait abnormalities that involve significant frontal and transverse plane mechanics, they were excluded for the same reason the material properties of the phantom-foot were simplified with respect to the anatomical foot; to provide a simplified target to achieve within the first iteration of the test platform (Bruening , Petersen, & Ridge, 2024; Tavares C, 2018). Figure 34 describes the steps taken to setup the actuation system.

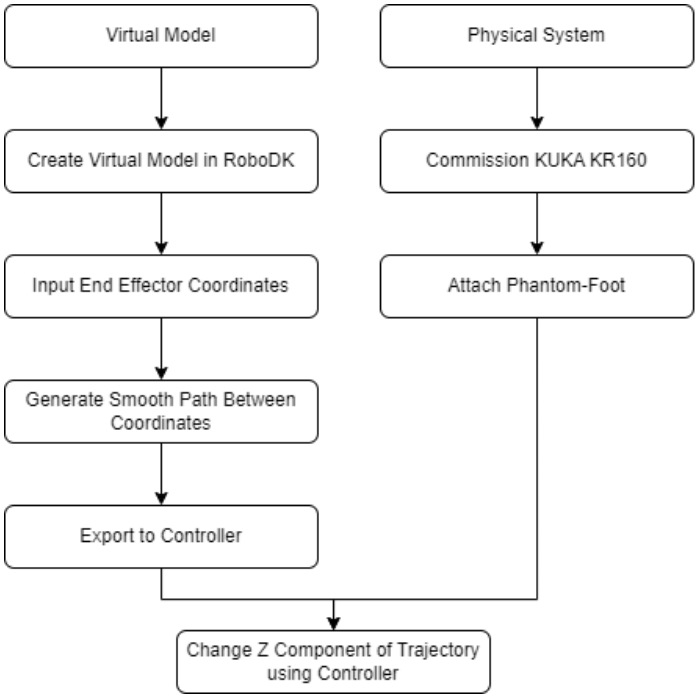

Figure 34: Setup process for robotic arm

Once the system was commissioned, the virtual environment was created in RoboDK simulation software which allowed an industrial environment to be created and motion paths for the arm to be programmed in a realistic setting. The phantom-foot model could then be imported, and 3D coordinates plotted to describe the position of the end effector i.e., the calcaneus-tibia segment angle and position of the phantom-foot with respect to the ground. This angle was imported from Jarvis et al and represented the average position across 100 healthy in-vivo participants. A smooth trajectory between each coordinate via a series of movement commands was generated, tested within the virtual environment, and exported to the real-world KUKA controller. This test routine could then be altered to apply more/less loading force by changing the z component of each defined coordinate, which satisfied specification point S6 (see Table 22). The following section describes the target trajectory and loading profile.

3.7.2. Actuation and loading profiles

Harlaar describes the gait cycle as consisting of the following events: loading response, early stance, terminal stance, pre-swing, early swing, and terminal swing (Harlaar, 2014). The role of extrinsic muscles to produce motions around the ankle joint could be realised by a direct connection between robotic arm and the phantom-foot, and the role of intrinsic muscles on the plantar aspect largely satisfied by the passive plantar tissue and pseudo-ligamentous structures. However, the internal foot motions observed in the midfoot and forefoot cannot be realised without additional actuators, meaning confidence in the recreation of COP, PPD and GRF in later stance phases may be lower at the outset of using the test platform. Hence, the first portion of gait (from loading response until mid-stance) was of greatest interest within this project to describe the performance of an orthotic with the plantar surface of the foot under load. Figure 35 shows the typical GRF profile produced during walking. The key characteristics of the curve are 1) the heel strike transient, 2) initial and secondary peaks and 3) transient between the peaks.

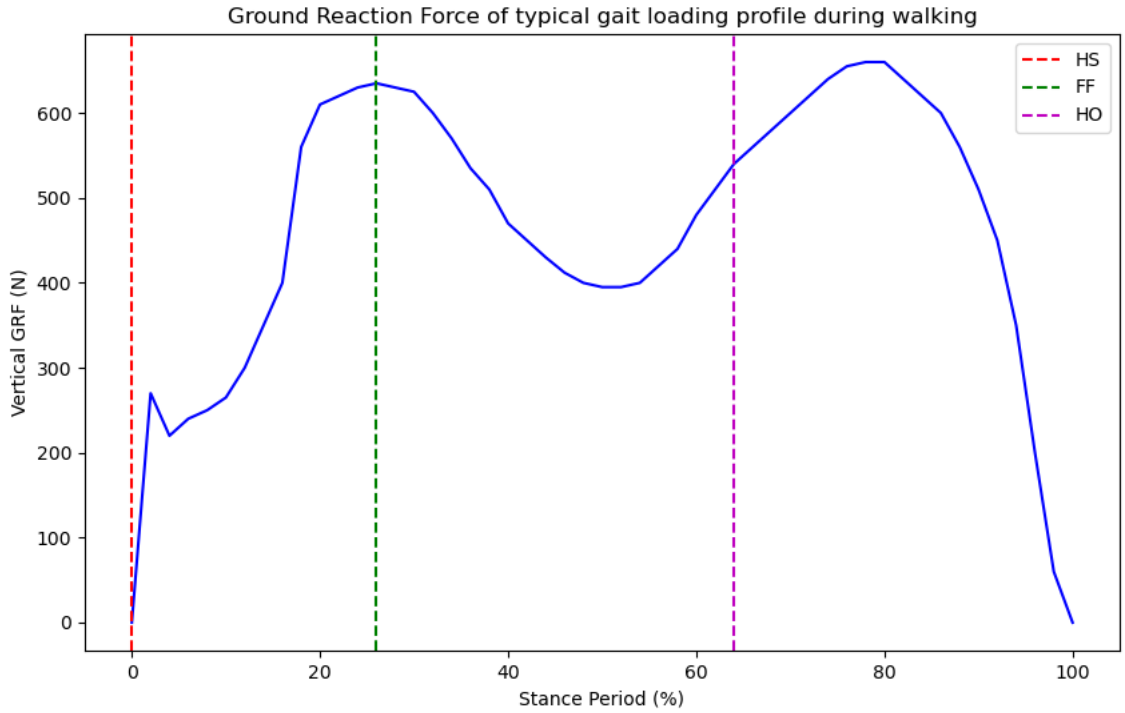

Figure 35: Ground reaction forces of typical gait loading profile during walking. HS = Heel Strike, FF = Foot flat, HO = Heel Off.

The heel strike transient is described as a high frequency vertical impulsive event occurring in early stance phase (Verdini, Marcucci, Benedetti, & Leo, 2006), at approximately 3% in Figure 35. It was unclear whether the heel-strike transient would be achievable within the actuation system due to the high loading rate required. The two peaks are the result of the

foots collision with the ground (passive peak) and the force applied by the intrinsic muscles to push off from the ground (active peak) (Jiang, Napier, Hannigan, Eng, & Menon, 2020). Due to the omission of tendinous structures to actuate the forefoot, the second peak wasn't achievable without applying additional force through the tibia, i.e., changing the trajectory in the coronal plane; this may have impacted the characterisation of the products. Hence, the closest achievable trajectory achievable without significant changes to the trajectory of the forefoot was selected. The calcaneus-tibia segment joint angle during walking was obtained from Jarvis (Nester, Jarvis, Jones, Bowden, & Liu, 2014), where the sagittal plane motion was extracted (see Figure 36). Velocity data for the in-vivo participants was not available as the data had been anonymised and down-sampled to 100 points.

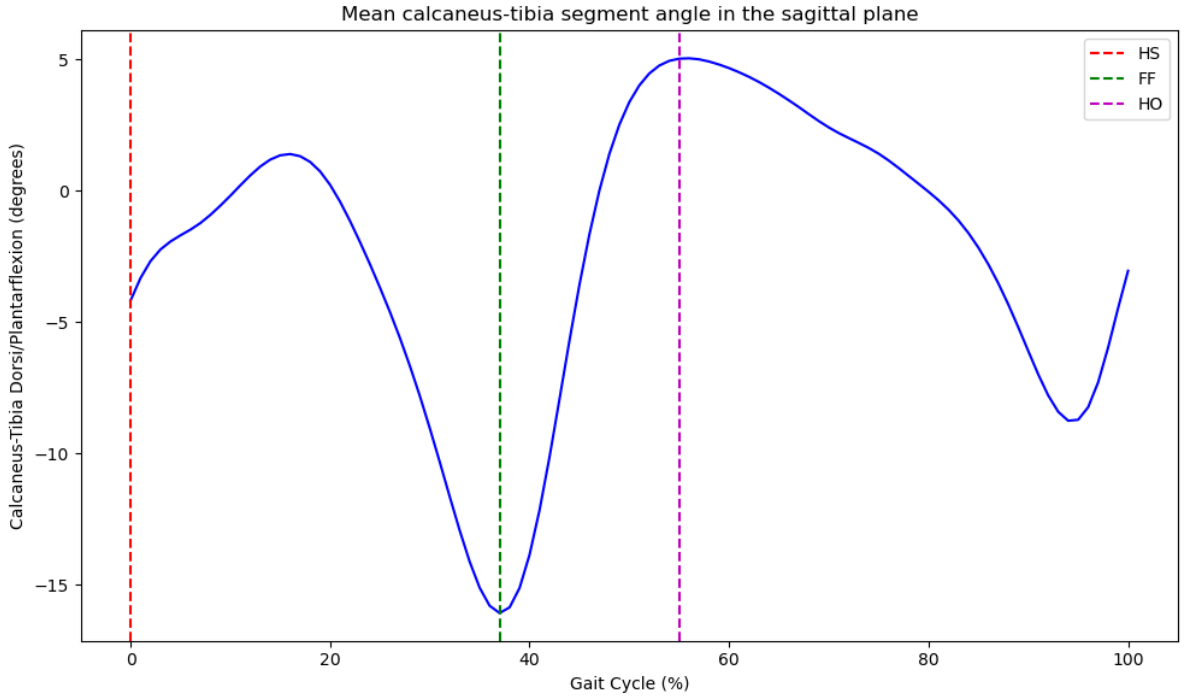

Figure 36: From Jarvis et al: Mean calcaneus-tibia segment angle in the sagittal plane during walking trials. HS = Heel Strike, HO = Heel Off, TO = Toe Off, DF = Dorsiflexion, PF = Plantarflexion

The calcaneus-tibia segment angle for the heel strike, heel-off and toe-off were used to define the coordinates within RoboDK: the plantar surface of the heel of the phantom-foot was defined as the end effector, and the arm rotated around this point to recreate the 'rollover' motion of the human foot during stance phase (see Figure 37). Although the foot involves coronal plane motion during stance phase i.e. the foot transitions from inversion to eversion, the coronal plane was constrained in the test platform to simplify the actuation trajectory (Arnold, Caravaggi, Fraysse, Thewlis, & Leardini, 2017). The 3D position of the end effector was positioned such that the trajectory could be completed close to the base of the robotic

arm; this would allow the camera capture volume to be as small as possible, such as to reduce complexity in arranging the measurement system.

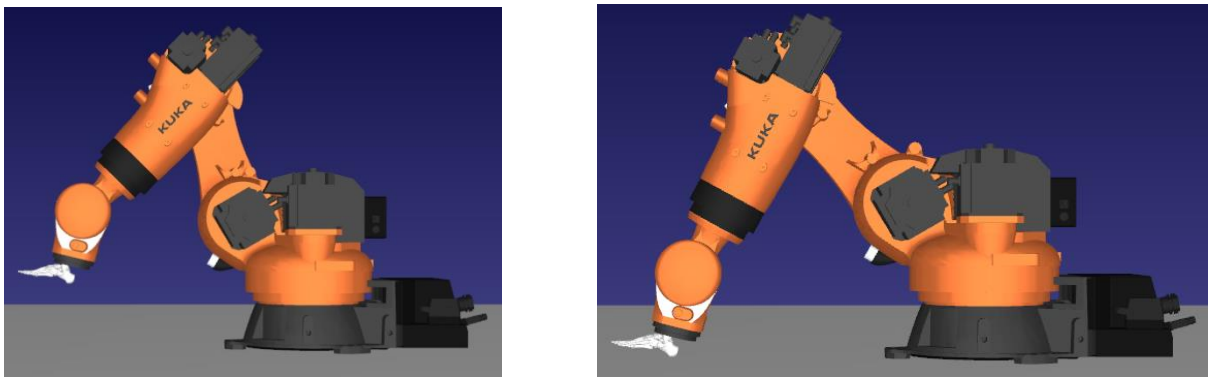

Figure 37: RoboDK test platform model demonstrating the home position (left) and joint changes to achieve a heel-strike position (right).

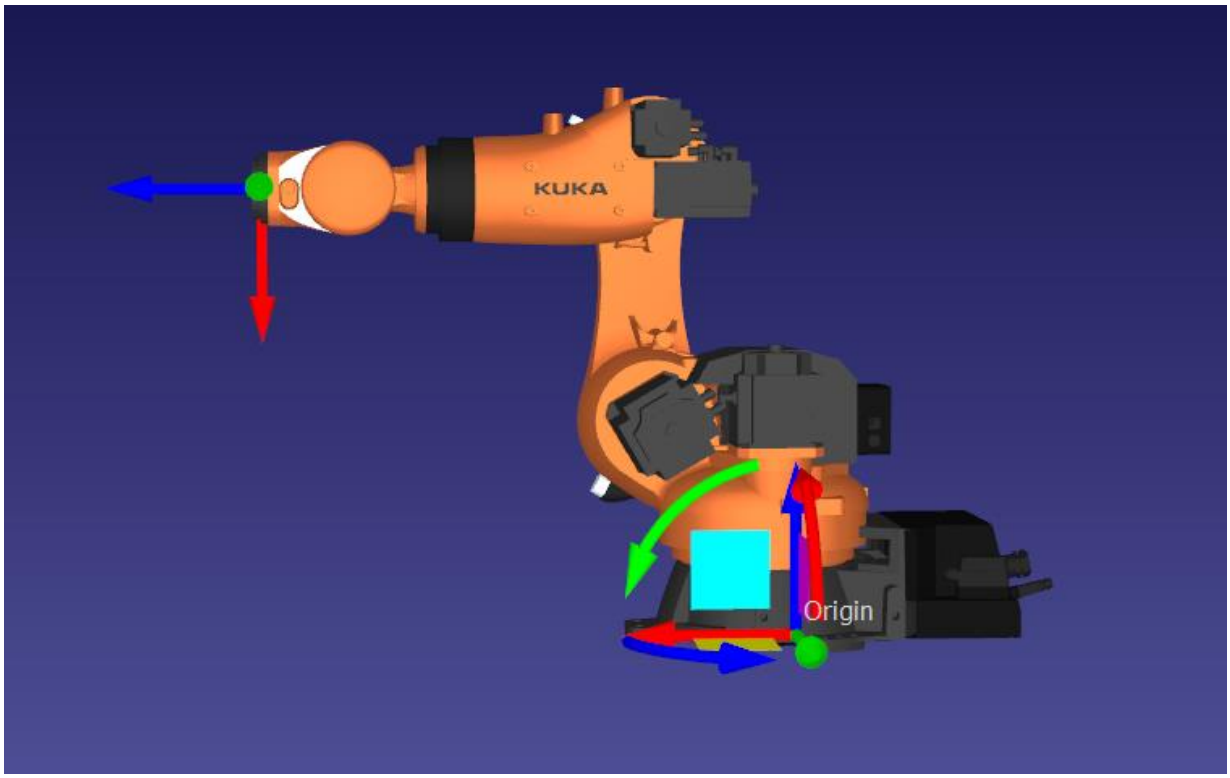

Figure 38: Robotic arm with coordinate systems representing the origin and end effector. The origin represents the coordinates 0,0,0.

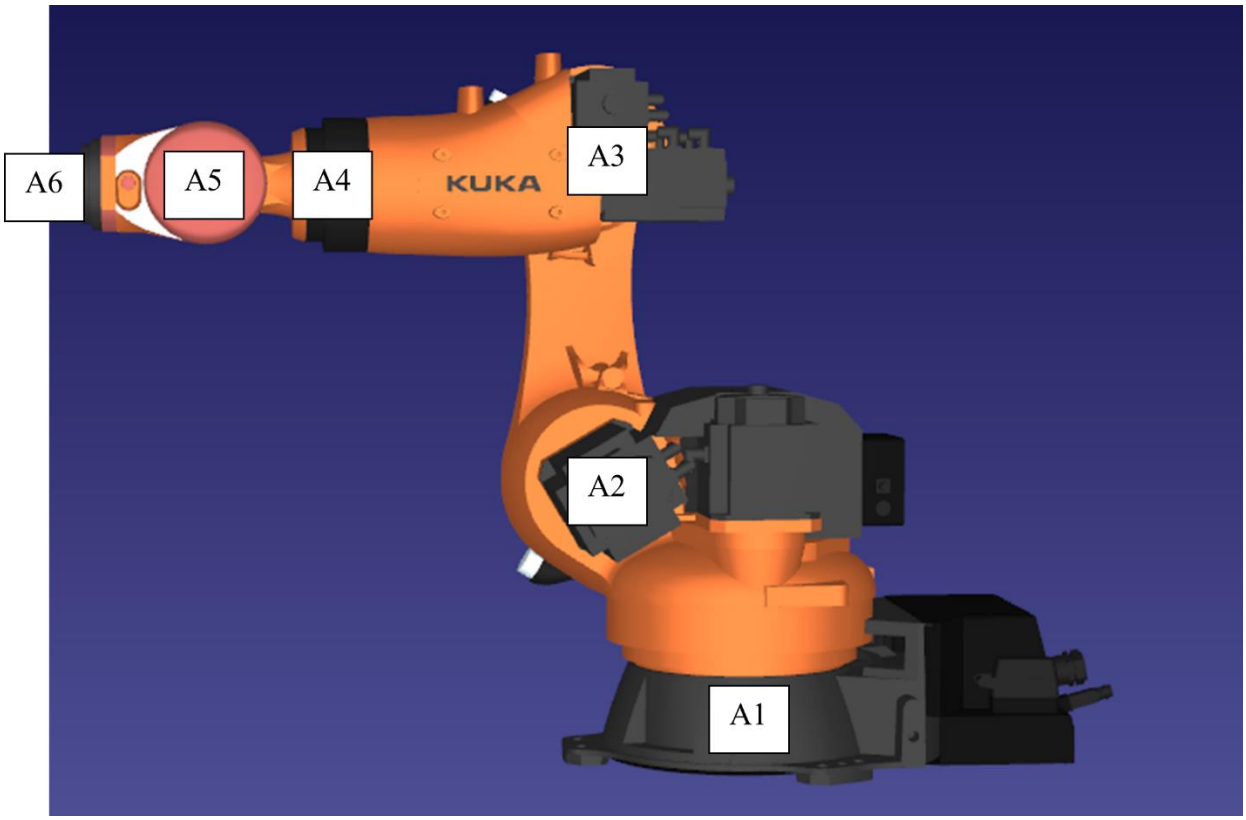

Figure 39: The robotic arm with each joint labelled

Table 23: Robotic arm axis data – the range of motion per joint.

Axis	Axis label	Range of motion, software limited (°)	Speed with rated payload (°/s)
1	A1	+180 to -180	123
2	A2	+45 to -45	114
3	A3	+145 to -130	86
4	A4	+350 to -350	179
5	A5	+120 to -120	172
6	A6	+350 to -350	220

Following the arrangement of the actuation system, the measurement system was required to facilitate tuning of the loading force applied by the robotic arm and enable validation of the test platform against in-vivo data. This is because the robotic arm was position controlled and required an external measurement system to determine the loading force applied to the phantom-foot.

3.8. Measurement system design and setup

Chapter 1 outlined the product performance criteria required within this project, which required the use of measurement tools to capture force, plantar pressure, and the kinematics of the phantom-foot. Following the literature reviews, the suggested tools were a force plate, in-shoe plantar pressure measurement system and camera-based motion capture system.

3.8.1. Ground reaction force measurements

3.8.1.1. Equipment and arrangement

Force measurements, specifically ground reaction force (GRF) are highly important to the operation of the test platform as they provide a method of tuning the trajectory of the robotic arm to vary the force applied, and therefore, the mass of the sample represented by the test platform. Force plates use a series of load cells to determine three dimensional forces however, only the vertical component of this force was utilised within the test platform as shear forces were not modelled. A Kistler 9286AA force plate (Kistler Group, Winterthur, Switzerland) was employed alongside a Kistler 5691A amplifier, with data captured within Bioware proprietary software (Kistler Group, Winterthur, Switzerland) with a sampling rate of 1000Hz (satisfied requirements R18-R19, and specification S7). Bioware is a software package designed for data acquisition and signal processing of force plates and other analogue devices (satisfied specification point S9). The force plate was placed on a table, directly underneath the robotic arm; this would prevent potential damage to the robotic arm if it attempted to drive the phantom-foot into the floor due to erroneous trajectory data. A spirit level was used to ensure that the floor and table were level before the force plate was zeroed. Live data capture was employed to tune the phantom-foots trajectory until the robotic arm recreated loading forces representative of the sample chosen (see Figure 40).

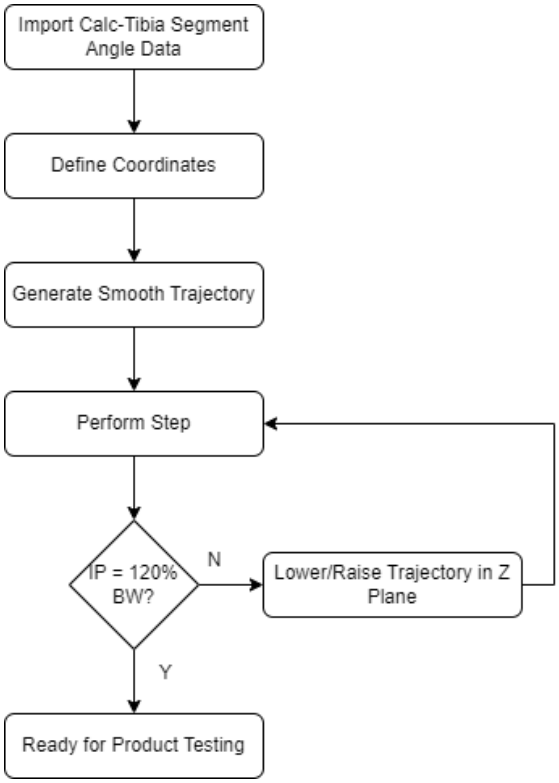

Figure 40: Implementation of force plate to tune robotic arm loading force. IP = Initial Peak, BW = Body Weight of sample

The test protocol was configured within Bioware software to define the duration of the test cycle and enable automatic data collection if an input threshold was exceeded. The generated trajectory refers to Figure 36. Data was saved directly to the cloud to reduce the chance of corruption.

3.8.1.2.Calibration and constraints

The force plate was zeroed within Bioware software prior to any testing at the beginning of each test protocol. A controller connected to the robotic arm via an extendable cable was used to initiate the trajectory and perform emergency stops if required.

The following test conditions were defined:

1) Sample rate (set to 1000Hz),
2) Minimum force threshold to trigger data collection (set approximately to 10N to avoid accidental triggering due to noise),
3) Test duration (set to 2400s)
4) Force components to record i.e., x, y and z components. In this initial implementation of the test platform, only the z component of force was selected as shear force recreation was not considered.

3.8.1.3.Data management and analysis

Raw force data is exported from Bioware software and saved as a text file. Next, Microsoft Excel is used to import and delimit the data into two columns: 1) Time (s) and 2) Force (N). Each 'step' is comprised of 4000 data points; this represents the stance phase only and represented a duration of 2.4 seconds. The robotic arm loads the phantom-foot at a consistent loading rate meaning that no drift occurred over multiple cycles and the loading response wouldn't be affected by a change in velocity. A macro which determines the first peak force every 4000 data points is then applied to determine the peak force per step (occurring in the heel region), which can then be graphed to determine the force loading response of the phantom-foot over time. As each step has fixed data points an average loading profile can be generated for each condition which might allow evaluation against a known loading profile.

3.8.1.4.Outcomes measures

1. Peak force per step describes the sample represented by the phantom-foot, the loading repeatability and changes in its' behaviour caused by degradation over time.

3.8.2. Pressure measurements

3.8.2.1.Equipment and arrangement

Plantar pressure measurements satisfy the majority of the product performance criteria as they describe the interaction of the product and plantar surface of the foot. An XSENSOR (XSENSOR Technology Corporation, Canada) in-shoe plantar pressure system was elected for use within the test platform due to its recent assessment as an accurate in-shoe pressure measurement tool (Parker, Andrews, & Price, 2023). This satisfied requirements R11-R13 and specification points S7-S8. Data was available from a previous study investigating the gait of 100 healthy participants (Nester, Jarvis, Jones, Bowden, & Liu, 2014). This provided an initial means of checking the behaviour of the phantom-foot prior to complete validation, which is described in chapter 3. The phantom-foot was placed within a neutral trainer shoe, with a pressure capture insole placed between the phantom-foot and insole product/shoe insole (if only the phantom-foot was being loaded, without any product). A foot-only condition was not chosen following initial testing of the test platform, as the pressure capture insole would not reliably remain adjoined to the phantom-foot throughout loading. Additionally, a limited number of pressure capture insoles were available to the student, so

the in-shoe condition provided a lower risk (in that the sensor was less likely to suffer damage), more appropriate option. Despite not featuring a dorsum, the phantom-foot was stable as the laces could be tied tightly. The choice of shoe aligned with the studies extracted from literature review 1 and the type of products to be investigated within this PhD; comfort products intended to be worn over the course of the day. Moreover, this would be consistent with the shoes worn by participants during validation of the test platform against in-vivo data.

3.8.2.2.Calibration and constraints

The pressure capture insole was zeroed before the insole, phantom-foot and orthotic product (if one was being tested) was placed within the shoe and bolted to the end effector of the robotic arm via 5mm hex bolts.

The data collection protocol was defined within XSENSOR proprietary software:

1) Minimum activation threshold of 0.25N (defined as equal to the threshold of the force plate)
2) Test duration of 2400s
3) Capture rate of 100Hz.

3.8.2.3.Data management and analysis

XSENSOR software is used to segment the foot following data collection according by grouping sensors together. The default grouping template was used to define four regions whose details can be seen in Table 24 and Figure 41. Four regions were deemed sufficient for the first implementation of the test platform, however, could be further discretised e.g. when evaluating products which affect medial/lateral areas of the foot.

Table 24: Pressure capture insole sensor groups

Sensor Group	Number of Cells	Total Area (cm^2)
Left Heel	36	23.04
Left Midfoot	70	44.8
Left Metatarsal	76	48.64
Left Toe	51	32.64

The raw data, average pressure, peak pressure and contact area is then exported as a csv file and imported to Microsoft Excel. The average pressure, peak pressure and contact area per step can then be directly aligned with the force plate data and graphed to determine the pressure loading response of the phantom-foot over time.

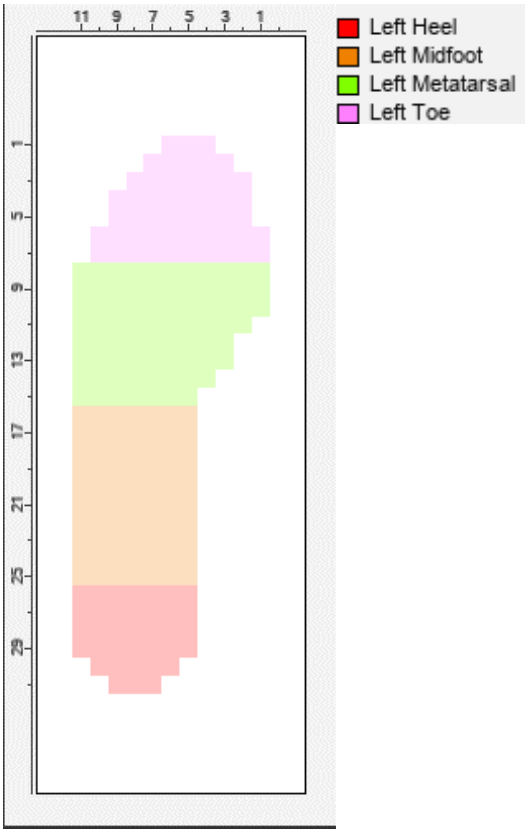

Figure 41: Sensor groups

3.8.2.4.Outcome measures

The outcome measures calculated were informed by the variables used within existing orthotic studies which were identified in literature review 1.

1. Peak pressure.
2. Pressure time integral.
3. Contact area.
4. Time to peak pressure.
5. Contact time.
6. Centre of pressure.

3.8.3. Kinematic measurements

3.8.3.1.Equipment and arrangement

3D foot kinematics provided the final measures required to evaluate product performance, specifically segment range of motion and changes made to foot kinematics following the application of an orthotic product. A six camera Qualisys (Qualisys, Sweden) motion capture system was used to track phantom-foot bone/segment motion with a capture rate of 100Hz; this satisfied requirements R14-R16 and specification point S7. This gold standard gait capture system allowed direct comparison of the movement of the phantom-foot to in-vivo participant data using retroreflective markers placed on the foot to define the Salford multi-segment foot model, which reflect infrared light to contrast starkly against their background. This allows the 3D coordinates of each marker to be calculated through data processing (Liu, Holt, & Evans, 2007). 3 markers were required per segment, with additional markers placed at the proximal and distal joint ends to define skeletal structures. The hindfoot markers were placed directly onto the surface of the shoe rather than onto the calcaneus by cutting holes into the shoe as it would provide a closer approximation between the phantom-foot and in-vivo participants, the latter of which could otherwise present skin movement artifacts. Qualisys Track Manager (QTM) software (Qualisys, Sweden) was utilised for data capture and the results imported into Visual3D (C-Motion, USA) for gait analysis, where foot segments were identified using the skin markers. Only the hindfoot and midfoot were defined according to the model, given the inability of the test platform to accurately recreate forefoot motion (particularly in terminal stance) due to the omission of tendinous structures. The marker placement protocol defined by Jarvis (Nester, Jarvis, Jones, Bowden, & Liu, 2014) as applied to the phantom-foot can be seen in Figure 42. Details of the marker placement protocol can be found in section 5.2.4.2. This satisfied requirement R17.

Figure 42: Marker placement protocol defined by Jarvis as adapted/implemented within the test platform.

6 cameras were placed around the robotic arm and force plate such that they could capture the entire work envelope (see Figure 43).

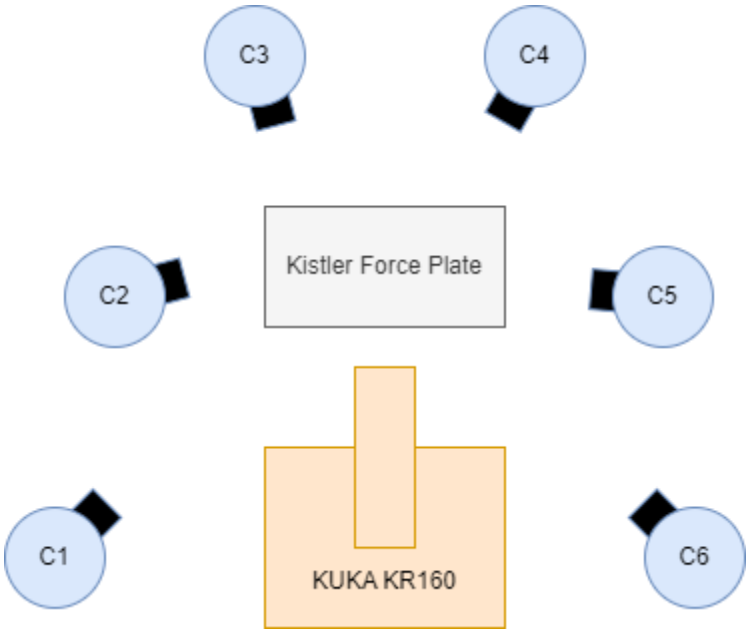

Figure 43: Motion capture and force plate arrangement around robotic arm, C = Camera

The cameras were angled downwards to reduce the number of artifacts picked up by reflections off objects in the workspace e.g., the camera tripods. As the test platform was not situated within a space dedicated to gait studies, the number of reflective surfaces required certain compromises: the work envelope was made as small as possible while keeping the cameras a safe distance away from the robotic arm, the number of overhead lights was reduced as much as possible and large masks were applied within QTM to effectively ignore

areas outside of where the phantom-foot was operating. In a permanent workspace, additional measures such as blackout curtains could be placed around the robotic arm and its reflective surfaces covered with a non-reflective tape, however, this was not possible within the university environment as it was a shared workspace, and cosmetic changes could not be made to the robotic arm. Consequently, the work envelope was much smaller than would typically be seen in a gait study.

Although the appropriate add-ons were not available to the student which would allow data capture from the force plate to be conducted within QTM as well, force, pressure, and kinematic data could be synchronised post data collection. Finally, the position, aperture and threshold of each camera was altered to ensure that the phantom-foot would be captured throughout the entire trajectory of the robotic arm. Figure 44 shows the complete test platform arrangement featuring the robotic arm, force plate, motion cameras and phantom foot placed within a shoe.

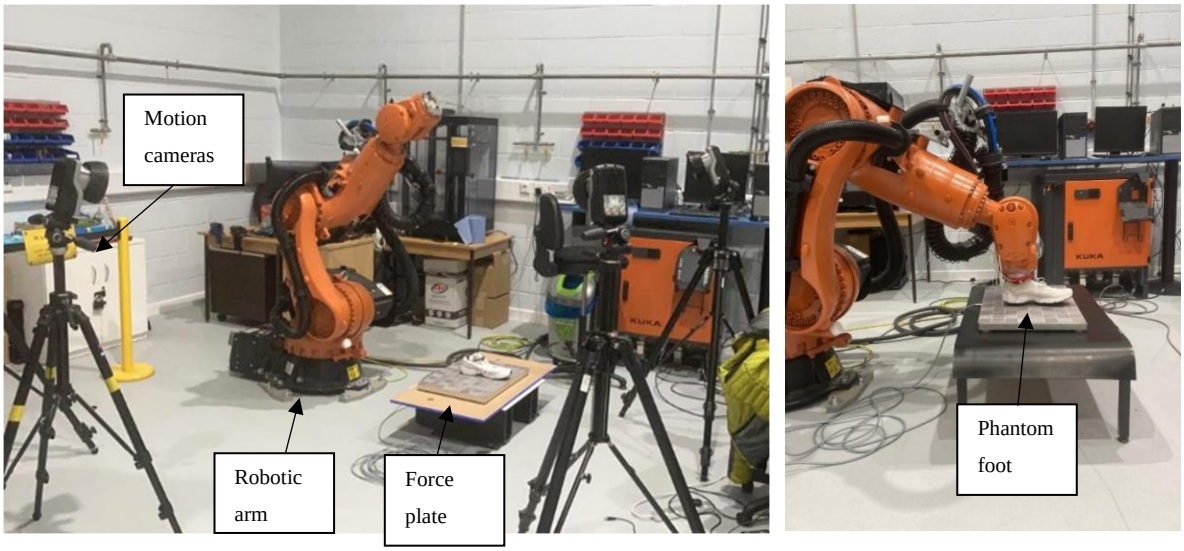

Figure 44: Arrangement of robotic arm, force plate, motion cameras and pressure capture insoles (placed within the shoe)

3.8.3.2.Calibration and constraints

The motion capture system suggests calibration each day in case a camera was accidentally moved. Calibration involves several steps: 1) camera aiming, 2) masking, 3) capture volume calibration and 4) volume origin definition. Cameras are aimed as described previously to capture a small volume around the robotic arm and force plate; markers placed on the force plate help ensure the force plate is visible to each camera. The input threshold and aperture of each camera is defined within QTM software to minimise the effects of noise caused by

reflective surfaces. Next, masking is manually applied to remove any remaining noise, with any unnecessary objects removed from the capture volume at this time. The system features a calibration wand which must be waved throughout the capture volume, ensuring that the markers on the wand are visible to the cameras. Care must be taken to avoid contact with the ground, force plate and robotic arm to avoid calibration errors. This is required until each camera indicated sufficient data had been captured and calibration had been completed. The number of points and average residual data is then reviewed to determine whether the calibration was successful or needed to be repeated; target values are not available from the manufacturer as calibration feedback data are based on factors such as the size of the capture volume and the camera lens type, hence general guidelines specific to the laboratory used are selected as optimal values (minimum 1000 points, maximum 1.0mm average residual). Finally, the volume origin i.e., global coordinate system, is defined via the placement of an L frame on the force plate; this defines the surface of the force plate as the ground. Table 25 displays the calibration results.

Table 25: Camera calibration results

Camera	X (mm)	Y (mm)	Z (mm)	Points	Avg. residual (mm)
1	-1068.86	1243.2	871.33	1717	0.70093
2	-1252.01	117	851.57	1988	0.48635
3	-1210.04	-504.34	970.31	1678	0.58051
4	373.64	-1185.36	1004.51	1793	0.60261
5	1296.54	-988.97	975.34	1956	0.64392
6	1412.85	448.97	846.13	1440	0.65995

The constraints were defined within QTM.

1) Test duration of 2400s
2) Capture rate of 100Hz.

3.8.3.3.Data management and analysis

Following data capture, a Butterworth 6Hz low-pass filter is applied to remove high frequency signals and individual markers are labelled within QTM software: the software determines the percentage of time each marker is visible throughout the data capture period, allowing phantom-markers caused by reflective surfaces to be identified and deleted (markers visible for <2% of the data collection period). Automatic marker labelling is then applied to determine the trajectory of a marker over the entire data collection period. Manual inspection of each marker trace is then required to identify errors caused by marker occlusion; any

obstruction of the marker will result in the breaking of a trace; however, separate traces can be grouped, and gap-fill functions performed to generate a complete trajectory. Polynomial gap-fill operations are the default option, and connect x,y, and z data through interpolation; to avoid errors a maximum number of 10 frames to be filled are used. Next, the trajectory of each marker is then exported to Visual3D, where a skeletal model is generated by defining segment boundaries using markers. The joint segment data is then exported to Microsoft Excel, where the range of motion of each segment per step can be analysed to determine the kinematic effects of an orthotic products on the phantom-foot. Events are identified through examining the position of the phantom-foot in relation to the force plate and force measurements i.e., the highest position above the force plate is the starting position, the first impact is heel-strike, and the point at which no force is detected is toe-off.

3.8.3.4.Outcome measures

1. Joint segment angles

3.8.4. Operational procedure

Once each measurement system is configured, the principal investigator must remain behind the safety barriers, with the robotic arm controller in hand. The controller must be used to initiate the test cycle, and an emergency stop button is available to cease operation if required. XSENSOR and QTM provide live results during data collection and can be used to monitor the operation of the test platform. The robotic arm will automatically cease operation and return to the home position once the test cycle is complete, at which point the data analysis protocol may begin.

The conclusion of the data analysis protocol results in a single Microsoft Excel file featuring outcome variable for the force, pressure and kinematic data collected by the test platform per each complete test cycle.

3.8.5. Synchronisation

The force plate, in-shoe pressure measurement system and motion cameras could not be synchronised within QTM as the force plate amplifier and pressure system were not compatible. Consequently, a single step event was used to synchronise each system using the moment of first contact between the phantom-foot and force plate, i.e. a minimum force of 3N which exceeded the maximum error threshold. Datasets were then aligned based on this

event. To validate the synchronisation, force, pressure, and motion data were visualised to ensure the alignment was correct.

3.8.6. Conclusion

Following information gathering in chapter 1 and an outlining of the needs of the industry partner to inform the design of the test platform a detailed specification was created to detail the requirements of the system. A conceptual design was developed to offer a pathway to address the requirements and specification established in Table 21 and Table 22, ensuring that each point was addressed. Next, the components selected to fulfil this specification were designed, developed, manufactured, and arranged. The data collection and analysis protocols were defined. Consequently, the completion of this chapter presented a test platform which required validation against human foot behaviour to determine its effectiveness in characterising orthotic and footwear products.

Chapter 4: Development and validation

4.1. Chapter overview

This chapter describes the development, and validation of the industrial test platform specified in chapter 3. Following production of the phantom-foot and arrangement of the actuation and measurement systems, the series of validation steps described includes:

(1) Validation of the robotic arm's ability to apply a repeatable load and trajectory to the phantom-foot, such that changes captured by the measurement system can be attributed solely to the phantom-foot and foot orthotic products.
(2) Confirmation that the phantom-foot provides a repeatable loading response to characterise orthotic product performance when loaded according to the represented sample i.e., 637.65N male. This includes inter and intra-phantom-foot model repeatability, and hence also describes the error caused due to manufacturing variation between different copies of the phantom-foot.
(3) Validation of the performance of a phantom-foot model in repeated assessments to assess its' longevity and inform the test protocols to be applied by the test platforms.

Completion of these validation steps leads to quantifying the minimal detectable change in orthotic products by the test platform, representing the inherent error in the system. Consequently, changes in foot function (such as loading, pressure, and joint kinematics) larger than this error can be attributed to the evaluated orthotic products. This is particularly important as it establishes the design constraints that can be explored using the test platform in industry. It also guides the design iteration process, for example, by determining the effect of varying the heel wedge height. Following the validation steps, a series of steps were completed to compare the performance of the test platform to in-vivo data.

These steps included:

(1) Comparison of the loading profile of the phantom-foot to in-vivo data during gait.
(2) Comparison of the pressure profile and contact area of the phantom-foot to in-vivo data during gait.
(3) Comparison of the segment kinematics to in-vivo data during gait.

The outcome of this chapter is a complete industrial test platform ready for implementation in evaluating the performance of orthotic devices, and an informed test protocol.

4.2. Test platform validation pathway

A validation pathway was required to ensure that the industrial test platform was able to fulfil the use contexts agreed upon with the industry partner (see page 108) and adequately capture orthotic product performance. First, the repeatability of the actuation system was evaluated based on its ability to produce a repeatable loading force and trajectory. Next, the repeatability of the loading response between different copies of the phantom-foot was evaluated based on the ability to produce comparable loading responses based on the same inputs. Finally, the capability of the phantom-foot to be used in repeated assessments was evaluated by repeating a test cycle following a rest period. The purpose, research question/hypothesis, test methodology and results of each validation stage are described below.

4.2.1. Validation of actuation system repeatability

4.2.1.1. Purpose

The test platform is required to capture changes made to the phantom-foot by an orthotic product (according to the product performance criteria). Consequently, the actuation system is required to produce a repeatable trajectory (and thereby a repeatable loading force) to ensure deviations in these variables applied by the actuation system aren't falsely attributed to the phantom-foot/product. This is critical because of the position-based open-loop control strategy adopted by the test platform; there is no corrective action to return the actuation system to the correct input if drift occurs. The capability of the test platform to produce the correct loading force relates to the position as variations in the position of the end-effector will impact the loading of the phantom-foot on the force plate. The robotic arm has a manufacturer stated pose accuracy and pose repeatability of ± 0.06 mm, following the guidelines of ISO 9283 (International Organization for Standardization, 1998). The angular accuracy is not stated. Previous studies have investigated the repeatability of similar robotic systems. Goldsmith found high repeatability in a 6 DOF robotic system for in vitro mechanical testing (Goldsmith, et al., 2015) however, the removal and installation of different specimens (in a protocol similar to that to be employed with the test platform) has been shown to produce substantial changes to a system's inter-specimen repeatability (Goldsmith, Smith, Jansson, LaPrade, & Wijdicks, 2014). Although this may be attributed to the use of cadaveric samples to determine these results. The primary control variables found

to affect positional repeatability include speed and the motion type: keeping the maximum speed significantly within capacity improved repeatability (Sirinterlikci, Tiryakioğlu, Bird, Harris, & Kweder, 2009).

4.2.1.2. Research question/hypothesis

Research question: Can the robotic arm reproduce repeatable loading patterns and trajectories within the manufacturer stated pose repeatability of the system, such that changes in the loading response of the phantom-foot can be declared independent of the actuation system?

Hypothesis: A correctly commissioned and calibrated robotic arm (according to ISO 9283) will reproduce ± 0.06 mm pose accuracy and pose repeatability throughout the applied trajectory and over the course of the entire test protocol.

4.2.1.3. Test methodology

The test platform was intended to apply loading force representative of the sample used to model the phantom-foot; hence a 637.65N male sample. The trajectory applied to the phantom-foot was informed by the average calcaneus-tibia sagittal plane joint angles from Jarvis study of 100 healthy participants (Nester, Jarvis, Jones, Bowden, & Liu, 2014). The calcaneus-tibia angle at key gait events was used to define coordinates, between which a smooth trajectory was generated to produce a path which represented the first portion of the gait cycle. A solid resin block was fitted to the end effector of the robotic arm to act as a stiff indenter to be applied to the force plate; this would prevent damage to the force plate if the robotic arm was applied directly. 100 cycles of the given trajectory were applied to the force plate, with the load and positional characteristics compared to determine the repeatability of the actuation system. Figure 45 shows the protocol performed during this validation step.

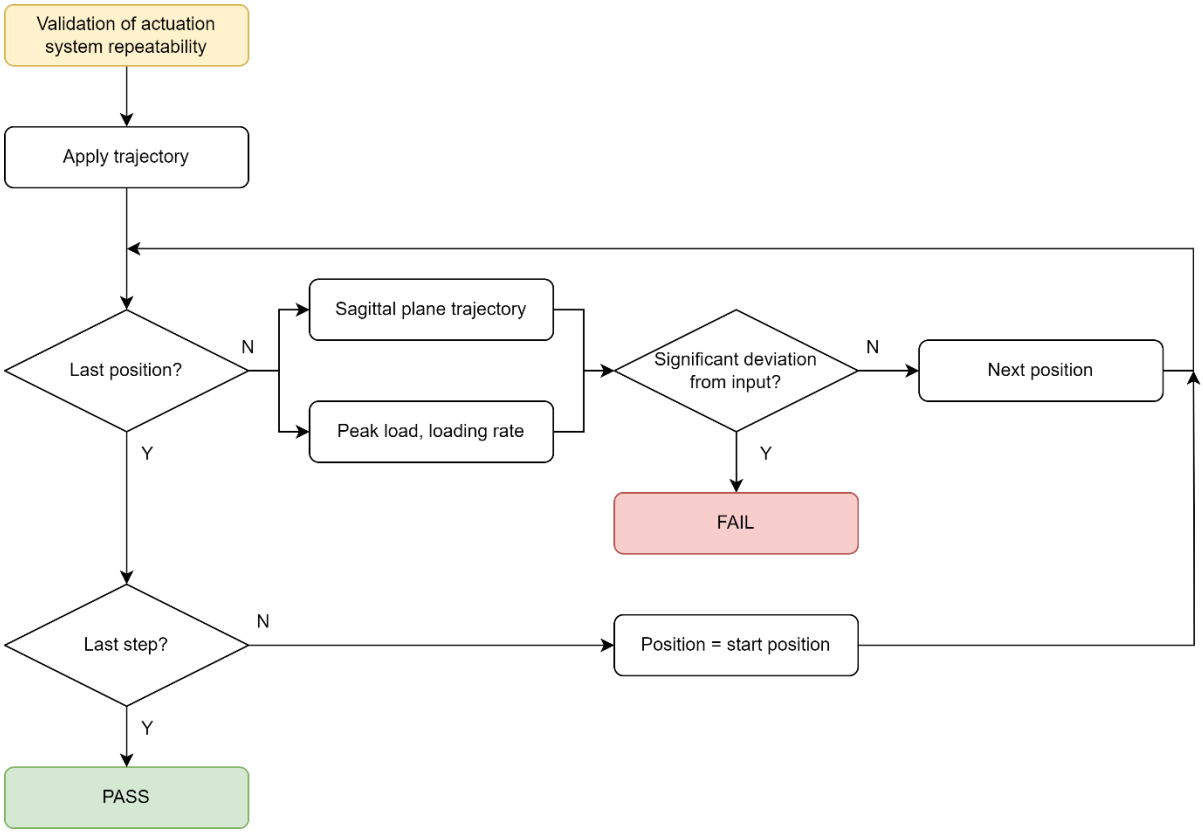

Figure 45: Validation of actuation system repeatability pathway. A significant deviation from the input is defined as ±0.06mm

4.2.1.4. Results

The force and position repeatability data for the test platform are reported as the standard deviation (see Table 26). Force repeatability is reported as differences in the average and peak force. Positional repeatability is examined at the home position, heel-strike, mid-stance, and toe-off which were the specified positions between which a smooth loading trajectory was generated. Figure 46 shows the test platform loading repeatability, Figure 47 the positional repeatability in the "Z" axis which corresponds to the coronal plane and Figure 48 the positional repeatability in the "Y" axis which corresponds to the sagittal plane.

Table 26: Test platform force and positional repeatability data

	Step										
Variable	**1**	**10**	**20**	**30**	**40**	**50**	**60**	**70**	**80**	**Mean**	**SD**
Average force (N)	297.14	297.83	297.54	297.54	297.73	297.73	297.64	297.34	297.93	297.64	0.20
Peak force (N)	583.99	583.60	584.68	584.68	588.11	588.40	589.78	587.72	587.42	586.44	2.26
Y position at home (m)	0.23	0.23	0.23	0.23	0.23	0.23	0.23	0.23	0.23	0.23	0.0003
Z position at home (m)	0.39	0.39	0.39	0.39	0.39	0.39	0.39	0.39	0.39	0.39	0.0030
Y position at heel-strike (m)	0.24	0.24	0.24	0.24	0.24	0.24	0.24	0.24	0.24	0.24	0.0002
Z position at heel strike (m)	0.00	0.00	0.01	0.01	0.01	0.01	0.01	0.01	0.01	0.01	0.0011
Y position at mid-stance (m)	0.24	0.24	0.24	0.24	0.24	0.24	0.24	0.24	0.24	0.24	0.0001
Z position at mid-stance (m)	0.08	0.09	0.10	0.08	0.09	0.11	0.09	0.10	0.08	0.09	0.011
Y position at toe-off (m)	0.24	0.24	0.24	0.24	0.24	0.24	0.24	0.24	0.24	0.24	0.0001
Z position at toe-off (m)	0.17	0.18	0.17	0.17	0.17	0.18	0.17	0.18	0.17	0.17	0.0037

The test platform demonstrated high repeatability with respect to loading in both the average force per step (297.64N ± 0.20) and peak force (586.44N ± 2.26) variables. This corresponded to a maximal deviation when representing a 637.65N sample of 0.07% and 0.38% respectively. The maximum acceleration was limited to 55ms^{-2} to ensure the robotic arm could be stopped rapidly in case of emergency; this aligned with requirement 7 in Table 21. Positional repeatability in both the Y and Z axes was high, however, the Y axis achieved a lower SD across each recorded position. The most significant deviation (±0.0108m) occurred in the Z axis at mid-stance, which exceeded the manufacturer stated pose repeatability of ± 0.06 mm.

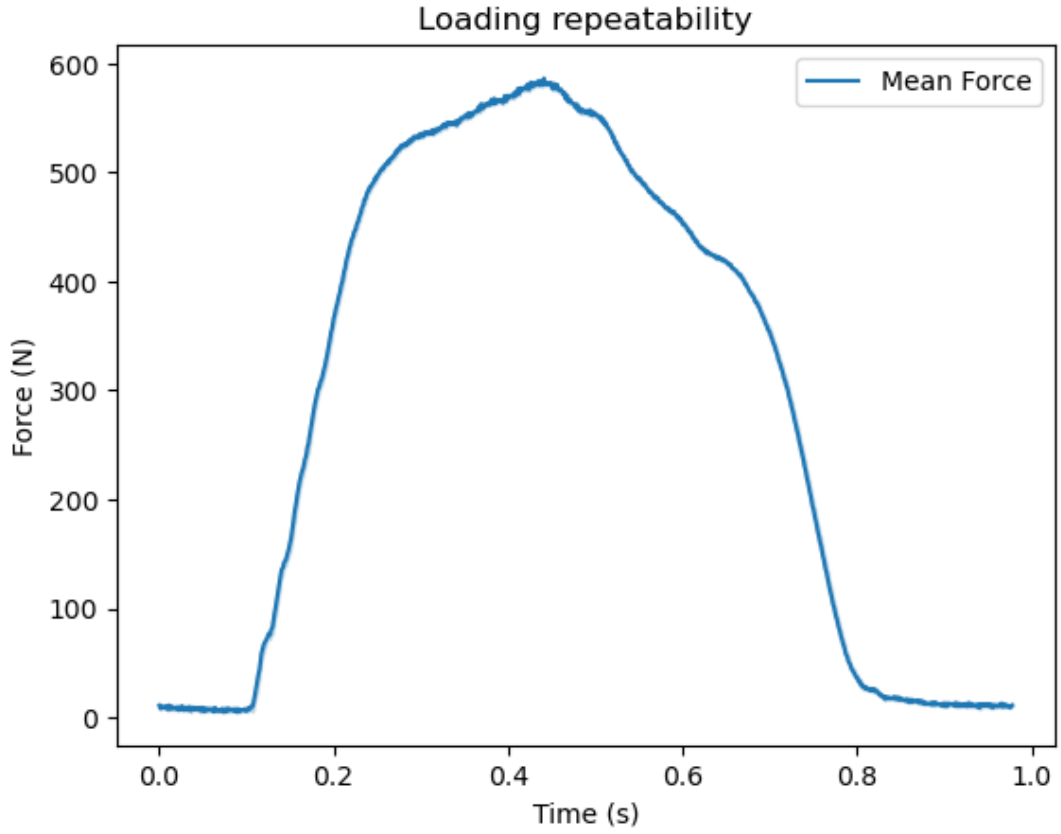

Figure 46: Test platform loading repeatability. This represents the closest approximation of stance phase produced by the first implementation of the test platform. The latter stages of stance phase, particularly toe-off, could not be represented accurately given the lack of muscular control.

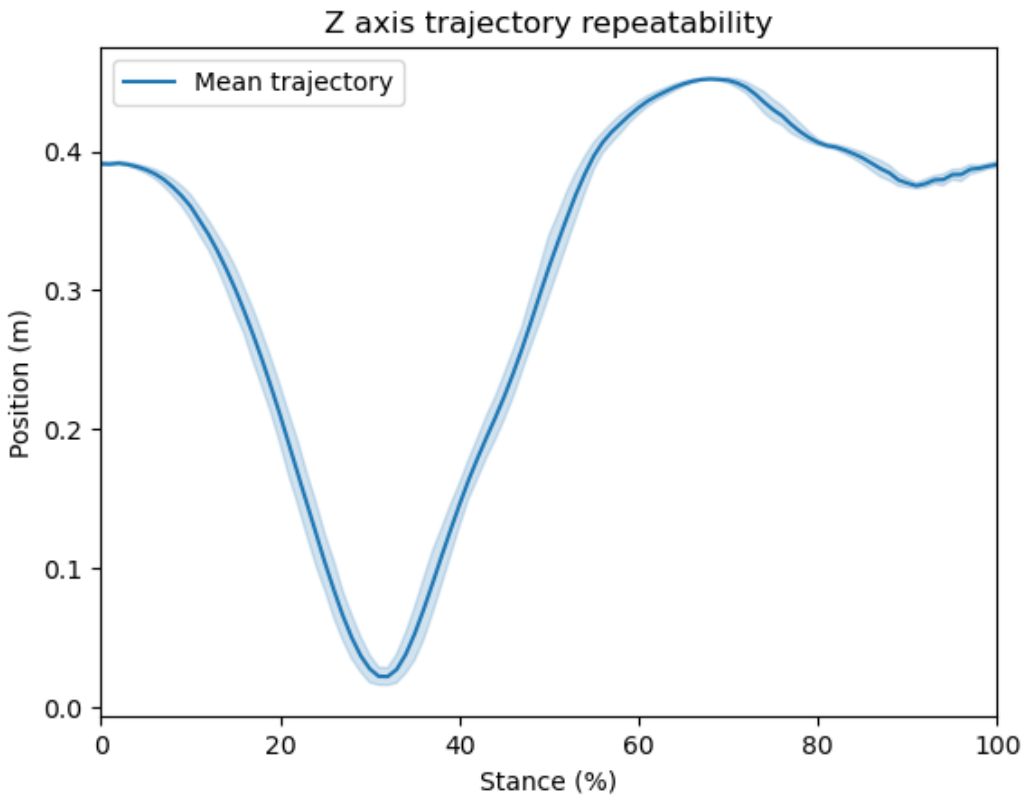

Figure 47: Z axis trajectory repeatability

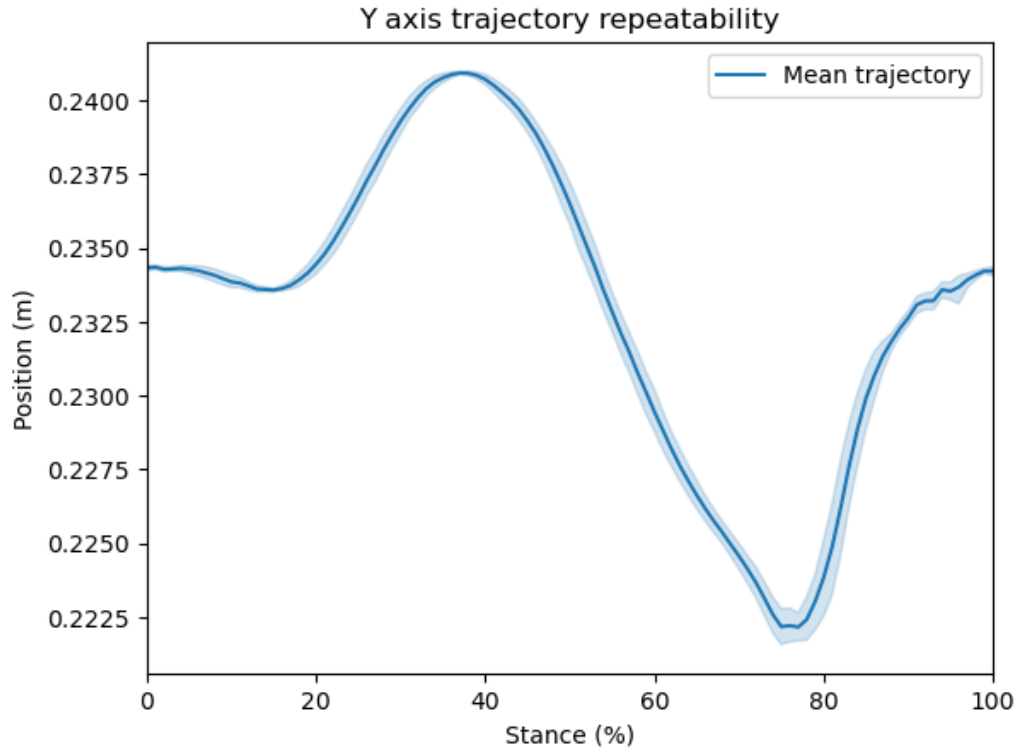

Figure 48: Y axis trajectory repeatability

4.2.1.5. Discussion

This validation step was required to define the error associated with the actuation system in order to ensure that its' repeatability is greater than the minimum change effected by the orthotic products on the phantom-foot. The loading error was noticeably small despite the open-loop control system employed, with the greatest variation occurring at the maximum loading/unloading rates. Each step aligned with the manufacturer stated positional repeatability (±0.06mm) aside from the Z position at mid-stance. This was most likely affected due to the open-loop control strategy which does not account for the compression of the phantom-foot over time, which would affect the Z position during the period where the phantom-foot is in contact with the force plate. Irrespective of this, the test platform performs at a consistent repeatability which is much greater than the inter-participant repeatability of human participants i.e., the steps produced by the robotic arm do not vary compared to the natural in-vivo gait. Additionally, changes in the loading response of the phantom-foot can be declared independent of the actuation system.

4.2.2. Validation of phantom-foot loading response repeatability

4.2.2.1. Purpose

The phantom-foot was designed according to the morphology and material properties of the components that comprise the human foot. This validation had two purposes: to assess the repeatability of the load as applied by the phantom-foot, and to confirm that each phantom-foot copy of a given sample was equivalent in terms of morphology and performance. This was critical to the operation of the test platform to ensure that testing across multiple phantom-foot copies when testing different orthotic products would be consistent and reliable. Previous orthotic product assessments in industry have required a minimum of 200 steps to characterise product performance. However, clinical assessments have a much lower requirement to fulfil, as it is not feasible timewise to capture hundreds of steps per participant and per condition. Fewer than 50 steps have been indicated to be sufficient, meaning that both use-contexts could be satisfied by the phantom-foot achieving 200 repeatable steps (Kroneberg, et al., 2017; Kribus-Shmiel, Zeilig, Sokolovski, & Plotnik, 2018).

The test platform was not capable of recreating all the characteristics of the typical in-vivo loading curve. Specifically, the latter portion of gait (from mid-stance onwards) where load would be applied by the forefoot in human participants but could not be performed using the

test platform given that loading was only applied through the tibia. Hence, only the loading pattern produced by the phantom-foot during the first 50% of the gait cycle (from heel-strike to mid-stance) was of interest within this validation step.

4.2.2.2. Research question/hypothesis

Research questions:

1) Can the phantom-foot reproduce a repeatable loading response representative of a 637.65N sample and present stable behaviour for the minimum number of steps required to characterise orthotic products?
2) Does each phantom-foot copy of a given sample produce the same loading response under the same test platform conditions? Does each phantom-foot present equivalent morphology?

Hypotheses:

1) A phantom-foot with material properties comparable to a human foot, which has a realistic trajectory applied to it (i.e., speed and position informed by in-vivo data) will produce a loading response repeatable to within 5% of the peak load per cycle following pre-conditioning, for a minimum of 200 steps. The loading response would be expected to vary over time as the plantar tissue material degrades, with the lattice network weakening/failing, or material fatigue propagating cracks which weaken the material until it can no longer sustain the peak load.
2) The mechanical response of the phantom foot is not dependent on manufacture and on post-production processes. There is no statistically significant difference in the morphology of each phantom-foot.

4.2.2.3. Test methodology

During prototyping and calibration of the test platform, initial testing showed that the phantom-foot required pre-conditioning at much higher loading forces, to ‘settle’ at the correct magnitude (637.65N). This was attributed to the mechanics of the plantar tissue changing over the course of testing including heating up, compressing and degrading. Trial and error were used to determine an initial peak loading force of approximately 1030.05N to pre-condition the phantom-foot such that a loading response in the region of 637.65N would be produced post conditioning. This pre-conditioning step was included within the test protocol itself and steps prior to producing a stable response would be characterised as such.

Three phantom-foot copies were manufactured according to the protocol detailed in chapter 3. These steps included: 1) 3D printing the skeletal model and post-processing to remove support material and join bones via the pseudo-ligamentous structures, 2) 3D printing the plantar tissue model and post-processing to remove excess resin, cure, dry and join both pieces of the model together and 3) joining the skeletal and plantar tissue models together to form the phantom-foot. Following manufacture, each phantom-foot was visually inspected. The transparent plantar tissue model allowed careful examination of the lattice structure to determine defects and manufacturing inconsistency, which would ultimately produce functional differences between each phantom-foot copy.

1000 steps were applied within the protocol to ensure that the response of the phantom-foot during pre-conditioning and normal operation were captured, such that the minimum of 200 repeatable steps could be satisfied. Moreover, this accounted for changes in loading pattern caused by permanent changes made to the phantom-foot (i.e., irreversible deformation or degradation) to be captured, to determine the expected lifespan of each phantom-foot model. The protocol was repeated using three phantom-foot copies representing the same 637.65N sample and manufactured using the same process.

The force plate was employed to track the loading response of the phantom-foot. Following the completion of the test, the peak load, time to peak load and maximum loading/unloading rate per step were derived. The force profile of each phantom-foot under the same loading trajectory would demonstrate functional differences between each phantom-foot copy including the time required for pre-conditioning, duration of the stable region and the points at which it would begin/end. Greater than 5% change in the peak load following conditioning was considered ‘unstable’, hence the greatest period where the peak load remained within 5% of a given value was selected as the stable period. The period where each phantom-foots’ stable regions overlapped would then be validated as the repeatable stable period and point at which orthotic performance could be characterised by the test platform. Figure 49 shows the protocol performed during this validation step.

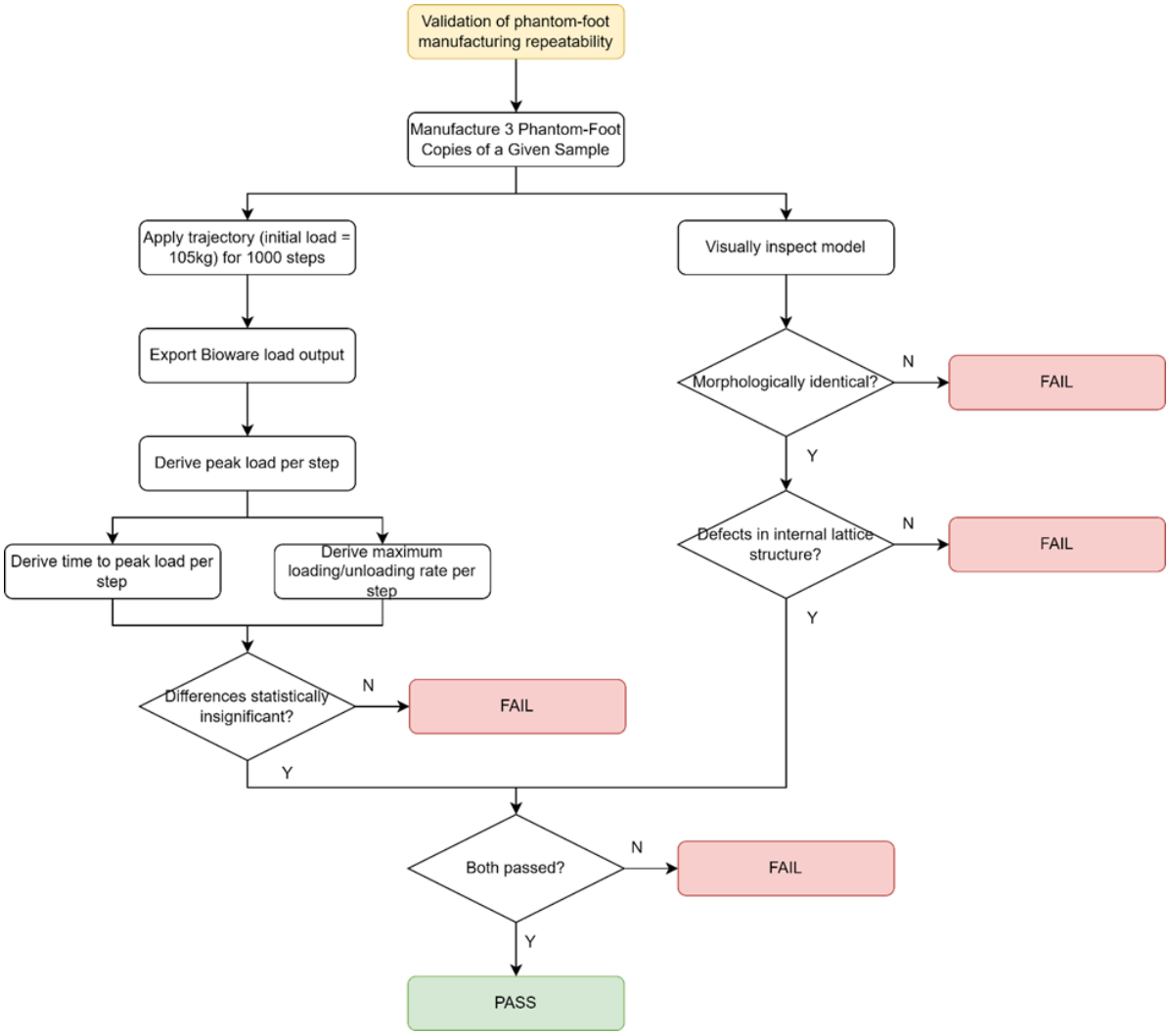

Figure 49: Validation of phantom-foot loading response repeatability pathway

4.2.2.4. Results

The phantom-foot repeatability data is represented as the standard deviation across the three phantom-foot copies. The average peak load per step across the three phantom-foot copies was calculated and plotted in Figure 53. Figure 54 shows the inter-phantom-foot standard deviation, with the stable region highlighted.

Table 27: Variation between phantom-foot copies

Variable	Phantom-foot 1	Phantom-foot 2	Phantom-foot 3	Mean	SD
Preconditioning steps	589	524	551	554.67	32.65
Steps in stable region	333	397	337	355.67	35.85
Time to mid-stance (s)	0.232	0.232	0.232	0.232	0
Time to peak load (s)	0.144	0.144	0.144	0.144	0
Time to peak load (% gait cycle)	22	22	22	22	0

At the beginning of the test cycle, the phantom-foot models demonstrated unstable behaviour for approximately 500 steps, which could be described as the conditioning period. The greatest stable loading response produced was 268 steps within 5% of 600.00N before the load fell below the stable threshold. Figure 55 shows the typical GRF curve applied per step within the stable region; the first and final steps within the stable region are included. While the peak load varied within the stable region between 615.00N to 585.00N, the time to peak load remained consistent, occurring at 22% of the gait cycle (0.144s). The standard deviation was greatest during steps 0-100, with an average of 63.57N. However, this reduced to 3.24N within the stable region; this was due to the stabilisation of the phantom-foot materials.

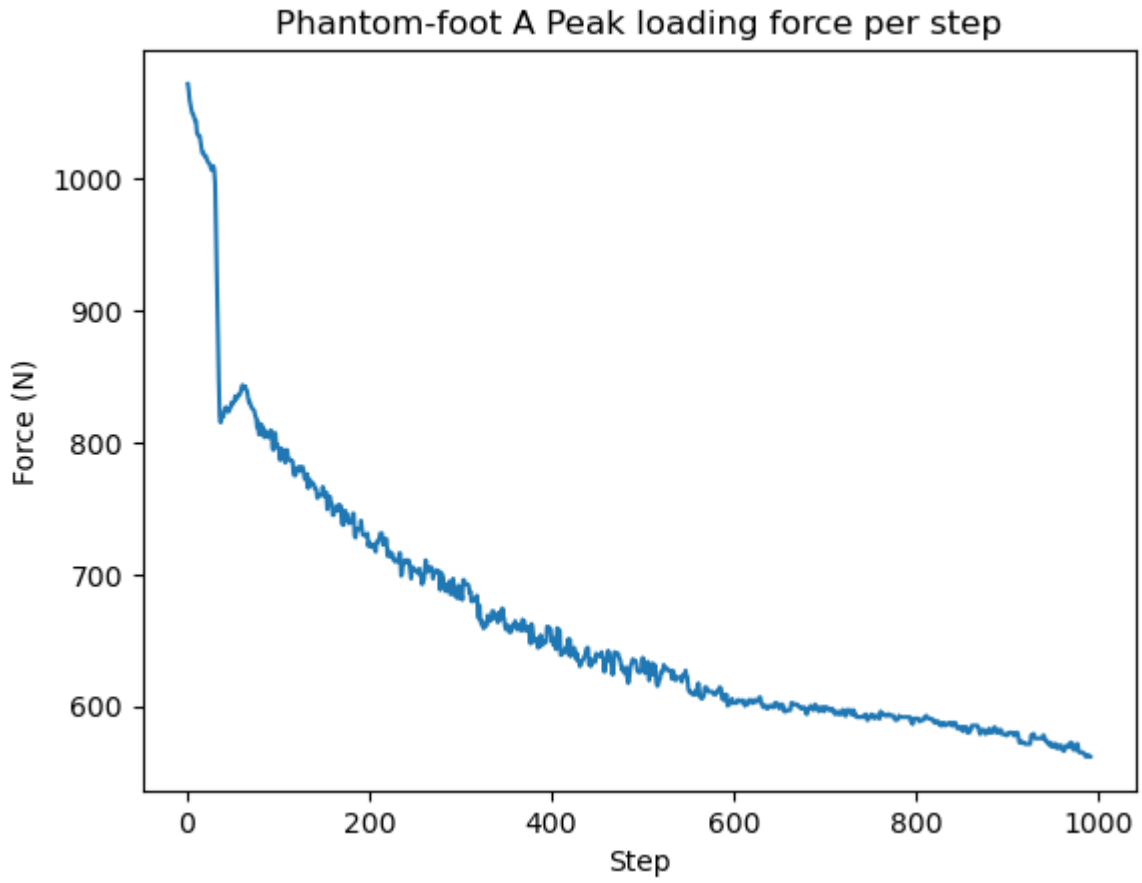

Figure 50: GRF over 1000 steps with phantom-foot copy A

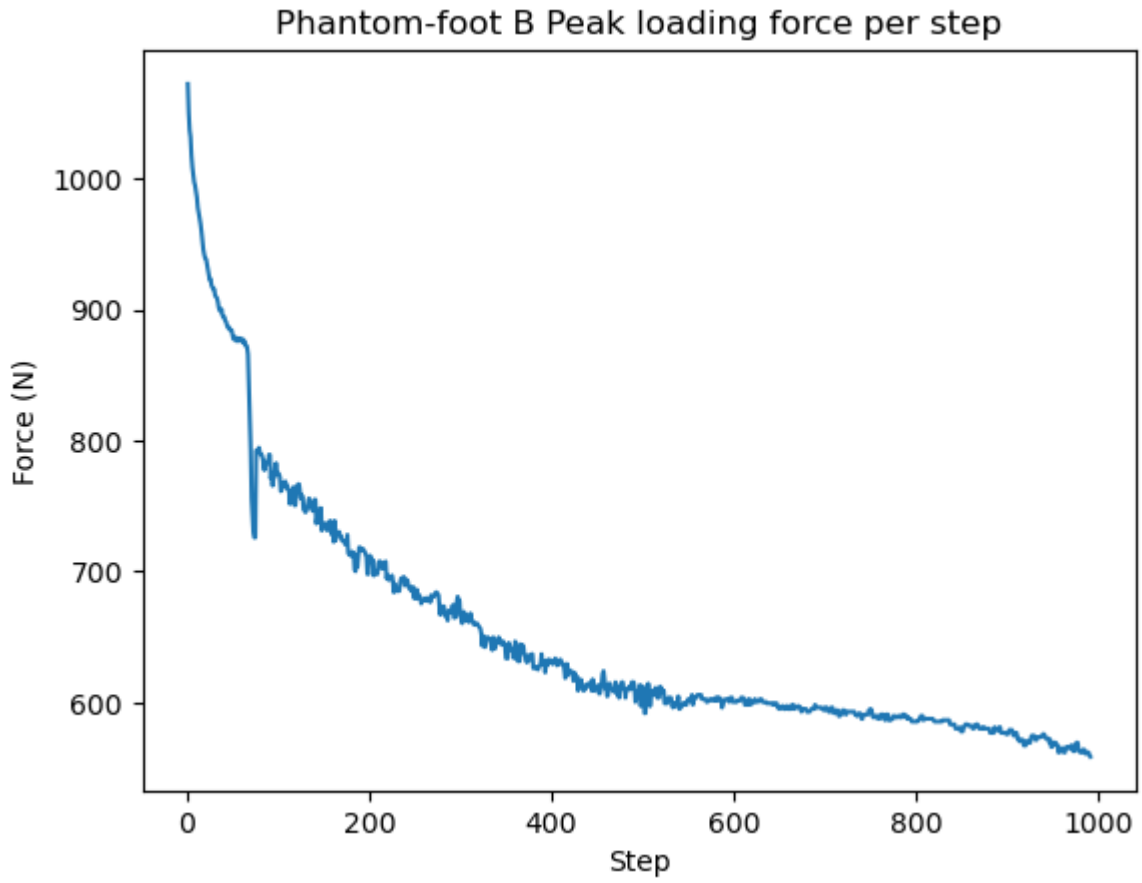

Figure 51: GRF over 1000 steps with phantom-foot copy B

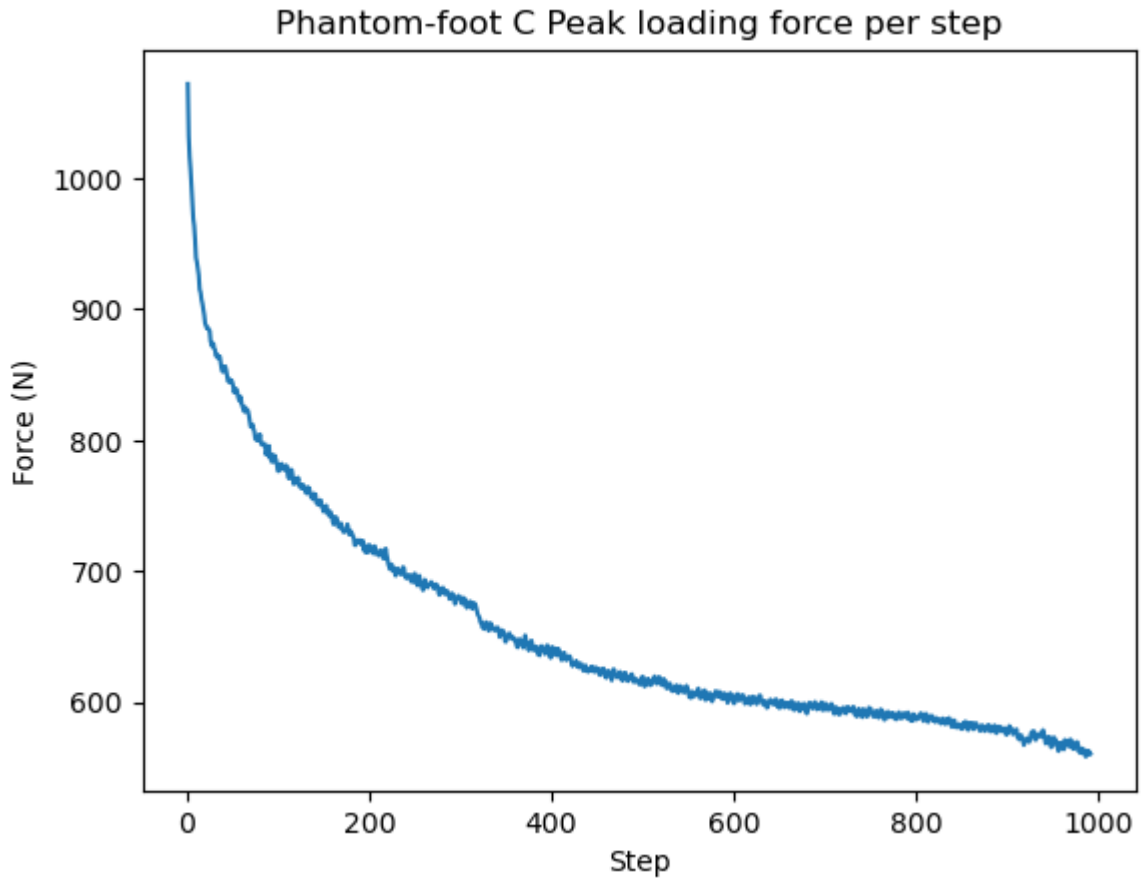

Figure 52: GRF over 1000 steps with phantom-foot copy C

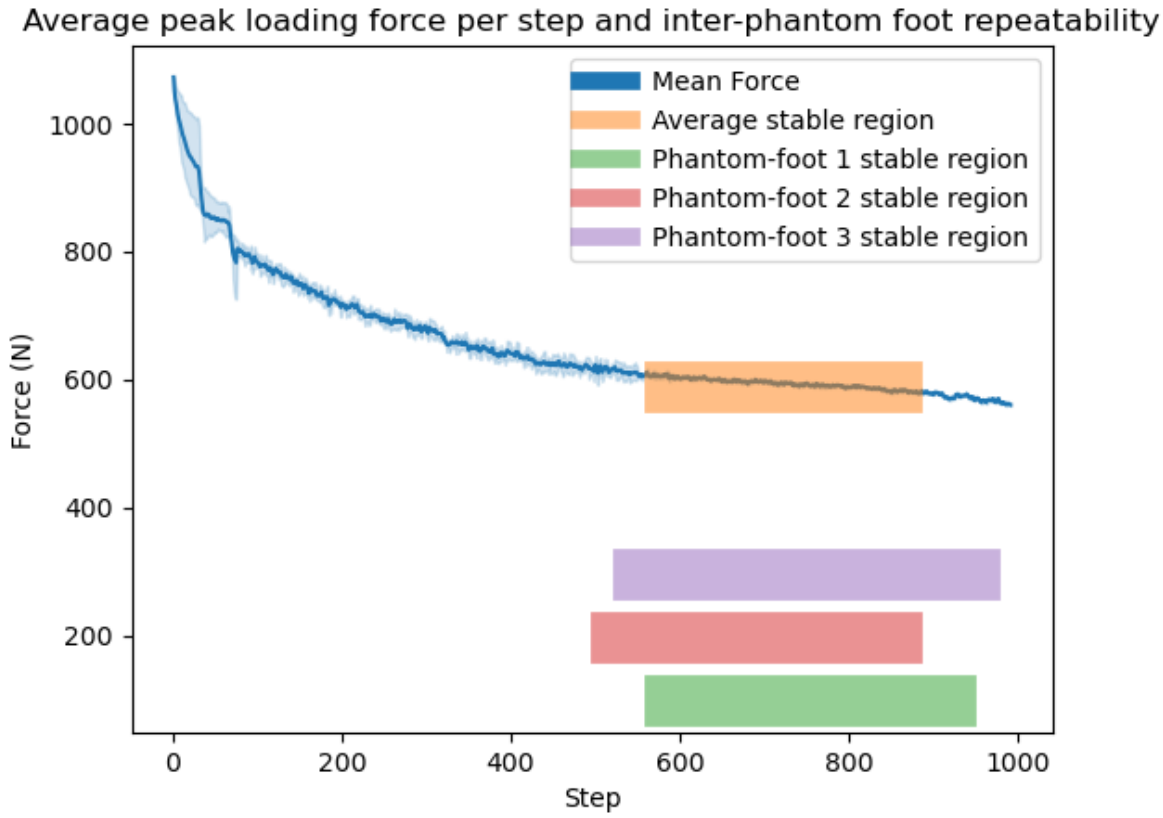

Figure 53: GRF over 1000 steps with stable region highlighted, and standard deviation between phantom-foot copies (shaded in blue). The average stable region is defined as the period during which all phantom-foot copies produced a force within 5% of 600N.

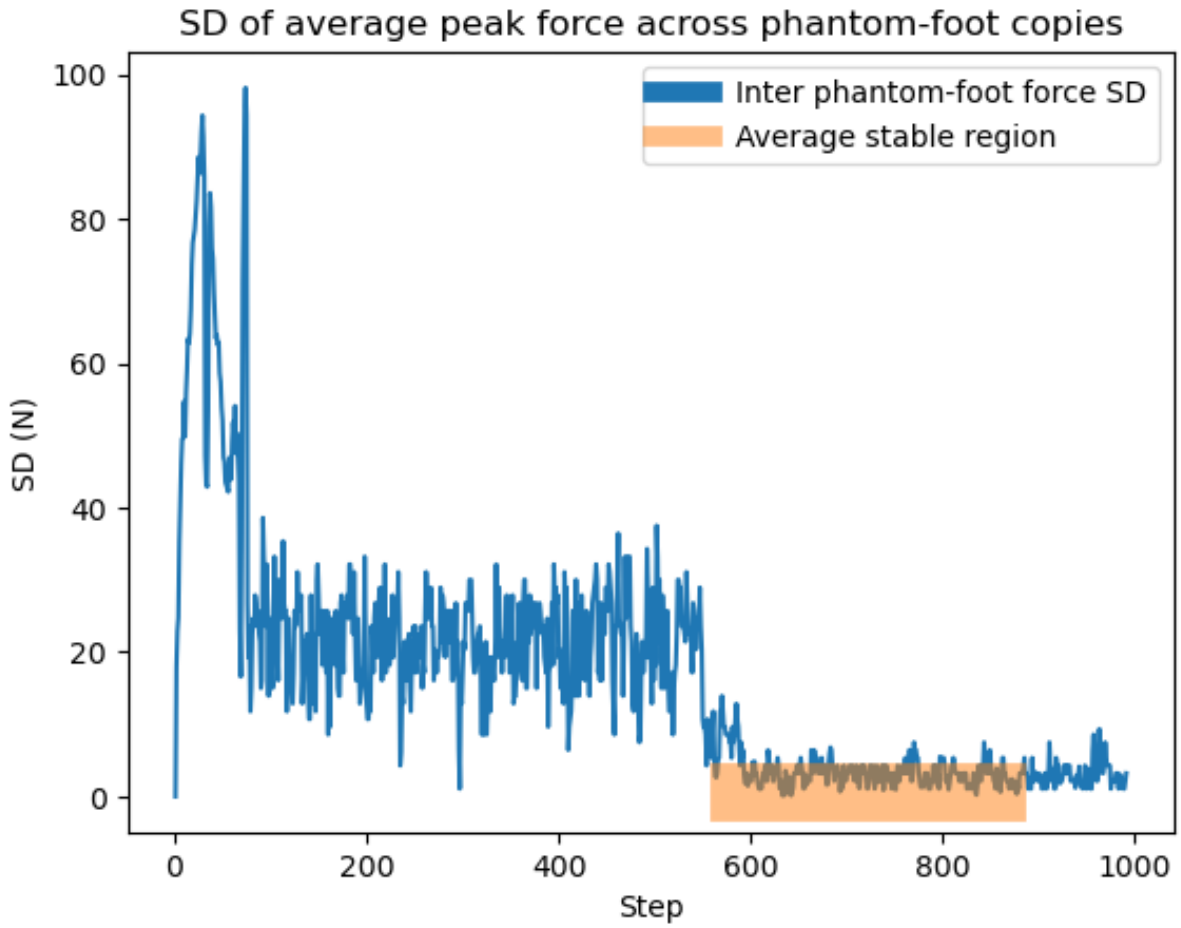

Figure 54: SD of average peak force across each phantom-foot copy during a test cycle of 1000 steps.

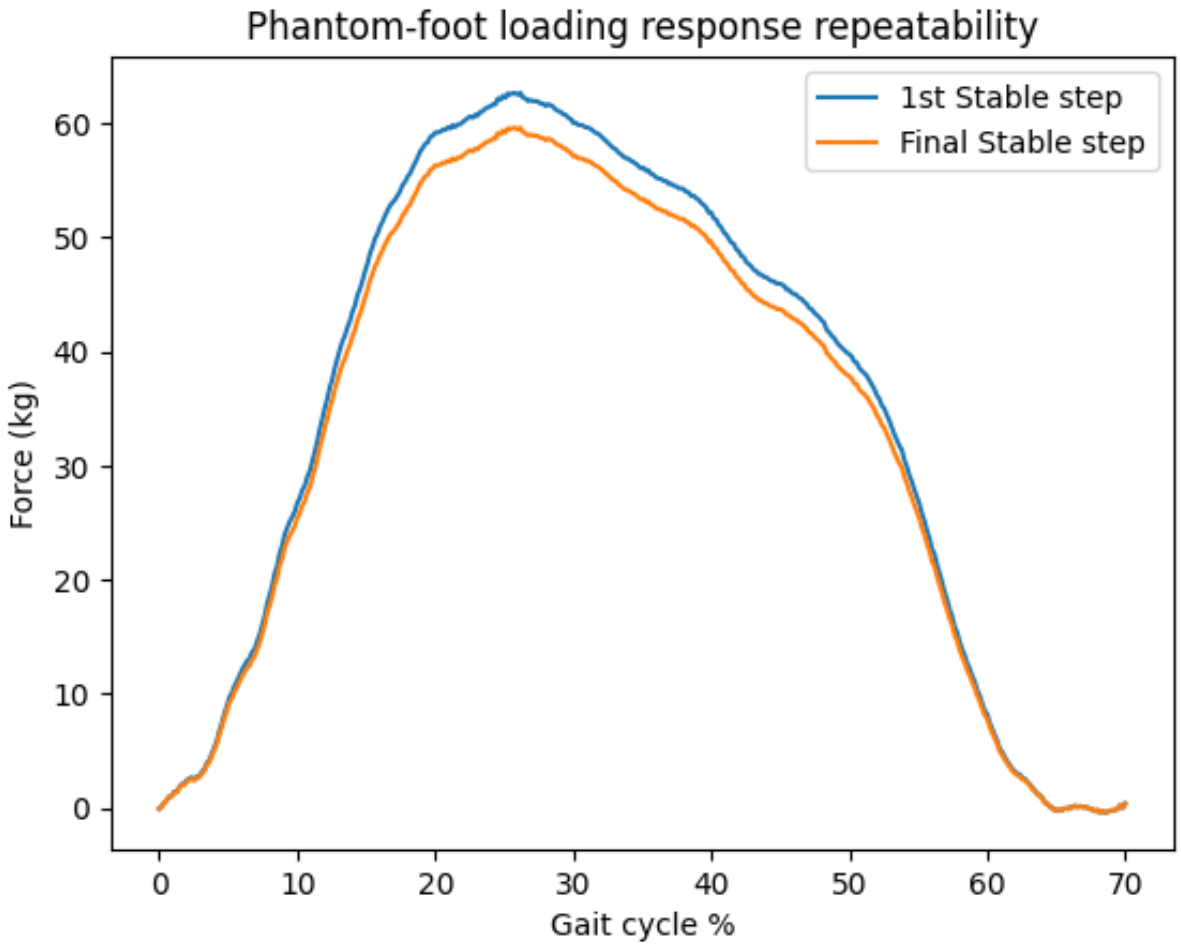

Figure 55: Change in loading trajectory from 1st and last step in stable loading region

4.2.2.5. Discussion

As the phantom-foot was loaded during each step, the plantar tissue material compressed and relaxed to return to its original shape. Over time, the degree to which the material recovered after loading reduced until, and alongside material degradation this lowered the loading force applied to the force plate by the test platform. Consequently, to achieve the correct magnitude of loading post conditioning, the initial load parameters had to be set significantly higher. This was the case within the test platform primarily as an open-loop control strategy was adopted. Alternatively, if a method of load control existed, the test platform would be able to account for the behaviour of the phantom-foot over the course of a test to maintain a specified loading force.

The phantom-foot models took a greater number of steps to stabilise than expected, with approximately 500 steps required before the period of stability was achieved. Each phantom-foot displayed differences in the exact period defined as stable. Nevertheless, an average stable period of 268 steps across all copies of the phantom-foot was achieved, hence both

validation conditions were able to be satisfied by the test platform. For steps within the stable region, Figure 55 showed that the trajectory of the loading curve remains consistent, but the peak force reduced. This was expected given the highly repeatable loading mechanism; only the degradation of the phantom-foot reduced the peak loading force over time.

Despite passing this validation step there were notable limitations which could be improved upon. Firstly, the large number of preconditioning steps required to stabilise the material of the phantom-foot and non-linear behaviour of the phantom-foot prior to conditioning made tuning the trajectory difficult; a much higher than expected initial loading force was required to be applied such that the phantom-foot reached stability at the correct GRF. This required trial and error to tune the loading force, however, the final loading profile produced was still lower than expected to represent the 637.65N sample (600.00N). The use of a different material and perhaps a solid structure rather than a lattice would produce a stable response immediately, before fatiguing and failing. Alternatively the application of a closed loop control system could eliminate the variation caused by the compression of the phantom-foot by enabling consistent loading throughout testing. Rather than choosing a position (as in the open-loop system), a target load could be specified within the test platform control system. Consequently, the loading repeatability would increase, as the displacement of the phantom-foot changes over time as the material compresses would be accounted for.

4.2.3. Validation of phantom-foot repeated assessments

4.2.3.1. Purpose

Materials undergoing cyclic indentation testing experience fatigue compression over the course of testing, which results in material deformation and damage (Xu, Chen, & Yue, 2019). In practical terms, this means the force-displacement behaviour of the phantom-foot would change as it is unable to fully relax and return to its original shape. It was unclear over the course of the previous validation steps whether a phantom-foot model would be able to recover following testing such that it could be used in multiple test cycles, or if the material fatigue experienced had resulted in permanent, irreversible damage. Therefore, the purpose of this validation step was to evaluate how the phantom-foot would perform after completing a complete test cycle, given a rest period of 24 hours between tests.

4.2.3.2. Research question/hypothesis

Research question: Can a phantom-foot model reproduce a repeatable loading response and present stable behaviour for the minimum number of steps required to characterise orthotic products in multiple test cycles of 1000 steps?

Hypothesis: The phantom-foot would not be able to recover sufficiently subsequent to the completion of a test cycle of 1000 steps. The degradation of the phantom-foot over the course of a test cycle would result in permanent deformation, requiring the use of a new phantom-foot model in each ensuing test cycle.

4.2.3.3. Test methodology

The same protocol was applied to the phantom-foot models employed in the previous validation step following a rest period of 24hrs. The loading response produced in the second test cycle was then compared to the first; the peak load produced in the first 100 steps would establish the degree to which the phantom-foot recovered following the rest period. A visual inspection would be performed between test cycles to determine material degradation. If material degradation was excessive, or the phantom-foot was unable to produce a stable response for 200 steps, the validation step would be considered unsuccessful. Figure 56 shows the protocol performed during this validation step.

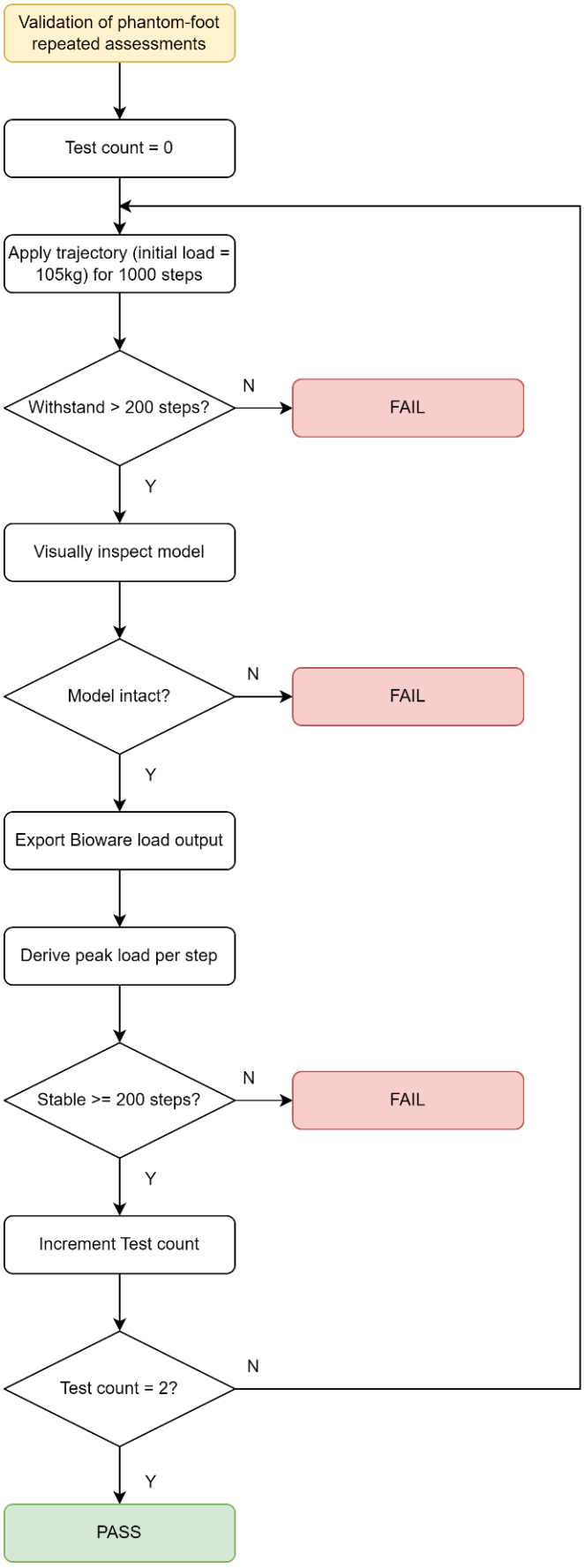

Figure 56: Validation of phantom-foot repeated assessments

4.2.3.4. Results

The phantom-foot repeated assessments feasibility is described in Figure 57. Figure 58 shows the degradation of the phantom-foot following the completion of a test cycle of 1000 steps, with a large cavity in the posterior lateral heel. There was an initial recovery to 637.65N in the first step of test cycle 2, however, the phantom-foot then demonstrated unstable behaviour with a significantly lower load. Test cycle 2 was terminated early given the loading trend presented and degradation of the phantom-foot beginning to detach it from the robotic arm.

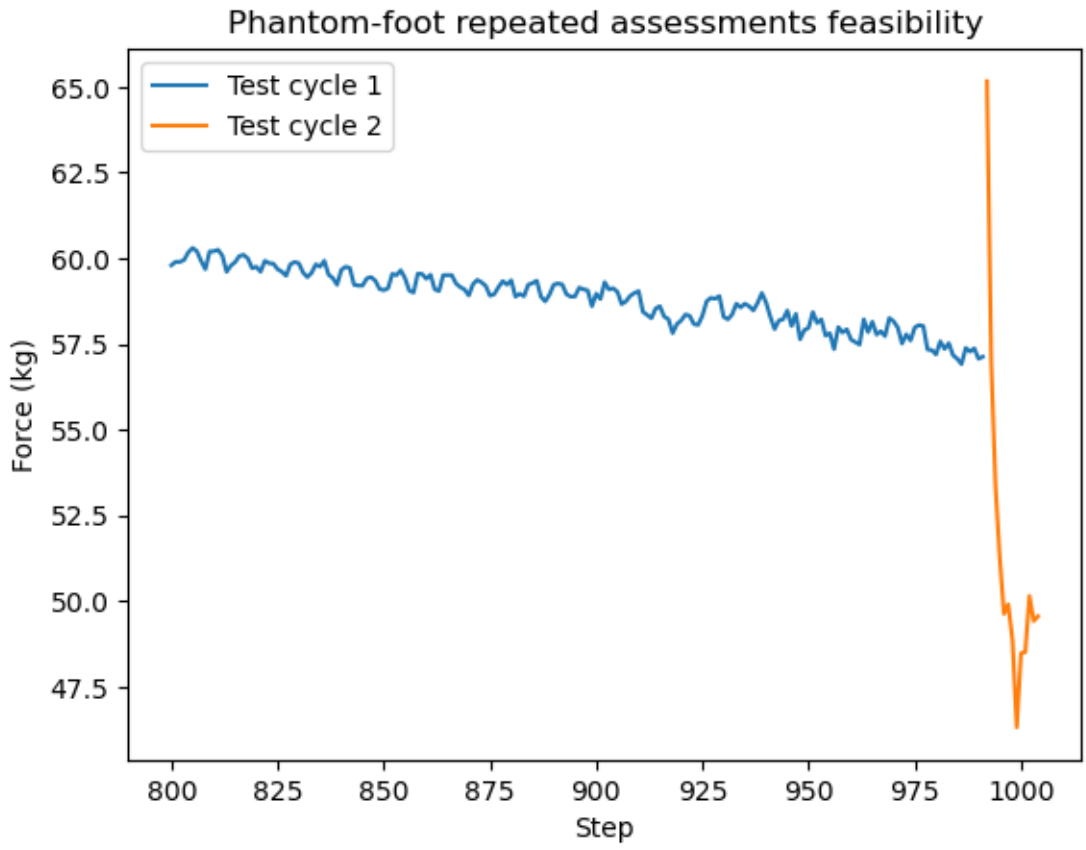

Figure 57: Phantom-foot repeated assessments feasibility validation

Figure 58: Damage to the tissue component of the phantom-foot following cyclic loading of 1000 steps

4.2.3.5. Discussion

This validation step failed as, even when provided a rest period to allow material recovery, the phantom-foot degraded beyond the minimum threshold required to undergo further testing. This was determined by repeating the protocol with the same phantom-foot, which was unable to sustain any significant period of stability.

This inability to run longer test cycles, or multiple cycles with the same phantom-foot could be attributed to the lattice structure. Inherently, a lattice structure features points of weakness around the connecting points between repeating structures. As these areas are damaged/rupture under repeated loading, it causes a cascading effect where greater load is transferred to the remaining intact lattice, which then degrades at a faster rate. A visual inspection following each 1000 step protocol revealed the damage the phantom-foot sustained during testing because of this effect (see Figure 58). The area where the phantom-foot sustained damage was consistent across phantom-foot copies, which indicated the lattice network rather than the impact force was the primary factor causing degradation.

This could be addressed by manufacturing the phantom-foot tissue as a solid structure rather than a lattice structure which would also likely increase the duration of the period the phantom-foot remains stable. However, this would introduce greater issues around repeatability (if an alternative to 3D printing was elected) or cost (if Polyjet printing rather

than SLA printing was chosen). For example, a Polyjet printer can cost upwards of £30,000. Within the use-contexts for the test platform, the current phantom-foot design is sufficient to characterise orthotic product performance and the requirement to use a new phantom-foot model for each test does not significantly impact its implementation, provided there was no statistical significance to changing between models; this was confirmed in the previous validation step.

4.3. Test platform comparison to in-vivo data

Following validation, comparison against in-vivo data was required to determine how closely the test platform could recreate realistic plantar pressure distribution and joint kinematics. This would enable a more detailed evaluation of orthotic product performance, as absolute changes made to the phantom-foot (described using the product performance criteria) could be inferred, rather than trends e.g., a reduction of peak plantar pressure in the heel region by a given percentage of bodyweight. Firstly, the loading profile produced by the test-platform on the phantom-foot was compared to that of in-vivo participants. Next, the pressure profile and contact area produced by the test-platform on the phantom-foot were compared to the same cohort. Finally, the joint segment kinematics produced by the test-platform on the phantom-foot were compared.

4.3.1. Loading profile agreement

4.3.1.1. Purpose

The previous chapter validated the loading repeatability of the actuation system and the change in loading response of the phantom-foot over a test cycle. Next, it is important to ensure that the loading profile applied by the test platform aligns with in-vivo i.e., the magnitude and timings of peak loads and the rate of loading/unloading. There exists a high degree of inter-participant variability with respect to body mass, stride length and walking speed. Therefore, the test platform will be compared to in-vivo participants of similar anthropometrics, loading will be presented as a function of bodyweight percentage and the walking speed presented as a function of gait cycle percentage to minimise these effects.

4.3.1.2. Research question/hypothesis

Research question: Does the phantom-foot produce a loading response equivalent to in-vivo for the first portion of the gait cycle?

Hypothesis: The phantom-foot and in-vivo datasets will align with the peak load (bodyweight %) and timing of events, however, there will be significant variation within the in-vivo group.

4.3.1.3. Test methodology

1000 steps were applied to 3 phantom-foot copies, and the average loading response per step in the stable region evaluated. The average phantom-foot group was then compared to a similar cohort (i.e., comparable anthropometrics such as mass and height) of healthy participants. This data was collected from an existing source where participants had given consent for secondary analysis (Nester, Jarvis, Jones, Bowden, & Liu, 2014). The two individuals chosen as part of the comparable cohort can be found in Table 28. More than one individual was preferred given the natural variation in gait between individuals; the test platform was intended to represent a generic gait pattern rather than a specific individual.

Table 28: Phantom-foot and comparable in-vivo cohort

Sample	Age	Mass (N)	Height (cm)
Phantom-foot	22	637.65	172.8
Individual 1	Not stated	618.03	173.4
Individual 2	23	627.84	174.2

Comparison metrics included peak load (expressed as bodyweight %), time to gait events and maximum loading rate. T tests on each of these metrics were performed to determine statistical differences between each group. Figure 59 shows the protocol performed during this validation step.

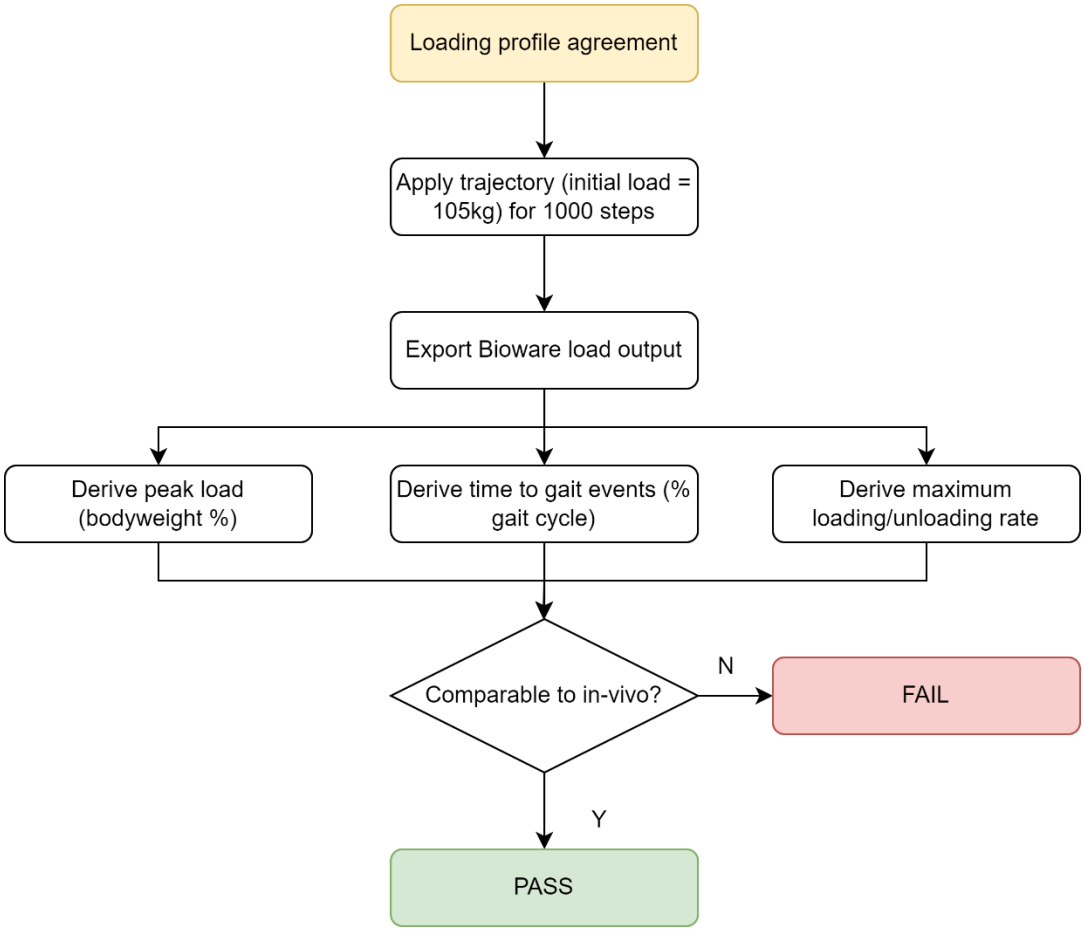

Figure 59: Loading profile agreement pathway.

4.3.1.4. Results

Table 29 presents the loading profile agreement between the test platform and the in-vivo comparable cohort. Figure 60 shows the loading profile of test platform and comparable in-vivo participants. There were significant differences between the test platform and in-vivo group in the peak load at heel strike, time to mid-stance and maximum unloading rate. Moreover, the test platform only demonstrated variability between steps in the peak load, whereas the in-vivo group showed variation across each metric. The test platform produced a lower peak load (10% lower than in-vivo) but operated at a higher loading rate. However, the heel-strike transient occurring at the beginning of the in-vivo loading profile was not recreated by the test platform.

Table 29: Mean (SD) loading profile agreement between the test platform and in-vivo comparable cohort

Variable	Test platform (stable region) (%)	In-vivo comparable cohort (%)	T-value	P value
Peak load at heel-strike (% bodyweight)	94.10 (3.33)	104.09 (6.27)	2.21	0.035
Time to mid-stance (% gait cycle)	40.18 (0)	48.76 (3.82)	3.13	0.004
Time to heel-strike peak load (% gait cycle)	26.54 (0)	25.52 (3.72)	0.38	0.71
Maximum loading rate (% bodyweight/% gait cycle)	8.73 (0)	8.32 (2.11)	0.27	0.79
Maximum unloading rate (% bodyweight//% gait cycle)	7.44 (0)	2.69 (1.35)	4.90	<0.001

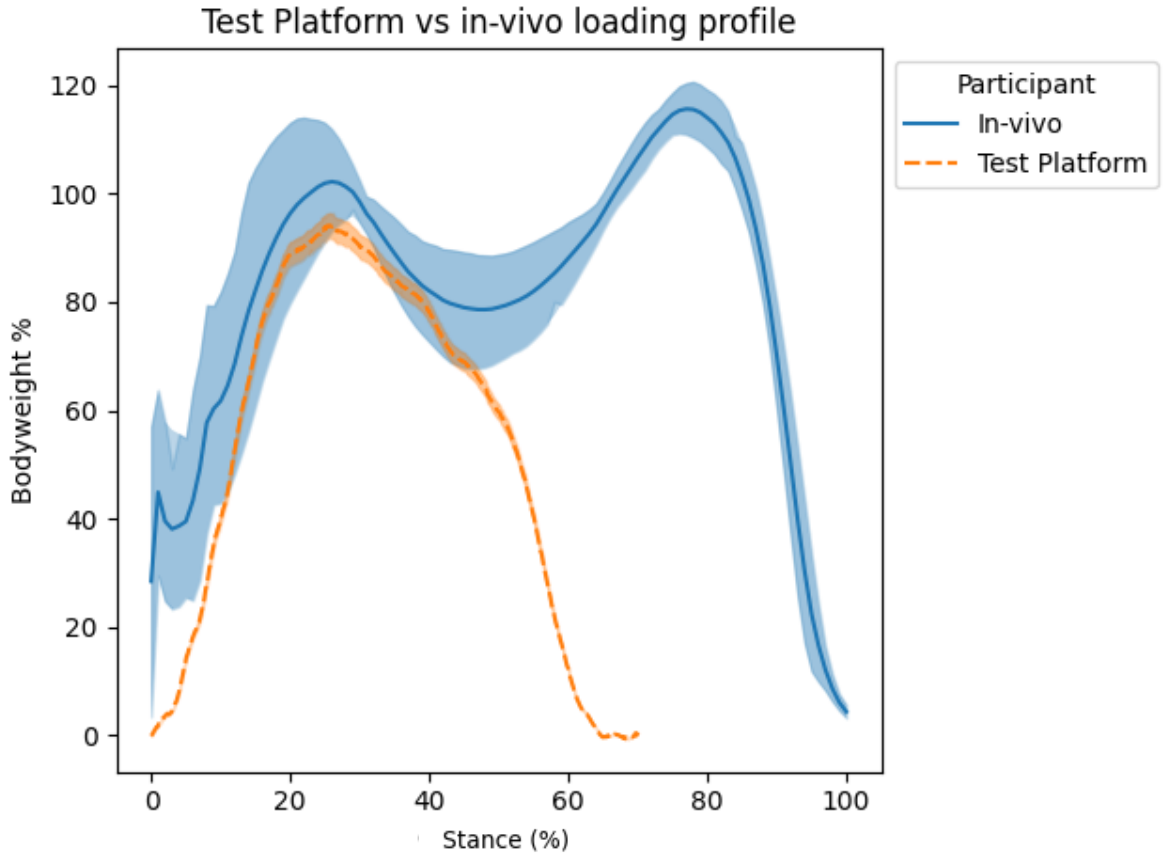

Figure 60: Loading profile (mean and standard error) of test platform within the stable region and comparable in-vivo participants. Each profile was generated using 10 steps, and the in-vivo cohort included 2 participants.

4.3.1.5. Discussion

The test platform produced a loading profile which largely lies within 1 SD of the mean in-vivo loading pattern represented in Figure 60, with the most significant difference being the unrepresented heel strike transient. The significant differences between the test platform and in-vivo group could be attributed to several factors. Firstly, as demonstrated in the Validation of phantom-foot loading response repeatability, the open-loop control system employed and requirement for a conditioning phase for the phantom-foot until it produced a stable response resulted in a lower-than-expected peak load at heel-strike. Similarly, the method employed to develop the trajectory and loading pattern resulted in differences between the timing of events and unloading rate; the implementation of a control system to generate more realistic loading patterns would likely result in improved alignment to in-vivo gait loading patterns.

In-vivo gait naturally varies in magnitude and loading rate. Conversely, robotic systems can produce highly repetitive motions, which results in significantly less variation across all metrics. The impact of these differences highlights the benefits of using the test platform to characterise products; changes made to the phantom-foot can solely be attributed to the

applied product, which would not be possible with in-vivo participants. However, given the products will ultimately be used by humans and subjected to step-by-step variation, it does not reduce the need for clinical studies involving humans as well.

4.3.2. Pressure profile and contact area agreement.

4.3.2.1. Purpose:

The purpose of this validation step was to evaluate whether the plantar pressure profile produced by the phantom-foot was comparable to in-vivo, such that the performance of orthotic products could accurately be captured by the test platform. In this initial test platform, the hindfoot region of the phantom-foot was of greatest interest given the orthotic products to be tested. Pressure variables of interest included centre of pressure, peak pressure, and location of peak pressure in the hindfoot region.

4.3.2.2. Research question/hypothesis:

Research question: Does the test platform produce a centre of pressure, peak pressure, location of peak pressure and contact area comparable to the in-vivo foot during gait?

Hypothesis: The phantom-foot will produce comparable centre of pressure, peak pressure and pressure distribution to the in-vivo foot due to the comparably stiff plantar tissue material.

4.3.2.3. Test methodology:

1000 steps were applied to 3 phantom-foot copies, and the plantar pressure metrics per step in the stable region evaluated. The average phantom-foot group was then compared to the in-vivo group of 100 healthy participants (Nester, Jarvis, Jones, Bowden, & Liu, 2014). Comparison metrics included peak pressure, total pressure, peak pressure distribution map and contact area. T tests on each of these metrics were performed to determine statistical differences between each group. Figure 61 shows the protocol performed during this step and Figure 62 shows the method employed to concatenate the pressure profile of the heel region per step.

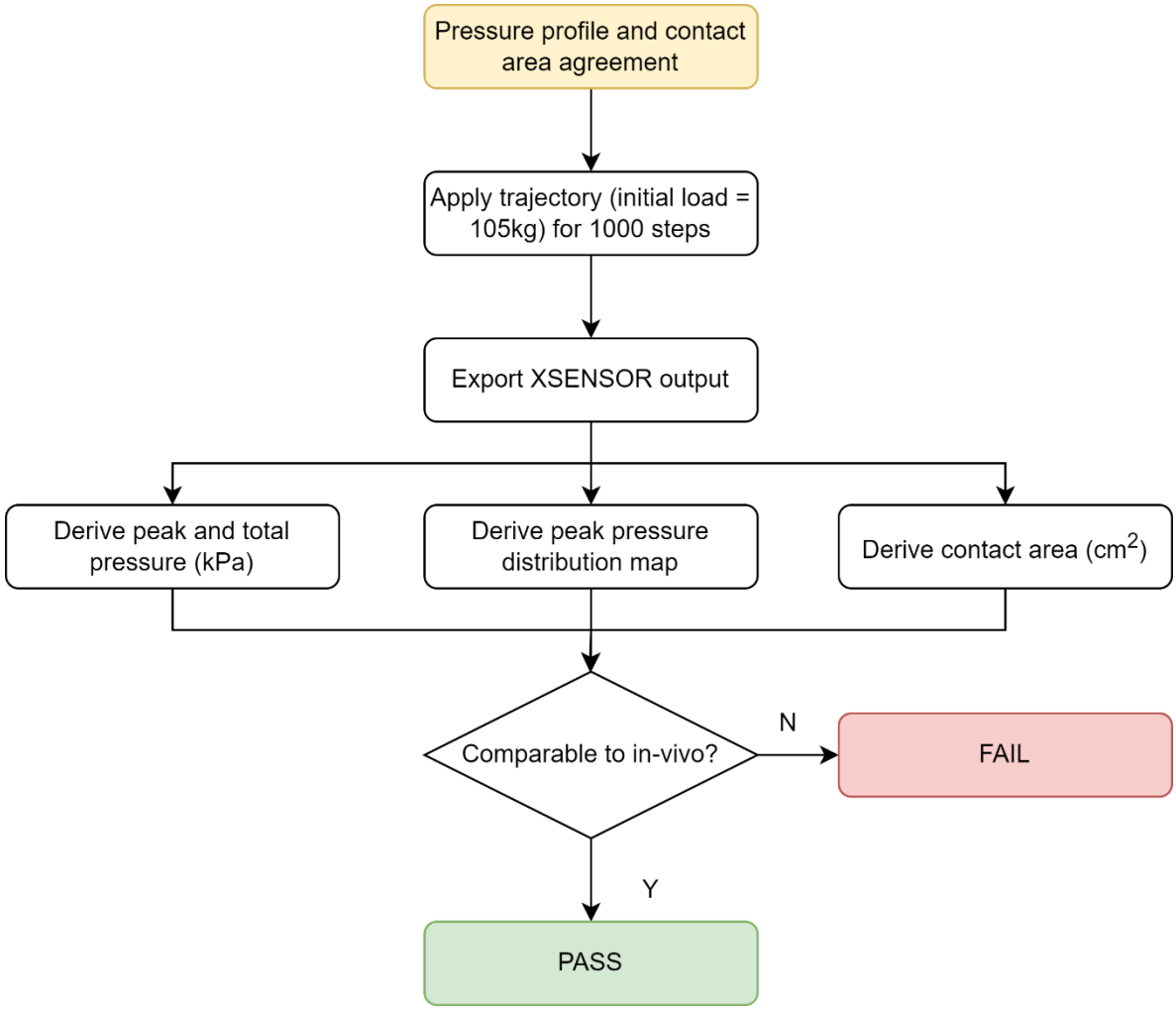

Figure 61: Phantom-foot pressure profile and contact area validation pathway

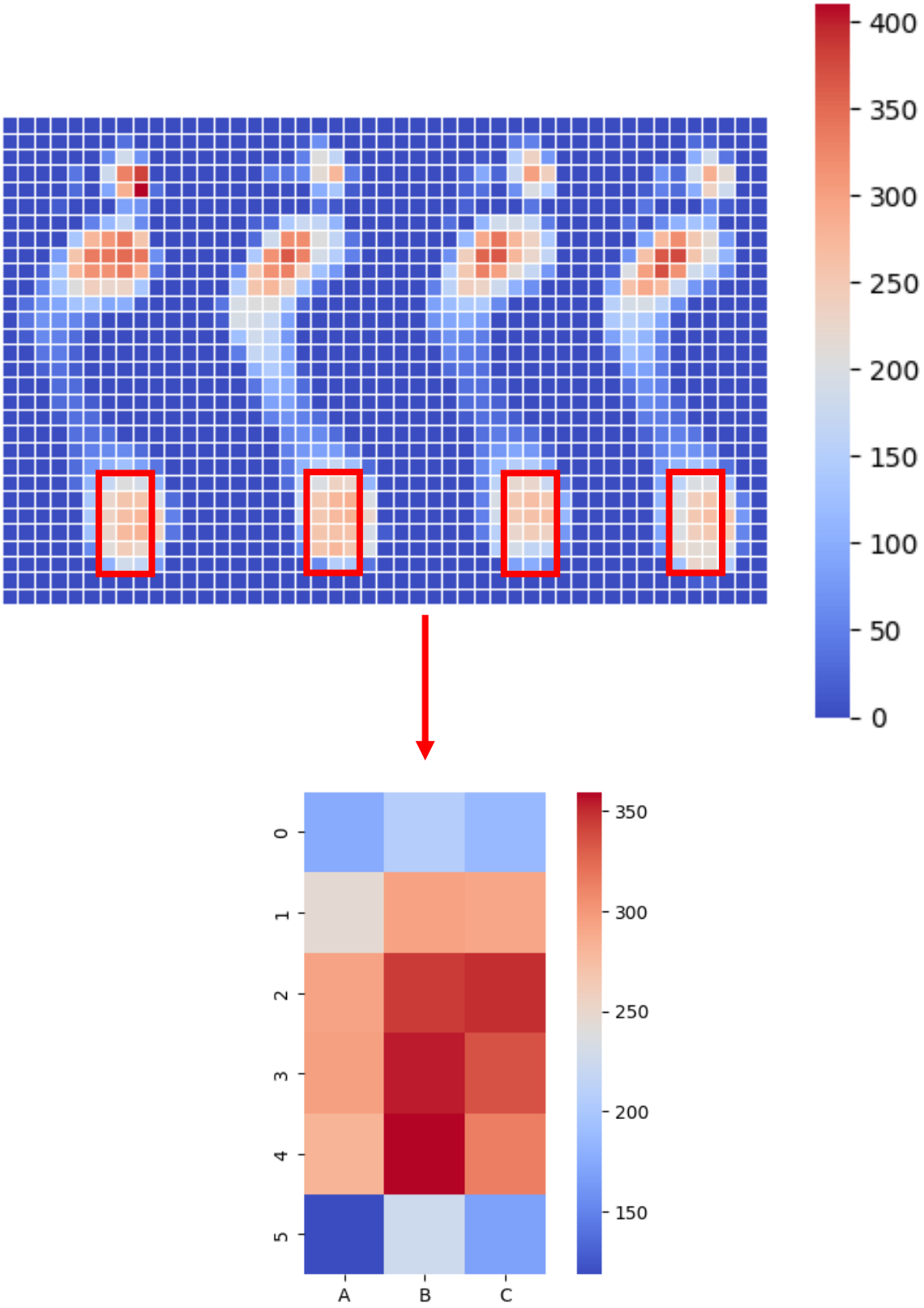

Figure 62: Individual steps averaged per participant, with the region of interest highlighted. Only the heel region is included (excluding the lateral and posterior borders) as the forefoot produced a significantly lower pressure distribution and was not of interest within the first implementation of the test platform.

4.3.2.4. Results:

Table 30 shows the mean and standard deviation of the heel region peak pressure for in-vivo group and test platform. Figure 63 presents the pressure heatmaps of the heel region for each participant from Jarvis dataset comprising the in-vivo group. Figure 64 presents the mean pressure heatmap of the heel region for this in-vivo group and test platform and Figure 65 shows the in-vivo and test platform average heel region contact area map. Finally Figure 66 and Figure 67 show Tukey plots comparing the peak pressure of the in-vivo group and the test platform (mean and 95% confidence interval).

Although there was overlap in between the peak pressure produced by the test platform and in-vivo group (see Figure 66), the location of peak pressure was significantly different. The test platform produced a high concentration of pressure in the posterior-lateral heel region (sensors rows A4 and A5), while the in-vivo group demonstrated a concentration around the centre-posterior heel. This could have been related to degradation of the phantom-foot, or the lack of coronal plane control; the phantom-foot may have been slightly everted when attached to the robotic arm. There were also differences in the shape of the contact area between the test platform and in-vivo cohort, specifically in the heel region captured. The in-vivo participants that produced a peak pressure within the 95% confidence interval of the test platform were 30.23 ± 10.06 years old, weighed 662.96 ± 130.57N and had a height of 166.81 ± 8.34 cm. This closely aligned with the sample used to model the phantom-foot (22-year-old, 637.65N, 172cm). 7 female and 26 and male participants aligned with the male test platform sample.

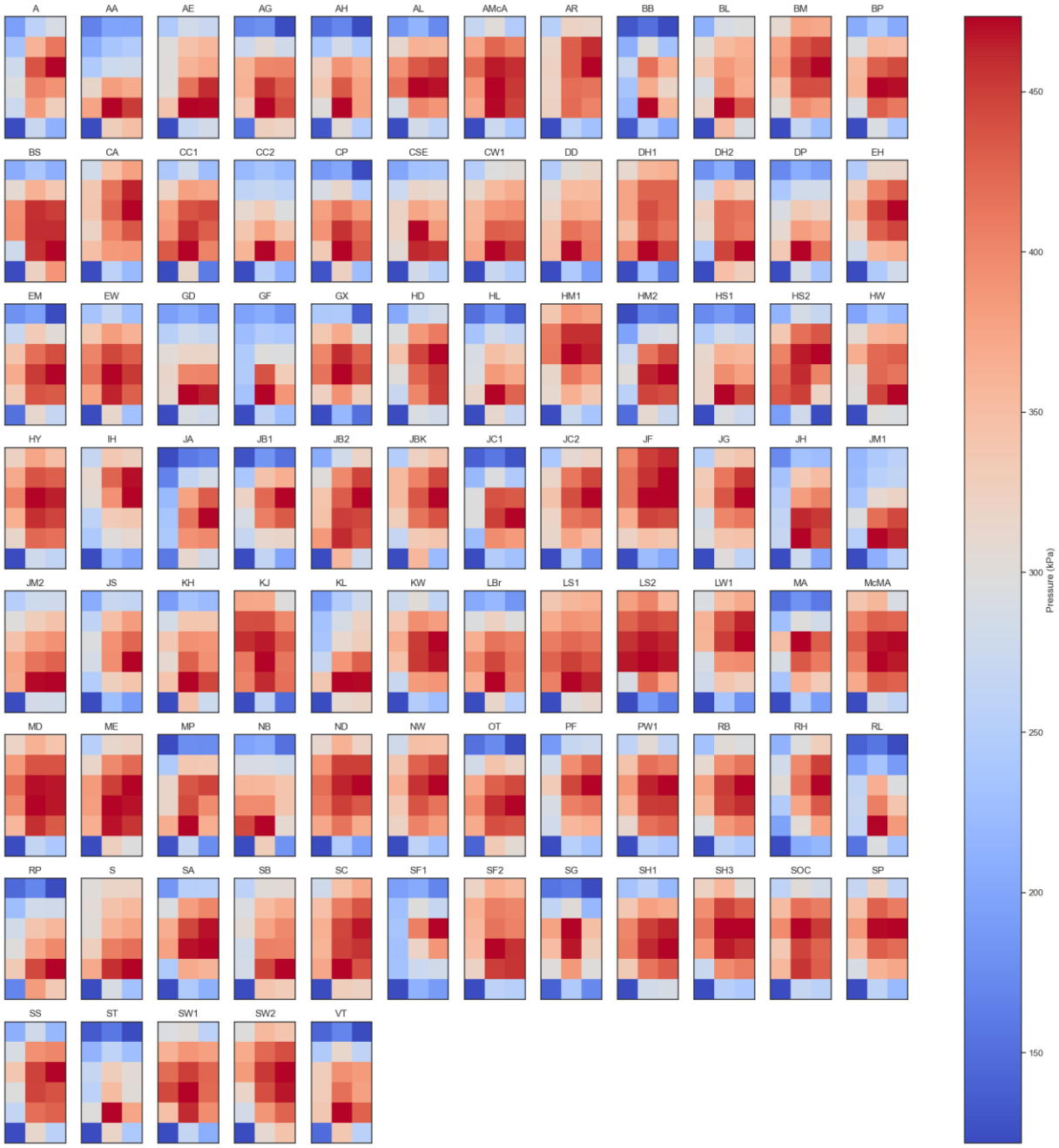

Figure 63: Pressure heatmaps of the heel region for each participant from Jarvis dataset

Table 30:Heel region peak pressure for in-vivo whole group (IVWG) and test platform (TP)

Heel region peak pressure (kPa)						
Sensor column/row	**A**		**B**		**C**	
Group	**IVWG**	**TP**	**IVWG**	**TP**	**IVWG**	**TP**
0	182.78 (54.87)	13.24 (4.36)	219.25 (66.28)	32.17 (10.41)	202.32 (80.74)	1.22 (2.99)
1	248.96 (55.61)	80.59 (24.86)	304.59 (70.84)	66.76 (20.58)	302.32 (81.51)	53.6 (16.63)
2	290.55 (63.06)	147.59 (44.82)	359.72 (87.79)	105.76 (32.02)	362.99 (85.39)	74.48 (22.44)
3	284.97 (67.84)	250.98 (76.00)	376.12 (98.44)	161.82 (48.75)	367.93 (98.88)	89.52 (26.9)
4	269.05 (81.54)	359.26 (108.04)	382.96 (142.7)	247.59 (74.39)	359.27 (118.5)	98.37 (29.57)
5	97.97 (25.63)	315.6 (95.43)	241.55 (70.94)	202.25 (61.17)	209.54 (67.47)	100.55 (30.59)

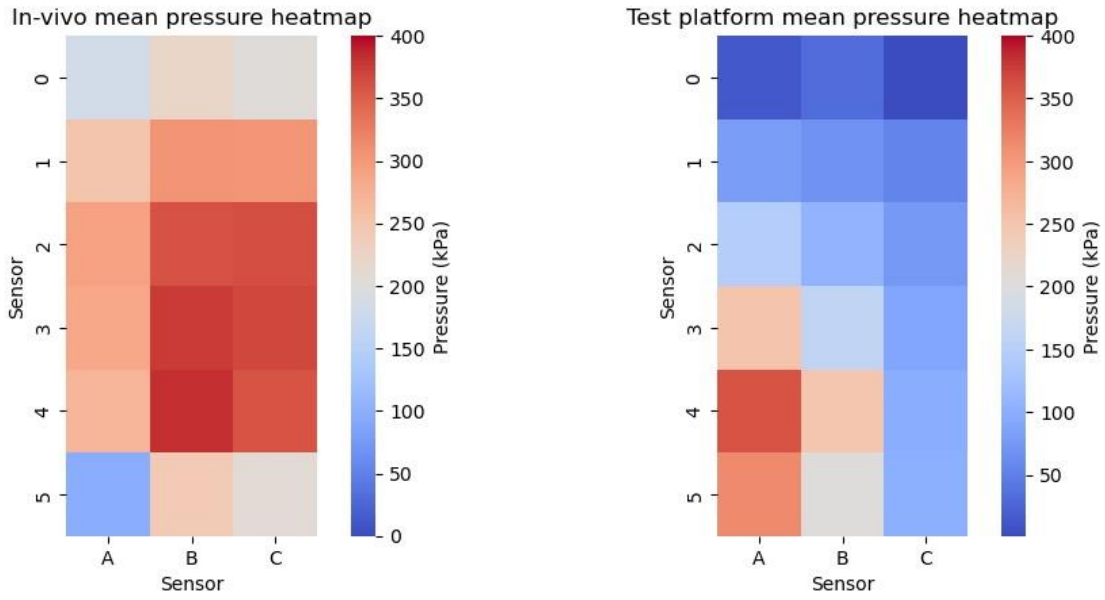

Figure 64: Mean pressure heatmap of the heel region for the in-vivo group and test platform.

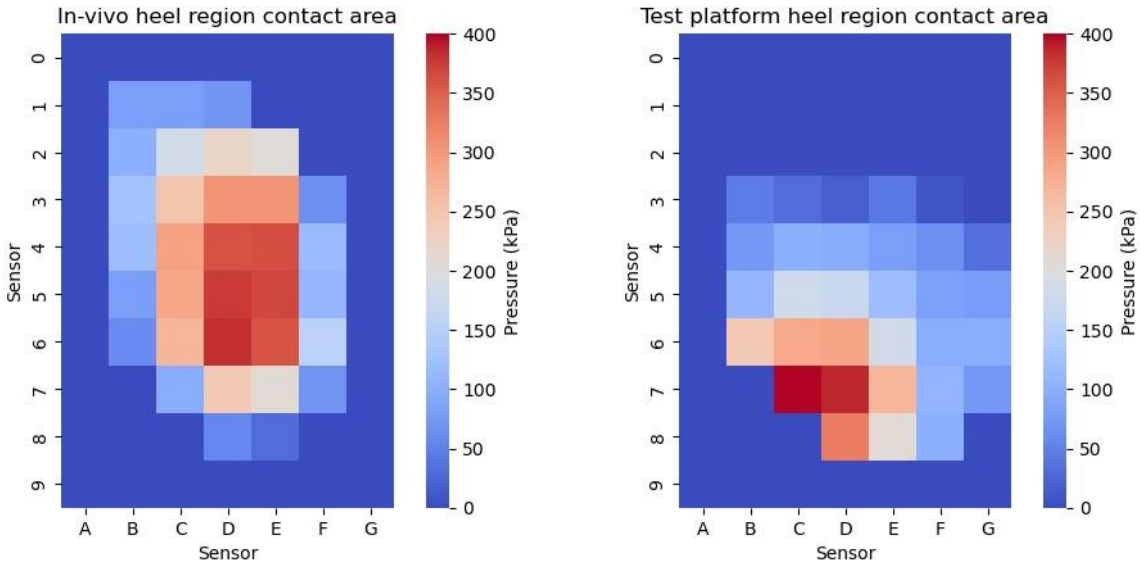

Figure 65: In-vivo and test platform average heel region contact area map.

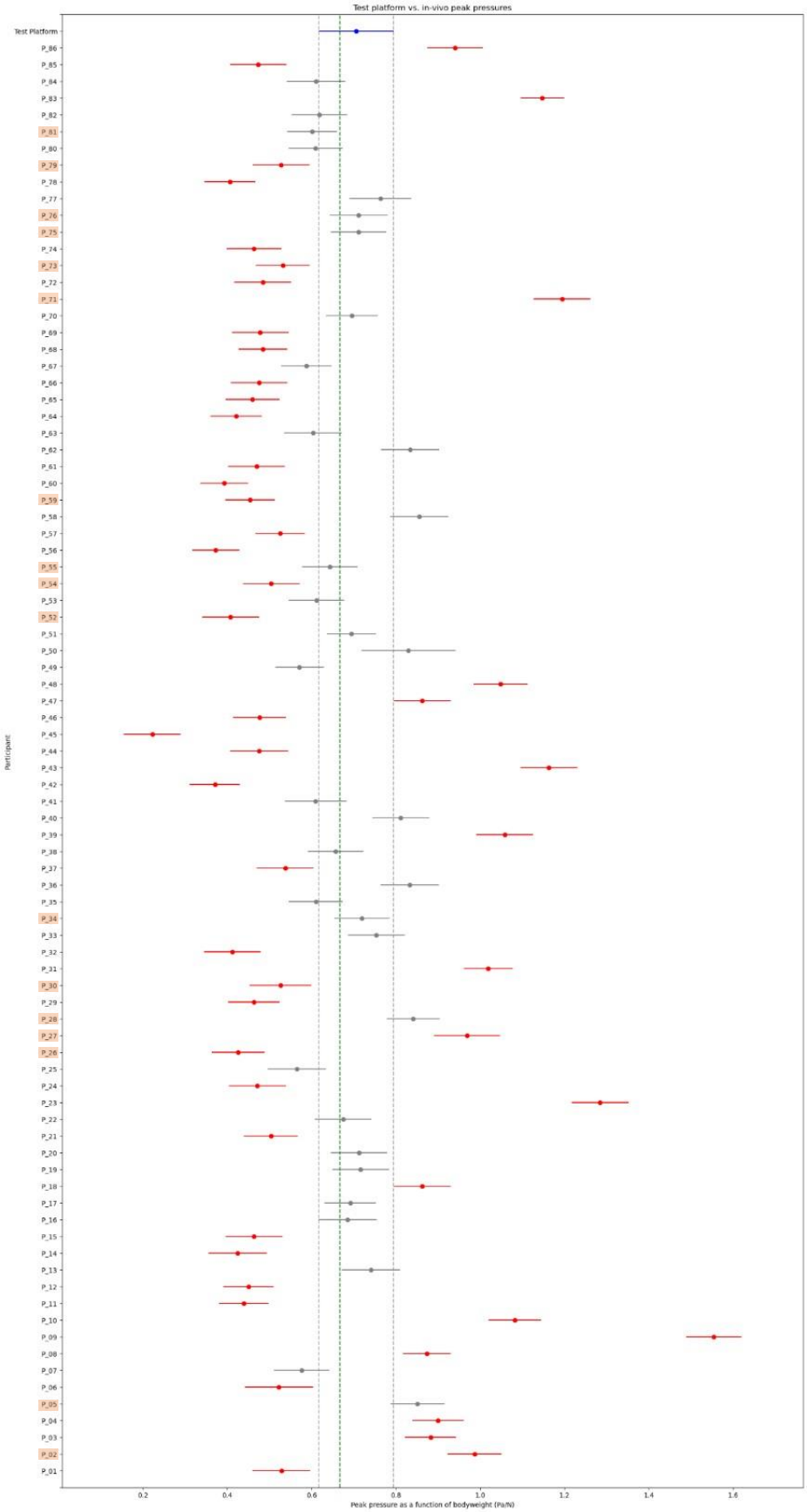

Figure 66: Tukey plot describing multiple comparisons between all pairs for peak plantar pressure. Shaded participants align within 5% of the phantom-foot samples mass and height. Grey plots represent participants which lie within the 95% confidence intervals, red participants lie out of this range, and the green line represents the mean of all in-vivo participants.

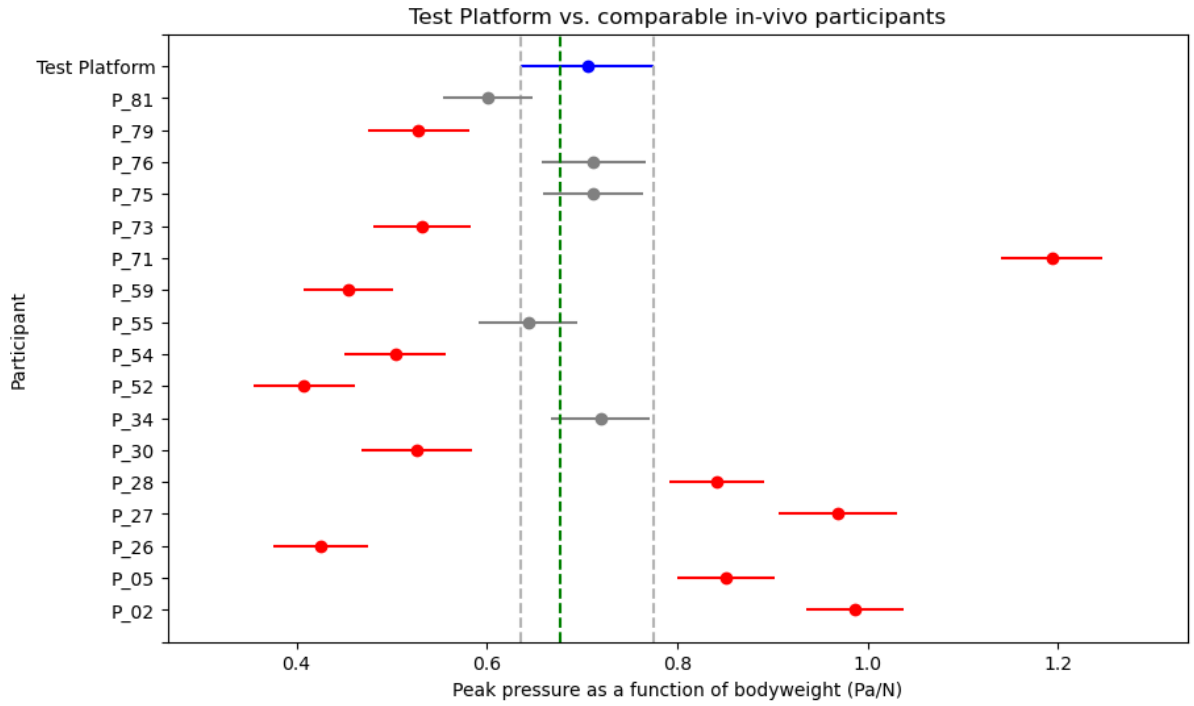

Figure 67: Tukey plot describing multiple comparisons between all pairs for peak plantar pressure, for participants with comparable mass and height to the phantom-foot sample. Grey plots represent participants which lie within the 95% confidence intervals, red participants lie out of this range, and the green line represents the mean of all in-vivo participants.

4.3.2.5. Discussion:

There was significant variation in the age, mass, and height of the in-vivo participants, so it was expected that the test platform would not align with every individual. Within this group there were a number of participants with comparable heights and masses to the phantom-foot sample, however, even within this cohort there was significant variation in the peak plantar pressure as a function of bodyweight (typical variation in pressure) and the test platform only aligned with 5 participants. Comparable anthropometrics didn't seem to improve alignment between in-vivo participants and the test platform, which indicates that other factors such as variation in gait patterns or foot/shoe size may have greater effects.

The test platform demonstrated much greater repeatability than the in-vivo participant group, indicated by the much smaller spread in peak pressures, producing a point pressure map. This difference in the location of peak pressure between the test platform and in-vivo group may be attributed to the geometry of the skeletal component of the phantom-foot, which may have concentrated pressures around a sharp feature on the calcaneus. This will also have contributed to the findings of the validation of phantom-foot repeated assessments feasibility, as the point of failure in the plantar tissue component of the phantom-foot aligns with this region of peak pressure (see Figure 58).

With respect to the contact area, the phantom-foot utilised a plantar tissue material which didn't exhibit the same viscoelastic behaviour as in-vivo plantar tissue and was not expected to deform as much, producing a lower contact area. However, unexpectedly the phantom-foot appeared to deform more than the average in-vivo maps (see Figure 65). This may be ascribed to differences in measurement equipment; the in-vivo cohort was evaluated using a pressure plate compared to an in-shoe system for the test platform. Hence a comparison using the same measurement system would allow for more appropriate comparisons to be made.

Given the highly repeatable behaviour of the test platform, differences applied by products should be indicative of product performance (for this region). However, improvements could be made to improve performance of the test platform and enable more in-depth product performance testing. Firstly, identifying the design changes required to "smooth" the region of high-pressure present in the lateral-posterior region of the phantom-foot would enable a more accurate plantar pressure map to be produced, and hence more easily allow changes applied by orthotic products to be identified by the test platform. Additionally, the current design of the phantom-foot didn't allow the propagation of force through the midfoot section of the plantar surface (given the gap between the skeletal structures and plantar tissue) and hence no clear contact area/ peak pressure measurements. By filling this gap, changes made to this region of the foot by products could also be analysed. Unfortunately, improvements made to the forefoot pressure map would only be possible with significant additions to the actuation system by the addition of motion control i.e., muscular control of the forefoot. This is because the forefoot is difficult to load solely through the tibia, with the greatest concentration of force being transferred to the hindfoot.

4.3.3. Joint segment kinematics agreement

4.3.3.1. Purpose:

In addition to the location of peak pressure, the test platform was intended to recreate the internal foot kinematics of the human foot. Therefore, the purpose of this stage was similar to the previous validation step, however, centred around the alignment of the segment joint range of motion to in-vivo values. This would also ensure that kinematic changes made by orthotic products could be accurately assessed by the test platform. Kinematic variables of interest included segment range of motion and the timings of peaks in each plane.

4.3.3.2. Research question/hypothesis:

Research question: Does the test platform produce bone/segment kinematics comparable to the in-vivo foot during gait?

Hypothesis: The phantom-foot is expected to produce similar sagittal plane motion as the in-vivo foot however, different coronal and transverse plane motion due to the omission of shear force control in the actuation system. In particular, the hindfoot is expected to produce more accurate motion than the forefoot due to the design of the phantom-foot and actuation system excluding tendinous control. A paired t-test will evaluate how closely the phantom-foot and in-vivo data align.

4.3.3.3. Test methodology:

During loading, the phantom-foot is intended to reflect the behaviour of a human foot. As defined in the use-contexts of this project, an important indicator of the alignment of the phantom-foot to a real foot is the bone/joint segment motion, including the range of motion of each joint and their motion profiles throughout the gait trajectory. The marker placement protocol established in Figure 42 was applied. As before, 1000 steps were applied to 3 phantom-foot copies, and the joint kinematics per step in the stable region evaluated. The average phantom-foot group was then compared to a similar cohort (i.e., comparable anthropometrics such as mass and height) of 100 healthy participants. The chosen participants had masses of 618.03N and 627.84N, and heights of 173.4cm and 174.2cm respectively. Comparison metrics included joint segment range of motion, maximum movement in each plane and the joint angle at key gait events. For each foot segment combination and plane of motion, the mean, 95% CI of the angle of the phantom-foot at IC, FFL and HO, and the total range of motion during stance were calculated. Figure 68 shows the protocol performed during this step.

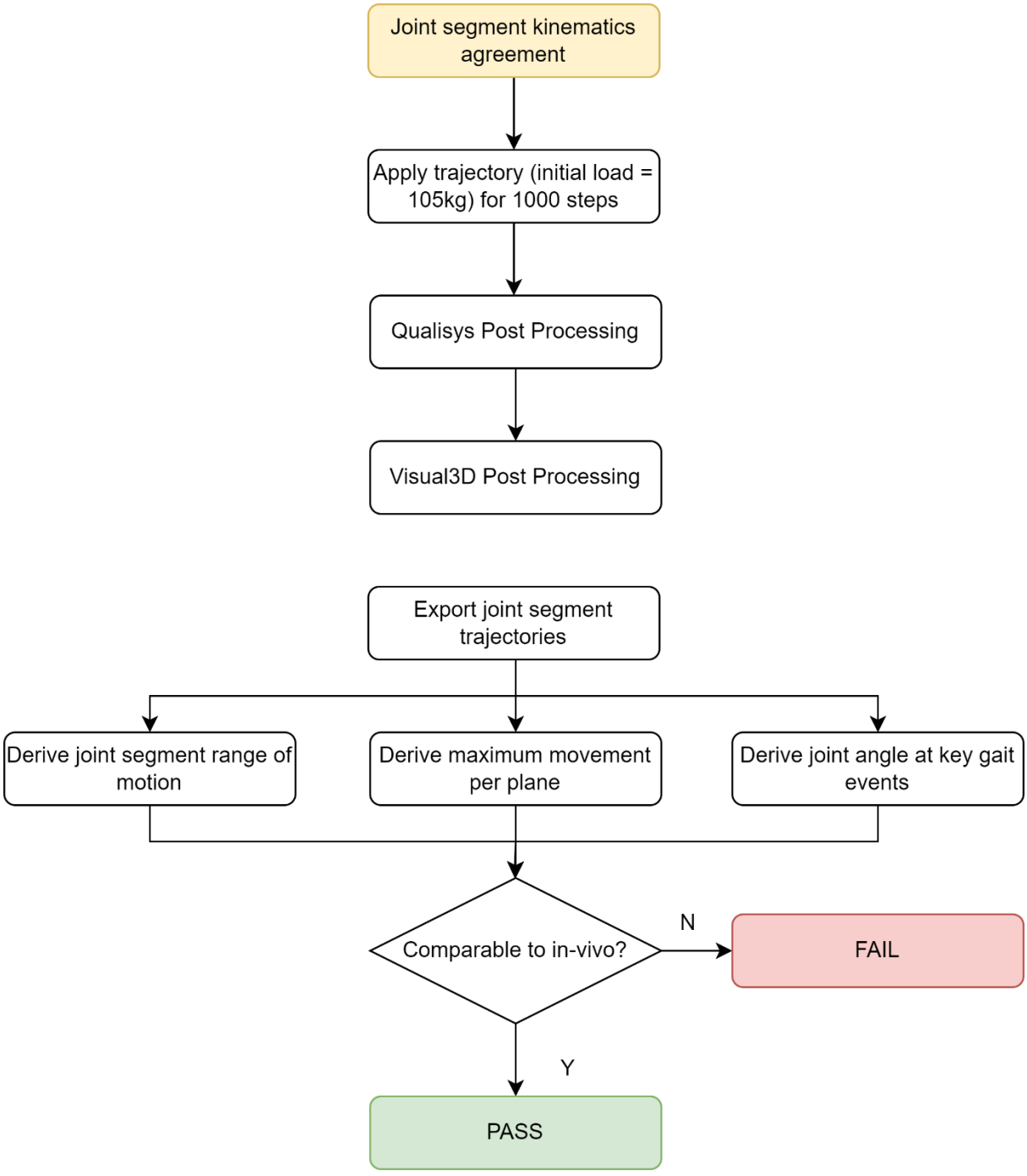

Figure 68: Joint Segment Kinematics Conformance Validation Pathway

4.3.3.4. Results:

The joint segment kinematics for the test platform and two comparable participants from a cohort of 100 healthy participants are presented in Figure 69. Only stance period is represented. Table 31 shows the mean joint angle at initial contact (IC), full foot loading (FFL) and heel off (HO), 95% confidence interval and range of the in-vivo group and test platform per segment in each plane. Both in-vivo participants exhibited similar trends i.e., timings of peaks, range of motion, however, with different behaviour in late midstance in the

midfoot-calcaneus coronal and midfoot-shank coronal planes; participant 2 exhibiting abduction in contrast to the adduction presented by participant 1. The test platform demonstrated poor alignment to both participants, producing significantly simpler motion paths across each segment. Between IC and FFL, there was agreement in the change in joint segment angle in the calcaneus-tibia (sagittal plane), midfoot-calcaneus (frontal and coronal plane) and midfoot-shank (frontal and coronal plane) segments. However, between FFL and HO there was little to no motion per segment, likely as a consequence of not representing muscles within the phantom-foot.

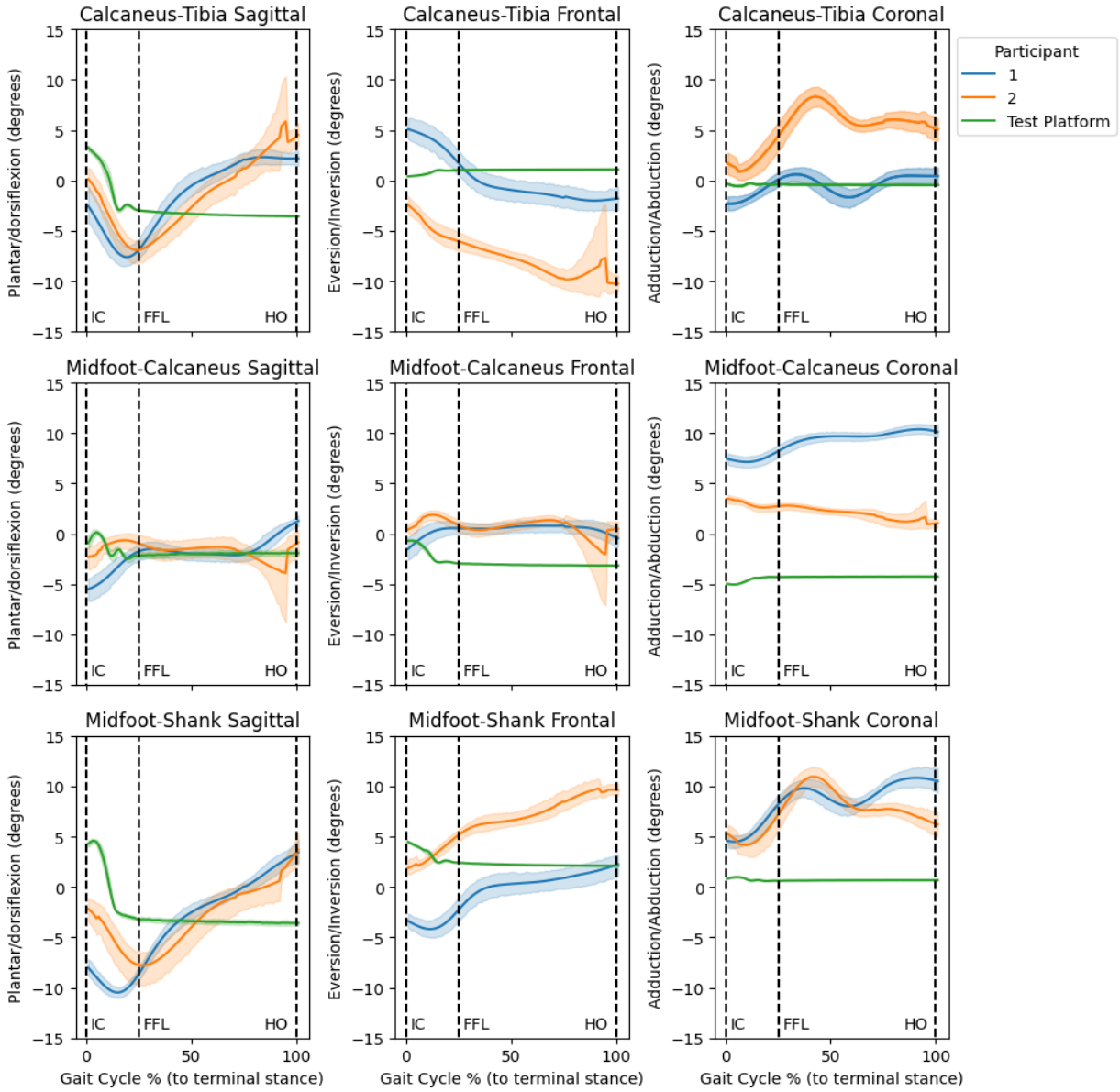

Figure 69: Joint segment kinematic data for calcaneus-tibia, midfoot-calcaneus and midfoot-shank segments occurring between heel-strike to terminal stance for comparable in-vivo participants and the test platform

Table 31: For each foot segment combination and plane of motion, mean, 95% CI of the angle of the phantom-foot at IC, FFL and HO, and the total range of motion during stance.

			In-vivo			Test Platform				
Event	**Column**	**Plane**	**Mean**	**95% CI**	**Range**	**Mean**	**95% CI**	**Range**	**T-Statistic**	**P-Value**
IC	Calc-Tib	Sag	-1.193	-2.429, 0.042	5.723, -5.486	3.256	2.923, 3.59	3.73, 2.223	-7.186	<0.01
		Frt	1.333	-0.333 ,2.998	8.728, -6.473	0.405	0.371, 0.439	0.511, 0.357	1.143	0.263
		Trn	-0.302	-1.354, 0.751	6.32, -4.072	-0.334	-0.421, -0.247	-0.21, -0.6	0.062	0.951
	Mid-Calc	Sag	-3.913	-4.976, -2.851	0.312, -10.192	-0.919	-1.75, -0.088	1.461, -2.043	-4.746	<0.01
		Frt	-0.535	-1.309, 0.239	2.034, -5.252	-0.692	-0.711, -0.673	-0.656, -0.73	0.415	0.681
		Trn	5.451	4.584, 6.318	9.228, 1.217	-4.986	-5.074, -4.898	-4.874, -5.215	24.6	<0.01
	Mid-Tib	Sag	-5.091	-6.48, -3.703	0.944, -10.881	4.308	3.882, 4.734	5.405, 3.767	-13.398	<0.01
		Frt	-0.737	-1.912, 0.439	5.638, -5.468	4.486	4.321, 4.65	4.69, 3.964	-9.046	<0.01
		Trn	4.929	4.288, 5.57	8.17, 1.32	0.847	0.749, 0.944	1.136, 0.72	12.944	<0.01
FFL	Calc-Tib	Sag	-6.889	-7.689, -6.09	-0.839, -12.75	-2.972	-3.018, -2.926	-2.899, -3.098	-10.076	<0.01
		Frt	-1.843	-3.643, -0.043	6.558, -8.767	1.042	1.037, 1.046	1.055, 1.034	-3.301	0.003
		Trn	2.073	0.871, 3.276	8.506, -1.792	-0.361	-0.397, -0.325	-0.298, -0.425	4.168	<0.01
	Mid-Calc	Sag	-1.385	-2.062, -0.709	1.342, -6.379	-2.187	-2.535, -1.839	-1.207, -2.613	2.219	0.034
		Frt	0.69	0.237, 1.143	2.537, -1.715	-2.943	-2.983, -2.903	-2.832, -3.001	16.463	<0.01
		Trn	5.68	4.492, 6.868	10.029, 0.786	-4.292	-4.345, -4.239	-4.219, -4.417	17.27	<0.01
	Mid-Tib	Sag	-8.235	-9.195, -7.275	-5.429, -17.57	-3.216	-3.497, -2.936	-2.444, -3.561	-10.416	<0.01
		Frt	1.149	-0.546, 2.844	6.859, -5.551	2.426	2.391, 2.46	2.487, 2.352	-1.55	0.134
		Trn	7.731	6.777, 8.685	11.342, 2.49	0.621	0.586, 0.656	0.731, 0.586	15.335	<0.01
HO	Calc-Tib	Sag	3.231	2.415, 4.046	7.346, 0.574	-3.544	-3.595, -3.494	-3.464, -3.631	17.113	<0.01
		Frt	-5.858	-7.784, -3.931	1.865, -12.412	1.101	1.096, 1.107	1.111, 1.093	-7.456	<0.01
		Trn	2.697	1.456, 3.937	8.576, -3.444	-0.441	-0.462, -0.419	-0.402, -0.472	5.221	<0.01
	Mid-Calc	Sag	0.133	-0.727, 0.992	2.719, -6.299	-1.923	-2.267, -1.579	-0.975, -2.466	4.647	<0.01
		Frt	0.042	-0.652, 0.736	3.01, -2.257	-3.153	-3.202, -3.104	-3.047, -3.238	9.484	<0.01
		Trn	5.777	3.813, 7.74	13.374, -0.41	-4.242	-4.302, -4.183	-4.142, -4.385	10.527	<0.01
	Mid-Tib	Sag	3.365	2.447, 4.283	9.133, 0.429	-3.575	-3.902, -3.247	-2.777, -4.132	14.862	<0.01
		Frt	5.775	4.062, 7.488	11.852, -2.486	2.111	2.077, 2.146	2.175, 2.065	4.415	<0.01
		Trn	8.507	7.227, 9.787	16.853, 2.171	0.678	0.646, 0.71	0.773, 0.63	12.622	<0.01

4.3.3.5. Discussion:

The lack of segment motion presented post FFL by the test platform may have resulted due to several factors. 1) The method used to link segments together and lack of support between the skeletal and plantar tissue models resulted in the midfoot and calcaneus decoupling and misrepresented their motion. 2) The single point-of-actuation and coupling of the phantom-foot and robotic arm effectively represented a fixed ankle-joint; this resulted in no significant motion between the calcaneus segment and the final joint of the robotic arm, effectively 'bottoming out' the sagittal range of motion. These were expected to impact the motion significantly, as in-vivo foot motion involves several points of actuation performed by a complex arrangement of components. 3) The environment in which the test platform was operated significantly impacted the ability of the motion capture system to accurately track joint segment due to the large number of reflections and poor segment tracking. The robotic arm obscured some markers during motion; this in combination with the large number of reflections resulted in more than 100,000 trajectories over the course of a test cycle.

Improvements in these three factors would result in a test platform more capable of representing in-vivo joint motion, and therefore capture kinematic changes produced by products more adequately. However, complete alignment to in-vivo kinematics is not necessarily required; demonstrating changes in the trend e.g., peak dorsi-plantarflexion would still describe the effects of a product.

4.3.4. Review of test platform validation and in-vivo agreement

4.3.4.1. Test platform validation

A validation pathway was created to determine the test platforms capability to capture orthotic product performance. The pathway comprised three stages: actuation system loading and trajectory repeatability, repeatability of the loading response of the phantom-foot and feasibility of using a phantom-foot for multiple assessments. In the first phase, the test platform demonstrated highly repeatable loading and trajectory execution. It far outperformed the repeatability of in-vivo gait, enabling clear distinctions between the error present within the actuation system and the effects of the product to be characterised by the test platform. Moreover, adjustments to the control system strategy adopted could improve upon this further, were greater resolution required in future test protocols.

Whilst the actuation system was highly repeatable, the loading response of the phantom-foot was non-linear and unstable prior to a conditioning period. This was attributed to several factors, including the lattice network used to design the plantar tissue component. As the phantom-foot was loaded, regions across the plantar tissue experiencing high loads/pressures degraded as weak portions of the internal lattice network fractured. This in turn caused the phantom-foot to degrade faster, as greater loads were applied to the remaining structure, which collapsed over time. Accordingly, the behaviour of the phantom-foot changed significantly over the course of the test platform. As a consequence of the unstable behaviour of the plantar tissue component, a conditioning phase was required prior to data collection, with a duration of 500 steps required on average. Following this period, the performance of the test platform improved significantly and a stable load (within 5% of the peak load) could be achieved over 268 steps, which far exceeded the step count used to characterise products within clinical studies.

Ideally, in an industrial environment each phantom-foot model would enable several test protocols (i.e., the assessment of several products) to be carried out. The final validation step assessed the feasibility of using a single phantom-foot model over numerous test cycles of 1000 steps, with a rest period of 24 hours between test cycles to allow material recovery. However, it was apparent that the phantom-foot degraded beyond the point of usage following one complete test cycle. Whilst disappointing, the impact on the suitability of the test platform to industrial testing would be limited. Different copies of the phantom-foot demonstrated consistent, predictable behaviour with a small margin of error, validating the repeatability of the manufacturing process elected. Consequently, the test platform sufficiently passed the validation steps, offering repeatable operation with a low margin of error.

4.3.4.2. In-vivo agreement

Three steps were completed to establish the performance of the test platform compared to in-vivo data: comparison of the loading profile, pressure profile (and contact area) and joint segment kinematics to in-vivo data during gait. The loading profile produced by the test platform aligned closely with the average in-vivo profile, with consistent timing of peak load, and maximum loading rate. However, there were some discrepancies in the peak load at heel-strike, time to mid-stance and maximum unloading rate where the open-loop control strategy and inaccurate trajectory input reduced the agreement with the in-vivo profiles. Similar trends

appeared in the second phase concerning plantar pressure, with partial alignment to in-vivo behaviour.

Plantar pressure metrics varied considerably between in-vivo participants, but the test platform aligned closely with the average in-vivo peak pressure as a function of bodyweight. The location of this peak pressure in-vivo primarily occurred in the centre of the heel region, although different participants commonly exhibited medial/lateral movement in the peak pressure. Conversely, the test platform produced significantly different pressure maps, with peak pressures occurring in the posterior-lateral heel. This difference was attributed to two factors. Firstly, the trajectory of the actuation system resulting in the load transferring through the posterior region of the phantom-foot, with the lack of an 'ankle' joint resulting in minimal load transfer towards the forefoot through stance. And secondly, the geometry of the phantom-foot producing areas of concentrated pressure, specifically under the calcaneus, skewing the pressure and contributing to aggravated wear and tear of the plantar tissue component.

The contact area across the plantar surface varies significantly between the phantom-foot and in-vivo population. Namely, the midfoot is not clearly represented, likely due to the separation of skeletal and plantar tissue models at this portion of the phantom-foot. This in combination with the inability of the robotic arm to transfer force through the 'ankle' joint during the latter stages of stance resulted in a lack of clarity in the plantar pressure distribution map produced. However, when considering only the hindfoot region, the contact areas were similar. Some difference in the reduced medial/lateral spreading of the phantom-foot was present but may be attributed to the difference in measurement equipment used (in-shoe pressure capture as opposed to a pressure plate). A direct comparison between the test platform and in-vivo participants using the same measurement technique would bring greater clarity to the evaluation of this measure; this approach was adopted in the implementation of the test platform, which is described in the following chapter. Overall, given a comparable heel region contact area and peak pressure, changes in the magnitude and location of this peak pressure would still indicate changes applied due to products and thus characterise product performance.

Finally, the joint segment kinematics were expected to be the most difficult aspect to accurately represent with the test platform due to the complexity of natural in-vivo foot ambulation. Given the single point-of-actuation at the tibia, the test platform was unable to accurately recreate in-vivo kinematics. Additionally, the loose connection between bone

segments may have dampened the internal motions following heel-strike, resulting in poor alignment to in-vivo. Moreover, the laboratory setup represented a substantial obstacle to data collection due to the large number of reflective surfaces present, and the movement of the robotic arm blocking certain markers during motion. Consequently, individual marker traces had to be concatenated together for processing and gap-filling operations applied, which reduced accuracy and significantly increased data processing and analysis times. The result of this in-vivo alignment stage is a test platform capable of indicating changes in trends i.e., reduction in motion in a given segment and plane, but not absolute changes.

Chapter 4 described the validation steps and comparisons to in-vivo data used to confirm the test platform (1) accurately and repeatedly recreated the behaviour of the human foot and (2) addressed the industrial problem through the fulfilment of the specification defined in chapter 3. The completion of this chapter enabled the implementation of the test platform to test real products to determine the capability of the initial design/iteration to inform clinical testing through comparison against in-vivo testing similar to a clinical product evaluation.

Chapter 5: Test platform implementation

5.1. Chapter overview

This chapter describes the implementation of the first design/iteration of the industrial test platform in testing two existing orthotic products available on the market, following its validation in the previous chapter. The two products tested included a ‘knee to heel pain relief’ insole situated under the heel and arch, and a ‘lower back pain relief’ insole fitted under the entire foot. Each of these products claims to ‘stabilise the position of your feet to support your natural walking style’ (Scholl products, 2024). In-vivo tests were completed using a range of participants of comparable foot size to the sample represented by the phantom-foot in the initial iteration of the test platform, comparing the performance of the test platform, specifically the phantom-foot, in accurately representing human foot behaviour during gait with each product. The outcome of this chapter is clear data on the ability of the test platform to capture product performance compared to in-vivo testing broadly similar to clinical testing used to validate products classed as medical devices, and hence guide (1) its implementation by the industry partner and (2) further design iterations required to improve its performance.

5.2. Implementation

The initial design/iteration of the industrial test platform was validated in chapter 4 to capture differences in the behaviour of the phantom-foot due to the application of different orthotic products. However, the agreement of these changes to those experienced by the in-vivo foot, e.g., during clinical product testing, was required, to determine to what extent product performance could be determined by the test platform such that product claims could be established pre-clinical testing i.e., whether absolute changes to the pressure/kinematics of the phantom-foot or only trends would align with human foot behaviour. Two products with comfort (pain-relieving) claims via the unloading of areas of peak plantar pressure were investigated: the performance of each product was characterised by the test platform and compared against in-vivo participants with similar foot sizes to the initial design/iteration of the phantom-foot. These products were chosen as described in the industrial considerations and partnership section (see page 107).

An ethics application (University of Salford Ethics Panel: ID 6755, 10/10/2022) was completed and the relevant documents including participant information sheet, consent form and data protection plan can be found in appendices B – F.

5.2.1. Product Selection

Figure 70: Scholl Knee to heel pain relief insole (right), lower back pain relief insole (centre) and cream control insole (right) used for testing.

Two therapeutic, off-the-shelf orthotic products were selected for testing. Both products claim to contour to the shape of the users' feet to provide pressure relief and to stabilise the position of the foot to support a natural walking style. Additionally, the knee to heel pain relief insoles claim to provide structured arch support. To verify the claims of these insole products, a neutral control insole was manufactured in-house using low density EVA with a shore hardness of 40A. The products were selected as they enabled an assessment of a product situated solely underneath the hindfoot, and one fitted under the entire plantar surface. Additionally, they are products which could benefit from testing using the test platform as clinical tests are not required for non-medical devices; despite claiming pain relief through changing foot function, very little evidence has been gathered to determine the effectiveness in these products to perform as marketed. The knee to heel pain relief insole has been labelled as "red insole", lower back pain relief insole as "orange insole" and control insole as "cream insole".

5.2.2. Purpose:

The purpose of testing two orthotic products using the industrial test platform and via in-vivo testing was to quantify the ability of the test platform to establish product trends/absolute effects on the foot, to inform clinical testing and facilitate product claims. Trends were not

sufficient in allowing product performance claims to be made, however, guided subsequent designs/iterations of the test platform to better satisfy the industry partner's needs. Trends were described as changes greater than the known error of the system i.e., changes which could be attributed directly to the product rather than changes in the material response of the phantom-foot over time.

5.2.2.1. Research question/hypothesis:

Research question: Does the test platform quantify the absolute effects of a product the behaviour of the phantom-foot (plantar pressure, kinematics) or trends/indications of performance?

Hypothesis 1: The initial iteration of the test platform will not sufficiently capture absolute changes made to the kinematics of the foot by a product, however, will suggest product performance trends.

Hypothesis 2: The changes made to the plantar pressure distribution will be more easily quantified than foot kinematics provided the mass of the sample and in-vivo participants are normalised.

Hypothesis 3: Both the knee to heel pain relief and lower back pain relief insoles will reduce peak plantar pressure but have limited effects on joint segment kinematics.

5.2.3. Participant selection

This study was approved by institutional review from the University of Salford prior to recruitment (application ID 6755). The inclusion criteria for this study were:

1. Participants must be asymptomatic.
2. Participants must have no impairments affecting their gait.
3. Both male and female participants are eligible for inclusion (the phantom-foot is a male sample but changes to the foot may occur independent of sex).
4. Participants must have a UK shoe size between 7 – 10, to match the phantom-foot sample size of UK 8.5. This size range was selected to allow participants of similar foot characteristics to the phantom-foot to be evaluated to ensure that foot size would not be an influential factor within the study.
5. Participants must be either students or staff of the University of Salford.

The exclusion criteria were:

1. Any participant presenting symptoms or impairments affecting their gait.
2. Individuals outside the UK shoe size range of 7 – 10.
3. Individuals who are not students or staff of the University of Salford.
4. Anyone unwilling or unable to complete the health questionnaire or provide informed consent.
5. Anyone who cannot or will not wear shorts for the study, which is essential for placing reflective markers on their leg.

Both male and female participants are eligible for inclusion.

5.2.4. Instrumentation

5.2.4.1. Devices

A multi-use clinical gait laboratory was used to carry out the study. The lab featured 8 Vicon (Vicon Motion Systems, Oxford, UK) motion capture cameras mounted around the perimeter of the room. Although different to the system employed by the test platform, the Vicon system operates via the same mechanism, and there were only minor differences in the software utilised by each system. Both systems used the same capture rate and have demonstrated comparable performance with respect to accuracy (Richards, 1999). Placement of the cameras above the workspace enabled the floor space to be maximised and prevented cameras being moved accidentally post-calibration. Embedded within the floor approximately midway across the laboratory were two Kistler Portable 9286AA force plates fully configured within the Vicon proprietary software system, however, only a single force plate was used to ease the data capture process (it was easier to ensure that participants made contact cleanly with a single force plate rather than two). This enabled force measurements to be captured and synced alongside kinematic measurements; force data was captured at a sampling rate of 1000Hz and kinematic data at 100Hz, but Vicon automatically up sampled the kinematic data to 1000Hz. Brower TC PhotoGate A&B wireless timing gates (Brower Timing Systems, Draper, US) were placed at each end of the laboratory, centred around the force plate to help guide participants to walk across the centre of the laboratory. They could be operated remotely ensuring the principal investigator could remain at the computer throughout testing and the value was manually recorded during each trial. The timing gates ensured that participants gait patterns didn't deviate significantly during testing. This may have occurred as a result of participants trying to adjust their gait to step onto the correct

force plate or slowing/speeding up their gait resulting in an unnatural gait. If a significant deviation occurred (greater than ±5% of the average), that trial was excluded, and the participant completed additional trials until the correct number was achieved.

5.2.4.2. Calibration and setup

Calibration of the Vicon camera system involved the same steps as the Qualisys system: 1) camera aiming, 2) masking, 3) calibration and 4) set volume origin. Camera aiming involved placement of the cameras to ensure that the entire capture volume would be captured: the principal investigator was not required to complete this step as the gait laboratory is a regularly maintained clinical research facility. Next, masking was completed via the automated masking tool; any unnecessary objects were removed from the capture volume at this time. The Vicon system features a calibration wand which must be waved throughout the capture volume, ensuring that the markers on the wand are visible to the cameras. This was required until each camera indicated calibration sufficient data had been captured and calibration had been completed. The wand count and image error data could then be reviewed to determine whether the calibration was successful or needed to be repeated; target values were not available from the manufacturer as calibration feedback data are based on factors such as the size of the capture volume and the camera lens type, hence general guidelines specific to the laboratory used were selected as optimal values. This calibration process was repeated each day in accordance with the manufacturer's recommendations. Finally, the volume origin i.e., global coordinate system, was defined via the placement of three markers in fixed locations on the floor.

Markers were placed onto the shoe and leg according to the Salford model established by Jarvis (Nester, Jarvis, Jones, Bowden, & Liu, 2014). Jarvis manufactured rigid plastic plates designed to represent different foot segments, which could then be placed onto to the dorsum and markers applied on top. The primary reasons to use rigid plates rather than place the markers directly onto the foot was to reduce motion occurring due to sliding of the skin and increase the available marker size, which would reduce vibration of the marker (Nester, et al., 2007). Typically, studies testing footwear and orthotics modify the footwear to achieve marker placement directly onto the foot and avoid the chance that they miss movement of the foot within the shoe. However, in this case markers were placed onto the shoe because of clear differences between the subjects to be compared. The phantom-foot did not feature a skin cover over the skeletal model; markers were placed directly onto the bone segments.

This would obviously not be achievable with in-vivo subjects, where markers would need to be placed onto the skin, thus introducing skin artifact errors. Therefore, a direct comparison would not be accurate. Consequently, the most appropriate method was to place markers onto the shoe for both the phantom-foot and in-vivo participants, and to use individual markers as opposed to rigid plates.

Similarly, to Jarvis, the calibrated anatomical system technique (CAST) was implemented to place the retroreflective markers onto the leg (Cappozzo, Cappello, Della Croce, & Pensalfini, 1997). Markers were placed at anatomical markers to define proximal and distal ends of each segment; these markers were not required during data collection, but only during static measurements to generate the segment model. Markers used during dynamic measurements were placed onto each segment to track segment position and orientations and remained attached to participants throughout data collection. At least three markers were required per segment; 9.5mm markers were used to define the calcaneus-talus and midfoot as forefoot motion was ignored during this study. The markers were large enough to be easily detected by the Vicon system, aligned with the same size used within the test platform, and did not cause cross-marker interference as they could be adequately spaced apart. The placement of the markers is described in Table 32 and can be seen in Figure 71.

Figure 71: Location of tracking markers for motion capture

Table 32:Placement of retro-reflective markers on the in-vivo foot to define the SFM.

Segment	Bones represented	Location of Markers	Position of Anatomical Markers
Tibia	Tibia	Four markers were placed 10cm above the lateral malleolus on the lateral aspect of the tibia.	Additional markers were placed on the lateral and medial epicondyles to help define the bony segment.
Calcaneus-Talus	Calcaneus and Talus	Three markers were placed at the medial, lateral, and posterior aspects of the calcaneus.	Additional markers were placed onto the medial and lateral malleolus.
Midfoot	Navicular and Cuboid	Three markers were placed onto the medial, central, and lateral aspects of the midfoot.	N/A

5.2.5. Data collection protocol

The study was divided into two phases: 1) collection of anthropometric data and explanation of experimental protocol and 2) instrumented gait analysis. Participants were anonymised through the designation of a participant ID.

5.2.5.1. Anthropometric data

Each participant was provided with a health questionnaire which requested their height, weight, foot length (maximum length from heel to hallux), foot width (length from base of 1st MTP to 5th MTP) and UK shoe size. They were measured using standard lab equipment and only the left foot of each participant was measured, as this would be the foot fitted with reflective markers and the pressure capture insole.

Measurement	Method of Examination	Photo	Significance of Parameter

Height	The participant was asked to stand erect against a stadiometer, with both feet flat on the floor.		The height of each participant would be compared to the height of the individual used to model the phantom-foot to compare their anthropometrics.

Mass	The participant was asked to stand in a relaxed position on a weighing scale. This value was multiplied by 9.81 to convert the weight into a mass.		The mass of each participant would be recorded as force-based results would be calculated as a percentage of bodyweight.
Foot Length and Width	1) The participant is seated, barefoot and with both feet on the floor in a relaxed position. 2) A ruler is placed under the centre of the heel, up to the anterior edge of the Hallux, and	 	The foot length and width were recorded to make note if participants had foot shapes which may have been impacted by the application of off-the-shelf orthotic products e.g., narrow feet, wide feet.

	the length recorded. 3) The ruler is then placed underneath the 1st MTP and the distance to the 5th MTP is measured.		UK shoe size may also differ according to brand hence the foot length and width provided an alternative foot size measure.
Shoe Size	The participant was asked for their UK shoe size and was given the appropriate shoe. Verbal confirmation ensured the size they requested fitted their feet correctly.		UK shoe size would be the easiest method of assigning the correct product size to each participant during implementation.

5.2.5.2. Instrumented gait analysis

Markers were placed onto participant as described on page 195. Next, the pressure capture insoles were fitted within the shoe between the product and the participants foot and zeroed with the foot unloaded. As with the test platform, the XSENSOR software was configured to define the test duration: this was specified to a maximum of 1hr and manually controlled by the principal investigator. Pressure data was collected continuously per each test condition i.e., no insole, cream insole, red insole, orange insole. The force plate was zeroed and a static measurement of each participant with one foot placed on the force plate was completed prior to dynamic assessment to ensure all markers were visible and the pressure capture insole was functioning correctly.

Participants were asked to stand on one foot (the side without the pressure capture insole) for a few seconds prior to starting each trial to allow for trials to be separated in post processing. During each trial, participants were asked to walk from one side of the gait lab to the other in a natural walking pattern i.e., at a self-selected speed. The timing gates were used to record the time taken to complete each trial and exclude trials with significant variations in walking speed. Several practice runs were completed, and the starting position of each participant altered until clean contact with the force plate was made during each pass; this was checked visually by the principal investigator during each subsequent trial. Within QTM each trial was recorded separately and trimmed to include 3 steps pre and post contact with the force plate; recording began prior to signalling the participant to begin walking and stopped after they passed the second timing gate to ensure no data was lost. Each test condition was repeated until 10 successful trials were completed by each participant, with the force plate and pressure capture insole zeroed after each test condition was completed.

5.2.6. Data analysis protocol

In-vivo data analysis was similar to the process described to analyse the data produced by the test platform in chapter 4. The only difference was the automatic synchronisation (via up-sampling of the kinematic data) of force plate and kinematic data within Vicon software during data collection. Two participants were excluded due to data loss caused by the pressure capture insole failing midway through trials; due to repeated usage, the connection point between the insole and module was loose, which resulted in data loss. These participants data force and motion data were also excluded from the study. However, the results for the remaining participants are displayed below (n=8). Tukey plots and repeated measures of two-way ANOVA (analysis of variance) were used to determine the change in plantar pressure and segment kinematics across conditions. A Tukey plot visually summarizes the distribution of a dataset by displaying the median, quartiles, and potential outliers using a rectangular box and "whiskers" extending to the minimum and maximum values. A repeated measures two-way ANOVA is a statistical technique used to analyze the effects of two categorical independent variables on a continuous dependent variable measured repeatedly from the same subjects across different conditions/time points.

5.2.7. Results

10 in-vivo participants were compared to the test platform in each condition, however, only 8 participants results were recorded due to sensor failure (n=8). Joint motion data was excluded for these participants for consistency.

5.2.7.1. Plantar pressure

In this comprehensive study, a variety of metrics associated with heel pressure in in-vivo participants across different test conditions were scrutinized. Table 33 serves as the cornerstone by detailing each participant's demographic information. Focusing on pressure metrics

Table 34, Table 35 and Table 36 respectively provide insight into the average, peak pressures and contact area in the heel region under various conditions, with Table 37 describing the statistical significance of these results. Figure 72 employs a Tukey plot to clarify variations in peak pressure, with a blue plot designated for the control condition where no insole was worn. For a nuanced comparative analysis, Figure 73 takes this a step further by amalgamating data on average pressure, peak pressure, and heel contact area across all conditions. Each of these metrics are visually synthesized in Figure 75, Figure 76 and Figure 77, which depict the average peak pressure maps (for individuals and the whole group average). Figure 74 quantifies the total effect size of each condition on these metrics, offering a comparative baseline to the shoe-only condition. Time-based metrics are exhaustively explored in Table 38, Table 39 and Table 40. The location of peak pressure differed between participants, with some exhibiting greater lateral (e.g., participant 1), posterior (e.g., participant 3) or anterior (e.g., participant 2) components of pressure. However, the average pressure profile across all participants showed a centre-lateral peak pressure, with the surrounding areas decreasing in pressure as the distance from the peak pressure point increasing. The test platform produced high pressures in the posterior lateral heel region.

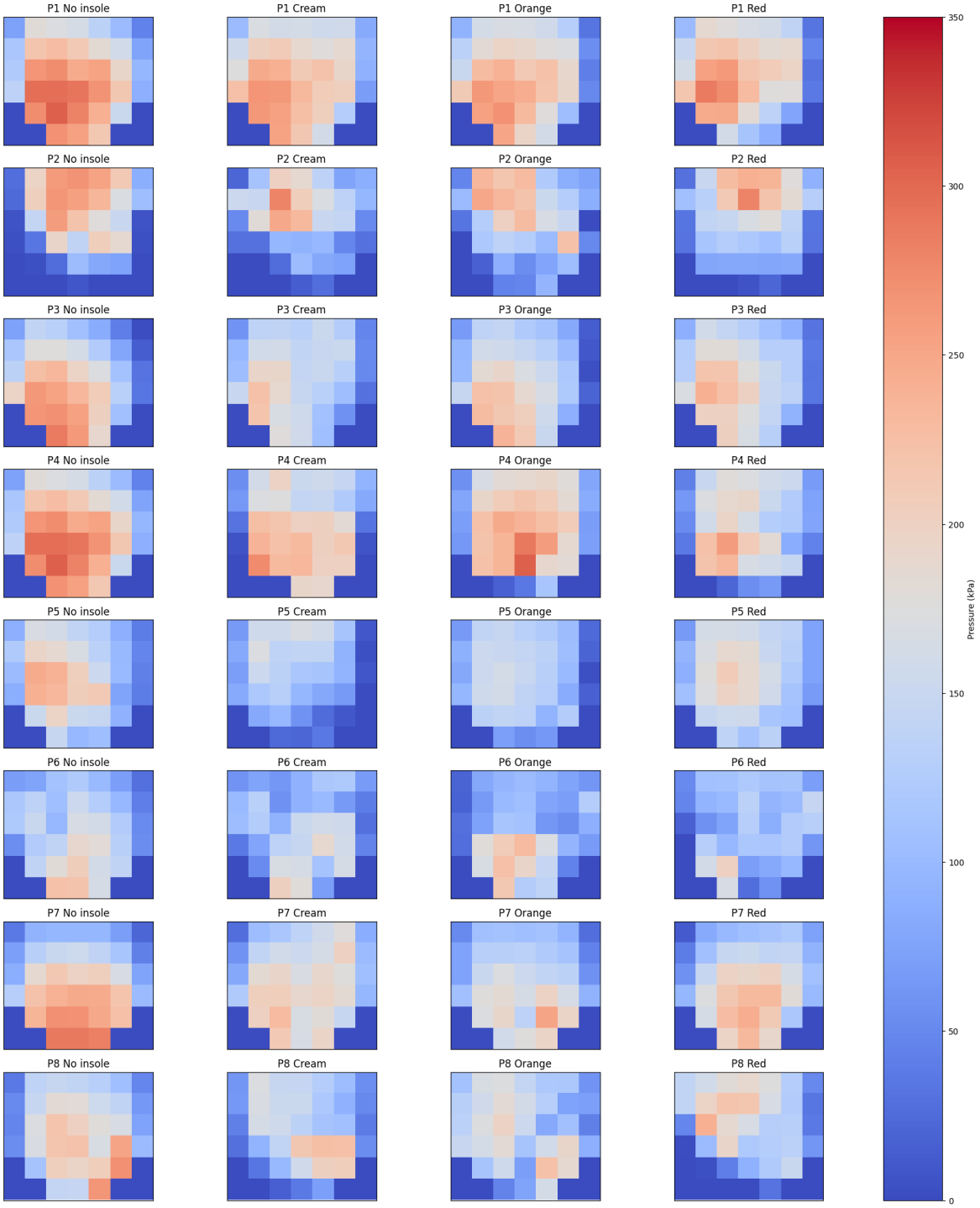

Figure 75: Average peak pressure in the heel region of each participant and each test condition. Cream = control insole, Red = knee to heel pain relief insole, Orange = lower back pain relief insole

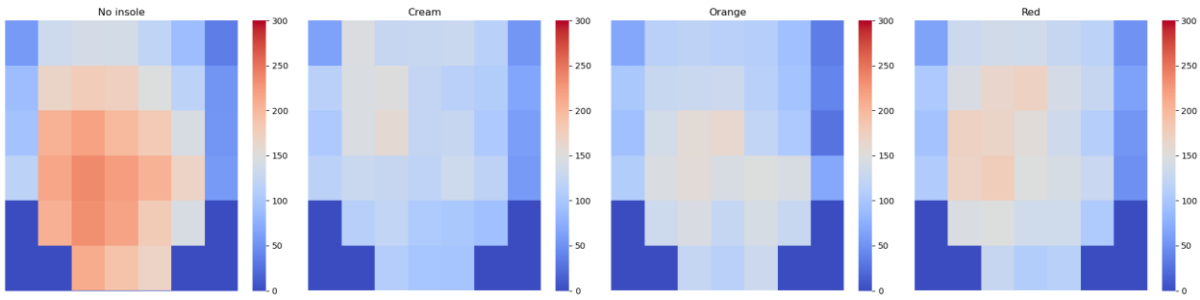

Figure 76: Average peak pressure in the heel region across all in-vivo participants for each test condition. Cream = control insole, Red = knee to heel pain relief insole, Orange = lower back pain relief insole

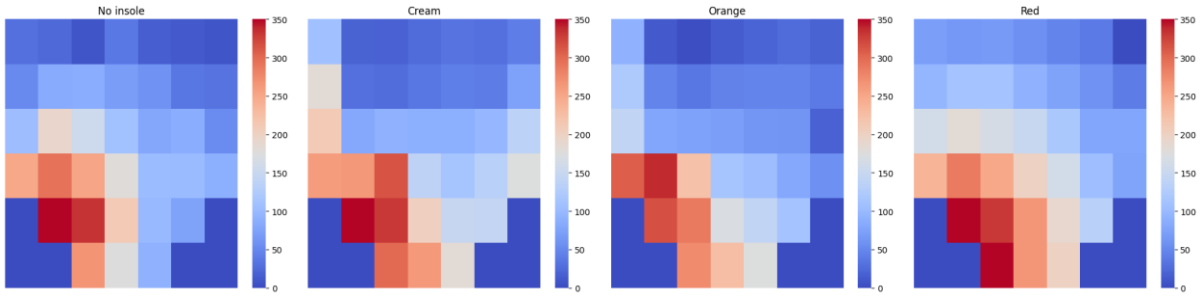

Figure 77: Average peak pressure in the heel region using the test platform for each test condition. Cream = control insole, Red = knee to heel pain relief insole, Orange = lower back pain relief insole

Variations in contact time were small between conditions and no statistical significance was observed. The pressure-time integral reduced significantly due to the application of each insole condition although the orange and red insoles did not produce a significant change when compared to the cream insole. An equivalent statistical result was observed with the time to peak pressure, granting variations between conditions were small. Finally, changes to the centre of pressure were inconsistent across in-vivo participants, although the test platform noted a shift towards the centre when using the orange and red insoles.

Table 38, Table 39 and Table 40, which elaborate on contact time, the pressure-time integral, and time to reach peak pressure, respectively. Table 41 describes the statistical significance of these results. Lastly, Table 42 contributes to the understanding of how the centre of pressure varies across conditions, captured both in-vivo and on the test platform.

The application of each condition resulted in differences across participants, but on average produced a statistically significant reduction in peak pressure compared with the shoe only condition, with the orange insole having the greatest effect. This effect was reflected by the test platform as well, with slight differences in effect size (within a difference of 20kPa). However, when comparing the orange and red insoles against the cream insole, there was no statistically significant change.

Similarly, the average pressure across the heel region decreased with application of each condition, with the orange and red insoles reducing the pressure by similar magnitudes. Once again, the application of each insole produced a statistically significant change, but the difference between cream, orange and red insoles was insignificant. No change of statistical significance was observed to the contact area.

Table 33: Demographic information for in-vivo participants

Participant	Sex	Height (cm)	Mass (N)	Foot Length (cm)	Foot Width (cm)	Foot Size (UK)
P1	F	178	588.60	24	9	7.5
P2	M	175	755.37	26.5	10.5	9.5
P3	F	167	735.75	23	9	8
P4	M	176.5	745.56	26.5	10	9.5
P5	M	184	784.80	26	9.5	9.5
P6	M	177	696.51	26	9.5	9.5
P7	F	169	804.42	24	9	6
P8	M	178.5	922.14	26	9.5	9

Table 34: Average pressure of the heel region per test condition. Cream = control insole, Red = knee to heel pain relief insole, Orange = lower back pain relief insole

Average Pressure (kPa)				
Participant	**No insole**	**Cream Insole**	**Orange Insole**	**Red Insole**
P1	168.82 (8.82)	160.80 (13.95)	151.84 (12.67)	146.38 (17.76)
P2	109.21 (3.59)	91.04 (12.03)	104.10 (14.37)	103.64 (5.50)
P3	135.74 (6.21)	114.45 (3.88)	118.56 (9.05)	124.30 (11.64)
P4	168.82 (5.27)	133.26 (21.38)	145.70 (10.37)	116.59 (12.13)
P5	120.04 (9.92)	76.85 (15.50)	93.65 (8.18)	118.95 (13.97)
P6	108.40 (5.71)	93.12 (6.12)	91.93 (9.42)	84.40 (10.33)
P7	141.66 (4.16)	132.97 (19.39)	114.69 (7.46)	126.41 (9.87)
P8	129.88 (9.55)	99.46 (18.76)	113.95 (10.37)	101.08 (15.94)
Average in-vivo	168.72 (31.93)	119.12 (34.73)	120.78 (29.53)	135.90 (28.63)
Test Platform	131.47 (1.42)	125.24 (3.11)	98.94 (1.80)	110.58 (4.13)

Table 35: Peak pressure of the heel region per test condition. Cream = control insole, Red = knee to heel pain relief insole, Orange = lower back pain relief insole

Peak Pressure (kPa)				
Participant	**No insole**	**Cream Insole**	**Orange Insole**	**Red Insole**
P1	305.96 (24.76)	265.42 (19.72)	268.27 (17.95)	285.97 (23.25)
P2	267.50 (6.42)	279.78 (26.02)	248.99 (28.81)	279.21 (41.97)
P3	286.49 (16.75)	222.56 (10.10)	236.84 (20.96)	240.94 (17.06)
P4	305.96 (13.24)	274.00 (52.21)	305.00 (51.02)	258.57 (39.46)
P5	245.60 (25.02)	171.17 (26.44)	163.23 (12.18)	208.81 (18.54)
P6	222.04 (15.82)	201.00 (21.98)	228.51 (18.27)	200.11 (23.85)
P7	287.79 (14.17)	228.77 (27.48)	252.57 (14.04)	243.96 (17.05)
P8	270.64 (29.31)	224.34 (25.09)	221.88 (21.31)	241.41 (26.45)
Average in-vivo	331.20 (72.74)	235.39 (64.86)	228.03 (61.20)	252.79 (55.19)
Test Platform	407.60 (6.58)	360.24 (3.63)	350.39 (8.13)	368.97 (8.93)

Table 36: Contact area of the heel region per test condition. Cream = control insole, Red = knee to heel pain relief insole, Orange = lower back pain relief insole

Contact Area (cm^2)				
Participant	**No insole**	**Cream Insole**	**Orange Insole**	**Red Insole**
P1	13.67 (3.39)	24.05 (0.00)	23.97 (0.56)	23.62 (1.17)
P2	14.71 (3.05)	19.10 (0.78)	19.56 (3.84)	20.22 (0.69)
P3	21.82 (1.67)	28.97 (0.99)	23.48 (0.47)	24.05 (0.00)
P4	31.62 (4.00)	18.12 (4.10)	23.94 (0.25)	23.84 (0.48)
P5	27.14 (3.13)	22.03 (2.88)	23.51 (0.47)	24.05 (0.00)
P6	27.25 (2.17)	23.16 (0.44)	23.37 (1.53)	23.26 (0.30)
P7	10.37 (3.38)	24.05 (0.00)	24.05 (0.00)	23.96 (0.23)
P8	27.60 (2.69)	23.38 (2.08)	23.91 (0.38)	20.57 (1.63)
Average in-vivo	23.13 (1.97)	22.39 (2.60)	23.45 (1.65)	23.29 (1.45)
Test Platform	19.74 (0.24)	19.81 (0.15)	21.23 (0.34)	22.40 (0.14)

Table 37: Statistical analysis using repeated measures of two-way ANOVA to assess the significance of different insoles (Cream = control, Red = knee to heel pain relief, Orange = lower back pain relief) on average pressure, peak pressure, and contact area.

		Average Pressure (kPa)		**Peak Pressure (kPa)**		**Contact Area (cm^2)**	
Participant	**Comparison**	**T-statistic**	**P-value**	**T-statistic**	**P-value**	**T-statistic**	**P-value**
Average in-vivo	No Insole vs Cream Insole	-24.11	<0.01	-22.77	<0.01	-5.72	<0.01
	No Insole vs Orange Insole	-22.40	<0.01	-23.57	<0.01	2.25	0.02
	No Insole vs Red Insole	-14.44	<0.01	-16.87	<0.01	1.06	0.29
	Cream Insole vs Orange Insole	0.78	0.43	-3.62	<0.01	7.83	<0.01
	Cream Insole vs Red Insole	2.25	7.46	-0.25	0.81	6.30	<0.01
Test Platform	No Insole vs Cream Insole	4.74	<0.01	2.08	0.04	1.12	0.26
	No Insole vs Orange Insole	1.32	0.19	-1.26	0.21	1.59	0.11
	No Insole vs Red Insole	2.90	<0.01	1.08	0.28	2.18	0.03
	Cream Insole vs Orange Insole	-3.64	<0.01	-3.62	<0.01	0.68	0.54
	Cream Insole vs Red Insole	-0.12	0.91	-0.25	0.81	1.10	1.53

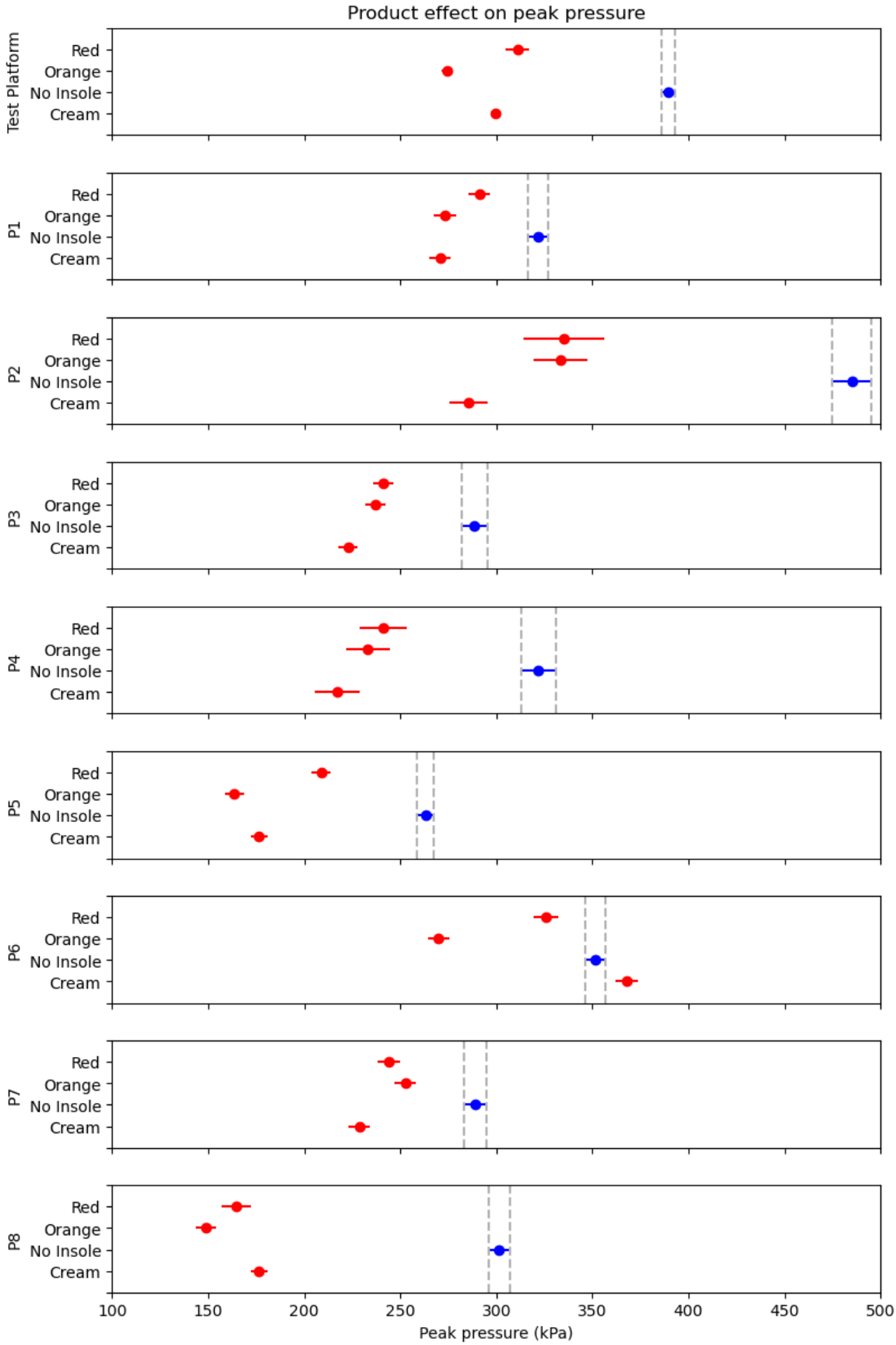

Figure 72: Tukey plot describing differences in peak pressure per condition. The blue plot represents the no-insole condition. Cream = control insole, Red = knee to heel pain relief insole, Orange = lower back pain relief insole

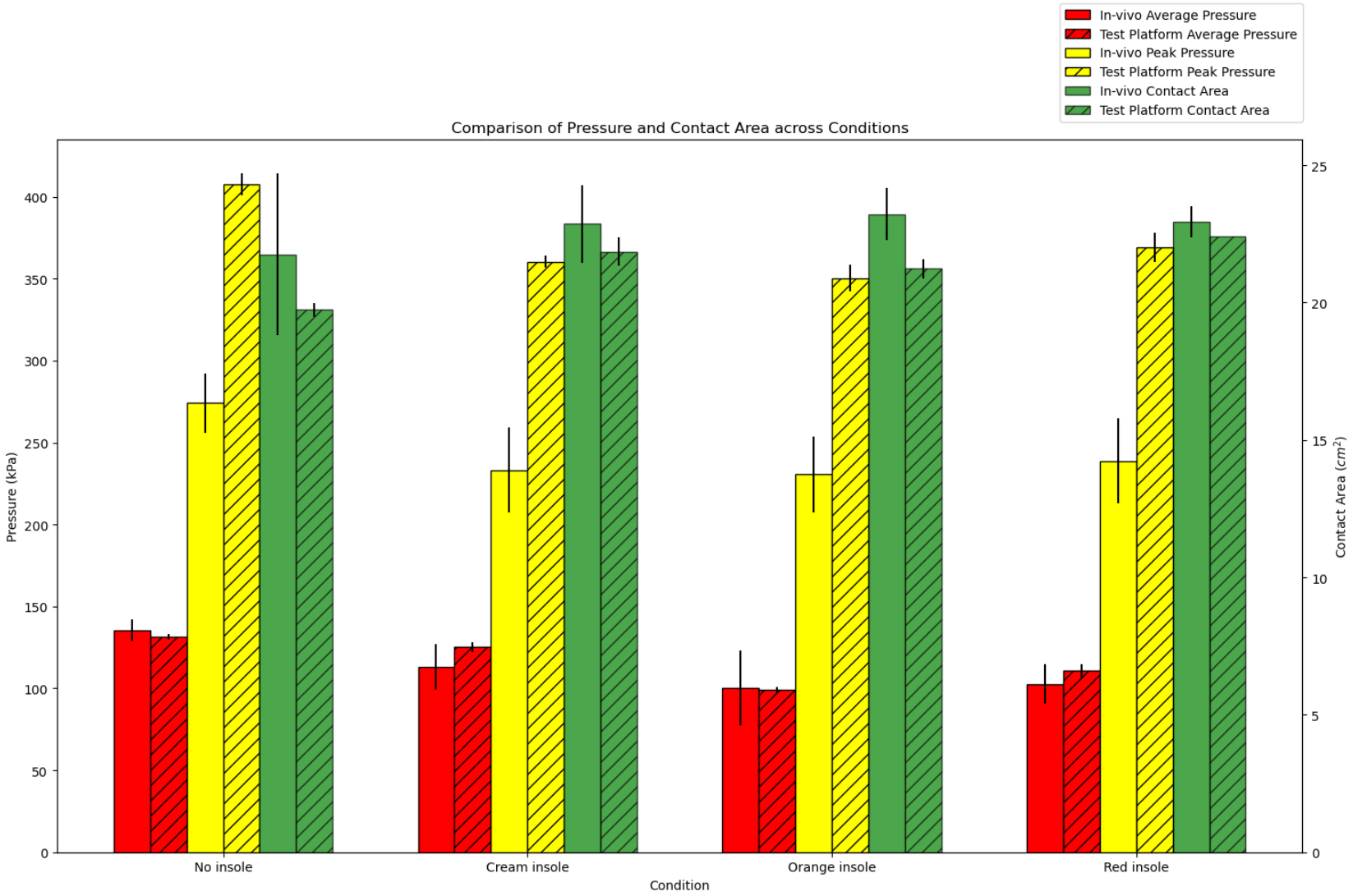

Figure 73: Average pressure (kPa), peak pressure (kPa) and heel contact area (cm^2) across each condition. Cream = control insole, Red = knee to heel pain relief insole, Orange = lower back pain relief insole

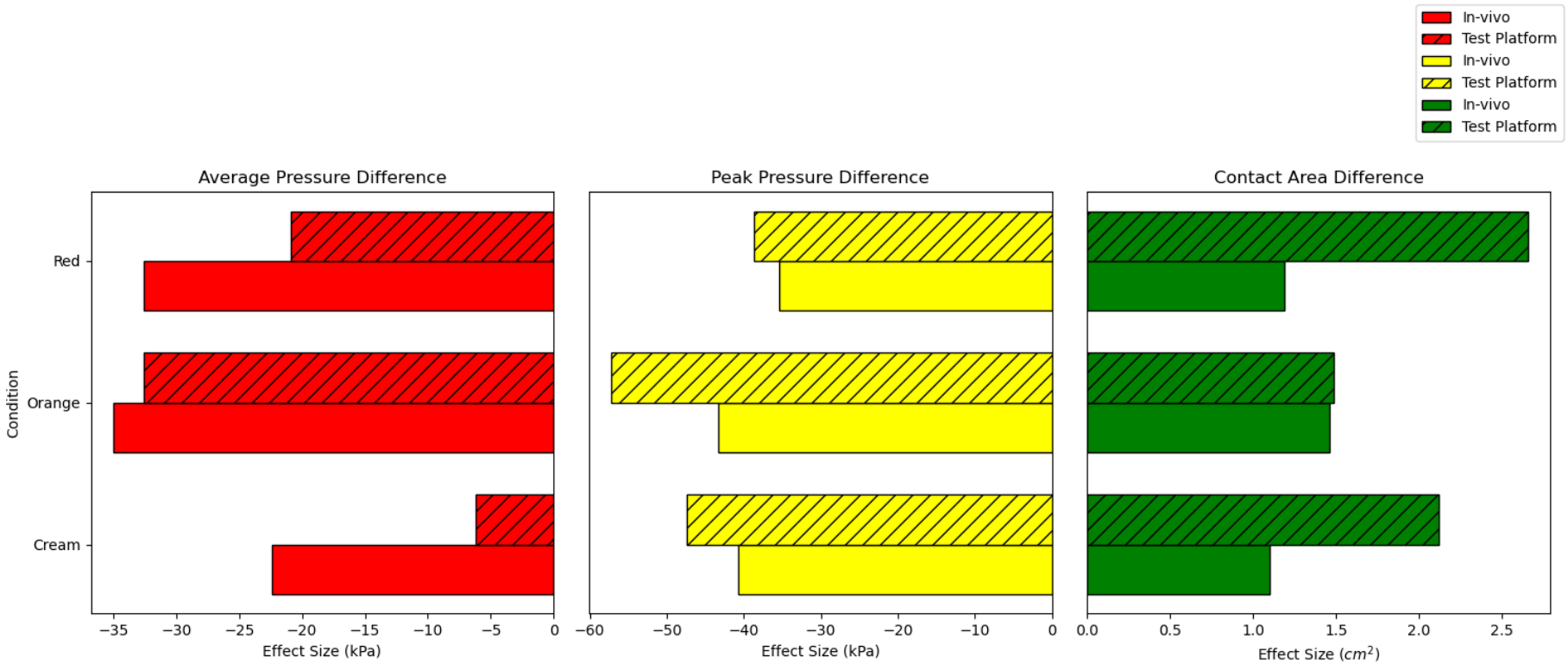

Figure 74: Effect size for average pressure (kPa), peak pressure (kPa) and contact area (cm^2) with respect to the shoe only condition. Cream = control insole, Red = knee to heel pain relief insole, Orange = lower back pain relief insole

The location of peak pressure differed between participants, with some exhibiting greater lateral (e.g., participant 1), posterior (e.g., participant 3) or anterior (e.g., participant 2) components of pressure. However, the average pressure profile across all participants showed a centre-lateral peak pressure, with the surrounding areas decreasing in pressure as the distance from the peak pressure point increasing. The test platform produced high pressures in the posterior lateral heel region.

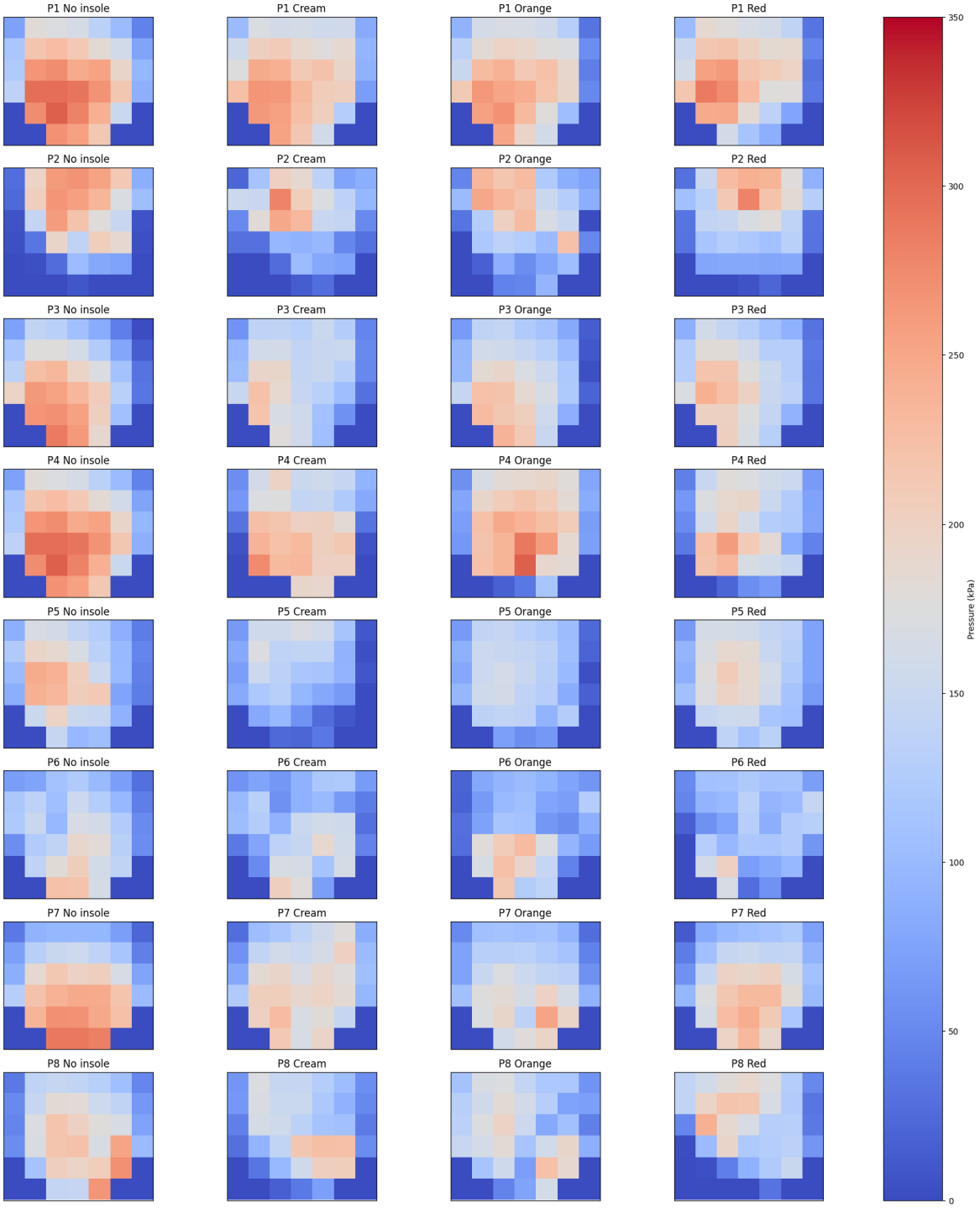

Figure 75: Average peak pressure in the heel region of each participant and each test condition. Cream = control insole, Red = knee to heel pain relief insole, Orange = lower back pain relief insole

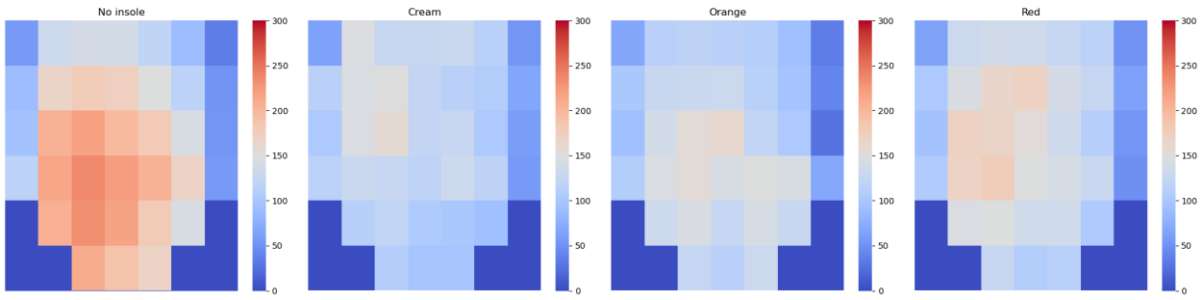

Figure 76: Average peak pressure in the heel region across all in-vivo participants for each test condition. Cream = control insole, Red = knee to heel pain relief insole, Orange = lower back pain relief insole

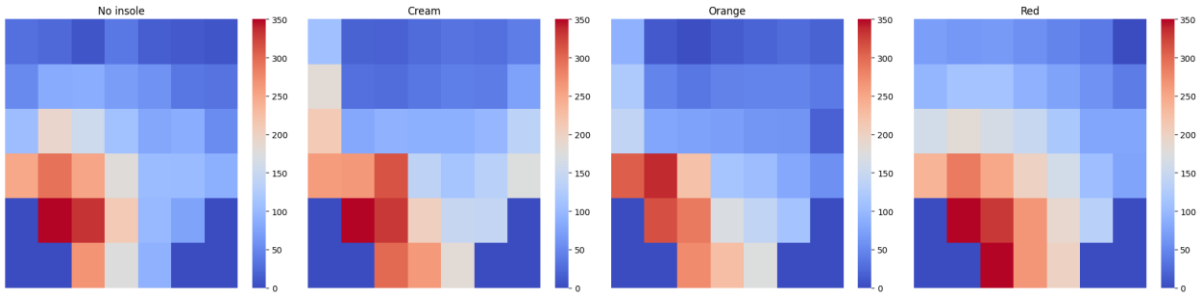

Figure 77: Average peak pressure in the heel region using the test platform for each test condition. Cream = control insole, Red = knee to heel pain relief insole, Orange = lower back pain relief insole

Variations in contact time were small between conditions and no statistical significance was observed. The pressure-time integral reduced significantly due to the application of each insole condition although the orange and red insoles did not produce a significant change when compared to the cream insole. An equivalent statistical result was observed with the time to peak pressure, granting variations between conditions were small. Finally, changes to the centre of pressure were inconsistent across in-vivo participants, although the test platform noted a shift towards the centre when using the orange and red insoles.

Table 38: In-vivo and test platform contact time. Cream = control insole, Red = knee to heel pain relief insole, Orange = lower back pain relief insole

Contact Time (s)				
Participant	**No Insole**	**Cream Insole**	**Orange Insole**	**Red Insole**
P1	0.51 (0.02)	0.61 (0.01)	0.52 (0.05)	0.53 (0.03)
P2	0.57 (0.01)	0.70 (0.01)	0.62 (0.03)	0.58 (0.05)
P3	0.56 (0.07)	0.51 (0.01)	0.49 (0.01)	0.51 (0.04)
P4	0.77 (0.10)	0.52 (0.06)	0.58 (0.03)	0.64 (0.04)
P5	0.67 (0.05)	0.52 (0.01)	0.62 (0.03)	0.50 (0.02)
P6	0.69 (0.01)	0.60 (0.02)	0.19 (0.02)	0.59 (0.01)
P7	0.52 (0.02)	0.53 (0.03)	0.53 (0.07)	0.53 (0.02)
P8	0.49 (0.02)	0.55 (0.03)	0.54 (0.03)	0.64 (0.07)
Average in-vivo	0.54 (0.14)	0.57 (0.08)	0.51 (0.14)	0.57 (0.09)
Test Platform	0.40 (0.00)	0.40 (0.01)	0.37 (0.01)	0.39 (0.01)

Table 39: In-vivo and test platform pressure-time integral (kPa.s). Cream = control insole, Red = knee to heel pain relief insole, Orange = lower back pain relief insole

Pressure-Time Integral (kPa.s)				
Participant	**No Insole**	**Cream Insole**	**Orange Insole**	**Red Insole**
P1	51.64 (0.73)	50.8 (0.67)	41.45 (0.64)	42.55 (0.58)
P2	45.72 (0.54)	34.49 (0.34)	32.58 (0.36)	32.26 (0.39)
P3	35.42 (0.54)	34.29 (0.46)	34.38 (0.49)	31.44 (0.49)
P4	55.87 (0.54)	26.63 (0.29)	34.48 (0.37)	35.76 (0.35)
P5	28.17 (0.36)	25.36 (0.32)	33.79 (0.38)	30.24 (0.41)
P6	39.83 (0.45)	30.04 (0.28)	29.12 (0.30)	30.90 (0.36)
P7	41.77 (0.63)	41.49 (0.55)	33.24 (0.43)	37.28 (0.52)
P8	39.80 (0.54)	30.45 (0.37)	22.79 (0.31)	21.44 (0.25)
Average in-vivo	42.28 (0.32)	34.19 (0.26)	32.73 (0.25)	32.73 (0.26)
Test Platform	122.53 (0.46)	64.62 (0.25)	62.15 (0.26)	63.11 (0.53)

Table 40: In-vivo and test platform time to peak pressure (s). Cream = control insole, Red = knee to heel pain relief insole, Orange = lower back pain relief insole

Time to peak pressure (s)				
Participant	**No Insole**	**Cream Insole**	**Orange Insole**	**Red Insole**
P1	0.09 (0.01)	0.11 (0.05)	0.09 (0.00)	0.09 (0.01)
P2	0.10 (0.01)	0.12 (0.01)	0.13 (0.02)	0.11 (0.03)
P3	0.56 (0.01)	0.11 (0.01)	0.10 (0.01)	0.09 (0.01)
P4	0.77 (0.03)	0.17 (0.01)	0.16 (0.01)	0.13 (0.05)
P5	0.67 (0.02)	0.11 (0.01)	0.13 (0.01)	0.13 (0.03)
P6	0.69 (0.01)	0.11 (0.02)	0.12 (0.01)	0.12 (0.02)
P7	0.52 (0.01)	0.09 (0.02)	0.11 (0.03)	0.10 (0.00)
P8	0.49 (0.01)	0.11 (0.01)	0.11 (0.01)	0.12 (0.02)
Average in-vivo	0.49 (0.24)	0.12 (0.04)	0.12 (0.03)	0.14 (0.37)
Test Platform	0.19 (0.01)	0.19 (0.00)	0.16 (0.00)	0.16 (0.01)

Table 41: Statistical analysis using repeated measures of two-way ANOVA to assess the significance of different insoles (Cream = control, Red = knee to heel pain relief, Orange = lower back pain relief) on average pressure, peak pressure, and contact area.

		Contact Time (s)		Pressure-Time Integral (kPa.s)		Time to peak pressure (s)	
Participant	**Comparison**	**T-statistic**	**P-value**	**T-statistic**	**P-value**	**T-statistic**	**P-value**
In-vivo	No Insole vs Cream Insole	0.65	0.54	2.37	0.05	4.14	<0.01
	No Insole vs Orange Insole	1.32	0.23	3.15	0.02	4.18	<0.01
	No Insole vs Red Insole	0.9	0.40	3.59	0.01	4.25	<0.01
	Cream Insole vs Orange Insole	1.02	0.34	0.60	0.57	-0.48	0.65
	Cream Insole vs Red Insole	0.09	0.93	0.66	0.53	0.68	0.52
Test Platform	No Insole vs Cream Insole	5.87	<0.01	-5.46	<0.01	0.95	0.35
	No Insole vs Orange Insole	-53.66	<0.01	-48.15	<0.01	13.48	<0.01
	No Insole vs Red Insole	14.91	<0.01	-9.50	<0.01	21.63	<0.01
	Cream Insole vs Orange Insole	51.40	<0.01	11.19	<0.01	-16.73	<0.01
	Cream Insole vs Red Insole	-9.78	<0.01	-0.56	0.58	-34.68	<0.01

Table 42: Centre of pressure changes across conditions captured in-vivo and using the test platform (TP). Cream = control insole, Red = knee to heel pain relief insole, Orange = lower back pain relief insole

	No Insole	Cream Insole	Orange Insole	Red Insole
P1	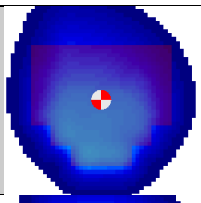	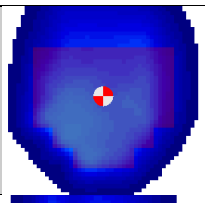	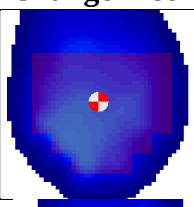	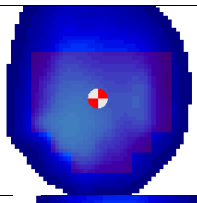
P2	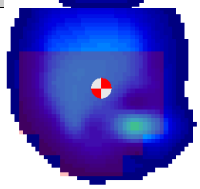	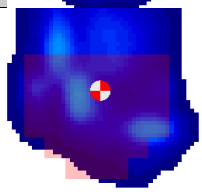	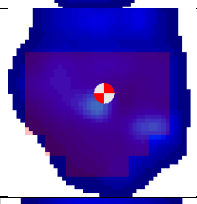	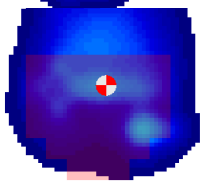
P3	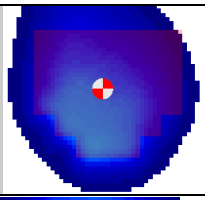	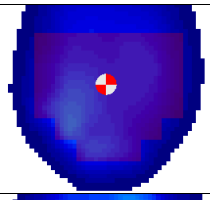	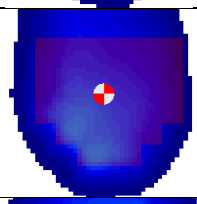	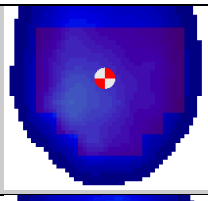
P4	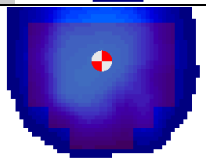	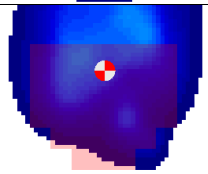	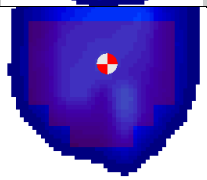	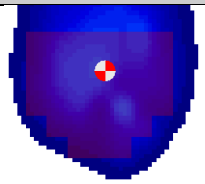
P5	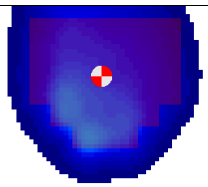	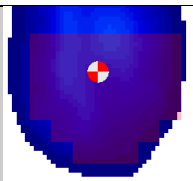	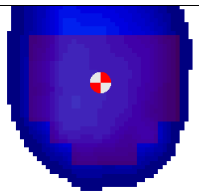	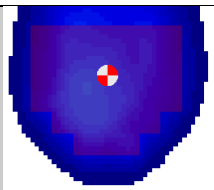
P6	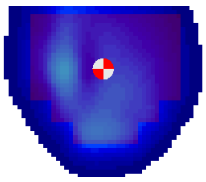	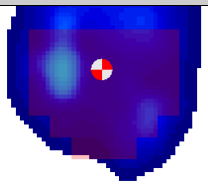	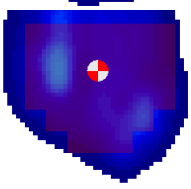	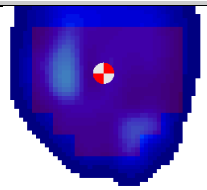
P7	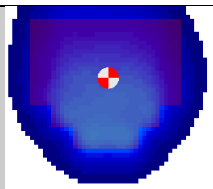	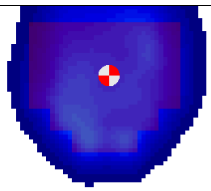	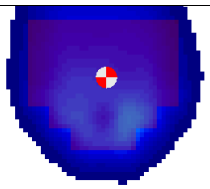	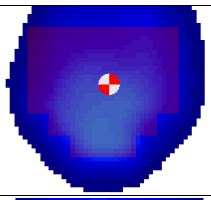
P8	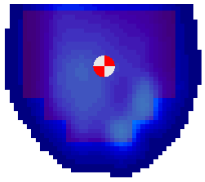	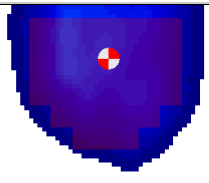	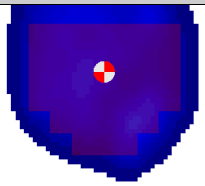	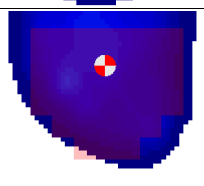
TP	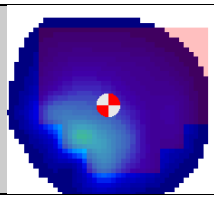	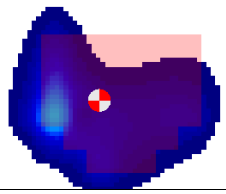	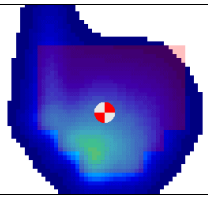	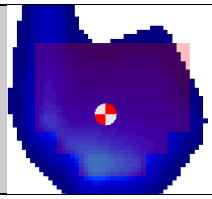

5.2.7.2. Joint segment data

Figure 78 shows the average in-vivo joint segment kinematic data and Figure 79 the equivalent test platform kinematic data. Figure 80, Figure 81 and Figure 82 show the joint segment effect sizes at IC, FFL and HO. Product performance criteria

Table 43: Product performance criteria results - cream insole

Product Performance Criteria	Measure		Impact	Comments
Impact on gait	Rearfoot angle at contact		Yes	Coronal plane only
Impact on gait	Maximum rearfoot angle		Yes	Coronal plane only
Impact on gait **Impact on shock absorption** **Impact on loading pattern**	Kinetic data	Vertical force	No	-
		Vertical impulse	No	-
Impact on shock absorption **Impact on loading pattern**	Peak pressure	Heel	Yes	Reduction in peak pressure
Impact on shock absorption **Impact on loading pattern**	Pressure time integral	Heel	Yes	Reduction in pressure-time integral
Impact on shock absorption **Impact on loading pattern**	Force time integral		No	-
Impact on shock absorption **Impact on loading pattern**	Contact area	Heel	No	-
Impact on loading pattern	Time to peak pressure	Heel	Yes	Reduction in pressure-time integral
Impact on loading pattern	Contact time	Heel	No	-
Impact on stability/balance	Centre of pressure and mass displacement	Displacement of centre of pressure	Yes	

				Inconclusive if COP is shifted to the centre of the heel.

Table 44 and Table 45 details the product performance criteria results for each insole. Although none of the products appeared to significantly alter in-vivo gait patterns, some effects were noted. In several segments, the absolute position of the foot appeared to shift between conditions; this produced large effect sizes. However, the range of motion in the majority of cases did not change, so these effects could be disregarded. The orange, red and cream insoles reduced the range of motion of the calcaneus-tibia segment in the frontal and coronal planes, decreasing both inversion/eversion and abduction/adduction. The cream and red insoles decreased the range of motion of the midfoot-calcaneus segment in the frontal and coronal planes; however, this behaviour was not replicated in the coronal plane of the midfoot-shank. The test platform did not present a coherent picture of the impact of each insole on the phantom-foot with respect to the in-vivo participants. This could be attributed to several factors: the lack of control of the mid and forefoot, lack of structures to limit the motion of each segment and significant errors introduced due to reflections in the robotics lab workspace.

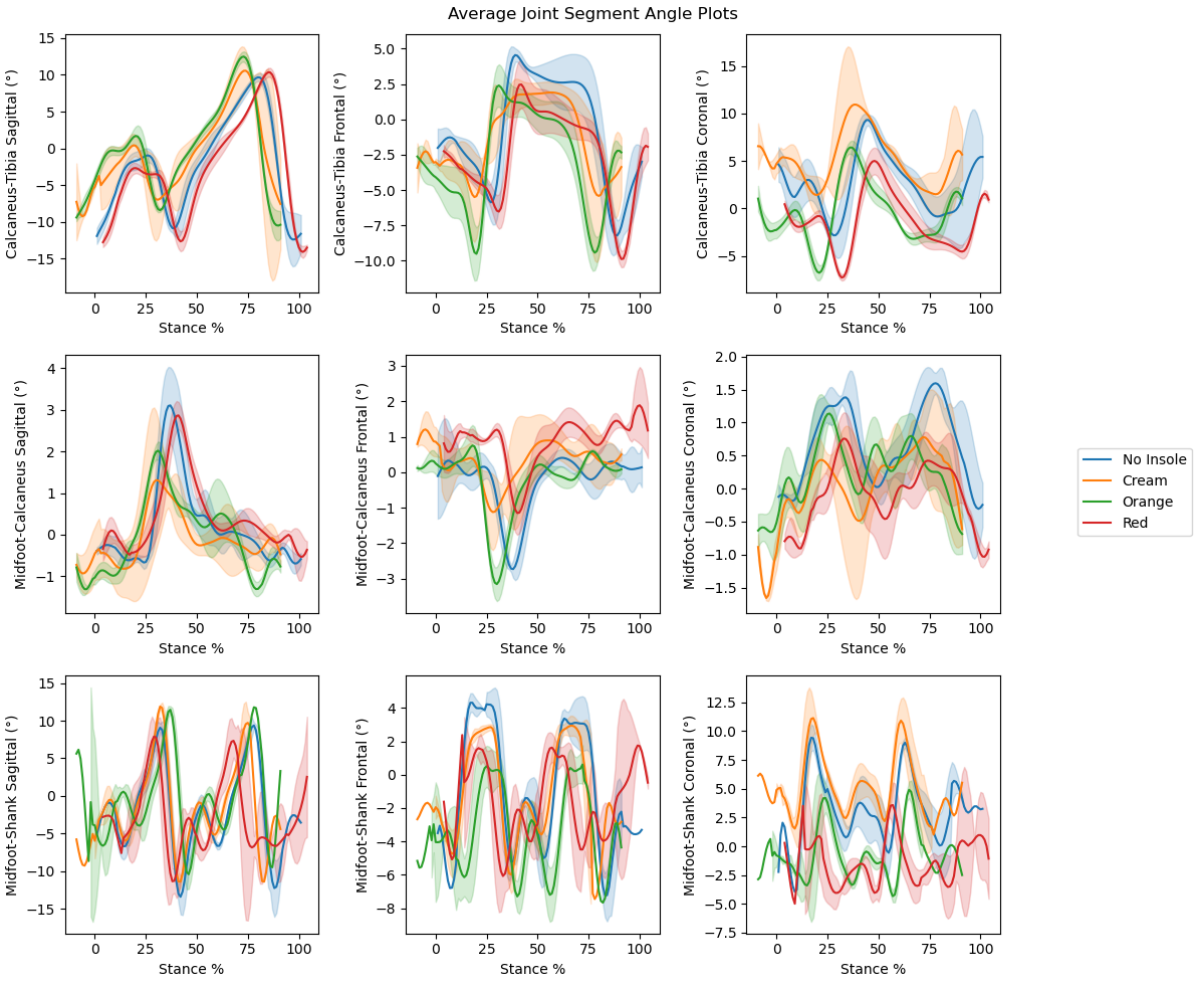

Figure 78:Average in-vivo joint segment kinematic data

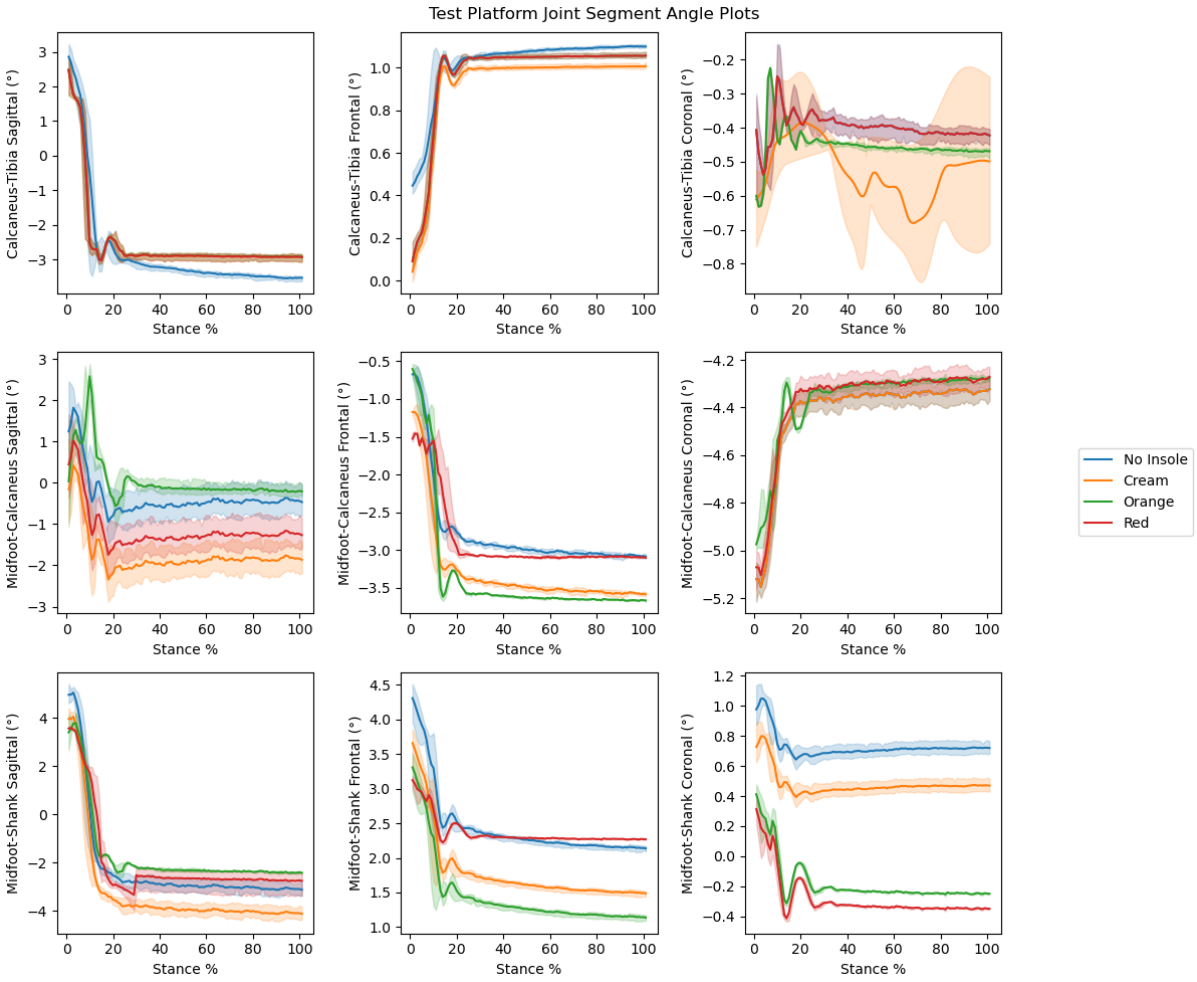

Figure 79: Test platform joint segment kinematic data

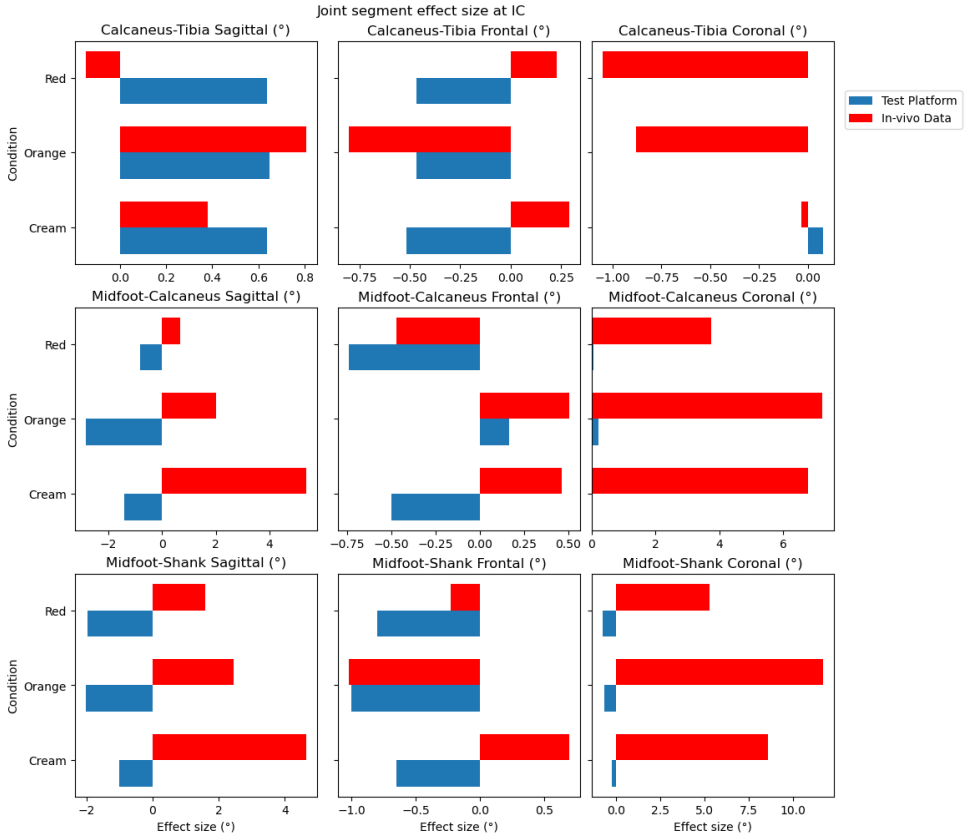

Figure 80: Joint segment effect size at initial contact (IC)

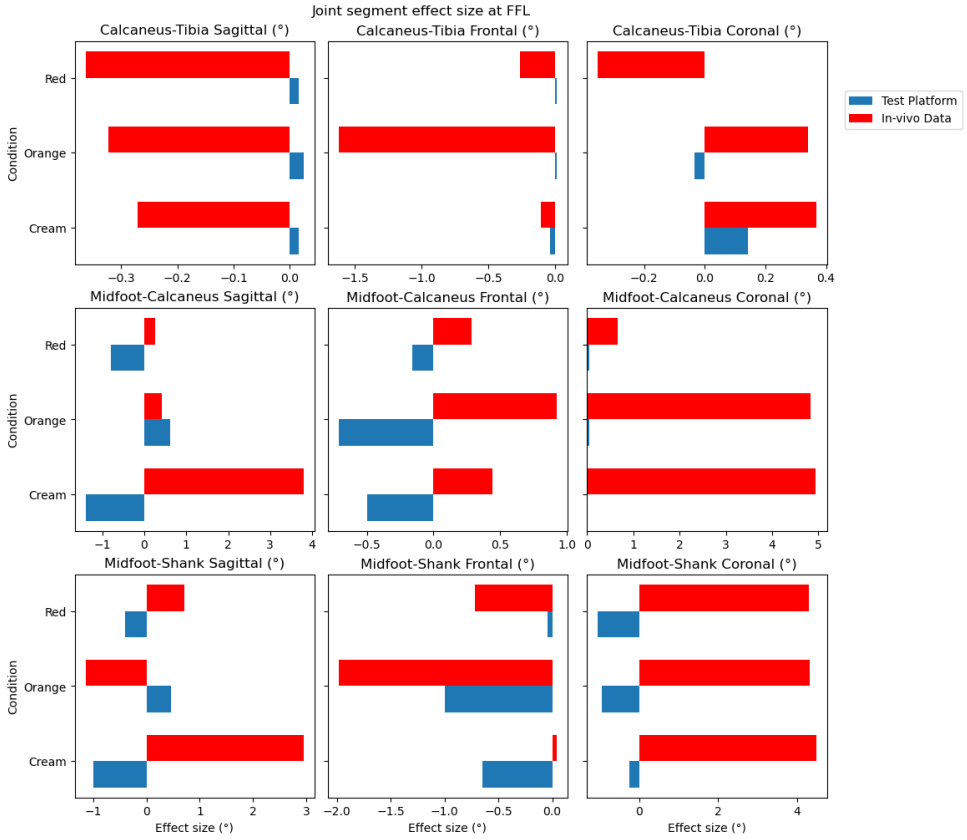

Figure 81: Joint segment effect size at full foot loading (FFL)

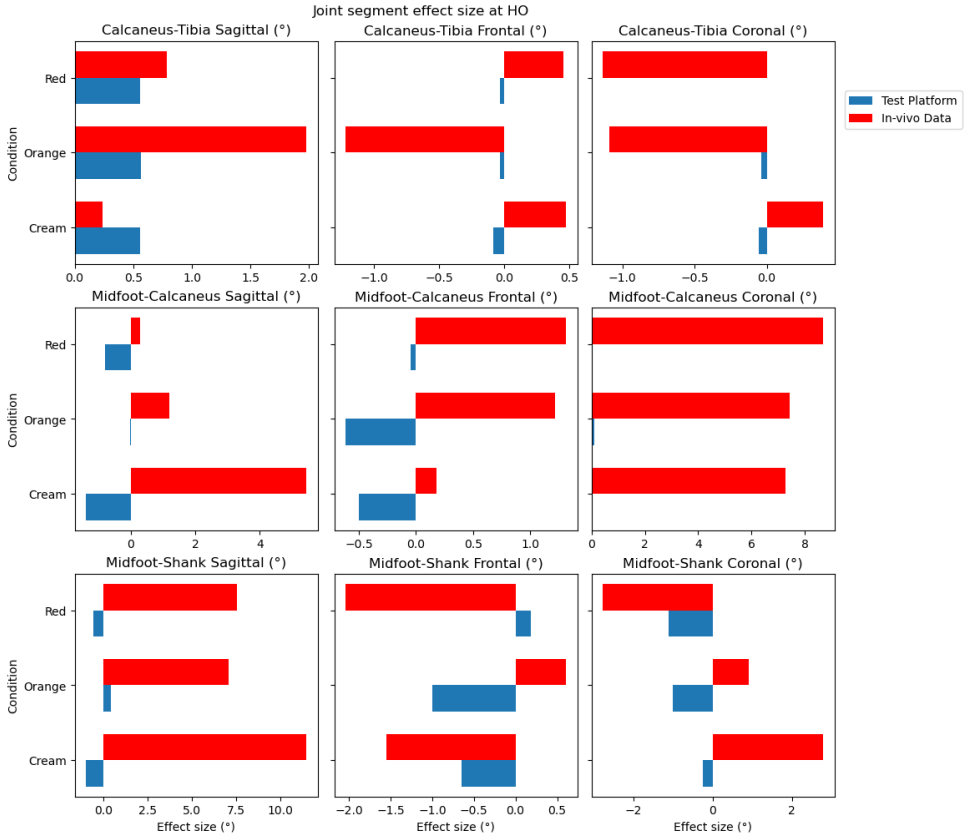

Figure 82: Joint segment effect size at heel off (HO)

5.2.7.3. Product performance criteria

Table 43: Product performance criteria results - cream insole

Product Performance Criteria	Measure		Impact	Comments
Impact on gait	Rearfoot angle at contact		Yes	Coronal plane only
Impact on gait	Maximum rearfoot angle		Yes	Coronal plane only
Impact on gait **Impact on shock absorption** **Impact on loading pattern**	Kinetic data	Vertical force	No	-
		Vertical impulse	No	-
Impact on shock absorption **Impact on loading pattern**	Peak pressure	Heel	Yes	Reduction in peak pressure
Impact on shock absorption **Impact on loading pattern**	Pressure time integral	Heel	Yes	Reduction in pressure-time integral
Impact on shock absorption **Impact on loading pattern**	Force time integral		No	-
Impact on shock absorption **Impact on loading pattern**	Contact area	Heel	No	-
Impact on loading pattern	Time to peak pressure	Heel	Yes	Reduction in pressure-time integral
Impact on loading pattern	Contact time	Heel	No	-
Impact on stability/balance	Centre of pressure and mass displacement	Displacement of centre of pressure	Yes	Inconclusive if COP is shifted to the centre of the heel.

Table 44: Product performance criteria results - red insole

Product Performance Criteria	Measure		Impact	Comments
Impact on gait	Rearfoot angle at contact		Yes	Coronal plane only
Impact on gait	Maximum rearfoot angle		Yes	Coronal plane only
Impact on gait **Impact on shock absorption** **Impact on loading pattern**	Kinetic data	Vertical force	No	-
		Vertical impulse	No	-
Impact on shock absorption **Impact on loading pattern**	Peak pressure	Heel	Yes	Reduction in peak pressure
Impact on shock absorption **Impact on loading pattern**	Pressure time integral	Heel	Yes	Reduction in pressure-time integral
Impact on shock absorption **Impact on loading pattern**	Force time integral		No	-
Impact on shock absorption **Impact on loading pattern**	Contact area	Heel	No	-
Impact on loading pattern	Time to peak pressure	Heel	Yes	Reduction in pressure-time integral
Impact on loading pattern	Contact time	Heel	No	-
Impact on stability/balance	Centre of pressure and mass displacement	Displacement of centre of pressure	Yes	Inconclusive if COP is shifted to the centre of the heel.

Table 45: Product performance criteria results - orange insole

Product Performance Criteria	Measure		Impact	Comments
Impact on gait	Rearfoot angle at contact		Yes	Coronal plane only
Impact on gait	Maximum rearfoot angle		Yes	Coronal plane only
Impact on gait **Impact on shock absorption** **Impact on loading pattern**	Kinetic data	Vertical force	No	
		Vertical impulse	No	
Impact on shock absorption **Impact on loading pattern**	Peak pressure	Heel	Yes	Reduction in peak pressure
Impact on shock absorption **Impact on loading pattern**	Pressure time integral	Heel	Yes	
Impact on shock absorption **Impact on loading pattern**	Force time integral		No	-
Impact on shock absorption **Impact on loading pattern**	Contact area	Heel	No	-
Impact on loading pattern	Time to peak pressure	Heel	Yes	Reduction in pressure-time integral
Impact on loading pattern	Contact time	Heel	No	-
Impact on stability/balance	Centre of pressure and mass displacement	Displacement of centre of pressure	Yes	Inconclusive if COP is shifted to the centre of the heel.

5.2.8. Discussion

The aim of this study was to identify the impact of two products on the pressure and joint kinematics of the foot during normal gait, when compared to a control insole and shoe-only condition, and to compare the test platform's ability to capture these changes in comparison to an in-vivo experimental protocol. Both products made claims around shock absorption, stabilisation, and pressure redistribution. Each product resulted in a reduction of peak and average plantar pressures in the heel region and an increase in time to peak pressure compared to the shoe-only condition. However, according to the results of the repeated measures two-way ANOVA, these changes were not statistically significant when compared to the control condition. No clear changes in joint kinematics were observed. The outcome of the study indicates the test platform can indicate certain performance trends caused by the application of different orthotic products with respect to plantar pressure but lacks the capability to capture kinematic changes in its current implementation.

5.2.8.1. Effect of the FOs on plantar pressure

As previously identified in chapter 2, soft orthoses provide shock absorption and reduce shear forces (Janisse & Janisse, 2008). This informed the hypothesis that both products would reduce peak plantar pressure and the pressure-time integral, which was corroborated by both the in-vivo and test platform results. Though the link between these metrics and pain reduction is unclear, as previous studies have found no relationship between peak pressure and pain (Postema, Burm, Zande, & Limbeek, 1998).

The red orthoses featured a heel cup, which have been used in previous studies to reduce heel strike force, although primarily used during running studies (Hajizadeh, Desmyttere, Carmona, Bleau, & Begon, 2020). Given the similarity in plantar pressure metrics between the orange and red insoles, there didn't appear to be any significant effect caused by this specific geometry; this may be due to the insole material, as previous studies have indicated plastic heel cups have a significant effect on contact area (Wang, Cheng, Tsuang, Hang, & Liu, 1994). Nevertheless this insole produced statistically significant changes in average pressure in the hindfoot region compared to the control condition within the in-vivo group and test platform (19.45% decrease in the in-vivo group and 15.89% decrease in the test platform). There was also a statistically significant change in peak pressure within the in-vivo group, but this was not reflected in the test platforms results. The orange orthosis similarly produced a statistically significant change in contact area with respect to the control

condition, however, changes in the average and peak pressures were conflicting between the test platform and the in-vivo group. The conflicting results may be a result of the variation in effect size between in-vivo participants, as trends were largely consistent across participants. Additionally, the difference in trajectory between the test platform and in-vivo participants may have also contributed to differences between groups.

5.2.8.2. Effect of the FOs on kinematics

Insoles made using soft materials have been found to reduce peak angles in the hip, knee, and ankle, with the most significant effects occurring in the ankle joint (Alsenoy, et al., 2023). Contoured insoles have been found to significantly affect kinematics; however, no studies have specifically investigated the effects of heel cups (Qiu-Qiong, Pui-Ling, Kit-Lun, Jiao, & Qi-Long, 2022). It was much more difficult to substantiate the two insoles product claims around stabilisation. In-vivo results indicated products may have shifted joint angle start and end positions but did not impact joint segment range of motion in most cases. Differences between conditions were noted in the calcaneus-tibia and calcaneus-midfoot segments, with each of the insoles decreasing the range of motion compared to a shoe-only condition. However, neither the red nor orange insole appeared to produce a significantly different effect to the cream control insole. No significant effects were captured by the test platform and alignment to in-vivo kinematics was poor; aspects which may have impacted joint kinematics were addressed in the previous chapter.

5.2.8.3. Product performance criteria

Concerning the product performance criteria, the red and orange insoles effectively impacted the same measures and claims for each product could be made on impact on each criterion: impact on gait, shock absorption, loading pattern and stability/balance. Although claims on the impact on gait would be limited, given that changes in joint kinematics were only observed in one plane. Finally, the effectiveness of each product to affect these criteria varies between individuals. The dataset size may have contributed to these results; given the natural variation in gait between participants which was identified in the previous chapter, a larger dataset may be required to effectively show significant product effects.

5.2.8.4. Study limitations and strengths

There were some limitations associated with the study. Firstly, the two products investigated had similar product claims around shock absorption, stabilisation, and pressure redistribution and were constructed from the same materials. Investigating products with larger differences e.g., a heel wedge and metatarsal bar or products of different stiffnesses, may have more clearly identified the performance of the test platform with respect to the in-vivo group, and the effects of each product with respect to the control condition. Secondly, the test platform was limited in its ability to capture kinematics changes applied by each product. This was expected given the simplified actuation method utilised, however, it matched the complexity of the existing industrial test systems used to test the durability of orthotic products such as the Satra Pedatron. Improvements could be made by utilising a more appropriate environment for motion capture and adding complexity to the actuation system to actuate the forefoot of the phantom-foot. Finally, the sample size of the in-vivo group was relatively small, which reduced the clarity of each products effect on plantar pressure metrics (Faber & Fonseca, 2014). Orthotic evaluations usually involve 20 participants to reduce the effects of natural variation in gait; consequently, increasing the number of participants would likely result in closer alignment between the test platform and in-vivo results.

Despite these weaknesses, there were also strengths associated with the study. Firstly, the inclusion of both a shoe-only condition and control orthotic allowed the products to be compared against a generic insole; this further establishes product claims and allows individual design component effects to be established e.g., heel cups. Moreover, the repeatability of the test platform is significantly higher than individual in-vivo participants and groups. This offers much greater sensitivity on product effects and effect sizes per product and per metric.

5.2.9. Conclusion

The present study aimed to investigate the performance of two specific insoles, focusing on their impact on foot pressure and joint kinematics during normal gait, and therefore verify or build upon the claims made by the manufacturer. The findings offered insights into how these products performed against a control condition and a shoe-only condition with in-vivo participants and in the test platform.

Firstly, the test platform was generally effective in capturing the same performance characteristics as the in-vivo tests in terms of pressure on the foot. Both settings revealed that the products could reduce peak and average pressure on the heel, thus partially substantiating claims around shock absorption and pressure redistribution. However, there were differences in the magnitude of effect sizes between the platform and in-vivo settings, likely due to the inherent variability among in-vivo participants. This suggests that while the test platform provides valuable insights, the variation expected between in-vivo participants would be difficult to predict prior to clinical studies.

When it comes to joint segment kinematics, the test platform was ineffective. It did not capture significant effects that were, albeit minimally, observed in in-vivo settings—particularly the calcaneus-tibia segment in the frontal plane. This indicates that while the test platform has its merits, it is less equipped to substantiate claims concerning stabilization, at least in the context of joint kinematics.

The absolute error in the test platform's readings was lower compared to that of the in-vivo participants, providing a clearer lens through which the effects of the products can be evaluated. However, the results indicated that neither the red nor the orange insoles led to significant changes beyond what was observed with the control insole. This suggests that the claims about these products should be cautiously interpreted. Future research should involve additional testing against this control condition to validate these claims more robustly. Finally, despite the noted limitations, there was a consistency in the trends between the test platform and in-vivo results. This congruence lends some confidence to the applicability of our findings to real-world scenarios.

In summary, while both products showed some efficacy in affecting foot pressure, their impact on joint kinematics was minimal, and in neither case did they significantly outperform the control insole. These findings warrant further investigation and suggest that any claims regarding these products should be carefully qualified. The test platform, although not fully aligned with in-vivo results, serves as a useful tool for preliminary assessment, especially given its lower error rate. Further studies using a more diverse sample and additional control conditions are recommended to fully substantiate the claims made by these products.

Chapter 6: Test platform evaluation and future development pathway

5.1. Chapter overview

This chapter evaluates the test platform in this first implementation, describing the primary advantages and disadvantages in the design of the phantom-foot, actuation system and measurement system. A series of future developments to improve each element of the test platform was also suggested, depending on the future test requirements of the industrial partner. Suggestions have also been proposed to create future research opportunities e.g., the representation of populations experiencing foot pathology. The outcome of this chapter is a critical appraisal of the test platform and suggestions for future developments depending on the requirements of the industrial partner.

5.2. Achievements of the research

Three aims were established for the test platform following the conception of the project, literature reviews and needs analysis (see page 104):

1) To create a phantom-foot model that replicates the material and mechanical properties of the human foot during gait for orthotic testing purposes
2) To develop a comprehensive test platform that accurately assesses orthotic product designs under realistic loading conditions.
3) To evaluate the effectiveness of the developed test platform through comparison with in-vivo orthotic experimental protocols

Each of the objectives were completed for aim 1; the material and mechanical properties of the components that comprise the foot were identified and informed the design of the phantom-foot, which was then validated against in-vivo subject data. However, not all components of the foot were modelled in the phantom-foot and those which feature several layers which exhibit different properties e.g., the heel pad, were represented by single structures. Consequently, the complex viscoelastic, anisotropic behaviours exhibited by the human foot were simplified into a linear, much simpler loading response.

The objectives of aim 2 were also satisfied through the use of a robust, durable, flexible robotic arm capable of highly accurately and repeatedly loading the phantom-foot, even

without force-feedback control. Consequently, its inclusion within the test platform to facilitate orthotic performance assessment was well justified. Finally, aim 3 represents the shortcomings of the test platform in its first iteration to inform clinical studies. Ultimately, the test platform demonstrated a capability of determining performance trends, but not comprehensive effect sizes with respect to different design parameters. However, additional testing would be required to quantify the minimum detectable change with respect to various design parameters, as it was not feasible to complete this within the timeframe of the PhD. This would involve varying design parameters e.g. stiffness and adjudging if there is a perceptible change in loading response of the phantom-foot. Regarding the hypotheses formulated during the implementation of the test platform, they were proven to be correct. The test platform was able to suggest product performance trends, was more capable of capturing changes in plantar pressure than joint kinematics and found minimal effects cause by the two therapeutic products tested.

Requirements R1 to R19 informed the decision-making process including the materials used to construct the phantom-foot, parameters which guided the selection and operation of the robotic arm, and choice of measurement equipment. With respect to the specification, S1 to S3 were achieved in part but simplifications in the design of the phantom-foot reduced its correspondence to realistic human foot biomechanics, tissue deformation and joint stability. S4 to S9 were satisfied to a greater degree, however, an actuation system which did not include any muscular control was limited in recreating realistic foot motion. Consequently, the most significant improvement in future implementations would be a more complex actuation system capable of achieving representative foot kinematics.

The primary contribution of this work is the demonstration of a feasible approach to testing foot health medical devices to inform clinical studies, and gauge product performance for therapeutic products which would otherwise have poorly supported claims. This method of constructing a phantom-foot for the purpose of characterising the functional performance of orthotic products is novel. As such, this work has resulted in a series of recommendations and improvements which could be introduced in future iterations of the test platform which discussed in the following section.

5.3. Critical appraisal of the test platform and suggested developments

The test platform was successfully validated in chapter 4; however, several limitations were highlighted in the current implementation. A critical appraisal of the decision-making process to produce the test platform and each subsystem's advantages and disadvantages are described below. These decision pathways were developed following the industrial needs analysis and literature reviews to produce a test platform capable of fulfilling the specification, while remaining a realistic target within the PhD timeframe. Whilst informed by the industrial needs analysis, the decisions were solely made by the student. Often, pragmatic choices were made due to limitations in funding and the impact of Covid-19 e.g., choosing a robotic arm that was readily available within the University of Salford.

5.3.1. Phantom-foot

5.3.1.1. Decision pathway

Figure 83 describes the key decisions made in the design, manufacture, and arrangement of the phantom-foot within the test platform.

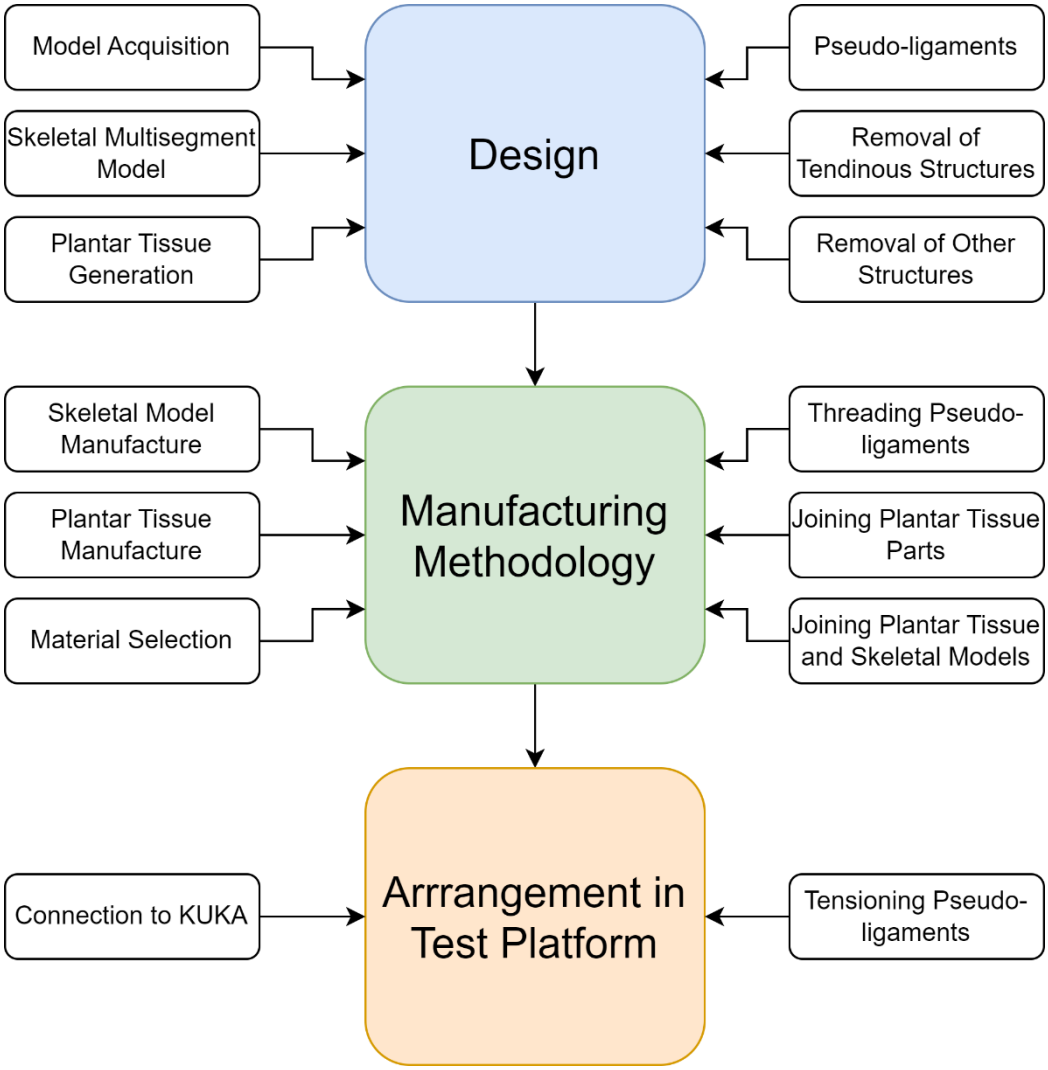

Figure 83: Phantom-foot decision pathway

5.3.1.2. Design

5.3.1.2.1. Model acquisition: Use of online repository BodyParts3D to design phantom-foot

Model acquisition was required to inform the geometry of the phantom-foot, to ensure its design aligned with the anatomy of the human foot. Several methods exist for the capture and generation of a 3D model including surface 3D scanning, magnetic resonance imaging (MRI), computed tomography scanning (CT) and ultrasound. Surface 3D scanning is limited to producing a model of the external geometry of the foot without capturing any internal structures, and hence was not appropriate for this application. Previous literature has compared the generation of 3D models using CT, MRI and ultrasound imaging techniques and found MRI to be the best tool given its high resolution and capacity to display clear boundaries between muscles and bone (Mehta, Rajani, & Sinha, 1997). Consequently, MRI

was selected as the most appropriate method to generate the 3D model which would inform the design of the phantom-foot.

MRI involves significant costs and post processing to produce a 3D model and individualize components. Subsequently, an existing repository of anatomical components was utilized which included a skin model and musculoskeletal model, including individualized components, which saved significant time and money. The disadvantages associated with this decision were the noted differences in geometry between healthy Japanese feet and healthy Caucasian feet; this may have impacted the comparison between the phantom-foot (generated according to the Japanese model) and in-vivo participants, the majority of who were Caucasian. To capture product performance more accurately within different populations, a dataset of foot models representative of healthy individuals from populations with noted geometric foot differences would be generated using MRI, but this was not feasible within this PhD project. It is unclear whether the use of a Japanese model impacted on the product performance criteria, however, given the plantar pressure behaviour aligned closely between the test platform and in-vivo participants it is unlikely.

5.3.1.2.2. Skeletal MSM: choice of Salford MSM to simplify the phantom-foot model.

The Salford MSM was selected in the design of the phantom-foot as it has previously been shown to represent key motions, motion pattern and timing of motion within the foot and was considered an achievable design to implement (Nester, Jarvis, Jones, Bowden, & Liu, 2014). Additionally, a large dataset of 100 healthy participants whose gait was analysed using the Salford MSM was available. During production of the phantom-foot, the grouping of the segments helped improve the durability of the skeletal model, particularly the smaller phalanx bones which would have broken more easily if individualised. Moreover, during implementation within the test platform, the segments were large enough to easily place the 3 retro-reflective markers required for tracking within the motion capture system and ensured larger markers which are more easily detected could be utilised. Placing markers directly onto the skeletal model differs from in-vivo studies which use skin-mounted markers, instead resembling bone-pin studies such as Nester et al. (Nester C. J., 2009). The benefits of this include the removal of skin artifacts which would have misrepresented joint segment motion, however, this made validation of the model against in-vivo subjects more difficult to achieve (Fiorentino, et al., 2017).

The primary disadvantage attributed to the selection of this MSM to model the phantom-foot was the misrepresentation of joint segment motion, which was highlighted by the misalignment of the test platform to in-vivo kinematics. However, this misalignment could not solely be attributed to the MSM selection, with additional factors such as the use of pseudo-ligaments to link segments together damping motion significantly, a simplified actuation system with no controllable internal foot motion and environmental issues when using the motion camera system with the robotic arm. Consequently, until these additional factors can be resolved, the suitability of the Salford MSM cannot be critically judged to have impacted the test platform in its evaluation of product performance.

5.3.1.2.3. Plantar tissue generation: 3D modelling technique and lattice generation to vary Young's modulus.

A plantar tissue model was not available within the online repository and was therefore required to be generated within 3D modelling software. A Boolean command was used to produce a solid of the space between the skeletal and skin models, which was defined as the plantar tissue model. The advantage of this method was that indentations could also be designed in areas of the plantar tissue e.g., the heel, phalanges, to help align the skeletal and ultimately join it to the plantar tissue. Following this, a lattice structure could be used and applied to the solid model to vary the stress/strain properties (measured via Young's modulus) to achieve properties which aligned more closely with in-vitro tissue. The ease with which the process could be carried out was a key advantage, new samples could be modelled and manufactured rapidly for implementation. Additionally, the high repeatability with which phantom-foot models could be produced; copies of the same model were validated to show no significant difference in loading response. This is comparable to the cadaveric simulators identified in chapter 2 e.g., Peters et al. (Peeters, et al., 2013) .

Alongside these benefits, there were some disadvantages associated with the plantar tissue design process. Firstly, the plantar tissue was represented as a single layer of given material properties, which is a simplification of the tissue structure of the human foot. Separation of the structure into layers would likely produce a more realistic response, particularly with regards to contact area as the phantom-foot would spread more under load. Finally, the tissue depth varies across the foot (as identified in chapter 2), but this was not represented with the plantar tissue model. This likely reduced the accuracy with which the location of peak pressure aligned with in-vivo foot behaviour but could be addressed within the 3D modelling

software by varying the position of the skeletal model relative to the skin model prior to performing the Boolean function to produce the plantar tissue model. Next, the validation process identified weaknesses in this design strategy as the phantom-foot degraded over the course of a single test protocol. Although this would require a new phantom-foot copy per test protocol, this was not perceived as a significant impact given the high repeatability between copies and low production costs (approximately £100). However, a solid phantom-foot model may provide a longer 'stable' region in which product performance can be evaluated, hence allowing longer test protocols to be carried out.

5.3.1.2.4. Pseudo-ligaments: using NinjaFlex filament to link segments together

To join bone segments together, flexible NinjaFlex filament was threaded through the core of each segment and glued into the distal phalanges. The resulting skeletal model could be made more/less flexible depending on the tension under which the filament was held, and the number of filament strands used to link segments, although the model was compliant even under the maximum applicable tension. This offered a simple, adaptable method of linking segments and varying the range of intersegmental motion.

As mentioned in section 2.1.2.2. the pseudo-ligaments may have contributed to the laxity of the phantom-foot and the resultant lack of intersegmental motion. This was likely due to the material chosen, as the filament would break when held under high tension, or slide during the operation of the robotic arm, reducing the tension linking the segments together. By changing the material to a more durable alternative such as neoprene, the kinematic performance of the phantom-foot would improve. Additionally, this design featured a lack of motion restriction; in a human foot, ligaments permit/prevent fixed ranges of motion in each plane, but this was simplified within the phantom-foot model. If joint segment motion of a particular segment of portion of the foot was a point of interest during implementation of the test platform, additional neoprene structures could be applied between segments to achieve a more realistic segment range of motion by restricting movement in a chosen plane.

5.3.1.2.5. Pseudo-cartilage: using PET tape to line the joint endings of the phantom-foot

Articular cartilage lines the joint endings within the human foot to allow bones to slide more easily over each other with little friction. PET tape was selected to mimic this function in the phantom-foot, similar to the method employed by Zhu in an anthropometric robotic finger (Zhu, Wei, Ren, Luo, & Shang, 2023). The PET tape ensured that the rough surface finish of

the 3D printed bones didn't cause wear or impact the freedom of movement of any segment. However, it is unclear whether the addition of PET tape impacted the joint kinematics of the phantom-foot, and additional studies would be required to understand the effects of its inclusion.

5.3.1.2.6. 3D model processing: removal of muscular/tendinous structures

BodyParts3D was used to obtain a complete musculoskeletal model and skin model, however, the foot model was simplified to present a more achievable target within the PhD timeframe. All muscular, ligamentous, and tendinous structures were removed from the model. The decision to remove these structures impacted the phantom-foot in two respects: firstly, the resulting phantom-foot could only be ambulated through the tibial connection, changing the action of the foot particularly in the latter stages of stance phase. Secondly, the removal of these structures reduced the number of components maintaining the shape of the phantom-foot and transferring load underneath the midfoot. This resulted in greater forces applied to the pseudo-ligaments which degraded more quickly and reduced the plantar pressure under the midfoot during stance. The generation of a solid phantom-foot model, where the skeletal model would be encapsulated by the plantar tissue model, would help to alleviate the latter issues as the skeletal system would be more adequately supported and load would be transferred more realistically. However, the limitation around gait recreation is dictated by the choice of actuation system; this is addressed in the appraisal of the actuation system.

5.3.1.3. Manufacturing methodology

5.3.1.3.1. Skeletal model manufacture: selection of 3D printing

The skeletal model obtained from the BodyParts3D was downloaded, processed and 3D printed. 3D printing was chosen due to its high repeatability, accuracy, low manufacturing costs and relatively quick production time. Moreover, manufacture of the phantom-foot was intended to involve as little manual work as possible to ensure high repeatability between phantom-foot copies of the same sample. This was achieved as it was validated that there was no statistical significance associated with the manufacturing methodology. An Ultimaker S5 3D printer was selected to produce the skeletal model using PLA filament, a strong, low-cost material which is readily available.

5.3.1.3.2. Plantar tissue manufacture: selection of SLA 3D printing

Several manufacturing methods were considered during the development of the test platform involving varying degrees of manual labour, ranging from minimal to extensive manual effort. A relatively low-effort solution was 3D printing, which features its high repeatability, accuracy, low manufacturing costs and relatively quick production time. Additionally, new designs could be modelled and manufactured rapidly. An alternative method with a more involved manufacturing process was resin casting, which would allow high customisability of material properties and lower manufacturing costs compared to 3D printed options, potentially at the cost of lower repeatability due to manufacturer error and less flexibility in design changes.

Ultimately, high repeatability and flexibility in the production of different phantom-foot models (e.g., of different sizes and shapes) led to the selection of 3D printing as the method used to produce the phantom-foot. A Formlabs Form 3 SLA 3D printer was selected to manufacture the plantar tissue model as it was capable of printing to a resolution of 25 microns, which enabled complex lattices to be produced and hence greater variation of the stress/strain properties. Additionally, the printer could use flexible and elastic resins which would produce compliant models, whose behaviour under load would align more closely with the human foot. The manufactured plantar tissue models fulfilled the criteria established with the industry partner and reproduced peak plantar pressure in the heel region consistent with in-vivo data.

Despite this success, there was a clear disadvantage associated with this manufacturing methodology. The implementation of a lattice structure rather than a solid, although successful in varying the material properties, ultimately compromised the durability of the phantom-foot and reduced its effectiveness as a test system. Significant improvements could be made by changing the 3D printing technology implemented from SLA to polyjet, which would enable variation of the material properties via multi-materials and produce a solid plantar tissue model. Alternatively, filling the generated lattice structure with a compliant silicon or material of similar properties could improve the durability of the model without adding additional manufacturing costs.

5.3.1.3.3. Material selection: selection of PLA and Formlabs flexible 80A resin

PLA filament was chosen for the manufacture of the skeletal model due to its low cost, wide availability, and low tendency to warp during printing. The material was able to fulfil the

requirements of the phantom-foot to sustain 1000 loading cycles without any notable impact. Although if the test platform was required to perform tests of longer duration, PLA may not be appropriate given its biodegradability (meaning prints would degrade over time) and poor mechanical characteristics in comparison to ABS, PETG or Nylon. Additionally, support material had to be manually removed (rather than dissolved as in the case of PVA) which was time consuming and sometimes resulted in non-smooth finishes.

Formlabs flexible 80A resin was selected to manufacture the plantar tissue model. The stress/strain properties of this material were significantly greater than required to correspond with the in-vitro properties collected in chapter 2, however, could be tuned through the implementation of the lattice structure. Although the material required time-consuming post-processing, its durability, elastomericity and transparency (which made it easier to examine the lattice structure post-testing to determine degradation and points of failure) justified it as an appropriate choice.

5.3.1.3.4. Threading pseudo-ligaments: linking segments using pseudo-ligaments and gluing them to the phalanges.

Each pseudo-ligament was glued to a phalanx and threaded through each segment to be linked together, with the number of pseudo-ligaments passed through a segment dictating its ability to rotate in the coronal plane. This method functioned to hold the skeletal model in place and the holes drilled in each segment didn't impact the durability during implementation of the test platform. However, there was no method used to maintain a set distance between segments: only the tension applied to the pseudo-ligaments dictated the spacing between segments and supported the shape of the skeletal model. The repeatability of the joint kinematics could be improved by gluing the pseudo-ligaments within each segment to define and maintain joint spacing. Moreover, this would prevent the segments with only a single pseudo-ligament (i.e., the phalanges) from spinning freely in the coronal plane.

5.3.1.3.5. Joining plantar tissue parts

The plantar tissue component was larger than the maximum print volume of the Formlabs Form 3. Consequently, it was split into two parts, with alignment pins and holes used to mate the parts together post-printing. The primary benefit from this technique was the potential reduction in manufacturing time, as the same forefoot could be used with different hindfoot parts given that the forefoot was not extensively loaded due to the lack of 'rollover' achievable by the robotic arm in transferring load towards the forefoot.

Despite this, the design presented two disadvantages. Firstly, separating the plantar tissue into two parts changed the lattice structure, as a solid boundary enclosed each volume. This effectively introduced a hard boundary between the parts, with different stiffness properties which may impact the kinematics around the midfoot in late stages of stance phase. Similarly, the pegs used to mate the parts together may reduce the flexibility of the phantom-foot around the midfoot. Therefore, a clear improvement in the design and manufacture of the plantar tissue component would be the use of a 3D printing method capable of producing the entire component in a single piece.

5.3.1.3.6. Joining plantar tissue and skeletal models together

As the plantar tissue and skeletal model components were manufactured individually, they needed to be joined together to form the phantom-foot. Several options were tested with varying results. Gluing the components together at the heel cup and indentations left to fit the phalanges did not produce a join strong enough to withstand loading and the flexing of the foot during actuation. Using screws in these regions was difficult due to the small size of some skeletal segments, particularly in the forefoot, and due to the tendency of the plantar tissue material to tear as the screws moved during loading. Consequently, the solution which was adopted was the use of two screws in the medial and posterior of the calcaneus, and tape to secure the forefoot in place. The advantages with this solution included the reusability of skeletal components, as they were not damaged during loading, and the ease with which each component could be oriented and joined together.

The phantom-foot design adopted showed low adherence to in-vivo kinematics, particularly around the midfoot. This was attributed in part due to the large gap between the plantar tissue and skeletal components in this region. Combined with the factors discussed in sections 5.3.1.3.2 and 5.3.1.3.5, it suggests the need for a phantom-foot model where both components are fixed together with no gaps e.g., where the parts are enveloped in a transparent material. This would ensure load is transferred through the phantom-foot in a manner akin to in-vivo.

5.3.1.4. Arrangement in test platform

5.3.1.4.1. Connection to robotic arm: connecting the phantom-foot via a flange.

The end effector of the robotic arm features a circular flange plate with several bolt holes, allowing the connection of grippers, claws etc in a chosen orientation. Therefore, to secure

the phantom-foot to the robotic arm, a flange plate was designed, and 3D printed alongside the skeletal model, where it was incorporated into the calcaneus-talus segment. This provided a durable, secure method of attachment which ensured each phantom-foot copy would be fixed to the robotic arm in the same orientation each time. However, due to the size of the flange plate and its geometry, it required a significant amount of support material during printing which wasteful and significantly increased printing time. A more appropriate connection method would be a metal flange plate with a point of connection to the phantom-foot; this would significantly reduce the material required to print the skeletal model and only require a single flange plate for all phantom-foot copies.

5.3.2. Actuation system

5.3.2.1. Decision pathway

Figure 84 describes the key decisions made in the selection and implementation of the robotic arm within the test platform.

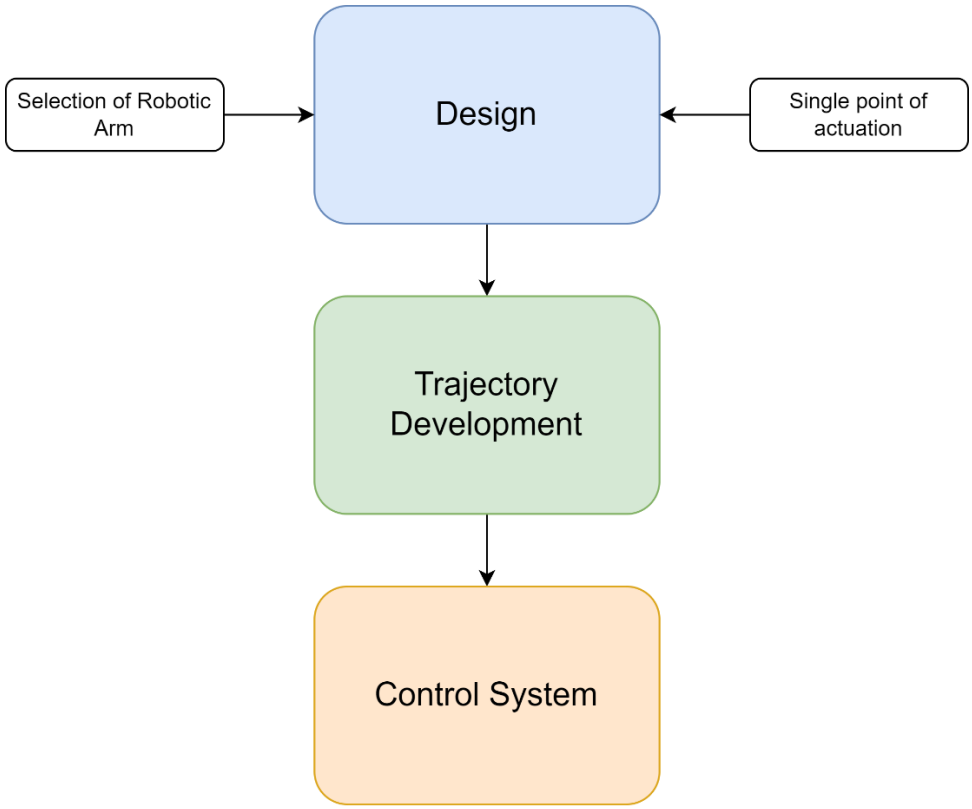

Figure 84: Actuation system decision pathway

5.3.2.2. Design

5.3.2.2.1. Selection of a robotic arm

A robotic arm was selected as the test platform's actuation system to load the phantom-foot given the flexibility with which the trajectory could be altered, high repeatability and capability of operating with open and closed loop control systems. The robotic arm was chosen as it fulfilled the defined specification and enabled a high degree of control of each joint to recreate a given trajectory. Additionally, RoboDK simulation software enabled the workspace to be modelled such that the trajectory of the robotic arm could be plotted prior to implementation. Despite the clear advantages behind the use of a robotic arm, it was only feasible for use within this PhD project due to its availability within the University of Salford. Moreover, there are significant barriers to use including the requirement of specialist training and workspace safety restrictions. These restrictions will require a specific workspace to be setup for operation of the test platform, with a technician or qualified professional responsible for its usage. But this is not considered a significant barrier to its implementation within the industrial partners product development pathway as these requirements are normal for large industrial test processes.

5.3.2.2.2. Single point of actuation

The human foot contains numerous components which act to change its shape and transfer load from rearfoot to forefoot during stance phase. The test platform simplified this motion significantly, given the complicated network of actuators which would be required to achieve this motion, and with the understanding that product performance evaluation may not require an exact recreation of in-vivo gait. As such, load transfer solely occurred through the point of connection between the phantom-foot and robotic arm, which was effectively the tibia. The advantages behind this decision were the simplified connection to the robotic arm and ease with which the trajectory could be designed. However, this oversimplification of gait contributed to the lack of agreement between the test platform and in-vivo. Therefore, if the test platform was required to investigate the performance of products designed to change foot kinematics, a more advanced actuation system would be required; this could include the addition of extensors to lift the forefoot on heel-strike and transfer load through the forefoot during terminal stance.

5.3.2.3. Trajectory development

The test platform was intended to load the phantom-foot and applied products in a manner comparable to in-vivo. RoboDK simulation software was utilised to model the entire workspace and create the trajectory to be applied to the phantom-foot. This trajectory was informed by in-vivo tibial sagittal motion, and calcaneus angles at key positions during the gait cycle. These positions were plotted, and a smooth spline applied to generate the entire trajectory. However, a key difference between the robotic arm and in-vivo gait was the effective lack of an ankle joint; the joint structure of the robotic arm would not enable motions around the ankle joint to be carried out, with the nearest joint acting as a knee instead. Consequently, the gait pattern would be more akin to an in-vivo participant with a fixed ankle joint. This lack of mobility around the ankle joint, together with the single point of actuation significantly reduced kinematic alignment to in-vivo, Although in this case, irrespective of the future intentions behind the test platform, the addition of an ankle joint e.g., through the connection of a prosthetic ankle device, would be a serious recommendation given the impact on load transfer towards the forefoot.

5.3.2.4. Control system

Although the robotic arm can be configured with a device offering feedback e.g., a load cell, an open-loop control system was elected for the test platform. This decision was influenced by two factors: the intention to deliver a system capable of fulfilling the specification, and the budget available during this PhD project. In the first case, alongside simplifications to the phantom-foot model, a simple open-loop control system presented an achievable target within the allotted PhD timeframe, including demands introduced by covid and access restrictions to the robotic arm's workspace. And the latter case dictated the feasibility of adding a load cell to the end effector of the robotic arm to configure impedance/force control feedback. As such, the loading applied by the test platform had to be configured through trial and error, changing the y component of the trajectory until the intended loading was achieved. The addition of a load cell and a closed loop control system would improve this process and ensure the exact load required would be applied by the test platform.

5.3.3. Measurement system

5.3.3.1. Decision pathway

Figure 85 describes the key decisions made in the selection and arrangement of the measurement devices used within the test platform.

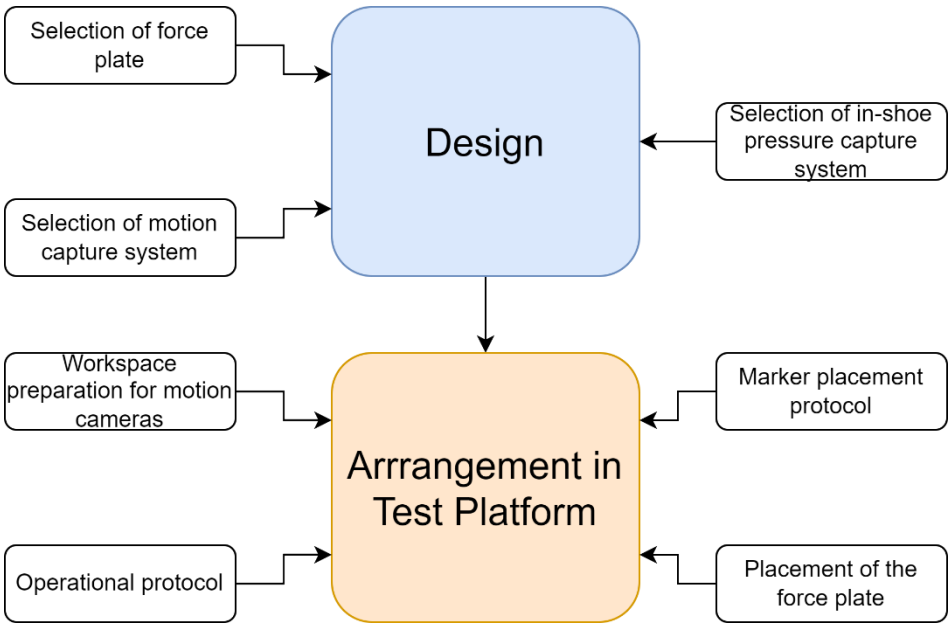

Figure 85: Measurement system decision pathway

5.3.3.2. Design

5.3.3.2.1. Selection of force plate

To precisely determine the load applied by the robotic arm, and the nuanced changes in loading affected by the product, several force measurement options, including a force plate, load cells, and piezoelectric sensors, were considered. The portable force plate was elected as the best choice. Given its ability to measure forces and moments in multiple directions it could capture shear forces and offer a comprehensive view of the entire load spectrum. Moreover, the force plate could reliably capture both static and dynamic measurements, including high speed changes. A software package supplied with the force plate made data acquisition and handling straightforward. This high degree of accuracy and precision, combined with its ease of installation and robust build, set the Kistler 9286AA apart. In contrast load cells typically only measure forces in a single direction, hence multiple sensors would be required to capture multi-directional force data. And piezoelectric sensors are susceptible to changes in temperature and can drift during long-duration static force

measurements. Therefore, the force plate was clearly the most appropriate solution for use within the test platform.

Although force plates are typically embedded into a walkway in gait laboratories, a portable system offers a better solution for industry. This is primarily due to the use of the robotic arm, which has the capability to drive itself into the ground if incorrectly programmed, ultimately destroying itself. Consequently, positioning the force plate onto a raised surface provides a safe solution to reduce the likelihood of this event occurring.

5.3.3.2.2. Selection of in-shoe pressure capture system

Within Jarvis' study, a pressure plate was used to capture plantar pressure data. This described the boundary between the foot/shoe and ground, but the test platform is required to define the interface between the foot and device. Consequently, an XSENSOR in-shoe pressure capture system was elected for use in the test platform. Although accurate and with sufficient battery life to record several test protocols, the pressure capture system presented several challenges. They were liable to fold when placed inside the shoe such that they were not flat against the sole of the shoe. Consequently, when the phantom-foot was placed on top, areas where the insole was not flat would not collect plantar pressure data correctly. Additionally, this could result in individual pressure sensors becoming damaged which would show significantly low/high pressure spots which skewed data; this affected in-vivo data collection more than testing with the test platform as individuals would struggle to avoid displacing the pressure capture insole when sliding their foot into the shoe. Attempts were made to remedy this issue by triggering a short data collection to confirm pressure data was being recorded correctly prior to completing a test protocol.

5.3.3.2.3. Selection of motion capture system

A motion capture system was selected to capture kinematic changes applied by the orthotics, due to its prevalence within clinical gait studies. These systems can capture changes with great accuracy, however, require dedicated laboratory spaces with dull surfaces and bright lighting to operate correctly. Otherwise they can be suspect to capturing reflections, thus influencing motion capture results. It may not be feasible to setup a gait laboratory with these conditions in industry hence it may not be an appropriate measurement system for use within the test platform. Moreover, the actuation system and phantom-foot design are not mature enough to fully simulate the intrinsic motion of the foot during a gait cycle, meaning its utilisation in capturing kinematic changes is limited. An alternative method exists, where the

motion capture system could be used to create a number of actuation profiles within the University of Salford. Given the high repeatability of the test platform, it could be pre-programmed using the motion capture system before a separate system which does not require the same laboratory setup (e.g., accelerometers) is used to capture kinematic changes. This would not offer the high accuracy of the motion capture system, but given the limited actuation system of the test platform this would not pose a significant barrier, and ultimately may be a more appropriate selection for industry.

5.3.3.3. Arrangement

5.3.3.3.1. Workspace preparation for motion cameras

Gait laboratories use low-reflective surfaces to ensure motion cameras can operate effectively. The robotic arm was situated in a robotic laboratory which was not configured for motion cameras, and contained several reflective surfaces including machinery, computer equipment and glossy flooring. It could not be moved due to university restrictions, so numerous strategies were adopted to reduce the effects of these environmental factors. Firstly, the motion cameras were placed in close proximity to the robotic arm to reduce the size of the workspace and ensure other equipment within the laboratory wouldn't interfere with kinematic data capture. Next, the number of light sources was reduced to a single point above the robotic arm to reduce reflectivity. Finally, the aperture and marker threshold for each camera was configured to reduce the sensitivity as much as possible while still allowing marker tracking. Masks were applied in areas with reflections where the phantom-foot would not move through, and hence no markers would be present.

Despite the adoption of these strategies, significant numbers of reflections were still present in the workspace. Crucially, as the robotic arm actuated the phantom-foot, the shiny surface of the robotic arm produced a significant number of reflections. Over the course of a test protocol comprising 1000 steps, this produced thousands of erroneous traces, which significantly contributed to data processing time and may have impacted motion data quality. The most significant improvement which could be made to alleviate these issues would be covering the exterior of the robotic arm with a dull finish. This would ensure that additional reflections wouldn't be generated during operation of the test platform, and masking would be more effective at reducing the number of reflections present.

5.3.3.3.2. Marker placement protocol

Markers were applied to the phantom-foot according to the Salford MSM but placed on top of the shoe rather than directly onto the skeletal model. During operation, the robotic arm obscured some markers (particularly around the calcaneus) which resulted in numerous traces within QTM rather than a single, continuous trace. This significantly increased the time required for data processing as individual traces had to be identified and concatenated together, with gap-fill methods applied to join traces where data was missing. Moreover, due to the large number of reflections, identifying markers and erroneous traces was difficult and likely reduced data quality for markers which had been obscured during operation.

As well as adopting the method previously described to reduce the number of reflections, changes could be made to reduce the number of markers covered during operation of the test platform. Firstly, the joint poses of the robot could be changed to extend the end effector of the test platform further away from the base. Consequently, the base would be less likely to obscure the calcaneus markers. Moreover, the addition of a greater number of markers on the phantom-foot and the robotic arm would bring clarity during data processing as it would be easier to identify the correct markers and ignore erroneous traces. This may require the application of markers on stalks rather than directly to the phantom-foot to increase the number of markers that can be applied.

5.3.3.3.3. Placement of the force plate

A portable force plate was placed under the robotic arm within the test platform, and effectively and reliably collected force data during operation. The force plate was positioned in the centre of a table; a heavy table was chosen to ensure it would not shift during operation of the test platform. However, as the phantom-foot came into contact with the force plate, the protective cover on its surface was pushed off over time due to the shear force applied during loading. Extra adhesive was applied to secure it to the surface of the force plate, but the embedding of the force plate into a table/mount would be a more appropriate long-term solution, to ensure the force plate doesn’t laterally shift over the course of a test protocol.

5.3.3.3.4. Operational protocol

The robotic arm is a robotic arm capable of delivering significant forces at high speeds within a large workspace. As such, there are stringent safety requirements associated with its use, such as the requirement for a trained technician to operate the machine and users to stand a

safe distance away during operation. To meet these requirements, safety barriers were erected outside the maximum reach of the robotic arm, with the controller placed on this boundary for use by the operator. However, the laptops used to operate the force plate acquisition software, motion capture software and pressure capture software had to be placed close to the test platform due to cable lengths. Consequently, the method of operation included running all 3 data acquisition programs, moving outside the safety barriers and using the robotic arm controller to trigger the test protocol.

Although functional, this resulted in separate force, pressure and motion data which had to be manually synchronised. This could be improved by configuring multiple data sources within a single data acquisition software; it is possible to integrate force plate data collection into QTM which would synchronise motion and force data upon collection. However, this was not feasible within this project as insufficient funding was available to purchase a Kistler amplifier compatible with QTM, and the pressure software was not supported within QTM. Furthermore, arranging the test platform such that all laptops are placed outside the safety barriers would be more appropriate for implementation of the test platform.

5.3.4. Reflections and conclusion

The current implementation of the test platform, while capable of characterising product performance in some metrics and largely fulfilling the specification, has also been accompanied by a significant number of drawbacks. Namely, the choice of a lattice network as opposed to a solid material for the plantar tissue component of the phantom-foot, simplification of the actuation system causing joint segment kinematic adherence to in-vivo to be poor, and poor test environment impacting data quality and processing times.

Some of these shortcomings can be ameliorated with adjustments to the test protocol or through the integration of straightforward measures e.g., changing materials and removing reflective surfaces from the test environment. However, others might necessitate more comprehensive modifications to the equipment or alterations in the environment in which the test platform functions e.g., buying new equipment to enable a closed loop control system or synchronicity in force and kinematic data capture. It's pivotal to note that the selection of changes to be added in future iterations of the test platform will largely hinge on the test protocols specified by the industrial partner and anticipated testing needs.

While there are limitations, I would also draw back to the fact that the phantom foot was able to demonstrate a similar response to the in vivo comparator data during the implementation tests and so can act as an effective pre-clinical design and evaluation tool.

Upon reflection, if it were possible to repeat the design of the test platform, I would produce a phantom-foot constructed from a solid material. A polyjet printer would offer multi-material printing capabilities such that the desired material properties could be recreated, and the skeletal system could be incorporated directly into the muscular and plantar tissue components. In addition, the use of a control system within the robotic arm would enable a more accurate method of loading the phantom-foot and reduce the trial and error required to achieve the desired force. Both of these changes would increase the cost of the test platform and as such would require additional industry or university support, but would likely produce better results. Moving forward, an actuation system of increased complexity would yield the most significant improvements, but will also require extra funding. Therefore, future iterations would be dependent on its availability.

Appendices

Appendix A: Papers reviewed in Literature review: foot material properties

Table 46: Young's Modulus (YM) values of plantar tissue regions of the foot. NS = not stated

Component	Reference	Sample	Protocol Conditions	YM (kPa)	SD
Heel	(Klaesner J. W., Commean, Hastings, Zou, & Mueller, 2001)	n = 5 (3M, 2F) age = 31.6 ± 7.2 y In-vivo	Force Range: (N) 2-9	160	NS
			Force Range: (N) 2-9	135	NS
			Force Range: (N) 1-3	90	NS
			Force Range: (N) 7-12	216	NS
	(Hsu, et al., 2009)	n = 16 age = 55.2 ± 4.2 In-vivo		221	45
	(Teoh, Shim, & Lee, 2014)	n = 25 (11M, 14F) age = 22.1 ± 1.6 H = 164.9 ± 8.0 cm M = 554.27 ± 82.40N In-vivo		198.5	24.8
		n = 25 age = 66.9 ± 5.9 H = 160.1 ± 8.4 cm M = 558.19 ± 89.27N In-vivo		260.7	64.7
Met 1	(Klaesner J. W., Commean, Hastings, Zou, & Mueller, 2001)	n = 5 (3M, 2F) age = 31.6 ± 7.2 y In-vivo	Force Range: (N) 2-9	159	NS
			Force Range: (N) 2-9	109	NS
			Force Range: (N) 1-3	59	NS
			Force Range: (N) 7-12	144	NS
	(Chao, Zheng, Huang, & Cheing, 2010)	n = 19 (11M, 8F) age = 27.11 ± 4.18 y H = 170 ± 8 cm M = 646.28 ± 129.00N In-vivo		32.91	14.41
		n = 11 (6M, 5F) age = 62.18 ± 5.72 y H = 166 ± 7 cm W = 629.12 ± 88.98N In-vivo		36.73	19.26
	(Hsu, et al., 2005)	n = 9 (5M, 4F) age = 24.0 ± 1.8 y In-vivo	Impact status: Low	300	12
			Impact status: Medium	324	14
			Impact status: High	402	16
		n = 10 (5M, 5F) age = 54.6 ± 3.3 y In-vivo	Impact status: Low	509	21
			Impact status: Medium	505	20
			Impact status: High	511	32
Met 2	(Teoh, Shim, & Lee, 2014)	n = 25 (11M, 14F) age = 22.1 ± 1.6 H = 164.9 ± 8.0 cm M = 554.27 ± 82.40N In-vivo	Weight Bearing MTPJ angle: 0°	73.6	21
			Weight Bearing MTPJ angle: 20°	110.3	27.9
			Weight Bearing MTPJ angle: 40°	134.4	17.3
		n = 25 age = 66.9 ± 5.9 H = 160.1 ± 8.4 cm M = 558.19 ± 89.27N In-vivo	Weight Bearing MTPJ angle: 0°	103.6	27.9
			Weight Bearing MTPJ angle: 20°	153.4	48.5
			Weight Bearing MTPJ angle: 40°	182.5	48.4
	(Chao, Zheng, Huang, & Cheing, 2010)	n = 19 (11M, 8F) age = 27.11 ± 4.18 y H = 170 ± 8 cm M = 646.28 ± 129.00N In-vivo		58.3	15.88
		n = 11 (6M, 5F) age = 62.18 ± 5.72 y H = 166 ± 7 cm W = 629.12 ± 88.98N		83.24	28.77

		In-vivo			
	(Hsu, et al., 2005)	n = 9 (5M, 4F) age = 24.0 ± 1.8 y In-vivo	Impact status: Low	362	19
			Impact status: Medium	402	18
			Impact status: High	539	46
		n = 10 (5M, 5F) age = 54.6 ± 3.3 y In-vivo	Impact status: Low	500	26
			Impact status: Medium	502	28
			Impact status: High	494	22
Met 3	(Klaesner J. W., Commean, Hastings, Zou, & Mueller, 2001)	n = 5 (3M, 2F) age = 31.6 ± 7.2 y In-vivo	Force Range: (N) 2-9	165	NS
			Force Range: (N) 2-9	127	NS
			Force Range: (N) 1-3	85	NS
			Force Range: (N) 7-12	180	NS
	(Hsu, et al., 2005)	n = 9 (5M, 4F) age = 24.0 ± 1.8 y In-vivo	Impact status: Low	365	20
			Impact status: Medium	401	24
			Impact status: High	471	19
		n = 10 (5M, 5F) age = 54.6 ± 3.3 y In-vivo	Impact status: Low	517	34
			Impact status: Medium	527	37
			Impact status: High	547	32
Met 4	(Hsu, et al., 2005)	n = 9 (5M, 4F) age = 24.0 ± 1.8 y In-vivo	Impact status: Low	363	20
			Impact status: Medium	394	24
			Impact status: High	455	33
		n = 10 (5M, 5F) age = 54.6 ± 3.3 y In-vivo	Impact status: Low	564	35
			Impact status: Medium	568	36
			Impact status: High	545	37
Met 5	(Klaesner J. W., Commean, Hastings, Zou, & Mueller, 2001)	n = 5 (3M, 2F) age = 31.6 ± 7.2 y In-vivo	Force Range: (N) 2-9	123	NS
			Force Range: (N) 2-9	84	NS
			Force Range: (N) 1-3	64	NS
			Force Range: (N) 7-12	148	NS
	(Hsu, et al., 2005)	n = 9 (5M, 4F) age = 24.0 ± 1.8 y In-vivo	Impact status: Low	324	24
			Impact status: Medium	352	17
			Impact status: High	492	48
		n = 10 (5M, 5F) age = 54.6 ± 3.3 y In-vivo	Impact status: Low	528	29
			Impact status: Medium	530	33
			Impact status: High	557	31
Hallux	(Teoh, Shim, & Lee, 2014)	n = 25 (11M, 14F) age = 22.1 ± 1.6 H = 164.9 ± 8.0 cm M = 554.27 ± 82.40N In-vivo		24.8	7
		n = 25 age = 66.9 ± 5.9 H = 160.1 ± 8.4 cm M = 558.19 ± 89.27N In-vivo		36	14.1

Table 47: Unloaded thickness (UT) values of plantar tissue regions of the foot. NS = not stated

Component	Reference	Participants	UT (mm)	SD
Heel	(Hsu, Wang, Tsai, Kuo, & Tang, 1998)	n = 20 (10M, 10F) age = 28.2 ± 4.5 y H = 164 ± 8.6cm M = 590.56 ± 107.91N	17.6	2
		n = 13 (7M, 6F) age = 68.0 ± 6.5 y H = 161 ± 6.7cm M = 649.42 ± 107.91N	20.1	2.4
	(Wearing, Hooper, Dubois, Smeathers, & Dietze, 2014)	n = 16 (6M, 10F) age = 45 ± 10 y H = 166 ± 10 cm W = 791.67 ± 105.95N	18.9	1.7
	(Tong, Lim, & Goh, 2003)	n = 14 (6M, 8F) age = 43.2 ± 17.6 y H = 162 ± 10 cm M = 578.79 ± 102.02N	15.5	2.4
	(Chen, Lee, & Lee, 2014)	n = 6 (2M, 4F) age = 26.6 ± 4.6 y H = 161 ± 16 cm M = 560.15 ± 88.29N	11.7	1.2

1st Met	(Klaesner J. W., Commean, Hastings, Zou, & Mueller, 2001)	n = 5 (3M, 2F) age = 31.6 ± 7.2 y	8	
	(Kwan, Zheng, & Cheing, 2010)	n = 7 (0M, 7F) age = 45.1 ± 3.3 y H = 157.3 ± 6.7 cm M = 538.57 ± 56.90N	9.19	2.77
		n = 19 (3M, 16F) age = 56.4 ± 2.4 y H = 158.4 ± 6.4 cm M = 599.39 ± 93.20N	8.9	2.73
		n = 17 (4M, 13F) age = 66.6 ± 2.8 y H = 154.9 ± 7.6 cm M = 559.17 ± 64.75N	9.35	2.27
		n = 17 (7M, 10F) age = 74.3 ± 3.3 y H = 155.9 ± 8.7 cm M = 569.96 ± 90.25N	8.75	2.29
	(Chao, Zheng, Huang, & Cheing, 2010)	n = 19 (11M, 8F) age = 27.11 ± 4.18 y H = 170.0 ± 8 cm M = 646.28 ± 129.00N	12.7	2.14
		n = 11 (6M, 5F) age = 62.18 ± 5.72 y H = 166 ± 7 cm M = 629.12 ± 88.98N	9.92	0.87
	(Sun, et al., 2011)	n = 54 (12M, 42F) age = 57.9 ± 6.1 y H = 158 ± 1 cm M = 564.08 ± 97.12N	8.25	0.28
	(Mo, Li, Yang, Zhou, & Behr, 2019)	n = 10 (6M, 4F) age = 20-29 H = 167 ± 7.7 cm M = 575.85 ± 79.46N	7.1	1
		n = 10 (6M, 4F) age = 30-39 H = 165.1 ± 6.8 cm M = 601.35 ± 115.76N	7	1.1
		n = 10 (6M, 4F) age = 40-49 H = 161.6 ± 8.2 cm W = 598.41 ± 105.95N	6.9	0.5
		n = 10 (6M, 4F) age = 50-59 H = 159.1 ± 7.9 cm W = 566.04 ± 88.29N	7.1	1.2
		n = 10 (6M, 4F) age = 60-69 H = 164 ± 7.5 cm W = 629.80 ± 99.08N	7.6	1
	(Ng, Zheng, Kwan, & Cheing, 2015)	n = 15 (7M, 8F) age = 20-28	11.19	1.05
			9.79	1.24
2nd Met	(Kwan, Zheng, & Cheing, 2010)	n = 7 (0M, 7F) age = 45.1 ± 3.3 y H = 157.3 ± 6.7 cm M = 538.57 ± 56.90N	9.97	0.94
		n = 19 (3M, 16F) age = 56.4 ± 2.4 y H = 158.4 ± 6.4 cm M = 599.39 ± 93.20N	9.14	1.56
		n = 17 (4M, 13F) age = 66.6 ± 2.8 y H = 154.9 ± 7.6 cm W = 559.17 ± 64.75N	9.52	1.77
		n = 17 (7M, 10F) age = 74.3 ± 3.3 y H = 155.9 ± 8.7 cm W = 569.96 ± 90.25N	8.73	1.85
	(Chao, Zheng, Huang, & Cheing, 2010)	n = 19 (11M, 8F) age = 27.11 ± 4.18 y H = 170.0 ± 8 cm	13.21	1.8

		W = 646.28 ± 129.00N		
		n = 11 (6M, 5F) age = 62.18 ± 5.72 y H = 166 ± 7 cm M = 629.12 ± 88.98N	10.63	1.78
	(Sun, et al., 2011)	n = 54 (12M, 42F) age = 57.9 ± 6.1 y H = 158 ± 1 cm M = 564.08 ± 97.12N	8.88	0.28
	(Teoh, Lim, & Lee, 2015)	n = 20 age = 23.7 ± 1.6 y H = 166 ± 8 cm M = 563.09 ± 97.12N	13.8	1.76
3rd Met	(Klaesner J. W., Commean, Hastings, Zou, & Mueller, 2001)	n = 5 (3M, 2F) age = 31.6 ± 7.2 y	11	
4th Met	(Mo, Li, Yang, Zhou, & Behr, 2019)	n = 10 (6M, 4F) age = 20-29 H = 167 ± 7.7 cm M = 572.90 ± 79.46N	7.5	0.9
		n = 10 (6M, 4F) age = 30-39 H = 165.1 ± 6.8 cm M = 601.35 ± 115.76N	7.7	1.5
		n = 10 (6M, 4F) age = 40-49 H = 161.6 ± 8.2 cm M = 598.41 ± 105.95N	7.3	0.8
		n = 10 (6M, 4F) age = 50-59 H = 159.1 ± 7.9 cm M = 566.04 ± 88.29N	7	0.6
		n = 10 (6M, 4F) age = 60-69 H = 164 ± 7.5 cm M = 629.80 ± 99.08N	7.4	0.8
5th Met	(Klaesner J. W., Commean, Hastings, Zou, & Mueller, 2001)	n = 5 (3M, 2F) age = 31.6 ± 7.2 y	9	
	(Kwan, Zheng, & Cheing, 2010)	n = 7 (0M, 7F) age = 45.1 ± 3.3 y H = 157.3 ± 6.7 cm M = 538.57 ± 56.90N	6.39	1.86
		n = 19 (3M, 16F) age = 56.4 ± 2.4 y H = 158.4 ± 6.4 cm M = 599.39 ± 93.20N	8.84	4
		n = 17 (4M, 13F) age = 66.6 ± 2.8 y H = 154.9 ± 7.6 cm M = 559.17 ± 64.75N	8.39	2.51
		n = 17 (7M, 10F) age = 74.3 ± 3.3 y H = 155.9 ± 8.7 cm M = 559.96 ± 90.25N	8.62	2.04
	(Ng, Zheng, Kwan, & Cheing, 2015)	n = 15 (7M, 8F) age = 20-28	8.43 7.47	1.44 1.27
Hallux	(Kwan, Zheng, & Cheing, 2010)	n = 7 (0M, 7F) age = 45.1 ± 3.3 y H = 157.3 ± 6.7 cm M = 538.57 ± 56.90N	5.37	0.86
		n = 19 (3M, 16F) age = 56.4 ± 2.4 y H = 158.4 ± 6.4 cm M = 599.39 ± 93.20N	7.18	2.96
		n = 17 (4M, 13F) age = 66.6 ± 2.8 y H = 154.9 ± 7.6 cm M = 559.17 ± 64.75N	6.29	1.55
		n = 17 (7M, 10F) age = 74.3 ± 3.3 y H = 155.9 ± 8.7 cm M = 569.96 ± 90.25N	6.74	1.25

	(Sun, et al., 2011	n = 54 (12M, 42F) age = 57.9 ± 6.1 y	5.16	0.18
	(Mo, Li, Yang, Zhou, & Behr, 2019)	n = 10 (6M, 4F) age = 20-29 H = 167 ± 7.7 cm M = 575.85 ± 79.46N	7.2	0.7
		n = 10 (6M, 4F) age = 30-39 H = 165.1 ± 6.8 cm M = 601.35 ± 115.76N	7	0.8
		n = 10 (6M, 4F) age = 40-49 H = 161.6 ± 8.2 cm M = 598.41 ± 105.95N	6.6	1.4
		n = 10 (6M, 4F) age = 50-59 H = 159.1 ± 7.9 cm M = 566.04 ± 88.29N	6.5	0.9
		n = 10 (6M, 4F) age = 60-69 H = 164 ± 7.5 cm M = 629.80 ± 99.08N	6.2	0.6
	(Ng, Zheng, Kwan, & Cheing, 2015)	n = 15 (7M, 8F) age = 20-28	9.03	1.34
			8.11	1.2

Appendix B: Ethics Application

Project Title:

Development of an industrial test platform for orthotic device and footwear testing

Project Type:

Postgraduate Research

Student ID Number:

00572096

Supervisor:

Dr Daniel Parker

Project Description (in layman's terms) including the aim(s) and objectives and justification of the project:

Medical devices for the foot encompass therapeutic inserts available over-the-counter such as insoles and protective pads, as well as devices prescribed by professionals, such as orthotics. The development of these devices involves new products being conceived, designed, samples being tested and validated against well-defined regulatory requirements, before moving into production and consumer/patient use. With a large number of product development processes involving marketing, design, innovation and product delivery professionals, there exists a risk of inefficiencies. The specific risk that this project relates to is how product design decisions are made and informed by testing of prototypes and how results of this testing relate to regulatory and marketing requirements. Consequently, this industry-linked project aims to develop a physical test platform that can identify the initial and long-term performance of a orthotic and footwear product and the key effects of these products on the internal behaviour of the foot, so that product design decisions and regulatory and marketing concepts can be informed prior to more expensive, risker clinical testing involving human participants.

In-vivo data collection is required to validate the behaviour synthetic foot model implemented within the test platform, to ensure it aligns with a real human and is sufficiently sensitive to capture changes made to the foot by orthotics. Therefore, the objectives are:

- To compare the performance of the phantom-foot to human participants using 2 different orthotic devices. Each product claims to reduce plantar pressure in different

regions of the foot to alleviate pain hence changes in peak plantar pressure will be the main performance metric.

- To evaluate these products using the pressure profile, force profile and bone/segment motion from heel strike to mid-stance against four product performance criteria used in previous clinical studies carried out by the industry partner: impact on gait, impact on shock absorption, impact on loading pattern and impact on stability/balance.
- To compare the performance of devices used to measure acceleration (accelerometers) against a gold-standard gait capture system in evaluating product performance. The average acceleration profile of the in-vivo participants for each product will be compared against those collected by the industrial test platform to determine if the changes made to normal gait by each product can be captured.

Proposed start date:

18/09/2022

School:

School of Health and Society

Statement about your personal data:

I understand that personal data about me in this application is required by the University, for the purpose of ethics review, and to evidence that the appropriate level of ethics review has been undertaken.

Such data will be stored and managed in accordance with the principles established in the General Data Protection Regulations (GDPR) and the Data Protection Act 2018.

The project involves the following types of activity:

Human Participants, Data

Will the activity involve any external organisation for which separate and specific approval is required? (e.g. NHS; school; any criminal justice agencies including the Police, Crown Prosecution Service, Prison Service or Probation Service; Ministry of Defence)?

No

How will the results of the project be disseminated?

Dissertation/Thesis, Peer reviewed journal – hard copy or online, Conference presentation

Your Research methodology:

Participants:

A total of 10 healthy participants are to be sourced from the students and staff from the University of Salford for this project. Participants must be free of lower limb injury/pathology (e.g. cerebral palsy, osteoarthritis) and have a UK shoe size between 7-10 to align with the sample represented by the test platform. Both male and female participants will be tested to determine whether gender is an influencing factor.

Orthotics:

Two orthotic products produced by the industry partner will be used within this project: Scholl Everyday Knee to Heel Pain Relief Insoles and Scholl Lower Back Relief Insoles. Both products claim to reduce peak plantar pressure and provide shock absorption to relieve pain. Additionally, tests will be performed with a flat control insole made of foam and without an insole in the participants own shoes to negate the effects of the footwear on testing. For all tests the participant will use neutral trainers provided by the university, for tests with an orthotic if the footwear has an existing liner/insole this will be removed and the test orthotic inserted.

Walking Assessment:

The 4 test conditions outlined above will be assessed through an in lab walking assessment within a gait lab at the University of Salford. Orthotic conditions will be randomised to generate a unique order for each participant prior to testing.

Prior to the walking assessment the participant will be asked to walk 4 lengths of the lab through a set of timing gates to establish their natural walking speed. When established subsequent walks will be assessed to confirm participant has maintained a steady pace (within 5% of original pace)

The participant will wear a plantar pressure measurement device, an on-shoe accelerometer and motion capture markers, these systems are described in full below.

Each walking assessment will involve the participant walking 10 lengths of the gait lab. Within each length they will walk over the force plate and have their pace checked for consistency using timing gates. If the participant misses the force plate or has a fast/slow pace they will be asked to repeat the length until a minimum of 10 lengths have been achieved or maximum of 20 minutes has elapsed. This is to ensure the test remains within the 2h timeframe specified within the participant information sheet (including a maximum of 30 minutes for experimental setup).

Health Questionnaire:

Prior to testing, each participant will be required to complete a health questionnaire (see attached documents). They will be asked to confirm they don't have any health issues which impact their foot health or walking pattern and their age, gender, height, mass, shoe size, foot length and foot width will be recorded. These will be used to determine whether certain participants align more closely to the sample represented by the test platform during comparisons between in-vivo and industrial test platform product testing.

Plantar Pressure:

An XSENSOR in-shoe pressure capture system will be used to capture plantar pressure during the walking assessment. The sensor will be placed in the shoe under each orthotic, with the control unit securely clipped to the outside of the shoe. The participant won't be required to change their gait to accommodate the system within the shoe.

To analyse the pressure data a regional mask will be applied to separate the heel, midfoot and forefoot sections, however, only the heel will be of interest within this project (to align with testing completed using the test platform). Steps related to mid gait walking will be selected for analysis. Average plantar pressure, peak plantar pressure and contact area under the heel will be captured by the system for each step: the mean and standard deviation per participant and per product will later be calculated. This will align with the impact on shock absorption and impact on stability/balance product performance criteria used by the industry partner in previous clinical studies.

Motion Capture:

A gold standard 6-camera Qualisys motion capture system and Kistler force plate will be used to capture foot kinematics during gait. A series of reflective markers will be secured onto the participants' shoes and legs with tape to enable a skeletal model to be generated for gait analysis, to determine the effect of each orthotic product on the foot kinematics of each participant: the participant will be required to wear shorts to allow for markers to be placed on their legs. The locations of these markers will follow the Salford Foot Model protocol to align with the segmented foot model represented by the test platform. To calibrate the cameras, the participant will be required to stand still in the centre of the capture volume, on the force plate, for 10s to ensure all markers are visible to the cameras.

Following data collection with each test condition using QTM (Qualisys proprietary software), motion data will be exported into Visual3D to allow for a skeletal model to be generated and each joints range of motion in each plane to be calculated. This will align with the impact on loading pattern and impact on gait product performance criteria used by the industry partner in previous clinical studies. The peak load and rate of loading will be extracted from the force plate data, to ensure test conditions between each orthotic are consistent and to allow for comparison with the industrial test platform.

Statistical Analysis:

Pressure, motion, and acceleration variables will be calculated as described above. Each variable will be assessed for normality and outliers will be assessed prior to a whole group average being generated. For two dimensional variables (e.g. pressure curve over each step) an average and Bollinger band analysis will be conducted using 95% confidence intervals.

The whole group average for each variable will be used as the gold standard for assessment of a bench test of the same products. Agreement and disagreement between bench test and the in-shoe test will be assessed using RMSE difference, ICC, t-test and Bland-Altman plots.

Does the activity involve Human Participants?

Yes

Will the participants be from any of the following groups? (Select all that apply.)

Students or staff of this University

Please justify their inclusion and your sampling.

A total of 10 healthy participants are to be sourced from the students and staff from the University of Salford for this project. Participants must be free of lower limb injury/pathology (e.g. cerebral palsy, osteoarthritis) and have a UK shoe size between 7-10 to align with the sample represented by the test platform. Both male and female participants will be tested to determine whether gender is an influencing factor.

Will your research involve a Clinical Trial?

No

Have you undertaken the Safeguarding and Prevent training relevant to your project?

Not applicable

Is a Disclosure and Barring Service (DBS) check required?

No

Please indicate exactly how participants in the study will be (i) identified, (ii) approached and (iii) recruited.

Participants will be identified within the research students and staff within the School of Health and Society according to their shoe size. The identified participants will then be approached in-person and virtually (via email). Finally, interested participants will be recruited by sharing the participant information sheet, health questionnaire and consent forms virtually, and arranging thereafter to perform the study.

Will consent be sought?

Yes

Please explain how consent will be obtained.

A written consent form will be provided to potential participants. The form will include relevant information about the study methodology (i.e. what is required of the participant), data management and means of withdrawal.

How long will the participants have to decide whether to take part in the research?

A minimum of 24 hours, so as to follow standard practice.

What mechanism is there for participants to withdraw from the project, at what interval(s) and how is this communicated to the participants?

Participants may withdraw at any point through verbal or written communication with no explanation required. Details of how to withdraw will be provided in the consent form

What arrangements have been made for participants who might not adequately understand verbal explanations or written information, or who have special communication needs?

Individuals with special communication needs (i.e. difficulty understanding verbal or written information) are not expected to be involved in this project as participants will be selected from University staff and students, however, those with additional needs can be supported by people (e.g. carers) who already have a relationship with them and can be present during the study.

Do you propose to pay or reward participants?

No

Does your project involve the potential imbalance of power/authority/status, particularly those which might compromise a participant giving informed consent?

No

Will deception of the participant be necessary during the project?

No

Does the activity involve any information pertaining to illegal activities or materials or the disclosure thereof?

No

Does the project involve any possible distress, discomfort or harm (or offense) to participants or researchers? (including physical, social, emotional, psychological and/or aims to shock / offend – e.g. Art)

No

Will you provide Debriefing, Support and/or Feedback to participants?

No

Is there any realistic risk of any participant or researcher experiencing either physical or psychological harm, distress or discomfort?

No

Does the research involve collecting personal data about human participants?

Yes

The research only involves analysis of already collected data, that exists in anonymous form, and for which participants have already given consent that it can be used in future research?

No

Please provide details of the storage, protection and destruction of any physical or electronic data collected during your research.

Data will only be stored on laptops owned by the University of Salford. No physical data will be collected. Personal data will not be shared at any point. Additional information on the data management plan is available in the document attached.

Will the project be using prospectively collected data that is anonymous to the researcher?

Yes

Will the project involve access to confidential information about people without their consent?

No

Will participants be identifiable (i.e. researchers may or will know the identity of participants and be able to return responses)?

No

Do participants have the consented option of being identified in any publication arising from the research?

No

Will the project involve the use of personal data (i.e. anything that may identify them – e.g. institutional role, video – see Data Protection checklist for further guidance)?

No

Does the activity involve work with human tissue, biological fluids or DNA samples?

No

Does the project involve Animals and / or animal tissue?

No

The project requires the use of hazardous substances.

No

The research involves non-human genetic resource.

No

Are there any other potential ethical or political concerns?#

No

Do you have any ethical concerns about collaborator company / organisation, e.g. its product has a harmful effect on humans, animals or the environment; it has a record of supporting repressive regimes; does it have ethical practices for its workers and for the safe disposal of products?

No

Appendix C: Data Protection Checklist

Data protection checklist:
Research and Related Activities

Activities which involve processing personal data must comply with the general data protection regulation (GDPR). This checklist outlines the requirements of the GDPR and the measures you must take when processing personal data for research; it also provides a mechanism for recording the steps you will take to ensure the personal data you are using are safeguarded and the reputation of the University is upheld.

Ensuring personal data are processed fairly and lawfully with due regard for individuals' privacy and ensuring that personal data remain secure are paramount. Demonstrating that we have considered the requirements of the GDPR when conducting our activities will provide assurances to research participants that their personal data is protected at Salford. Truly anonymised data (which cannot be reconstructed or linked to any other data you hold or may hold in the future to enable you to identify individuals from it) does not constitute personal data because it cannot be used to identify individuals.

What is *personal data*?

Personal data are data relating to a living individual who can be identified from those data. Personal data can be factual (such as name, address, date of birth) or can be an opinion (such as a professional opinion as to the causes of an individual's behavioural problems). Information can be personal data even if it does not include a person's name or other obvious identifiers; for example, a paragraph describing a specific event involving an individual or a set of characteristics relating to a particular individual may not include their name but would clearly identify them from the set of circumstances or characteristics being described or represented.

What is processing?

The GDPR is concerned with the processing of personal data. Processing means obtaining, recording or holding the information or data or carrying out any operation or set of operations on the information or data, including –

(a) the organisation, adaptation or alteration of the information or data,
(b) retrieval or use of the information or data,
(c) disclosure of the information or data by transmission or otherwise making available.

If your proposed activity involves processing personal data, you must complete the following checklist.
If you are unable to answer ***Yes*** to each applicable question, you must contact the Information Governance Team for advice before proceeding. If you require any further information or guidance to enable you to answer *Yes* to each question, please contact the Information Governance Team

Type of activity:	**Orthotic testing study**
Activity name/title:	**Validation of Industrial Test Platform**

Processing personal data fairly
The GDPR requires us to process personal data fairly and lawfully. In practice and in the context of research, we must: • have legitimate grounds (this is our public task); • not use the data in ways that have unjustified adverse effects on the individuals concerned; • be transparent about how you intend to use the data, and give individuals appropriate *privacy notices* when collecting their personal data; • handle people's personal data only in ways they would reasonably expect; and • make sure you do not do anything unlawful with the data.

If your activity involves *sensitive personal data*, have you checked and confirmed that you can satisfy a condition for processing this kind of personal data from the GDPR? Sensitive personal data includes: - data about racial or ethnic origin; political opinions; religious or similar beliefs; trade union membership; physical or mental health or condition; sexual life; commission or alleged commission of any offences; or any proceedings for any offence committed or alleged to have been committed.	Yes

If the intended use of the personal data would or would be likely to have an adverse effect on one or more individuals, have you considered and documented why that adverse effect is justified?	Not Applicable
Have you documented why you are collecting the specific items of information to demonstrate that you have legitimate grounds for doing so e.g. if you are carrying out research into how students' music preferences affect their degree classification and also collecting participants' shoe sizes, can you show you have a legitimate need for this information?	Yes
Have you included a research privacy notice in the Participant Information Sheet to provide to individuals? The privacy notice tells individuals how we will use their personal data once we have it, the purpose or purposes for which you intend to process the information; and any extra information you need to give individuals in the circumstances to enable you to process the information fairly, such as whether or not the information will be disclosed to a third party.	Yes

Security
Ensuring personal data are secure at all times is extremely important. The GDPR requires us to ensure that *appropriate technical and organisational measures shall be taken against unauthorised or unlawful processing of personal data and against accidental loss or destruction of, or damage to, personal data*. It is important that any personal data you collect or use during your activities remains secure until it is destroyed, which includes ensuring that only those who are authorised to access and use the data can do so. **For further guidance on information security, please see IT Security and Information Governance**

If you are intending to publish information, which could identify individuals, have you made those individuals aware that this will happen via our PIS and Consent Form and obtained their consent, if appropriate?	Not Applicable
Will papers, files, audio visual recordings, CDs, USB (memory) sticks or other media, which contain personal data, be kept in locked cabinets, cupboards, drawers etc. when the offices are vacated?	Yes
Do all individuals who will have access to or be using the personal data understand that it must not be provided to any unauthorised person (which includes disclosing information to family members or other representatives of data participants, unless the data participant has given consent for us to do this)?	Yes
Do all individuals, who will have access to or be using the personal data, understand their responsibilities under the GDPR and have they received data protection training?	Yes
Do you have appropriate procedures in place to ensure the security of the personal data if it is removed from Salford offices for any reason? Electronic data must only be removed if it is stored on encrypted devices or media e.g. an encrypted disc or USB stick, an encrypted laptop etc. Alternatively, it can be accessed remotely via a secure connection. If an unencrypted device containing personal data is lost or stolen, it is likely to lead to a substantial fine for a breach of the GDPR. Non-electronic records must be rigorously safeguarded at all times and not left unattended or in view of unauthorised people. Laptops, USB sticks and other devices, papers or any other form of personal data must not be left in cars.	Yes

Will the personal data be stored on the Salford network in a secure location with restricted access, to prevent unauthorised parties who have no right or need accessing the data?	Yes
Are all individuals who will have access to or use the personal data aware that personal information should not be stored off the Salford network and should only be stored on equipment owned or leased by Salford, unless exceptional circumstances apply? Storage under such exceptional circumstances must include the use of appropriate security measures. No personal information should be stored on any removable media e.g. USB sticks, CDs or devices e.g. laptops, smartphones unless they are encrypted.	Yes
Are all individuals, who will have access to or use the personal data, aware that any information accessed via remote working methods such as Outlook Web Access or similar must be treated securely in line with relevant legislation and all University guidelines? Salford business information, including personal data, should not be stored on personal, non-Salford equipment or devices unless exceptional circumstances apply.	Yes
Are all individuals who will have access to or use the personal data aware that non-university system email is not a secure method of communication and do they know how to encrypt documents so that they can be attached to an email and sent securely? N.B. Encryption passwords must be provided separately and never included in the same email as the encrypted attachment.	Yes
Are all individuals who will have access to or use the personal data aware that all non-electronic material which contains personal data and has been authorised for disposal must be disposed of via the University's confidential waste service (including handwritten notes, computer print-outs etc.)?	Yes

Are all individuals who will have access to or use the personal data aware that any paper documents, electronic media or hardware which has been designated for disposal must be kept in a secure location until it has been appropriately destroyed and any information it contains is no longer accessible or recoverable? Electronic media and hardware should be disposed of in line with LIS guidelines and procedures.	Yes
Can you confirm that if personal data will be transferred overseas (outside the EEA), you have taken advice from Information Governance to ensure the transfer can legally take place? This includes via email and by virtue of using 'cloud' providers which store your data on their servers based overseas.	Not Applicable

Once this form has been completed, it should be attached to your ethics application and submitted as directed. If your activity does not require further ethical approval, this form should be retained with your project documentation as a record of your considerations and data protection compliance.

You can find a variety of guidance documents and FAQs on the Information Governance web pages.

Appendix D: Participant Information Sheet

Centre for Rehabilitation and Human Performance Research
Brian Blatchford Building
Frederick Rd
University of Salford
Salford
M6 6PU

Participant Information Sheet (Healthy Volunteer)

Orthotics Testing

You are being invited to take part in a research study. Before you decide it is important for you to understand why the research is being done and what it will involve. Please take time to read the following information carefully. Talk to others about the study if you wish.

The purpose of the study is to investigate the differences in foot pressure, force and motion when using 2 orthotic products compared to no orthotic. This information will be used to validate the performance of an industrial test platform which will be used to test different orthotic and footwear products.

Why have I been invited?

You have been invited to take part in this study as a healthy individual free from any lower limb injury that impacts the way you walk.

Do I have to take part?

No. It is up to you to decide whether or not to take part. If you do, you will be given this information sheet to keep and be asked to sign a consent form, but you are free to withdraw at any time without giving a reason.

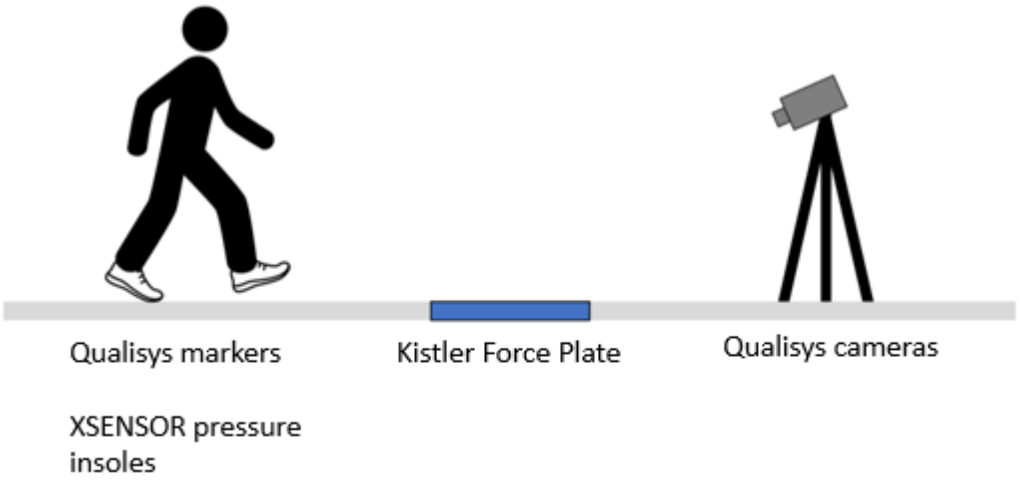

Figure 86: Representation of the data collection setup

What will be involved and what are the products being tested?

If you choose to take part you will be asked to walk wearing two different test insoles while we measure how you move and load your feet, this will take a maximum of 2 hours. You will be asked to put on a shoe in which two orthotic products will be placed, one at a time. Reflective markers and devices used to measure acceleration (accelerometers) will be placed onto the shoe and your leg; to allow these to be placed on the leg, you will be required to wear shorts. You will then be asked to walk at a specified normal pace between two markers on opposite sides of the room. During this, three measurements will be captured: pressure measurements captured using a device placed into the shoe, force data captured using a force plate under the on the floor which you will walk over and motion data using the camera system. You will be asked to repeat the walking test three times: while wearing the shoe with no insole, while wearing the shoe with insole 1 and while wearing the shoe with insole 2. The 2 products being investigated are expected to reduce the pressure in the heel during walk, to improve the wearers comfort.

Expenses and payments?

There will be no paid incentives as part of this study, this practice is not endorsed by the partnering company to maintain the integrity of the research and to allow for participation to be completely voluntary.

What are the side effects and other possible disadvantages and risks of taking part?

In preparation for this study, we have tested the products with healthy volunteers in the Gait Laboratory at Salford University. We have also tested the measurement devices which will be used to capture data and know that it is accurate and easy to use in this setting and now want to test on a larger group of healthy volunteers. The testing is low risk, as you will be using 2 orthotic products sold on the market and will only be walking for brief periods. It is considered that no increased risks, discomforts, or distresses are likely to result from the data collection above those associated with normal walking. A contact name and number will be provided to you for use if you have any queries about any part of your participation in the analysis and you are free to ask questions at any time.

What are the possible benefits of taking part?

You will not benefit directly from taking part in this research but, if successful, the research will inform the design of an industrial test platform used to test orthotic and footwear products.

What if there is a problem?

If you have a concern about any aspect of this study, you should ask to speak to the researcher Zain Shahid who will do their best to answer your questions. However, if you remain dissatisfied and wish to complain formally, please forward your concerns to Katy Szczepura, Chair of the Health Research Ethical Approval Panel, Room MS1.91, Mary Seacole Building, Frederick Road Campus, University of Salford, Salford, M6 6PU. Email K.Szczepura@salford.ac.uk

Will my taking part in this study be kept confidential?

The information obtained in this study will be collected and stored in line with the general data protection regulation in accordance with the Data Protection Act 1998. Any information obtained in connection with this study will be treated as privileged and confidential. All information will be anonymised so that you cannot be identified, except by a single paper form which will be stored securely in a lockable filing cabinet at Salford University. The research team, their colleagues, the sponsors, and people who need to audit the conduct of our research will have access to the identifiable forms. All computer records and the data will be coded so individuals cannot be identified. The data will be analysed to complete the study as outlined above. We will also keep the data for at least five years and may use it in future studies in the development of orthotic testing devices.to improve our understanding of the plantar tissue. For example, we may wish to combine the data from this study with that of future studies to enable us to use more powerful analysis techniques. Ethical approval will not normally be sought for these studies.

Involvement of the General Practitioner/Family doctor (GP)

Your GP will not be informed that you have taken part in the study, as it will not affect your health care, well-being, or lifestyle.

What will happen if I don't carry on with the study?

You may withdraw from the study at any time until the completion of the research study. Once you have completed the study you will no longer be able to withdraw your data from the research study. All data you have provided within the study until your time of withdrawal will be removed from inclusion within the study and deleted.

What will happen to the results of the research study?

The results of this study will be published in scientific and clinical journals and conferences. They will also be used for feedback and development of orthotic and footwear products. We also make regular reports to the industrial sponsor who funded this study and have an interest

in the progress of the study. None of the people who have taken part in the study will be identifiable from any of the results.

13. Who is organising or sponsoring the research?

The research is being organised by the primary researcher, working at Scholl in partnership with the University of Salford. The research is jointly funded by Scholl and the Centre for Doctoral Training in Prosthetics and Orthotics

Contact Details:

If you have any questions or would like more information, please do not hesitate to

contact:

Mr Z Shahid (PhD student)

Brian Blatchford Building, Frederick Rd Campus

University of Salford,

Salford, M6 6PU

Email: z.shahid@edu.salford.ac.uk

Appendix E: Consent Form

Centre for Rehabilitation and Human Performance Research
Brian Blatchford Building
Frederick Rd
University of Salford
Salford
M6 6PU

Consent Form for a Study of Healthy Volunteers

Orthotics Testing

Name of Researcher:

Please initial or tick the box

1. I confirm that I have read and understand the information sheet dated _____ 2022_____ version _____ for the above study and have had the opportunity to ask questions. ☐

2. I confirm that I have completed a health questionnaire ☐

3. I understand that my participation is voluntary and that I am free to withdraw at any time, without giving any reason, without my medical care or legal rights being affected. ☐

4. If I do decide to withdraw, I understand that the information I have given, up to the point of withdrawal, will not be used within the research study. ☐

The timeframe for withdrawal is until my participation within the study has been completed.

5. I understand that my personal details will be kept confidential and will not be revealed to people outside the research team. ☐

6. I understand that my anonymised data will be used in internal presentations, published journal articles, conference presentations, and PhD thesis. ☐

7. I agree to take part in the above study. ☐

_____ _____

Name of Participant Date Signature

_____ _____

Name of Person taking consent Date Signature
(if different from researcher)

_____ _____

Researcher Date Signature

Appendix F: Data Management Plan

Title:
Development of an Industrial Test Platform for Foot Health Device and Footwear Testing

Creator:
Zain Shahid

Affiliation:
University of Salford

Project Abstract:
Medical devices for the foot encompass comfort inserts available over the counter such as insoles and protective pads, as well as devices prescribed by professionals, such as orthotics. The development of these devices involves new products being conceived, designed, samples being tested and validated against well-defined regulatory requirements, before moving into production and consumer/patient use. With many product development processes involving marketing, design, innovation and product delivery professionals, there exists a risk of inefficiencies. The specific risk that this project relates to is how product design decisions are made and informed by testing of prototypes and how results of this testing relate to regulatory and marketing requirements.
It is important from an industry perspective to de-risk processes where possible and speed up any iterative processes. One key area of high risk is product testing which often involves clinical and laboratory studies with human participants, to assess how pressure under the heel might be affected by a specific shoe insert for example. These tests can be slow (take many months), costly (>£100k), and difficult to perform (e.g., require specialist skills/laboratories), and consequently impact the innovation process.
One solution to this problem is to develop models that are sufficiently realistic to appropriately test different product designs, but simplistic enough to enable testing to be repeatable, trustworthy (e.g., given regulatory requirements) and fast. Consequently, this industry-linked project aims to develop a physical test platform that can identify the initial and long-term performance of an orthotic and footwear product and the key effects of these products on the internal behaviour of the foot, so that product design decisions and regulatory and marketing concepts can be informed prior to more expensive, risker clinical testing involving human participants.

Start Date:
19-09-2022

Administrative Questions
Name of data management support staff consulted during the preparation of this plan.
Question not answered.

Date of consultation with support staff.
Question not answered.

I. Data description and collection or re-use of existing data
Provide a general description of the type of data you will be working with, including any re-used data:

Type of Data	File format	How will data be collected?	Purpose of processing	Storage location	Who will have access to the data
Qualisys motion capture data of feet	csv	Qualisys cameras (QTM software)	To determine bone/segment motion	Project drive	Researcher
Force plate data	csv	Kistler force plate (BioWare software)	To capture force profiles when using 2 different orthotic products	Project drive	Researcher
In-shoe pressure capture	csv	XSENSOR system (XSENSOR software)	To capture pressure profiles when using 2 different orthotic products	Project drive	Researcher

How much data storage will you require during the project lifetime?
<10Gb

II. Documentation and data quality
What documentation will accompany data?
Data dictionary explaining the variables used.
README file or other documentation explaining how data is organised.

III. Storage and backup during research process
Where will the data (and code, if applicable) be stored and backed-up during the project lifetime?
Project drive storage at the University of Salford

IV. Legal and ethical requirements, codes of conduct
Does your research involve human participants or 3rd party datasets collected from human participants?
Yes

Will you work with personal data? (information about an identified or identifiable natural person)
Yes

Will you work with any types of confidential or classified data or code as listed below? (tick all that apply)
No

How will ownership of the data and intellectual property rights to the data be managed?
During the active phase of research, the PhD student will oversee the access rights to data (and other outputs), as well as any requests for access from external parties.

Which personal data will you process? Tick all that apply.
Signed consent forms.
Gender, date of birth and/or age
Mass

Please list the categories of data participants
Students and staff at the University of Salford

Will you be sharing personal data with individuals/organisations outside of the EEA (European Economic Area)?
No

What is the legal ground for personal data processing?
Informed consent

Please describe the informed consent procedure you will follow:
All study participants will be asked for their written consent for taking part in the study and for data processing before the start of the interview.

Where will you store the signed consent forms?
Same storage solutions as explained in question 6.

Does the processing of the personal data result in a high risk to the data participants?
No.

What will happen with personal research data after the end of the research project?
Personal research data will be destroyed after the end of the research project. Anonymised or aggregated data will be shared with others.

How long will (pseudonymised) personal data be stored for?
For the duration of the research project. Research data won't be publicly made available.

Will your study participants be asked for their consent for data sharing?
Yes, in the consent form. Data will not be collected or deleted if consent is withdrawn later.

V. Data sharing and long-term preservation
Apart from personal data mentioned in question 17, will any other data be publicly shared?
No.

VI. Data management responsibilities and resources
Is the University of Salford the lead institution for this project?
Yes, it is the only institution involved.

If you leave the University of Salford (or are unavailable), who is going to be responsible for the data resulting from this project?
Dr Daniel Parker - d.j.parker1@salford.ac.uk

Appendix G: Risk Assessment Form

<table>
<tr><td>Task/Activity/Environment:
Gait analysis in gait lab to capture orthotic product performance</td><td>Location:
Mary Seacole Gait Laboratory</td><td colspan="2">Date of Assessment:</td></tr>
<tr><td colspan="2">Identify Hazards which could cause harm:
No. Hazard
1. Reflective Markers
2. Electrical (pressure sensor)</td><td colspan="2">Identify risks = what could go wrong if hazards cause harm:
No. Risk
1. Skin discomfort
2. Electrical shock injury</td></tr>
<tr><td colspan="3">List groups of people who could be affected:
Participants
Operator</td><td>What numbers of people are involved?
1 member of staff
No more than 5 participants per day</td></tr>
<tr><td colspan="3">What existing precautions are in place to reduce risks?

No.
1. Follow the procedure for good laboratory practise (HPL/8)
- explanation of walking over force plate
- participant will be instructed on route to seat
- where needed assistance from operator given to put on shoes
2. Follow the procedure for use of electrical equipment (HPL/1) Electrical testing conducted annually. (PAT Testing)
3. Ask if participant has any allergies</td><td>Risk level with existing precautions

low

low

low</td></tr>
<tr><td colspan="3">What additional actions are required to ensure precautions are implemented/effective or to reduce the risk further?

No.
1. Annual review of RA</td><td>Risk level with additional precautions

Low</td></tr>
<tr><td colspan="2">Is health surveillance required?
NO</td><td colspan="2">If YES, please detail:</td></tr>
<tr><td colspan="3">Who will be responsible for implementing precautions: Device Operator</td><td>By When:
Before test commences</td></tr>
</table>

Risk Evaluation = Level of Risk	No injury	First aid	<3 days absence	> 3days absence	Long term injury/ill health	Death or disabling
Almost impossible	I	I	I	I	I	I
Very unlikely	I	I	L	L	L	L
Unlikely <50/50 chance	I	L	L	L	M	M
Likely >50/50 chance	I	L	L	M	M	M
Very likely	I	L	M	M	M	**H**
Virtually certain	I	L	M	M	**H**	**C**

Risk Level	Action Required
I=Insignificant	No action
L=Low	Review controls to ensure they remain effective
If greater than low, identify additional controls to reduce risk further	
M=Medium	Identify additional actions to reduce risk further
H=High	Seek further advice
C=Critical	**STOP** seek further advice

Completed by: Zain Shahid

Date for review:

Reviewed by:

Signed:

Appendix H: Product Performance Criteria Definitions

Measures as per protocol		**Further Description**	**Units**
Joint orientation	Rearfoot angle at contact	Angle between the heel and the leg the moment the heel hits the ground in the frontal plane	°
	Maximum rearfoot angle	Maximum angle between the heel and the leg in the frontal plane	°
	Tibial rotation	Maximum internal rotation of the tibia relative to the heel	°
Body displacement	Displacement of centre of mass	Range of medial/lateral displacement of the pelvis relative to the laboratory	mm
Body velocity	Stride velocity	Quality control measure to measure walking speed	m/s
Joint angular velocity	Rearfoot eversion velocity	Maximum heel relative to the leg eversion velocity between 0% and 25% of stance	°/s
Kinetics	Vertical force	Maximum vertical ground reaction forces	BW
	Vertical impulse	Vertical force time integral	BW.s
	Ankle inversion moment	Maximum inversion moment at the ankle	BW.m
	Ankle eversion moment	Maximum eversion moment at the ankle	BW.m

Measures as per protocol		Further Description	Units
Force and pressure	BOF peak pressure	Maximum pressure that occurs at the BOF area	kPa
	Medial arch peak pressure	Maximum pressure that occurs at the medial arch area	kPa
	Heel peak pressure	Maximum pressure that occurs at the heel area	kPa
	BOF pressure time integral	Peak pressure time integral for the BOF area	kPa.s
	Medial arch pressure time integral	Peak pressure time integral for the medial arch area	kPa.s
	Heel pressure time integral	Peak pressure time integral for the heel area	kPa.s
	Force time integral	Force plate data: vertical force time integra	N.s
Contact area	Sole contact area	Total contact area of sole of foot	cm^2
	Medial arch contact area	Contact area in medial arch	cm^2
Contact time	BOF time to peak pressure	Time at which the peak pressure occurs in the BOF area	ms
	Medial arch contact area	Time at which the peak pressure occurs in the medial arch area	ms
	Heel time to peak pressure	Time at which the peak pressure occurs in the heel area	ms
	BOF contact time	Total time the BOF is in contact with the ground	ms
	Medial arch contact time	Total time the medial arch is in contact with the ground	ms
	Heel contact time	Total time the heel is in contact with the ground	ms
	Total contact time	Total time the foot is in contact with the ground	ms

Balance/Stability	Medial centre of pressure	Maximum medial excursion of centre of pressure	cm
	Lateral centre of pressure	Maximum lateral excursion of centre of pressure	cm

Appendix I: PLA Material Datasheet

FILAMENTIVE

Sustainable 3D Printing Materials

PLA/rPLA

PLA - short for polylactic acid - is a thermoplastic derived from renewable starches such as corn and sugarcane. PLA is biodegradable and produces few greenhouse gas emissions during its manufacture. PLA does not warp during print – ideal for 3D printers without a heated bed.

Dimensions

Size	Ø tolerance	Roundness
1,75mm	± 0,05mm	≥ 95%
2,85mm	± 0,10mm	≥ 95%

Physical properties

Description	Testmethod	Typical value
Specific gravity	ASTM D1505	1,24 g/cc
MFI	-	6,0 g/10 min
Tensile strength	ASTM D882	110 MPa (MD) 145 MPa (TD)
Elongation at break	ASTM D882	160% (MD) 100% (TD)
Tensile modulus	ASTM D882	3310 MPa (MD) 3860 Mpa (TD)
Impact Strength	-	7,5 KJ/m²

Thermal properties

Description	Testmethod	Typical value
printing temp.	-	180-210°C
melting temp.	-	210°C ± 10°C
melting point	ASTM D3418	145-160°C
vicat softening temp.	ISO 306	± 60°C

Features:

- Tougher and less brittle compared to regular PLA
- Easy to print at low temperature
- Low warping
- Biodegradable
- Limited smell

Additional info:

Due to its low tendency to warp PLA can also be printed without a heated bed. If you have a heated bed the recommended temperature is ± 35-60°C.
PLA can be used on all common desktop FDM or FFF technology 3D printers.
Storage: Cool and dry (15-25°C) and away from UV light. This enhances the shelf life significantly..

Filamentive Limited
InTechnology Enterprise Incubation Programme
Leeds Innovation Centre
103 Clarendon Road
Leeds
LS2 9DF
United Kingdom

www.filamentive.com
info@filamentive.com

Appendix J: Formlabs Flexible 80A Material Datasheet

Flexible 80A Resin Material Properties Data

	METRIC[1]		IMPERIAL[1]		METHOD
	Green	Post-Cured[2]	Green	Post-Cured[2]	
Mechanical Properties					
Ultimate Tensile Strength[3]	3.7 MPa	8.8 MPa	539 psi	1280 psi	ASTM D 412-06 (A)
Stress at 50% Elongation	1.5 MPa	3.1 MPa	218 psi	453 psi	ASTM D 412-06 (A)
Stress at 100% Elongation	3.5 MPa	6.3 MPa	510 psi	909 psi	ASTM D 412-06 (A)
Elongation at Break	100%	120%	100%	120%	ASTM D 412-06 (A)
Shore Hardness	70A	80 A	70A	80 A	ASTM 2240
Compression Set (23 °C for 22 hours)	Not Tested	3%	Not Tested	3%	ASTM D 624-00
Compression Set (70 °C for 22 hours)	Not Tested	5%	Not Tested	5%	ASTM D 395-03 (B)
Tear Strength[4]	11 kN/m	24 kN/m	61 lbf/in	137 lbf/in	ASTM D 395-03 (B)
Ross Flex Fatigue at 23 °C	Not Tested	>200,000 cycles	Not Tested	>200,000 cycles	ASTM D1052, (notched, 60° bending, 100 cycles/minute
Ross Flex Fatigue at 40 °C	Not Tested	>50,000 cycles	Not Tested	>50,000 cycles	ASTM D1052, (notched, 60° bending, 100 cycles/minute
Bayshore Resilience	Not Tested	28%	Not Tested	28%	ASTM D2632
Thermal Properties					
Glass transition temperature (Tg)	Not Tested	27 °C	Not Tested	27 °C	DMA

[1] Material properties can vary with part geometry, print orientation, print settings and temperature.

[2] Data was obtained from parts printed using Form 3, 100 µm, Flexible 80A settings, washed in Form Wash for 10 minutes and post-cured with Form Cure at 60 °C for 15 minutes.

[3] Tensile testing was performed after 24 hours at 23 °C, using a Die C specimen cut from sheets.

[4] Tear testing was performed after 24 hours at 23 °C, using a Die C tear specimen directly printed.

Solvent Compatibility

Percent weight gain over 24 hours for a printed and post-cured 1 x 1 x 1 cm cube immersed in respective solvent:

Solvent	24 Hour Weight Gain (%)	Solvent	24 Hour Weight Gain (%)
Acetic Acid, 5 %	0.9	Hydrogen Peroxide (3 %)	0.7
Acetone	27.4	Isooctane (pure gasoline)	1.8
Isopropyl Alcohol	11.7	Mineral Oil, light	0.1
Bleach, ~5 % NaOCl	0.8	Mineral Oil, heavy	<0.1
Butyl Acetate	51.4	Salt Water (3.5 % NaCl)	0.5
Diesel	2.3	Sodium hydroxide (aq), 0.025 %, pH = 10	0.8
Diethyl glycol monomethyl ether	16.3	Water	0.7
Hydrolic Oil	1.0	Xylene	64.1
Glycol 5	10.7	Strong Acid (HCl Conc)	28.6
Tripropylene Glycol Methyl Ether	13.8		

Appendix K: Ninjaflex Material Datasheet

NinjaTek
A division of Fenner Drives

Technical Specifications

NinjaFlex® 3D Printing Filament

Flexible Polyurethane Material for FDM Printers

NinjaFlex flexible filament leads the industry with superior flexibility and longevity compared to non-polyurethane materials. Its consistency in diameter and ovality (roundness) outpaces other polyurethane materials. Made from a specially formulated thermoplastic polyurethane (TPU) material, this patented technology contains a low-tack, easy-to-feed texture. The result is uniquely flexible, strong prints ideal for direct-drive extruders.

General Properties	Test Method	Imperial	Metric
Specific Gravity	ASTM D792	1.19 g/cc	1.19 g/cc
Moisture Absorption - 24 hours	ASTM D570	0.22 %	0.22 %

Mechanical Properties			
Tensile Strength, Yield	ASTM D638	580 psi	4 Mpa
Tensile Strength, Ultimate	ASTM D638	3,700 psi	26 Mpa
Tensile Modulus	ASTM D638	1,800 psi	12 Mpa
Elongation at Yield	ASTM D638	65%	65%
Elongation at Break	ASTM D638	660%	660%
Toughness (integrated stress-strain curve; calculated stress x strain)	ASTM D638	12,000 in-lbF/in³	82.7 m*N/m³ x10⁸
Hardness	ASTM D2240	85 Shore A	85 Shore A
Impact Strength (notched Izod, 23C)	ASTM D256	2.0 ft.lbf/in²	4.2 kJ/m²
Abrasion Resistance (mass loss, 10,000 cycles)	ASTM D4060	0.08 g	0.08 g

Thermal Properties			
Melting Point (via Differential Scanning Calorimeter)	DSC	420° F	216° C
Glass Transition (Tg)	DSC	-31° F	-35° C
Heat Deflection Temperature (HDT) @ 10.75psi/ 0.07 MPa	ASTM D648	140° F	60° C
Heat Deflection Temperature (HDT) @ 66psi/ 0.45 MPa	ASTM D648	111° F	44° C

NinjaTek filament is capable of being printed by a variety of printers in a variety of configurations. This specification sheet gives results as they pertain to the defined test standard and specimen details. Different slicing and/or printing configurations, test conditions, ambient environments, etc. may result in different results.

Impact Strength and Heat Deflection Temperature results were both provided by an accredited university testing laboratory. Specific Gravity and Hardness are innate characteristics of the material. Moisture Absorption, values associated with the Tensile Strength tests, Melting Point and Glass Transition data were prepared by Fenner Drives, Inc.

NinjaTek makes no warranties of any type, express or implied, including, but no lited to, the warranties of fitness for a particular application.

Test Specimen Details (by ASTM Test Number)
All printed specimens were created using the TAZ5 printer 0.75mm nozzle.
For ASTM D638 tests, the extrusion multiplier is 1.05.

Specific Gravity (D792): Results determined by nature of material.

Moisture (D570): 30g of filament tested in moisture analyzer evaluated at 125°C until the mass change is < 0.005% over 1 minute.

Tensile (D638): Dogbone Style IV, 100% fill, diagonal line fill.
Dimensions: 5mm thick. See drawing for other dimensions.

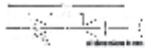

Hardness (D2240): Solid testing block.

Impact (D256): Un-notched test specimen, notch added post print by testing facility.

Abrasion (D4060): Rectangle block sized to fit tabor abrader.

HDT (D648): Bar shape.

NinjaTek.com +1-717-664-8254 support@ninjatek.com

Appendix L: PET Material Datasheet

PET (PET-P)

Technical Datasheet

SMITHS

Stable, tough, Load-Bearing Engineering Plastic — Service. Quality. Value.

Typical Applications

Mechanical engineering, automotive and general machinery construction - Especially suited to close tolerance bearings running in water. Plain bearings, coil bodies, guide & clutch parts, gears, cams, rollers, slide bearings, seal rings and guide rails.

Product Description

A high quality wear-resistant engineering plastic material with the chemical name polyethylene terephthalate. It is a crystalline material, a member of the polyester family of plastics, which should not be confused with the clear, amorphous version used to make bottles for carbonated drinks. PET exhibits particularly good dimensional stability and is available in a range of grades and forms to suit many applications.

Technical Description

Smiths' range of PET includes the following grade options:

Grade	Modification	Purpose
PET, natural and black	None.	Base material for general applications
PET + lubricant	Homogeneous dispersed solid lubricant	Additive to reduce friction, and increase wear resistance

Machinability

While not as fine as acetal, the machinability of the above grades of PET is excellent. As with all plastic materials, experience has shown that extra care must be taken with larger diameters, especially in the colder months when plastic materials lose some of their toughness and have less resistance to machining stresses. It's important that these materials are not machined while in a chilled condition. Full machining instructions may be supplied on request.

Dimensional Stability

PET is noted for its dimensional stability, enhanced by very low moisture absorption, 0.25%, and good creep resistance.

Chemical Resistance

PET has acceptable resistance to weak & diluted acids at 20ºC. Contact with alkalis is to be avoided, as is long-term contact with water above 70ºC because the material is sensitive to hydrolysis.

Product Attributes	Customer Benefits
Range of grades available	Correct grade selection for application is optimised.
Excellent dimensional stability - better than nylons and acetals.	
Minimal moisture absorption.	
Able to resist high mechanical loads.	Very good all-round product for diverse engineering applications.
Good creep resistance.	
Natural product may be used in contact with foodstuffs (subject to appropriate limits).	
May be varnished or polished.	Enables easy decoration or colouring.
Good sliding properties.	Long wear life in many industrial bearing, wear and gear applications.
High wear resistance.	
High surface hardness.	
Product sourced from longstanding manufacturer with ISO accreditation.	Consistent quality ensures uniform characteristics in machining and performance.

Product Availability *

Extruded round bar	Natural colour made up to 200mm dia, black to 100mm. Modified grades – please call for a quotation.
Extruded sheet/plate	Natural and black colour made to 100mm thk. Modified grades – please call for a quotation.

* Sizes not stocked are available on relatively short delivery time. 1, 2 or 3m lengths supplied or cut to customer requirements.

www.smithmetal.com sales@smithmetal.com

References

Abdallah, A. A. (2016). Effect of unilateral and bilateral use of laterally wedged insoles with arch supports on impact loading in medial knee osteoarthritis. *Prosthetics and orthotics international*, 231-9.

Abu-Dakka, F. J., & Saveriano, M. (2020). Variable Impedance Control and Learning—A Review. *Frontiers in Robotics and AI*.

Ahmadzadeh, S. M., & Hukins, D. W. (2014). Feasibility of using mixtures of silicone elastomers and silicone oils to model the mechanical behaviour of biological tissues. *Proceedings of the Institution of Mechanical Engineers. Part H, Journal of Engineering in Medicine*, 730-734.

al, C. J. (2019). Morphology and composition play distinct and complementary roles in the tolerance of plantar skin to mechanical load. *Sci. Adv.*

Allam, A. E., & Chang, K. V. (2022). *Plantar Heel Pain.* StatPearls Publishing.

Al-Munajjed, A. A., Rasmussen, J., Carbes, S., & Tørholm, S. (2013). The Glasgow-Maastricht AnyBody Foot Model to predict internal loads in the foo. *Combined Orthopedic Research Societies 2013.*

Alonso-Vázquez, A., Villaroya, M. A., Franco, M. A., Asín, J., & Calvo, B. (2008). Kinematic assessment of paediatric forefoot varus. *Gait and Posture*, 214-219.

Alsenoy, K. V., van der Linden, M. L., Ryu, J. H., Girard, O., Raisi, L. A., & Santos, D. (2023). Isolated and combined effects of EVA and TPU custom foot orthoses on constant speed, treadmill running kinematics. *Frontiers in earth science*.

Angin, S. M. (2018). Contributions of foot muscles and plantar fascia morphology to foot posture. *Gait & Posture*, 238-242.

Angin, S., & Demirbuken, I. (2020). Ankle and foot complex. In S. Angin, & I. Demirbuken, *Comparative Kinesiology of the Human Body* (pp. 411-439). Academic Press.

Annino, G., Palazzo, F., Alwardat, M. S., Manzi, V., Lebone, P., Tancredi, V., . . . Padua, E. (2016). Effects of long-term stimulation of textured insoles on postural control in health elderly. *The journal of sports medicine and physical fitness*, 377-384.

Arampatzis, A. a.-K. (2003). The effect of falling height on muscle activity and foot motion during landings. *Journal of Electromyography and Kinesiology*, 533-544.

Arch ES, S. S. (2016). Passive-dynamic ankle-foot orthosis replicates soleus but not gastrocnemius muscle function during stance in gait: Insights for orthosis prescription. *Prosthetics and Orthotics International*, 606-16.

Arnold, J. B. (2013). Repeatability of stance phase kinematics from a multi-segment foot model in people aged 50 years and older. *Gait and Posture*, 349-351.

Arnold, J. B., Caravaggi, P., Fraysse, F., Thewlis, D., & Leardini, A. (2017). Movement coordination patterns between the foot joints during walking. *Journal of Foot and Ankle Research*.

Asgari, N., Yeowell, G., & Sadeghi-Demneh, E. (2022). A comparison of the efficacy of textured insoles on balance performance in older people with versus without plantar callosities. *Gait and Posture*, 217-221.

Athanasiou, K. A., Liu, G. T., & Lavery, L. A. (1998). Biomechanical topography of the human articular cartilage in the first metatarsophalangeal joint. *Clinical Orthopaedics and Related Research, 348*, 269-281.

Aubin, P., Cowley, M., & Ledoux, W. (2008). Gait simulation via a 6-DOF parallel robot with iterative learning control. *IEEE Transactions on Biomedical Engineering, 55*(3), 1237-1240.

Azizan, N. A., Basaruddin, K. S., Salleh, A. F., Sulaiman, A. R., Safar, M. J., & Rusli, W. M. (2018). Leg Length Discrepancy: Dynamic Balance Response during Gait. *Journal of healthcare engineering*.

Baker, R. a. (2018). The conventional gait model - success and limitations. In *Handbook of Human Motion* (pp. 489--508). Springer International Publishing.

Balsdon, M. &. (2022). Custom-made foot orthoses with and without heel plugs and their effect on plantar pressures during treadmill walking. . *Prosthetics and Orthotics International*, 357-361.

Beckham, G., Suchomel, T., & Mizuguchi, S. (2014). Force Plate Use in Performance Monitoring and Sport Science Testing. *New Studies in Athletics*, 25-37.

Behforootan, S., Chatzistergos, P. E., Chockalingam, N., & Naemi , R. (2017). A Simulation of the Viscoelastic Behaviour of Heel Pad During Weight-Bearing Activities of Daily Living. *Annals of Biomedical Engineering*, 2750-2761.

Benedetti, M. G. (2011). A new protocol for 3D assessment of foot during gait: Application on patients with equinovarus foot. *Clinical Biomechanics*, 1033-1038.

Bennett, P. J., & Patterson, C. (1998). The foot health status questionnaire (FHSQ): a new instrument for measuring outcomes of foot care. *Australasian journal of podiatric medicine*, 55-9.

Bennett, P. J., Patterson, C., Wearing, S., & Baglioni, T. (1998). Development and validation of a questionnaire designed to measure foot-health status. *Journal of American Podiatric Medical Association*, 419-28.

Bhatt, A. (2019). New clinical trial rules: Academic trials and tribulations. *Perspectives in Clinical Research*, 103-105.

Bishop, C. a. (2012). Recommendations for the reporting of foot and ankle models. *Journal of Biomechanics*, 2185-2194.

Bone and Joint Specialists. (2024, 04 29). Retrieved from https://www.bone-joint.net/portfolio-items/foot-ankle-anatomy/

Bonnano, D. R., Landorf, K. B., Munteanu, S. E., Murley, G. S., & Menz, H. B. (2017). Effectiveness of foot orthoses and shock-absorbing insoles for the prevention of injury: a systematic review and meta-analysis. *British Journal of Sports*.

Bonnel, F., Teissier, P., Colombier, J. A., Toullec, E., & Assi, C. (2013). Biometry of the calcaneocuboid joint: biomechanical implications. *Foot and Ankle Surgery*, 70-5.

Boschetti, F., & Peretti, G. M. (2008). Mechanical Properties of Normal and Osteoarthritic Human Articular Cartilage . *Journal of Biomechanics, 41*(1).

Boyle, C. J. (2019). Morphology and composition play distinct and complementary roles in the tolerance of plantar skin to mechanical load. *Science Advances*.

Brodsky, J. W. (2011). Changes in Gait Following the Scandinavian Total Ankle Replacement. *Journal of Bone and Joint Surgery - Series A*, 1890-1896.

Brognara, L., Mazzotti, A., Rossi, F., & Lamia, F. (2023). Using Wearable Inertial Sensors to Monitor Effectiveness of Different Types of Customized Orthoses during CrossFit R Training. *Sensors*.

Bruening , D. A., Petersen, S. R., & Ridge, S. T. (2024). New perspectives on foot segment forces and joint kinetics -. *Annals of Biomedical Engineering*.

Campanelli, V., Fantini, M., Faccioli, N., Cangemi, A., Pozzo, A., & Sbarbati, A. (2011). Three-dimensional morphology of heel fat pad: an in vivo computed tomography study. *Journal of Anatomy*, 622-31.

Cappozzo, A., Cappello, A., Della Croce, U., & Pensalfini, F. (1997). Surface-marker cluster design criteria for 3-D bone movement reconstruction. *IEEE Transactions in Biomedical Engineering*, 1165-74.

Caravaggi, P. a. (2010). Kinematic correlates of walking cadence in the foot. *Journal of Biomechanics*, 2425-2433.

Caravaggi, P. a. (2011). Repeatability of a multi-segment foot protocol in adult subjects. *Gait and Posture*, 133-135.

Carson, M. C. (2001). Kinematic analysis of a multi-segment foot model for research and clinical applications: A repeatability analysis. *Journal of Biomechanics*, 1299-1307.

Chang, B. C., Wang, J. Y., Huang, B. S., Lin, H. Y., & Lee, W. C. (2012). Dynamic impression insole in rheumatoid foot with metatarsal pain. *Clinical Biomechanics*, 196-201.

Chao, C. Y., Zheng, Y.-P., Huang, Y.-P., & Cheing, G. L. (2010). Biomechanical properties of the forefoot plantar soft tissue as measured by an optical coherence tomography-based air-jet indentation system and tissue ultrasound palpation system. *Clinical Biomechanics*, *25*(6), 594-600.

Chapman, G. J. (2016). Comparability of off the shelf foot orthoses in the redistribution of forces in midfoot osteoarthritis patients. *Gait & posture*, 235-240.

Chatzistergos, P. E., Behforootan, S., Allan, D., Naemi, R., & Chockalingam, N. (2018). Shear wave elastography can assess the in-vivo nonlinear mechanical behavior of heel-pad. *Journal of Biomechanics*, 144-150.

Chatzistergos, P. E., Naemi, R., Sundar, L., Ramachandran, A., & Chocklingam, N. (2014). The relationship between the mechanical properties of heel-pad and common clinical measures associated with foot ulcers in patients with diabetes. *Journal of Diabetes and its Complications*, 488-493.

Chen, J. T.-N., Tang, A. C.-W., Hong, W.-H., & Tang, S. F.-T. (2015). The effects of heel-elevated total contact insole on rearfoot pressure reduction in heel injury patients who

had neurosensory impairment after receiving reconstructive flap operations. *Clinical Neurology and Neurosurgery*, 47-52.

Chen, W.-M., Lee, S.-J., & Lee, P. V. (2014). The in vivo plantar soft tissue mechanical property under the metatarsal head: implications of tissues' joint-angle dependent response in foot finite element modeling. *Journal of the Mechanical Behaviour of Biomedical Materials, 40*, 264-274.

Christopher, R. C., Drouin, J. M., & Houglum, P. A. (2006). The influence of a foot orthotic on lower extremity transverse plane kinematics in collegiate female athletes with pes planus. *Journal of Sports Science and Medicine*, 646-655.

Chuto, G., Richelme, E., Cermolacce, C., Nicaud, M., & Puech, B. (2018). *Bone SPECT/CT of Ankle and Foot.* Springer International Publishing.

Claassen, L., Luedtke, P., Yao, D., Ettinger, S., Daniilidis, K., Nowakowski, A., . . . Plaass, C. (2019). The geometrical axis of the talocrural joint-Suggestions for a new measurement of the talocrural joint axis. *Foot and Ankle Surgery*, 371-377.

Clancy NT, N. G. (2010). A new device for assessing changes in skin viscoelasticity using indentation and optical measurement. *Skin Research and Technology*, 210–228.

Colarusso, P., Kidder, L. H., Levin, I. W., & Lewis, N. E. (1999). Raman and Infrared Microspectroscopy. *Encyclopedia of Spectroscopy and Spectrometry*, 1945-1954.

Collier, R. (2011). Orthotics work in mysterious ways. *Canadian Medical Association Journal*, 416-417.

Cornwall, M. W., & McPoil, T. G. (1995). Footwear and foot orthotic effectiveness research: a new approach. *The journal of orthopaedic and sports physical therapy*, 337-44.

Cowley, M. S. (2001). *A multisegment kinematic and kinetic foot model for clinical decision making.* University of Utah.

Crossland, S. R., Sairally, F., Edwards, J., Culmer, P., & Brockett, C. L. (2024). Mechanical characteristics of diabetic and non-diabetic plantar skin. *Journal of the Mechanical Behaviour of Biomedical Materials*.

Cruz, A. B., Radke, M., Haninger, K., & Krüger, J. (2021). How can the programming of impedance control be simplified? *Procedia CIRP*, 266-271.

Curtis, D. J. (2009). Intra-rater repeatability of the Oxford foot model in healthy children in different stages of the foot roll over process during gait. *Gait and Posture*, 118-121.

Dalal, S., Widgerow, A. D., & Evans, G. R. (2015). The plantar fat pad and the diabetic foot – a review. *International Wound Journal*, 636-640.

Davis, R. B. (1991). A gait analysis data collection and reduction technique. *Human Movement Science*, 575-587.

Dawe, E. J., & Davis, J. (2011). Anatomy and biomechanics of the foot and ankle. *Orthopaedics and Trauma*, 279-286.

De Ridder, R. a. (2015). Multi-segment foot landing kinematics in subjects with chronic ankle instability. *Clinical Biomechanics*, 585-592.

Debbi, E. M. (2012). In-shoe center of pressure: indirect force plate vs. direct insole measurement. *The Foot*, 269-275.

Delgado, D. A., Lambert, B. S., Boutris, N., McCulloch, P. C., Robbins, A. B., Moreno, M. R., & Harris, J. D. (2018). Validation of Digital Visual Analog Scale Pain Scoring With a Traditional Paper-based Visual Analog Scale in Adults. *JAAOS: Global Research and Reviews*, 88.

Deschamps, K. a. (2012). Repeatability of a 3D multi-segment foot model protocol in presence of foot deformities. *Gait and Posture*, 635-638.

Deschamps, K. a. (2013). Comparison of foot segmental mobility and coupling during gait between patients with diabetes mellitus with and without neuropathy and adults without diabetes. *Clinical Biomechanics*, 813-819.

Dombroski, C. E., Balsdon, M. E., & Froats, A. (2014). The use of a low cost 3D scanning and printing tool in the manufacture of custom-made foot orthoses: a preliminary study. *British Medical Council Research Notes*.

Du Pasquier, R. A., Blanc, Y., Sinnreich, M., Landis, T., Burkhard, P., & Vingerhoets, F. J. (2003). The effect of aging on postural stability: a cross sectional and longitudinal study. *Clinical Neurophysiology*, 213-218.

Elatter, O., Smith, T., Ferguson, A., Farber, D., & Wapner, K. (2018). Uses of Braces and Orthotics for Conservative Management of Foot and Ankle Disorders. *Foot & Ankle Orthopaedics.*

Emanuel, E. J., Lowell, S. E., Deborah, K. Y., Levinson, J., & Lichter, A. S. (2003). The Costs of Conducting Clinical Research. *Journal of Clinical Oncology*.

Erdemir, A., Viveiros, M. L., Ulbrecht, J. S., & Cavanagh, P. R. (2006). An inverse finite-element model of heel-pad indentation. *Journal of Biomechanics*, *39*(7), 1279–1286.

Eun-tae, J., & Hwi-young, C. (2020). A Novel Method for Gait Analysis on Center of Pressure Excursion Based on a Pressure-Sensitive Mat. *Environmental Research and Public Health*.

Evans AM, R. K. (2022). Foot orthoses for treating paediatric flat feet. *The Cochrane Database of Systematic Reviews*.

Everett, J. S., & Sommers, M. S. (2012). Skin Viscoelasticity: Physiologic Mechanisms, Measurement Issues, and Application to Nursing Science. *Biol Res Nurs*, 338-346.

Excalibur: PDF Table Extraction for Humans. (2024, 05 14). Retrieved from https://excalibur-py.readthedocs.io/en/master/

Faber, J., & Fonseca, L. M. (2014). How sample size influences research outcomes. *Dental press journal of orthodontics*, 27-29.

Fact.MR. (2021). *Market Research Report: Insoles Market.* Fact.MR.

Farzadi, M., Safaeepoor, Z., Mousavi, M. E., & Saeedi, H. (2014). Effect of medial arch support foot orthosis on plantar pressure distribution in females with mild-to-moderate hallux valgus after one month of follow-up. *Prosthetics and Orthotics International*, 134-139.

Fiorentino, N. M., Atkins, P. R., Kutschke, M. J., Goebel, J. M., Foreman, B. K., & Anderson, A. E. (2017). Soft tissue artifact causes significant errors in the calculation of joint angles and range of motion at the hip. *Gait & Posture*, 184-190.

Fong, D. T., Lue, K. B., Chung, M. M., & Chu, V. W. (2020). An individually moulded insole with 5-mm medial arch support reduces peak impact and loading at the heel after a one-hour treadmill run. *Gait & Posture*, 90-95.

Fonseca, M., Bergere, M., Candido, J., Leboeuf, F., Dumas, R., & Armand, S. (2022). The Conventional Gait Model's sensitivity to lower-limb marker placement. *Scientific Reports*.

Fourchet, F., & Gojanovic, B. (2016). Foot core strengthening: Relevance in injury prevention and rehabilitation for runners. *Swiss Sports & Exercise Medicine*, 26-30.

Franklyn-Miller, A., Wilson, C., & Bilzon, J. (2011). Foot orthoses in the prevention of injury in initial military training: a randomized controlled trial. *American Journal of Sports Medicine*, 30-7.

Fukuchi, C. A., Lewinson, R. T., Worobets, J. T., & Stefanyshyn, D. J. (2016). Effects of lateral and medial wedged insoles on knee and ankle internal joint moments during walking in healthy men. *Journal of the American Podiatric Medical Association.*, 411-418.

Garrow, A. P., Papageorgiou , A. C., Silman, A. J., Thomas, E., Jason, M. I., & Macfarlane, G. J. (2000). Development and validation of a questionnaire to assess disabling foot pain. *Pain* , 107-113.

Gefen, A., Megido-Ravid, M., Itzchak, Y., & Arcan, M. (2000). Biomechanical analysis of the three-dimensional foot structure during gait: a basic tool for clinical applications. *Journal of biomechanical engineering*.

Gent, A. N. (1958). On the relation between indentation hardness and Young's modulus. *Institution of Rubber Industry - Transactions*, 46-57.

Giberti, H., Resta, F., Sabbioni, E., Vergani, L., Colombo, C., Verni, G., & Boccafogli, E. (2013). Development of a Bench for Testing Leg Prosthetics. *Conference Proceedings of the Society for Experimental Mechanics Series, 6*, 35-46.

Gibson, K. S., Woodburn, J., Porter, D., & Telfer, S. (2014). Functionally optimized orthoses for early rheumatoid arthritis foot disease: a study of mechanisms and patient experience. *Arthritis care & research.*, 1456–1464.

Goldsmith, M. T., Rasmussen, M. T., Turnbull, T. L., Trindade, C. A., LaPrade, R. F., Philippon, M. J., & Wijdicks, C. A. (2015). Validation of a six degree-of-freedom robotic system for hip in vitro. *Journal of Biomechanics*, 4093-4100.

Goldsmith, M. T., Smith, S. D., Jansson, K. S., LaPrade, R. F., & Wijdicks, C. A. (2014). Characterization of robotic system passive path repeatability during specimen removal and reinstallation for in vitro knee joint testing. *Medical engineering and physics*, 1331-7.

González-Sánchez, M., Ruiz-Muñoz, M., Li, G., & Cuesta-Vargas, A. (2018). Chinese cross-cultural adaptation and validation of the Foot Function Index as tool to measure patients with foot and ankle functional limitations. *Disability and Rehabilitation*.

Grewal, G. S., Baisch, R., Lee-Eng, J., Wu, S., Jarrett, B., Humble, N., & Najafi, B. (2015). Effect of Custom Foot Insoles on Postural Stability in Figure Skaters While on Ice. *Journal of Sport Rehabilitation*.

Gross, M. T., Mercer, V. S., & Feng-Chang, L. (2012). Effects of Foot Orthoses on Balance in Older Adults. *Journal of Orthopaedic & Sports Physical Therapy*, 649-657.

Grujičić, R. (2023, October 30). *Talocalcaneonavicular joint*. Retrieved from Kenhub: https://www.kenhub.com/en/library/anatomy/talocalcaneonavicular-joint

Guo, J. L. (2018). Biomechanical and mechanical behavior of the plantar fascia in macro and micro structures. *Journal of Biomechanics*, 160-166.

Haeun, Y., So Young, E., Yeokyeong, L., Jinah, K., Jihye, L., Jee Chin, T., & Taeyong , L. (2019). Investigation of the relationship between localized cumulative stress and plantar tissue stiffness in healthy individuals using the in-vivo indentation technique. *Journal of the Mechanical Behaviour of Biomedical Materials*, 157-162.

Hajizadeh, M. D. (2020). Can foot orthoses impose different gait features based on geometrical design in healthy subjects? A systematic review and meta-analysis. *The foot*.

Hajizadeh, M., Desmyttere, G., Carmona, J., Bleau, J., & Begon, M. (2020). Can foot orthoses impose different gait features based on geometrical design in healthy subjects? A systematic review and meta-analysis. *The Foot*.

Halstead, J., Chapman, G. J., Gray, J. C., Grainger, A. J., Brown, S., Wilkins, R. A., . . . Redmond, A. C. (2016). Foot orthoses in the treatment of symptomatic midfoot osteoarthritis using clinical and biomechanical outcomes: a randomised feasibility study. *Clinical rheumatology*, 987-996.

Hamerman, D. (1998). Biology of the Aging Joint. *Clinics in Geriatric Medicine, 14*(3), 417-433.

Harlaar, J. (2014). Phases of gait and gait events: Some redefining. *Gait & Posture, 39*, 100-101.

Hart HF, C. K. (2020). Immediate effects of foot orthoses on gait biomechanics in individuals with persistent patellofemoral pain. *Gait Posture*, 20-28.

Hashmi, F., Nester, C., Wright, C., Newton, V., & Lam, S. (2015). Characterising the biophysical properties of normal and hyperkeratotic foot skin. *Journal of foot and ankle research*.

Hawes, M. R., Sovak, D., Miyashita, M., Kang, S. J., Yoshihuku, Y., & Tanaka, S. (1994). Ethnic differences in forefoot shape and the determination of shoe comfort. *Ergonomics*, 187-196.

Hayes, W. K. (1972). A mathematical analysis for. *Journal of Biomechanics*, 541-551.

Headlee, L. D., Leonard, J. L., Hart, J. M., Ingersoll, D. C., & Hertel, J. (2008). Fatigue of the plantar intrinsic foot muscles increases navicular drop. *Journal of Electromyography and kinesiology*, 420-5.

Healthy Step. (2024, 04 29). Retrieved from https://www.healthystep.co.uk/shop/nine-to-five-insoles/nine-to-five-active-insole/

Heinemann, P., & Kasperski, M. (2017). Damping Induced by Walking and Running. *Procedia Engineering*, 2826-2831.

Herbert, R. D., & Gandevia, S. C. (2019). The passive mechanical properties of muscle. *Journal of Applied Physiology*.

Hillstrom, H. J., Song, J., & Kraszewski, A. P. (2013). Foot type biomechanics part 1: structure and function of the asymptomatic foot. *Gait Posture*, 445-451.

Hodge, M. C., Bach, T. M., & Carter, G. M. (1999). Orthotic management of plantar pressure and pain in rheumatoid arthritis. *Clinical Biomechanics*, 567-575.

Hsiao-Yun, C., Yun-Chi, C., Shih-Chung, C., & Chun-Hou, W. (2019). The effectiveness of rearfoot medial wedge intervention on balance for athletes with chronic ankle instability. *Medicine*.

Hsu, C. C., Tsai, W. C., Chen, C. P., Shau, Y. W., Wang, C. L., Chen, M. J., & Chang, K. J. (2005, 10). Effects of aging on the plantar soft tissue properties under the metatarsal heads at different impact velocities. *Ultrasound in Medicine and Biology, 31*, 1423–1429. doi:10.1016/j.ultrasmedbio.2005.05.009

Hsu, C. C., Tsai, W. C., Hsiao, T. Y., Tseng, F. Y., Shau, Y. W., Wang, C. L., & Lin, S. C. (2009, 10). Diabetic effects on microchambers and macrochambers tissue properties in human heel pads. *Clinical Biomechanics, 24*, 682–686. doi:10.1016/j.clinbiomech.2009.06.005

Hsu, T. C., Wang, C. L., Tsai, W. C., Kuo, J. K., & Tang, F. T. (1998). Comparison of the mechanical properties of the heel pad between young and elderly adults. *Archives of Physical Medicine and Rehabilitation, 79*, 1101–1104. doi:10.1016/S0003-9993(98)90178-2

Hsu, W.-H., Lewis, C. L., Monaghan, G. M., Saltzman, E., & Hamill, J. (2014). Orthoses posted in both the forefoot and rearfoot reduce moments and angular impulses on lower extremity joints during walking. *Journal of Biomechanics*, 2618-25.

Huang, J., Qin, Q., & Wang, J. (2020). A Review of Stereolithography: Processes and Systems. *Processes*.

Huerta, J. P., Moreno, J. M., Kirby, K. A., Carmona, F. J., & Garcia, A. M. (2009). Effect of 7-degree rearfoot varus and valgus wedging on rearfoot kinematics and kinetics during the stance phase of walking. *Journal of the American Podiatric Medical Association.*, 415-421.

Hurschler, C., Emmerich, J., & Wülker, N. (2003, 8). In vitro simulation of stance phase gait Part I: Model verification. *Foot and Ankle International, 24*, 614–622. doi:10.1177/107110070302400808

International Organization for Standardization. (1998, April). *Manipulating industrial robots — Performance criteria and related test methods (ISO Standard No. 9283).* Retrieved from https://www.iso.org/standard/22244.html

Ioannou, C. (2024, 04 29). *Exercising Health*. Retrieved from https://www.exercisinghealth.net/blog/how-to-fix-flat-feet

Isvilanonda, V., Li, E. Y., Iaquinto, J. M., & Ledoux, W. R. (2023). Regional differences in the mechanical properties of the plantar aponeurosis. *Journal of Biomechanics*.

Jackson, L., Binning, J., & Potter, J. (2004). Plantar pressures in rheumatoid arthritis using prefabricated metatarsal padding. *Journal of American Podiatric Medical Association*, 239-245.

Jameson, J. R. (2014). *Characterization of Bone Material Properties and Microstructure in Osteogenesis Imperfecta/Brittle Bone Disease.* Marquette University.

Janisse, D. J., & Janisse, E. (2008). Shoe modification and the use of orthoses in the treatment of foot and ankle pathology. *The Hournal of the American Academy of Orthopaedic Surgeons*, 152-8.

Jason M. Weber, L. G. (2005). Calcaneal stress fractures. *Clinics in Podiatric Medicine and Surgery*, 45-54.

Jastifer, J. R. (2023). Intrinsic muscles of the foot: Anatomy, function, rehabilitation. *Physical therapy in sport*, 27-36.

Jiang, X., Napier, C., Hannigan, B., Eng, J. J., & Menon, C. (2020). Estimating Vertical Ground Reaction Force during Walking Using a Single Inertial Sensor. *Sensors*.

Jimenez-Perez, I., Gil-Calvo, M., Aparicio, I., Cibrian Ortiz de Anda, R. M., & Perez-Soriano, P. (2021). Plantar pressure distribution during running with a self-customized foot orthosis in a home microwave. *Journal of Biomechanics*.

Jin, H. X. (2019). Use of 3D-Printed Heel Support Insoles Based on Arch Lift Improves Foot Pressure Distribution in Healthy People. *Medical science monitor : international medical journal of experimental and clinical research*, 7175–7181.

Johnson, L. (2018). *A Biomechanically and Anatomically Realistic Foot Model (BAREFOOT).* Tech. rep. Retrieved from https://digital.lib.washington.edu:443/researchworks/handle/1773/42470

Joshi, A., Kale, S., Chandel, S., & Pal, D. K. (2015). Likert Scale: Explored and Explained. *British Journal of Applied Science & Technology*, 396-403.

Jun-Na, Z., Wang, J., & Yu-Sheng, Q. (2019). Does Flexible Flatfoot Require Treatment?: Plantar Pressure Effects of Wearing Over-the-Counter Insoles when Walking on a Level Surface and Up and Down Stairs in Adults with Flexible Flatfoot. *Journal of the American Podiatric Medical Association*, 299-30.

Jurca, A., Zabkar, J., & Dzeroski, S. (2019). Analysis of 1.2 million foot scans from North America, Europe and Asia. *Scientific Reports*.

Ju-Wen, C., Wen-Chung, T., & Tung-Yang, Y. (2014). Gender-Related Effect of Aging on the Sonographic Appearance of Plantar Fascia. *Journal of Musculoskeletal Pain, 22*(1), 33-37.

Kaalund, S., & Madeleine, P. (2014). Effects of shock-absorbing insoles during transition from natural grass to artificial turf in young soccer players: a randomized controlled trial. *Journal of the American Podiatric Medical Association*, 444-450.

Kadaba, M. P. (1989). Repeatability of kinematic, kinetic, and electromyographic data in normal adult gait. *Journal of Orthopaedic Research*, 849-860.

Kadaba, M. P. (1990). Measurement of lower extremity kinematics during level walking. *Journal of Orthopaedic Research*, 383-392.

Karimi, H. R. (2022). How to deal with the complexity in robotic systems? *Complex Engineering Systems.* .

Keemink, A. Q., van der Kooij, H., & Stienen, A. H. (2018). Admittance control for physical human–robot interaction. *The International Journal of Robotics Research*.

Kelikian, A. S., & Sarrafian, S. K. (2011). *Sarrafian's anatomy of the foot and ankle : descriptive, topographical, functional.* Philadelphia: Wolters Kluwer Health/Lippincott Williams & Wilkins.

Khazzam, M., Long, J. T., Marks, R. M., & Harris, G. F. (2006). Preoperative gait characterization of patients with ankle arthrosis. *Gait & Posture*, 85-93.

Kidder, S. M., Abuzzahab, F. S., Harris, G. F., & Johnson, J. E. (1996). A system for the analysis of foot and ankle kinematics during gait. *IEEE transactions on rehabilitation engineering*.

Kim, E., Cho, H., Jung, T., Kim, S., & Chung, J. (2010). The Biomechanical Comparison of Functional Insoles. *World Congress of Biomechanics*.

Kim, J. H., & Oh, J. H. (2001). Development of an above knee prosthesis using MR damper and leg simulator. *Proceedings - IEEE International Conference on Robotics and Automation, 4*, pp. 3686–3691. doi:10.1109/ROBOT.2001.933191

Kim, K.-J., Kitaoka, H. B., Luo, Z.-P., Ozeki, S., Berglund, L. J., Kaufman, K. R., & An, K.-N. (2001, 5). In vitro simulation of the stance phase in human gait . *Journal of Musculoskeletal Research, 05*, 113–121. doi:10.1142/s0218957701000490

Kim, Y. S., Koh, M., Hwang, D. G., Han, J. J., & Lee, T. (2016). Prediction of plantar soft tissue stiffness based on gender. age, bodyweight, height and body mass. *Foot and Ankle Surgery, 22*(2), 42-43.

Klaesner, J. W., Commean, P. K., Hastings, 3. K., Zou, D., & Mueller, M. J. (2001). Accuracy and reliability testing of a portable soft tissue indentor. *IEEE Transactions on Neural Systems and Rehabilitation Engineering, 9*, 232–240. doi:10.1109/7333.928583

Klaesner, J. W., Commean, P. K., Hastings, M. K., Zou, D., & Mueller, M. J. (2001). Accuracy and reliability testing of a portable soft tissue indentor. *IEEE Transactions on Neural Systems and Rehabilitation Engineering, 9*, 232–240. doi:10.1109/7333.928583

Klein, T., Chapman, G. J., Lastovicka, O., Janura, M., & Richards, J. (2022). Do different multi-segment foot models detect the same changes in kinematics when wearing foot orthoses?. *Journal of Foot & Ankle Research*.

Kogler, G. F. (1996). Biomechanics of longitudinal arch support mechanisms in foot orthoses and their effect on plantar aponeurosis strain. *Clinical Biomechanics*, 243-252.

Kouchi, M. (1998). Foot dimensions and foot shape: Differences due to growth, generation and ethnic origin. *Journal of Anthropological Sciences*, 161-188.

Kribus-Shmiel, L., Zeilig, G., Sokolovski, B., & Plotnik, M. (2018). How many strides are required for a reliable estimation of temporal gait parameters? Implementation of a new algorithm on the phase coordination index. *Public Library of Science*.

Kroneberg, D., Elshehabi, M., Meyer, A.-C., Doss, S., Kühn, A., Maetzler, W., & Schmitz-Hübsch, T. (2017). How many steps are enough? Assessment of gait variability in realistically confined clinical settings. *Basal Ganglia*, 3-4.

Kwan, R. L., Zheng, Y. P., & Cheing, G. L. (2010, 7). The effect of aging on the biomechanical properties of plantar soft tissues. *Clinical Biomechanics, 25*, 601–605. doi:10.1016/j.clinbiomech.2010.04.003

Landorf, K. K. (2001). Foot orthosis prescription habits of Australian and New Zealand podiatric physicians. *Journal of the American Podiatric Medical Association*, 174-183.

Laribi , M., & Zeghloul, S. (2020). *Design and Operation of Human Locomotion Systems.* Academic Press.

Leardini, A. a. (1999). An anatomically based protocol for the description of foot segment kinematics during gait. *Clinical Biomechanics*, 528-536.

Ledoux, W. R., & Blevins, J. J. (2007). The compressive material properties of the plantar soft tissue. *Journal of Biomechanics, 40*(13), 2975–2981.

Ledoux, W. R., Rohr, E. S., Ching, R. P., & Sangeorzan, B. J. (2006). Effect of foot shape on the three-dimensional position of foot bones. *Journal of Orthopaedic Research*, 2176-2186.

Lee, S., & Kim, Y. J. (2012). Effects of Sampling Rates on Knee Kinematics and Kinetics during Single-leg landing. *Orthopaedic Research Society*.

Li, K., Zhang, Y., Wei, S., & Yue, H. (2018). Evolutionary Algorithm-Based Friction Feedforward Compensation for a Pneumatic Rotary Actuator Servo System. *Applied sciences*, 1623.

Liu, A., Nester, C. J., Jones, R. K., Lundgren, P., Lundberg, A., Arndt, A., & Wolf, P. (2012). Effect of an antipronation foot orthosis on ankle and subtalar kinematics. *Medicine & Science in Sports & Exercise*, 2384-2391.

Liu, H., Holt, C., & Evans, S. (2007). Accuracy and repeatability of an optical motion analysis system for measuring small deformations of biological tissues. *Journal of Biomechanics*, 210-4.

Logan, B. M., Sardesai, A. M., Daivajna, S., Robinson, A. H., & Hutchings, R. T. (2012). *McMinn's color atlas of foot and ankle anatomy.* Philadelphia: Elsevier/Saunders.

Lopes, L. R., Silva, A. F., & Carneiro, O. S. (2018). Multi-material 3D printing: The relevance of materials affinity on the boundary interface performance. *Additive Manufacturing*, 45-52.

M. F. Leyva-Mendivil, A. P. (2015). A mechanistic insight into the mechanical role of the stratum corneum during stretching and compression of the skin. *J. Mech. Behav. Biomed. Mater.* , 197-219.

Ma, C. Z., Wong, D. W., Lam, W. K., & Wan, A. H. (2016). Balance improvement effects of biofeedback systems with state-of-the-art wearable sensors: A systematic review. *Sensors*, 434.

Ma, C. Z.-H., Wong, D. W.-C., Wan, A. H.-P., & Lee, W. C.-C. (2018). Effects of orthopedic insoles on static balance of older adults wearing thick socks. *Prosthetics and orthotics international*, 357-62.

MacWilliams, B. A. (2003). Foot kinematics and kinetics during adolescent gait. *Gait and Posture*, 214-224.

Maghsoudi-Ganjeh, M., Wang, X., & Zeng, X. (2020). Nanomechanics and Ultrastructure of Bone: A Review. *Computer Modeling in Engineering & Sciences*, *125*(1), 1-32.

Mahaffey, R. a. (2013). Evaluation of multi-segmental kinematic modelling in the paediatric foot using three concurrent foot models. *Journal of Foot and Ankle Research*, 43.

Maithani, H., Ramon, J. A., & Mezouar, Y. (2019). Predicting Human Intent for Cooperative Physical Human-Robot. *IEEE 15th International Conference on Control and Automation (ICCA)* (pp. 1523-1528). Edinburgh: IEEE.

Marinelli, C., Giberti, H., & Resta, F. (2017). In vitro test method for the development of intelligent lower limb prosthetic devices. *Biocybernetics and Biomedical Engineering*, *37*, 11–23. doi:10.1016/j.bbe.2016.10.003

Martijn, H. A., Sierevelt, I. N., Wassink, S., & Nolte, P. A. (2023). Translation and Validation of 'Foot Health Status Questionnaire' in Dutch. *The Journal of foot and ankle surgery*, 31-34.

Mashiko, T., Konno, T., Kaneko, N., & Watanabe, E. (2015). Training in Brain Retraction Using a Self-Made Three-Dimensional Model. *World Neurosurgery*, 585-590.

Matt Appleton. (2024, 04 29). Retrieved from https://www.mattappleton.com.au/midfoot-foot-pain

Mckeon, P. O., & Fourchet, F. (2015). Freeing the foot: integrating the foot core system into rehabilitation for lower extremity injuries. *Clinics in sports medicine*, 347-61.

McKeon, P. O., Hertel, J., Bramble, D., & Davis, I. (2015). The foot core system: A new paradigm for understanding intrinsic foot muscle function. *British Journal of Sports Medicine*, *49*(5), 290.

Meaney, D. F. (2005). A Quasi-Linear, Viscoelastic, Structural Model of the Plantar Soft Tissue With Frequency-Sensitive Damping Properties . *Journal of Biomechanical Engineering*, *126*(6), 831 -.

Medicines & Healthcare products Regulatory Agency. (2002). Medical devices: legal requirements for specific medical products. Uk Government.

Mehta, B. V., Rajani, S., & Sinha, G. (1997). Comparison of image processing techniques (magnetic resonance imaging, computed tomography scan and ultrasound) for 3D modeling and analysis of the human bones. *Journal of Digital Imaging*, 203-6.

Melai, T., Herman, I. T., Schaper, N. C., de Lange, T. L., Willems, P. J., Meijer, K., . . . Savelberg, H. H. (2011). Calculation of plantar pressure time integral, an alternative approach. *Gait & Posture*, 379-383.

Melchels, F. P., Feijan, J., & Grijpma, D. W. (2010). A Review on Stereolithography and its Applications in Biomedical Engineering. *Biomaterials*, 6121-30.

Menz, H. (2015, 7). Biomechanics of the Ageing Foot and Ankle: A Mini-Review. *61*, 381–388. doi:10.1159/000368357

Menz, H. B., Auhl, M., Ristevski, S., Frescos, N., & Munteanu, S. E. (2014). Comparison of the responsiveness of the Foot Health Status Questionnaire and the Manchester Foot Pain and Disability Index in older people. *Health and Quality of Life Outcomes*.

Miller-Young, J. E., Duncan, N. A., & Baroud, G. (2002). Material properties of the human calcaneal fat pad in compression: experiment and theory. *Journal of Biomechanics*, 1523-1531.

Mo, F., Li, J., Yang, Z., Zhou, S., & Behr, M. (2019, 12). In Vivo Measurement of Plantar Tissue Characteristics and Its Indication for Foot Modeling. *Annals of Biomedical Engineering*, *47*, 2356–2371. doi:10.1007/s10439-019-02314-0

Molodov, D. A. (2013). *Microstructural Design of Advanced Engineering Materials.* Wiley-VCH.

Mombaur, K. D., Bock, H. G., Schlöder, J. P., & Longman, R. W. (2005). Open-loop stable solutions of periodic optimal control problems in robotics. *Journal of Applied Mathematics and Mechanics*, 499-515.

Mombaur, K., Longman, R., Bock, H., & Schlöder, J. (2005). Open-loop stable running. *Robotica*, 21-33.

Mootanah, R., Song, J., & Lenhoff, M. (2013). Foot type biomechanics part 2: are structure and anthropometrics related to function? *Gait Posture*, 452-456.

Morgan, E. F., Unnikrisnan, G. U., & Hussein, A. I. (2018). Bone Mechanical Properties in Healthy and Diseased States . *Annual Review of Biomedical Engineering, 20*, 119-143.

Morio, C., Lake, M. J., Guéguen, N., Rao, G., & Baly, L. (2009). The influence of footwear on foot motion during walking. *Journal of Biomechanics*, 2081-2088.

Morrison T, J. S. (2021). Reliability of ultrasound in evaluating the plantar skin and fat pad of the foot in the setting of diabetes. *PLoS One.*

Myers, K. A. (2004). Validation of a Multisegment Foot and Ankle Kinematic Model for Pediatric Gait. *IEEE Transactions on Neural Systems and Rehabilitation Engineering*, 122-130.

Naemi, R. B. (2015). Viscoelasticity in Foot-Ground Interaction. In M. F. El-Amin, *Viscoelastic and Viscoplastic Materials.* InTech.

Natali, A., Forestiero, A., Carniel, E., & Pavan, P. (2010). Investigation of foot plantar pressure: experimental and numerical analysis. *Medical & biological engineering & computing, 48*(12), 1167–1174.

Nester, C. J. (2009). Lessons from dynamic cadaver and invasive bone pin studies: do we know how the foot really moves during gait? *Journal of Foot and Ankle Research*.

Nester, C. J., Liu, A. M., Ward, E., Howard, D., Cocheba, J., Derrick, T., & Patterson, P. (2007). In vitro study of foot kinematics using a dynamic walking cadaver model. *Journal of Biomechanics, 40*, 1927–1937. doi:10.1016/j.jbiomech.2006.09.008

Nester, C., Jarvis, H., Jones, R. K., Bowden, P., & Liu, A. (2014). Movement of the human foot in 100 pain free individuals aged 18–45: implications for understanding normal foot function. *Journal of Foot and Ankle Research, 7*.

Neumann, E. E., Owings, T. M., Schimmoeller, T., Nagle, T. F., Colbrunn, R. W., Landis, B., . . . Erdemir, A. (2018, 9). Data descriptor: Reference data on thickness and

mechanics of tissue layers and anthropometry of musculoskeletal extremities. *Scientific Data, 5*, 1–10. doi:10.1038/sdata.2018.193

Ng, T. K., Zheng, Y. P., Kwan, R. L., & Cheing, G. L. (2015, 2). An innovative ultrasound foot scanner system for measuring the change in biomechanical properties of plantar tissue from sitting to standing. *International Journal of Rehabilitation Research, 38*, 68–73. doi:10.1097/MRR.0000000000000097

Niu, W., Wang, L., Feng, T., & Jiang, C. (2014). Effects of Bone Young's Modulus on Finite Element Analysis in the Lateral Ankle Biomechanics. *Applied Bionics and Biomechanics*, 189-195.

Nobili, C. O., Mannacio, E., Ciccarelli, A., Tajani, F., & Ripani, M. (2017). Analysis of modifications of the plantar parameters after the use of a proprioceptive insole: regular gait. *The journal of sports medicine and physical fitness*, 65-70.

Noble, L. D., Colbrunn, R. W., Lee, D. G., Van Den Bogert, A. J., & Davis, B. L. (2010, 2). Design and validation of a general purpose robotic testing system for musculoskeletal applications. *Journal of Biomechanical Engineering, 132*. doi:10.1115/1.4000851

Noginova, J. (2021). *Subtalar Joint Definition in Biomechanical Models.* Old Dominion University.

Novak, A. a. (2009). Gait changes following botulinum toxin a treatment in stroke. *Topics in Stroke Rehabilitation*, 367-376.

Novak, A. C. (2014). Gait analysis for foot and ankle surgeons - Topical review, part 2: Approaches to multisegment modelling of the foot. *Foot and Ankle International*, 178-191.

Nüchter, A. (2009). *3D Robotic Mapping: The Simultaneous Localization and Mapping Problem with Six Degrees of Freedom.* Berlin: Springer.

O'Leary, K., Vorpahl, K. A., & Heiderscheit, B. (2012). Effect of cushioned insoles on impact forces during running. *Journal of the American Podiatric Medical Association*, 503-508.

Oosterwaal, M., Carbes, S., Telfer, S., Woodburn, J., Torholm, S., Al-Munajjed, A. A., . . . Meijer, K. (2016). The Glasgow-Maastricht foot model, evaluation of a 26 segment kinematic model of the foot. *Journal of Foot and Ankle Research*.

Orvitz, K. (2015). Feet Hurt? *Chilton's industrial safety & hygiene news*, 54.

Pai, S., & Ledoux, W. R. (2010, 6). The compressive mechanical properties of diabetic and non-diabetic plantar soft tissue. *Journal of Biomechanics, 43*, 1754–1760. doi:10.1016/j.jbiomech.2010.02.021

Pai, S., & Ledoux, W. R. (2010). The compressive mechanical properties of diabetic and non-diabetic plantar soft tissue. *Journal of Biomechanics*, 1754-1760.

Palomo-Fernández, I., Martín-Casado, L., Marcos-Tejedor, F., Aldana-Caballero, A., Rubio-Arias, J., & Jiménez-Díaz, F. (2023). Lateral wedge insoles and their use in ankle instability. *Scandinavian Journal of Medicine & Science in Sports*, 1716-1725.

Pamungkas, D. S., Caesarendra, W., Soebakti, H., Analia, R., & Susanto, S. (2019). Overview: Types of Lower Limb Exoskeletons. *Electronics*, 1283.

Panichawit C, B. S. (2015). Effects of Foot Muscles Training on Plantar Pressure Distribution during Gait, Foot Muscle Strength, and Foot Function in Persons with Flexible Flatfoot. *J Med Assoc Thai*.

Papegaaij, S., & Steenbrink, F. (2017). *Clinical gait analysis: Treadmill-based vs overground.* Motek.

Parker, D. (2013, 6). Characterising the biomechanical properties of the plantar soft tissue under the conditions of simulated gait.

Parker, D., Andrews, J., & Price, C. (2023). Validity and reliability of the XSENSOR in-shoe pressure measurement system. *Public Library of Science*.

Partovifar, M., Safaeepour, Z., & Cham, M. B. (2021). The effect of pre-fabricated insole on plantar pressure distribution in patients with rheumatoid arthritis. *The Foot*.

Passmore, E. a. (2016). Defining the medial-lateral axis of an anatomical femur coordinate system using freehand 3D ultrasound imaging. *Gait and Posture*, 211-216.

Paterson, K. L., Hinman, R. S., Metcalf, B. R., McManus, F., Jones, S. E., Menz, H. B., . . . Bennell, K. L. (2022). Effect of foot orthoses vs sham insoles on first metatarsophalangeal joint osteoarthritis symptoms: a randomized controlled trial. *Osteoarthritis and Cartilage*, 956-964.

Patpatiya, P., Chaudhary, K., Shastri, A., & Sharma, S. (2022). A review on polyjet 3D printing of polymers and multi-material structures. *Proceedings of the Institution of Mechanical Engineers, Part C: Journal of Mechanical Engineering Science*.

Pawelka, S., Kopf, A., Zwick, E. B., Bhm, T., & Kranzl, A. (1997). Comparison of two insole materials using subjective parameters and pedobarography (pedar-system). *Clinical Biomechanics*, s6-s7.

Peeters, K., Natsakis, T., Burg, J., Spaepen, P., Jonkers, I., Dereymaeker, G., & Vander Sloten, J. (2013). An in vitro approach to the evaluation of foot-ankle kinematics: Performance evaluation of a custom-built gait simulator. *Proceedings of the Institution of Mechanical Engineers*.

Peters, A. a. (2012). A comparison of hip joint centre localisation techniques with 3-DUS for clinical gait analysis in children with cerebral palsy. *Gait and Posture*, 282-286.

Plooij, M., Wolfslag, W., & Wisse, M. (2015). Robust feedforward control of robotic arms with friction model uncertainty. *Robotics and Autonomous Systems*, 83-91.

Podiatry Station. (2024, 04 29). Retrieved from https://podiatrystation.com/the-5-benefits-of-custom-made-casted-orthotics/

Pollock, A. S., Durward, B. R., & Rowe, P. J. (2000). What is balance? *Clinical Rehabilitation*, 402-406.

Portinaro, N. a. (2014). Modifying the Rizzoli foot model to improve the diagnosis of pes-planus: Application to kinematics of feet in teenagers. *Journal of Foot and Ankle Research*.

Postema, K., Burm, P. E., Zande, v., & Limbeek, J. v. (1998). The influence of a custom moulded insole and a rockerbar on plantar pressure. *Prosthetics and Orthotics International*, 35-44.

Powell, D. W. (2013). A comparison of two multisegment foot models in Highand low-arched athletes. *Journal of the American Podiatric Medical Association*, 99-105.

Prisk, V. R., Imhauser, C. W., O'Loughlin, P. F., & Kennedy, J. G. (2010, 10). Lateral ligament repair and reconstruction restore neither contact mechanics of the ankle joint nor motion patterns of the hindfoot. *Journal of Bone and Joint Surgery - Series A, 92*, 2375–2386. doi:10.2106/JBJS.I.00869

Qi, H. J., Joyce, K., & Boyce, M. C. (2003). Durometer hardness and the stress-strain behaviour of elastomeric materials. *Rubber chemistry and technology*, 419-435.

Qian Z, J. Z. (2021). Morphology and Mechanical Properties of Plantar Fascia in Flexible Flatfoot: A Noninvasive In Vivo Study. *Front Bioeng Biotechnol*.

Qian, Z., Jiang, Z., Wu, J., Chang, F., Liu, J., Ren, L., & Ren, L. (2021). Morphology and Mechanical Properties of Plantar Fascia in Flexible Flatfoot: A Noninvasive In Vivo Study. *Frontiers in Bioengineering and Biotechnology*.

Qian, Z., Ren, L., Ding, Y., Hutchinson, J. R., & Ren, L. (2013). A Dynamic Finite Element Analysis of Human Foot Complex in the Sagittal Plane during Level Walking. *Public Library of Science*.

Qiu, F., Cole, M. H., Davids, K. W., Hennig, E. M., Silburn, P. A., Netscher, H., & Kerr, G. K. (2013). Effects of textured insoles on balance in people with Parkinson's disease. *The Public Library of Science*.

Qiu-Qiong, S., Pui-Ling, L., Kit-Lun, Y., Jiao, J., & Qi-Long, L. (2022). Influence of Contoured Insoles with Different Materials on Kinematics and Kinetics Changes in Diabetic Elderly during Gait. *International journal of environmental research and public health*, 12502.

Raffalt, P. C., McCamley, J., Denton, W., & Yentes, J. M. (2019). Sampling frequency influences sample entropy of kinematics during walking. *Medical & Biological Engineering & Computing*, 759-764.

Rasenberg, N. R. (2018). Efficacy of foot orthoses for the treatment of plantar heel pain: A systematic review and meta-analysis. *British Journal of Sports Medicine*.

Reddy, A. H., Davuluri, S., & Boyina, D. (2020). 3D Printed Lattice Structures: A Brief Review. *IEEE International Conference on "Nanomaterials: Applications & Properties"*.

Redmond, A. C., Landorf, K. B., & Keenan, A.-M. (2009). Contoured, prefabricated foot orthoses demonstrate comparable mechanical properties to contoured, customised foot orthoses: a plantar pressure study. *Journal of foot and ankle research*, 20.

Richards, J. G. (1999). The measurement of human motion: A comparison of commercially available systems. *Human Movement Science*, 589-602.

Richter, H., Simon, D., Smith, W. A., & Samorezov, S. (2015, 1). Dynamic modeling, parameter estimation and control of a leg prosthesis test robot. *Applied Mathematical Modelling, 39*, 559–573. doi:10.1016/j.apm.2014.06.006

Rizzo, D. C. (2015). *Fundamentals of anatomy & physiology*. Cengage Learning.

Robb, K. A., & Perry, S. D. (2020). Textured Foot Orthotics on Dynamic Stability and Turning Performance in Parkinson's Disease. *Journal of motor behaviour*, 396-403.

Rome K, C. H. (2017). Clinical effectiveness and cost-effectiveness of foot orthoses for people with established rheumatoid arthritis: an exploratory clinical trial. *Scandinavian Journal of Rheumatology*, 187-193.

Rome, K., & Brown, C. L. (2004). Randomized clinical trial into the impact of rigid foot orthoses on balance parameters in excessively pronated feet. *Clinical Rehabilitation*, 624-30.

Sangeux, M. a. (2011). Hip joint centre localization: Evaluation on normal subjects in the context of gait analysi. *Gait and Posture*, 324-328.

Sangeux, M. a. (2014). Which method of hip joint centre localisation should be used in gait analysis? *Gait and Posture*, 20-25.

Sauret, C. a. (2016). On the use of knee functional calibration to determine the medio-lateral axis of the femur in gait analysis: Comparison with EOS biplanar radiographs as reference. *Gait and Posture*, 180-184.

Schallig, W., van den Noort, J., Maas, M., Harlaar, J., & van der Krogt, M. M. (2021). Marker placement sensitivity of the Oxford and Rizzoli foot models in adults and children. *Journal of Biomechanics*.

Schimmoeller, T., Neumann, E. E., Owings, T. M., Nagle, T. F., Colbrunn, R. W., Landis, B., . . . Erdemir, A. (2020, 12). Reference data on in vitro anatomy and indentation response of tissue layers of musculoskeletal extremities. *Scientific Data, 7*, 1–10. doi:10.1038/s41597-020-0358-1

Scholl products. (2024, 05 16). Retrieved from Scholl: https://www.scholl.co.uk/products/scholl-lower-back-pain-relief-insoles-1

Sharkey, N. A., & Hamel, A. J. (1998, 9). A dynamic cadaver model of the stance phase of gait: Performance characteristics and kinetic validation. *Clinical Biomechanics*, *13*, 420–433. doi:10.1016/S0268-0033(98)00003-5

Shiba, N., Kitaoka, H. B., Cahalan, T. D., & Chao, E. (1995). Shock-absorbing effect of shoe insert materials commonly used in management of lower extremity disorders. *Clinical Orthopaedics and Related Research*, 130-136.

Shibuya, N., Kitterman, R., & Jupiter, D. C. (2013). Evaluation of the Rearfoot Component (Module 3) of the ACFAS Scoring Scale. *The Journal of Foot & Ankle Surgery*.

Shimaa Shehata, M. M.-H. (2022). Foot Anatomy. *NeuroQuantology*, 236-238.

Shoemaker, P. (1978). *Measurements of Relative Lower Body Segment Positions in Gait Analysis.* University of California.

Siciliano, B., & Khatib, O. (2017). Force Control. In *Springer Handbook of Robotics* (pp. 161-185). Springer International Publishing.

Siciliano, B., & Luigi, V. (2000). From Indirect to Direct Force Control: A Roadmap for Enhanced Industrial Robots. *Robotica*.

Siciliano, B., & Villani, L. (1999). Indirect Force Control. In *Robot Force Control.* Springer, Boston: The Springer International Series in Engineering and Computer Science.

Siegler, S., Block, J., & Schneck, C. D. (1988). The Mechanical Characteristics of the Collateral Ligaments of the Human Ankle Joint. *Foot & Ankle International, 8*(5), 234-242.

Simonsen MB, N.-A. K.-P. (2022). The effect of foot orthoses on gait biomechanics and pain among people with rheumatoid arthritis: A quasi-experimental study. . *Gait Posture*, 121-128.

Sirinterlikci, A., Tiryakioğlu, M., Bird, A., Harris, A., & Kweder, K. (2009). Repeatability and Accuracy of an Industrial Robot: Laboratory Experience for a Design of Experiments Course. *Technology Interface Journal*.

Snow SW, B. W. (1995). Anatomy of the Achilles Tendon and Plantar Fascia in Relation to the Calcaneus in Various Age Groups. *Foot & Ankle International*, 418-421.

Son, M., & Latt, D. (2019). Hindfoot Bone Viscoelasticity and Stress Relaxation. *Foot & Ankle Orthopaedics*.

Son, M., & Munroe, B. (2018). Viscoelastic Properties of the Hindfoot Bones. *Foot & Ankle Orthopaedics*.

Song, Q., Xu, K., Yu, B., Zhang, C., Sun, W., & Mao, D. (2015). Could Insoles Offload Pressure? An Evaluation of the Effects of Arch-supported Functional Insoles on Plantar Pressure Distribution during Race Walking. *Research in Sports Medicine*, 278-288.

Springett, K. p., Otter, S., & Barry, A. (2007). A clinical longitudinal evaluation of pre-fabricated, semi-rigid foot orthoses prescribed to improve foot function. *The Foot*, 184-189.

Stebbins, J. a. (2006). Repeatability of a model for measuring multi-segment foot kinematics in children. *Gait and Posture*, 401-410.

Stecco, C., Corradin, M., Macchi, V., Morra, A., Porzionato, A., Biz, C., & De Caro, R. (2013). Plantar fascia anatomy and its relationship with Achilles tendon and paratenon. *Jounral of Anatomy*, 665-676.

Strzalkowski, D. N., Triano, J. J., Lam, C. K., Templeton, C. A., & Bent, L. R. (2015). Thresholds of skin sensitivity are partially influenced by mechanical properties of the skin on the foot sole. *Physiological Reports, 3*(6).

Sun, J. H., Cheng, B. K., Zheng, Y. P., Huang, Y. P., Leung, J. Y., & Cheing, G. L. (2011, 9). Changes in the thickness and stiffness of plantar soft tissues in people with diabetic peripheral neuropathy. *Archives of Physical Medicine and Rehabilitation, 92*, 1484–1489. doi:10.1016/j.apmr.2011.03.015

Sutherland, D. a. (1972). Measurement of gait movements from motion picture film. *Journal of Bone and Joint Surgery*, 787-797.

Tahmasebi, R., Mohammad, K. T., Behnaz, S., & Francis, F. (2015). Evaluation of standing stability in individuals with flatfeet. *Foot and ankle specialist*, 168-74.

Tahririan, M. A. (2012). Plantar fasciitis. *Journal of research in medical sciences : the official journal of Isfahan University of Medical Sciences*, 799-804.

Tarrade, T., Doucet, F., Saint-Lo, N., Llari, M., & Behr, M. (2019). Are custom-made foot orthoses of any interest on the treatment of foot pain for prolonged standing workers?. *Applied Ergonomics*, 130-135.

Taş, S., & Çetin, A. (2019). An investigation of the relationship between plantar pressure distribution and the morphologic and mechanic properties of the intrinsic foot muscles and plantar fascia⋆. *Gait & Posture*, 217-221.

Tavares C, D. M.-N. (2018). Gait Shear and Plantar Pressure Monitoring: A Non-Invasive OFS Based Solution for e-Health Architectures. *Sensors (Basel)*.

Telfer, S., Abbott, M., Steultjens, M. P., & Woodburn, J. (2013). Dose–response effects of customised foot orthoses on lower limb kinematics and kinetics in pronated foot type. *Journal of Biomechanics*, 1489-1495.

Telfer, S., Woodburn, J., Collier, A., & Cavanagh, P. R. (2017). Virtually optimized insoles for offloading the diabetic foot: A randomized crossover study. *Journal of biomechanics.*, 157-161.

Teng, Z.-L., Yang, X.-G., Geng, X., Gu, Y.-J., Huang, R., Chen, W.-M., . . . Ma, X. (2022). Effect of loading history on material properties of human heel pad: an in-vivo pilot investigation during gait. *BMC Musculoskeletal Disorders*.

Tenten-Diepenmaat, M. D. (2019). Systematic review on the comparative effectiveness of foot orthoses in patients with rheumatoid arthritis. *Journal of Foot and Ankle Research*.

Teoh, J. C., Lim, Y. B., & Lee, T. (2015). Minimum indentation depth for characterization of 2nd sub-metatarsal head and heel pad tissue properties. *Journal of Biomechanics, 48*(10), 2096-2101.

Teoh, J. C., Shim, V. P., & Lee, T. (2014, 9). Quantification of plantar soft tissue changes due to aging in various metatarsophalangeal joint angles with realistic tissue deformation. *Journal of Biomechanics, 47*, 3043–3049. doi:10.1016/j.jbiomech.2014.06.033

Ting-Ting, W., Shin-Liang, L., Hui, C., Jeng-Sheng, Y., & Hsien-Te, P. (2022). Arch-Support Insoles Benefit the Archery Performance and Stability of Compound Archers. *International journal of environmental research and public health*.

Todros, S., Biz, C., Ruggieri, P., & Pavan, P. G. (2021). Experimental Analysis of Plantar Fascia Mechanical Properties in Subjects with Foot Pathologies. *Applied Sciences*.

Tong, J., Lim, C. S., & Goh, O. L. (2003, 6). Technique to study the biomechanical properties of the human calcaneal heel pad. *Foot, 13*, 83–91. doi:10.1016/S0958-2592(02)00149-9

Tran, K., & Spry, C. (2019). Custom-Made Foot Orthoses versus Prefabricated foot Orthoses: A Review of Clinical Effectiveness and Cost-Effectiveness. *Canadian Agency for Drugs and Technologies in Health*.

Tran, T. T., Nguyen, T. V., Dinh, T. T., & Tran, M. V. (2023). Development of a prototype 6 degree of freedom robot arm. *Results in Engineering*.

Tse, C. T., Ryan, M. B., Dien, J., Scott, A., & Hunt, M. A. (2021). An exploration of changes in plantar pressure distributions during walking with standalone and supported lateral wedge insole designs. *Journal of Foot and Ankle Research*, 1-11.

Turpin, K. M., De Vincenzo, A., Apps, A. M., Cooney, T., MacKenzie, M. D., Chang, R., & Hunt, M. A. (2012). Biomechanical and Clinical Outcomes With Shock-Absorbing Insoles in Patients With Knee Osteoarthritis: Immediate Effects and Changes After 1 Month of Wear. *Archives of Physical Medicine and Rehabilitation*, 503-508.

Understanding health research. (2023, January 11). Retrieved from UK Research and Innovation: https://www.ukri.org/councils/mrc/facilities-and-resources/find-an-mrc-facility-or-resource/mrc-regulatory-support-centre/understanding-health-research/ethical-approval/#:~:text=All%20studies%20which%20will%20involve,and%20wellbeing%20of%20research%20part

Verdini, F., Marcucci, M., Benedetti, M. G., & Leo, T. (2006). Identification and characterisation of heel strike transient. *Gait & Posture*, 77-84.

Vulović, A. Z., & Filipovic, N. (2020). The biomechanics of lower human extremities. In N. Filipovic, *Computational Modeling in Bioengineering and Bioinformatics* (pp. 179-210). Academic Press.

Wahmkow, G., Cassel, M., Mayer, F., & Baur, H. (2017). Effects of different medial arch support heights on rearfoot kinematics. *Public Library of Science*.

Wahmkow, G., Cassel, M., Mayer, F., & Baur, H. (2017). Effects of different medial arch support heights on rearfoot kinematics. *PLoS One*.

Walha, R. D. (2022). The effects of custom-made foot orthoses on foot pain, foot function, gait function, and free-living walking activities in people with psoriatic arthritis (PsA): a pre-experimental trial. . *Arthritis Research & Therapy*.

Wang, C.-L., Cheng, C.-K., Tsuang, Y.-H., Hang, Y.-S., & Liu, T.-K. (1994). Cushioning effect of heel cups. *Clinical Biomechanics*, 297-302.

Wang, D., Wang, W., Guo, Q., Shi, G., Zhu, G., Wang, X., & Liu, A. (2020, 10). Design and validation of a foot–ankle dynamic simulator with a 6-degree-of-freedom parallel mechanism. *Proceedings of the Institution of Mechanical Engineers, Part H: Journal of Engineering in Medicine, 234*, 1070–1082. doi:10.1177/0954411920938902

Wang, K., Raychoudhury, S., Hu, D., Ren, L., Liu, J., Xiu, H., . . . Qian, Z. (2021). The Impact of Locomotor Speed on the Human Metatarsophalangeal Joint Kinematics. *Frontiers in Bioengineering and Biotechnology*.

Wang, X. &.-F. (2012). A study of foot and ankle kinematics during stance phase of normal walking. *International Journal of Computer Applications in Technology*, 126-138.

Wang, Y., Li, Z., & Zhang, M. (2014). Biomechanical study of tarsometatarsal joint fusion using finite element analysis. *Medical Engineering and Physics*, 1394-400.

Wearing, S. C., Hooper, S. L., Dubois, P., Smeathers, J. E., & Dietze, A. (2014). Force-deformation properties of the human heel pad during barefoot walking. *Medicine and Science in Sports and Exercise, 46*, 1588–1594. doi:10.1249/MSS.0000000000000281

Wearing, S. C., Smeathers, J. E., Yates, B., Urry, S. R., & Dubois, P. (2009). Bulk compressive properties of the heel fat pad during walking: A pilot investigation in plantar heel pain. *Clinical Biomechanics*, 397-402.

Wendland, D. M., & Sprigle, S. H. (2018). The Characterization of Plantar Skin Across Environmental Condition and Time. *Adv Skin Wound Care*, 123-129.

West, M. (1993). The principles of dose limitation and the various means of dose reduction to the patient, including protection of the gonads, in Wootton R (ed). *Radiation Protection of Patients*, 5865.

Whittaker, G. L. (2020). Predictors of response to foot orthoses and corticosteroid injection for plantar heel pain. *Journal of Foot and Ankle Research*.

Whittle, M. W. (2014). *Gait Analysis: An Introduction.* Butterworth-Heinemann.

William R Ledoux, H. J. (2002). The distributed plantar vertical force of neutrally aligned and pes planus feet . *Gait & posture, 1*, 1-9.

Williamson, A., & Hoggart, B. (2005). Pain: a review of three commonly used pain rating scales. *Journal of Clinical Nursing*, 798-804.

Windle, C., Gregory, S., & Dixon, S. (1999). The shock attenuation characteristics of four different insoles when worn in a military boot during running and marching. *Gait and Posture*, 31-37.

Winiarski, T., & Woźniak, A. (2012). Indirect force control development procedure. *Robotica*, 465-478.

Winson, I. G. (1995). Metatarsal motion. *The Foot*, 91-94.

Withnall, R., Eastaugh, J., & Freemantle, N. (2006). Do shock absorbing insoles in recruits undertaking high levels of physical activity reduce lower limb injury? *Journal of the Royal Society of Medicine*, 32-7.

Wolfslag, W., Plooij, M., Babuška, R., & Wisse, M. (2015). Learning robustly stable open-loop motions for robotic manipulation. *Robotics and Autonomous Systems*, 27-34.

Wollseifen, T. (2011). Different methods of calculating body sway. *Pharmaceutical Programming*.

Wright, I. C., Neptune, R. R., van der Bogert, A. J., & Nigg, B. M. (1998). Passive regulation of impact forces in heel-toe running. *Clinical Biomechanics*, 521-531.

Wu, K. S., van Osdol, W. W., & Dauskardt, R. H. (2006). Mechanical properties of human stratum corneum: Effects of temperature, hydration, and chemical treatment. *Biomaterials*, 785-795.

Xu, B., Chen, X., & Yue, Z. (2019). Indentation Fatigue Mechanics. In G. Z. Voyiadjis, *Handbook of Nonlocal Continuum Mechanics for Materials and Structures* (pp. 401-431). Springer, Cham.

Yi, T. I., Lee, E. C., Son, N. H., & Sohn, M. K. (2022). Comparison of the Forefoot Pressure-Relieving Effects of Foot Orthoses . *Yonsei Medical Journal*, 864-872.

Yu-Ping, H., Hsien-Te, P., Wang, X., Zong-Rong, C., & Chen-Yi, S. (2020). The arch support insoles show benefits to people with flatfoot on stance time, cadence, plantar pressure and contact area. *Public Library Of Science*.

Yu-ping, H., Peng, H.-T., Wang, X., Zong-Rong, C., & Chen-Yi, S. (2020). The arch support insoles show benefits to people with flatfoot on stance time, cadence, plantar pressure and contact area. *The Public Library of Science*.

Zafar, A. Q., Zamani, R., & Akrami, M. (2020). The effectiveness of foot orthoses in the treatment of medial knee osteoarthritis: A systematic review. *Gait Posture*, 238-251.

Zelik, K. E., Scaleia, V. L., Ivanenko, Y. P., & Lacquaniti, F. (2015). Coordination of intrinsic and extrinsic foot muscles during walking. *European Journal of Applied Physiology*, 691-701.

Zhang, J., Shen, L., Shen, L., & Li, A. (2010, 12). Gait analysis of powered bionic lower prosthesis. *2010 IEEE International Conference on Robotics and Biomimetics, ROBIO 2010* (pp. 25–29). IEEE. doi:10.1109/ROBIO.2010.5723297

Zhang, X., Li, B., Kaiyun, L., Qiufeng, W., & Vanwanseele, B. (2016). An optimized design of in-shoe heel lifts reduces plantar pressure. *Gait & Posture*, 43-47.

Zheng, Y. P., Huang, Y. P., Zhu, Y. P., Wong, M., He , J. F., & Huang, Z. M. (2012). Development of a foot scanner for assessing the mechanical properties of plantar soft tissues under different bodyweight loading in standing. *Medical Engineering & Physics*, 506-11.

Zhu, Y., Wei, G., Ren, L., Luo, Z., & Shang, J. (2023). An Anthropomorphic Robotic Finger With Innate Human-Finger-Like Biomechanical Advantages Part I: Design, Ligamentous Joint, and Extensor Mechanism. *IEEE Transactions on Robotics*.